

Hiroshi Kimura, Kazuo Tsuchiya, Akio Ishiguro,
Hartmut Witte (Editors)

Adaptive Motion of Animals and Machines

Hiroshi Kimura, Kazuo Tsuchiya,
Akio Ishiguro, Hartmut Witte (Editors)

Adaptive Motion of Animals and Machines

With 241 Figures



Springer

Hiroshi Kimura
Graduate School of Information Systems
University of Electro-Communications
1-5-1 Chofu-ga-oka, Chofu, Tokyo 182-8585, Japan

Kazuo Tsuchiya
Department of Aeronautics and Astronautics
Graduate School of Engineering
Kyoto University
Yoshida-honmachi, Sakyo-ku, Kyoto 606-8501, Japan

Akio Ishiguro
Department of Computational Science and Engineering
Graduate School of Engineering
Nagoya University
Furo-cho, Chikusa-ku, Nagoya 464-8603, Japan

Hartmut Witte
Department of Biomechatronics
Faculty of Mechanical Engineering
Technical University of Ilmenau
Pf 10 05 65, D-98684 Ilmenau, Germany

Library of Congress Control Number: 2005936106

ISBN-10 4-431-24164-7 Springer-Verlag Tokyo Berlin Heidelberg New York
ISBN-13 978-4-431-24164-5 Springer-Verlag Tokyo Berlin Heidelberg New York

Printed on acid-free paper

© Springer-Verlag Tokyo 2006

Printed in Japan

This work is subject to copyright. All rights are reserved, whether the whole or part of the material is concerned, specifically the rights of translation, reprinting, reuse of illustrations, recitation, broadcasting, reproduction on microfilms or in other ways, and storage in data banks.
The use of registered names, trademarks, etc. in this publication does not imply, even in the absence of a specific statement, that such names are exempt from the relevant protective laws and regulations and therefore free for general use.

Springer is a part of Springer Science+Business Media
springeronline.com

Printing and binding: Hirakawa Kogyosha, Japan

Preface

• Motivation

It is our dream to understand the principles of animals' remarkable ability for adaptive motion and to transfer such abilities to a robot. Up to now, mechanisms for generation and control of stereotyped motions and adaptive motions in well-known simple environments have been formulated to some extent and successfully applied to robots. However, principles of adaptation to various environments have not yet been clarified, and autonomous adaptation remains unsolved as a seriously difficult problem in robotics.

Apparently, the ability of animals and robots to adapt in a real world cannot be explained or realized by one single function in a control system and mechanism. That is, adaptation in motion is induced at every level from the central nervous system to the musculoskeletal system. Thus, we organized the **International Symposium on Adaptive Motion in Animals and Machines (AMAM)** for scientists and engineers concerned with adaptation on various levels to be brought together to discuss principles at each level and to investigate principles governing total systems.

• History

AMAM started in Montreal (Canada) in August 2000. It was organized by H. Kimura (Japan), H. Witte (Germany), G. Taga (Japan), and K. Osuka (Japan), who had agreed that having a small symposium on motion control, with people from several fields coming together to discuss specific issues, was worthwhile. Those four organizing committee members determined the scope of AMAM as follows.

- + motion principles in nature
- + biologically inspired technical motion systems
- + nonlinear system dynamics and control
- + dynamic autonomous adaptation to terrain
- + dynamic adaptive mechanism
- + passive dynamic walking
- + autonomous pattern adaptation
- + evolution of mechanism and control/nervous system

These topics involve a broad range of background disciplines, i.e., biology, physiology, biomechanics, non-linear system dynamics, and robotics. It is usually difficult for people from different disciplines to discuss specific issues. Therefore, in order to ease this problem we invited nine speakers, each of whom had an impressive academic background in his field. Finally, 41 papers, including nine keynote lectures, were presented in single-track style over four days. Because the quality of each presentation, the intensive discussion concentrating on the single issue of adaptive motion, and the interaction

among people of different backgrounds were so well received, we agreed on holding the 2nd AMAM in Kyoto (Japan) in March 2003.

For the 2nd AMAM, the international organizing committee (AMAM IOC) was formally organized. We received sponsorship from the Japan Society for the Promotion of Science (JSPS) and co-sponsorship from the CREST Program of the Japan Science and Technology Corporation (JST). While keeping the symposium style of AMAM2000, 59 high-quality papers, including nine invited keynote lectures, were presented in single-track style over five days.

The 3rd AMAM was held in Ilmenau (Germany) in September 2005. The proceedings of AMAM2005 will be published on DVD. The members of the current AMAM IOC are:

Kazuo Tsuchiya, general chair
 Hiroshi Kimura, secretary
 Akio Ishiguro, treasurer
 Hartmut Witte

Auke Ijspeert
 Martin Buehler
 Avis H. Cohen

• Publication

This proceedings comprises 23 papers selected from the CD-ROM proceedings of the 1st and 2nd AMAMs. The topics can be loosely placed into six categories: (1) motion generation and adaptation in animals; (2) adaptive mechanics; (3) machine design and control; (4) bipedal locomotion utilizing natural dynamics; (5) neuro-mechanics and CPG and/or reflexes; and (6) adaptation at higher nervous levels.

• Towards the Future

What we discuss, e.g., science vs engineering or biology vs robotics, is not one of the key issues of AMAM. When we solve complicated problems, it is desirable to proceed with analysis and synthesis concurrently. It is well known that analysis by synthesis is a worthwhile and important methodology to understand underlying principles. We hope AMAM marks the beginning of a new interdisciplinary research field where science and engineering are merged.

Tokyo, Kyoto, Nagoya (Japan) and Ilmenau (Germany)
 November 2005

*Hiroshi Kimura
 Kazuo Tsuchiya
 Akio Ishiguro
 Hartmut Witte*

Contents

Part 1 Motion Generation and Adaptation in Animals

Overview of Adaptive Motion in Animals and Its Control Principles Applied to Machines	3
<i>Avis H. Cohen</i>	
Robust Behaviour of the Human Leg	5
<i>Reinhard Blickhan, Andre Seyfarth, Heiko Wagner, Arnd Friedrichs, Michael Günther, Klaus D. Maier</i>	
1 Introduction	5
2 Results	6
3 Perspective	14
Control of Hexapod Walking in Biological Systems	17
<i>Holk Cruse, Volker Dürr, Josef Schmitz, Axel Schneider</i>	
1 Walking: a nontrivial behavior	17
2 Control of the step rhythm of the individual leg	19
3 Control of the selector network: coordination between legs	19
4 Control of the swing movement	21
5 Control of the stance movement and coordination of supporting legs	24
6 Conclusion	26
Purposive Locomotion of Insects in an Indefinite Environment	31
<i>Masafumi Yano</i>	
1 Introduction	31
2 Motion control system	32
3 Central pattern generator model	35
4 Results	38
5 Discussion	38
Control Principles for Locomotion –Looking Toward Biology .	41
<i>Avis H. Cohen</i>	
1 Introduction to Central Pattern Generators and their sensory control	41
2 CPG and muscle activation	41
3 Sensory feedback	45
4 Summary and conclusions	49
Higher Nervous Control of Quadrupedal vs Bipedal Locomotion in Non-Human Primates; Common and Specific Properties ...	53
<i>Shigemi Mori, Futoshi Mori, Katsumi Nakajima</i>	
1 Introduction	53

2	Locomotor control CNS mechanisms including anticipatory and reactive control mechanisms	54
3	Emergence, acquisition and refinement of Bp locomotion in Juvenile Japanese monkeys	56
4	Common and different control properties of Qp and Bp locomotion	58
5	Similarity and difference in the kinematics of lower limbs during Bp walking between our monkey model and the human	59
6	Summary and discussion	60

Part 2 Adaptive Mechanics

Interactions between Motions of the Trunk and the Angle of Attack of the Forelimbs in Synchronous Gaits of the Pika (<i>Ochotona rufescens</i>)	69
--	----

Remi Hackert, Hartmut Witte, Martin S. Fischer

1	Introduction	70
2	Preliminary question: do pikas prefer one forelimb as trailing limb?	70
3	Trajectories of the centre of mass of pikas in half-bound gait	72
4	Does the angle of attack couple with speed?	74
5	Conclusions	75

On the Dynamics of Bounding and Extensions: Towards the Half-Bound and Gallop Gaits	79
--	----

Ioannis Poulakakis, James Andrew Smith, Martin Buehler

1	Introduction	79
2	Bounding experiments with Scout II	80
3	Self-stabilization in the SLIP	81
4	Modeling the Bounding Gait	82
5	Local stability of passive bounding	85
6	The half-bound and rotary gallop gaits	85
7	Conclusion	88

Part 3 Machine Design and Control

Jumping, Walking, Dancing, Reaching: Moving into the Future. Design Principles for Adaptive Motion	91
---	----

Rolf Pfeifer

1	Introduction	91
2	Design principles: overview	93
3	Information theoretic implications of embodiment	97
4	Exploring “ecological balance”—artificial evolution and morphogenesis	102
5	Discussion and conclusions	104

Towards a Well-Balanced Design in the Particle Deflection Plane	107
<i>Akio Ishiguro, Kazuhisa Ishimaru, Toshihiro Kawakatsu</i>	
1 Introduction	107
2 Lessons from biological findings	108
3 The model	109
4 Proposed method	110
5 Preliminary simulation results	111
6 Conclusion and future work	114
Experimental Study on Control of Redundant 3-D Snake Robot Based on a Kinematic Model	117
<i>Fumitoshi Matsuno, Kentaro Suenaga</i>	
1 Introduction	117
2 Redundancy controllable system	119
3 Kinematic model of snake robots	119
4 Condition for redundancy controllable system	122
5 Controller design for main-objective	123
6 Controller design for sub-objective	124
7 Experiments	125
8 Conclusion	125
<hr/>	
Part 4 Bipedal Locomotion Utilizing Natural Dynamics	
<hr/>	
Simulation Study of Self-Excited Walking of a Biped Mechanism with Bent Knee	131
<i>Kyosuke Ono, Xiaofeng Yao</i>	
1 Introduction	131
2 The analytical model and basic equations	132
3 The results of simulation	135
4 Conclusion	140
Design and Construction of MIKE; a 2-D Autonomous Biped Based on Passive Dynamic Walking	143
<i>Martijn Wisse, Jan van Frankenhuizen</i>	
1 Introduction	143
2 Foot shape	144
3 McKibben muscles as adjustable springs	146
4 Pneumatic system	148
5 Pressure control unit	149
6 Walking experiments	151
7 Conclusion	153

Learning Energy-Efficient Walking with Ballistic Walking	155
<i>Masaki Ogino, Koh Hosoda, Minoru Asada</i>	
1 Introduction	155
2 Ballistic walking with state machine	156
3 Energy minimization by a learning module	159
4 Comparing with human data	161
5 Discussion	163
Motion Generation and Control of Quasi Passsive Dynamic Walking Based on the Concept of Delayed Feedback Control	165
<i>Yasuhiro Sugimoto, Koichi Osuka</i>	
1 Introduction	165
2 Model of the walking robot	166
3 Stability of passive dynamic walking	167
4 DFC-based control method	168
5 Computer simulation	171
6 Conclusion and future work	174
<hr/>	
Part 5 Neuro-Mechanics & CPG and/or Reflexes	
Gait Transition from Swimming to Walking: Investigation of Salamander Locomotion Control Using Nonlinear Oscillators	177
<i>Auke Jan Ijspeert, Jean-Marie Cabelguen</i>	
1 Introduction	177
2 Neural control of salamander locomotion	178
3 Mechanical simulation	179
4 Locomotion controller	180
5 Discussion	186
Nonlinear Dynamics of Human Locomotion: from Real-Time Adaptation to Development	189
<i>Gentaro Taga</i>	
1 Introduction	189
2 Real-time adaptation of locomotion through global entrainment	190
3 Anticipatory adjustment of locomotion through visuo-motor coordination	195
4 Computational “lesion” experiments in gait pathology	197
5 Freezing and freeing degrees of freedom in the development of locomotion	199
6 Concluding comments	201
Towards Emulating Adaptive Locomotion of a Quadrupedal Primate by a Neuro-musculo-skeletal Model	205
<i>Naomichi Ogiwara, Nobutoshi Yamazaki</i>	

1	Introduction	205
2	Model	206
3	Results	211
4	Discussion	214
Dynamics-Based Motion Adaptation for a Quadruped Robot .		217
<i>Hiroshi Kimura, Yasuhiro Fukuoka</i>		
1	Introduction	217
2	Adaptive dynamic walking based on biological concepts	218
3	Entrainment between pitching and rolling motions	221
4	Adaptive walking on irregular terrain	223
5	Conclusion	225
A Turning Strategy of a Multi-legged Locomotion Robot ..		227
<i>Kazuo Tsuchiya, Shinya Aoi, Katsuyoshi Tsujita</i>		
1	Introduction	227
2	Model	228
3	Stability analysis of walking	229
4	Turning walk control	234
5	Conclusion	235
A Behaviour Network Concept for Controlling Walking		
Machines		237
<i>Jan Albiez, Tobias Luksch, Karsten Berns, Rüdiger Dillmann</i>		
1	Introduction	237
2	Activation, activity, target rating and behaviours	238
3	The walking machine BISAM	241
4	Implementing a behaviour network	242
5	Conclusion and outlook	243
Part 6 Adaptation at Higher Nervous Level		
Control of Bipedal Walking in the Japanese Monkey,		
<i>M. fuscata:</i> Reactive and Anticipatory Control Mechanisms ..		249
<i>Futoshi Mori, Katsumi Nakajima, Shigemi Mori</i>		
1	Introduction	249
2	Reactive control of Bp locomotion on a slanted treadmill belt	250
3	Reactive and anticipatory control of Bp locomotion on an obstacle-attached treadmill belt	253
4	Summary	257
Dynamic Movement Primitives –A Framework for Motor		
Control in Humans and Humanoid Robotics		261
<i>Stefan Schaal</i>		
1	Introduction	261

2	Dynamic movement primitives	263
3	Parallels in biological research	269
4	Conclusion	275

**Coupling Environmental Information from Visual System to
Changes in Locomotion Patterns: Implications for the Design
of Adaptable Biped Robots** 281

Aftab E. Patla, Michael Cinelli, Michael Greig

1	Introduction	281
2	The twelve postulates for visual control of human locomotion	282
3	Challenges for applying this knowledge to building of adaptable biped robots	284
4	Avoiding collisions with obstacles in the travel path	286
5	Avoiding stepping on a specific landing area in the travel path	293
6	Conclusions	296

Part 1

Motion Generation and Adaptation in Animals

Overview of Adaptive Motion in Animals and Its Control Principles Applied to Machines

Avis H. Cohen

University of Maryland, Biology Department and Institute for Systems Research,
College Park, MD 20742, USA
avis@isr.umd.edu

Animals have developed their locomotor strategies and control mechanisms under the intense pressure of the need to survive and reproduce. They must escape from predators and capture prey. They also must use as little energy as possible in order to preserve their resources. With this in mind, roboticists might well look to biology for design and control principles. Thus, in the articles that follow the reader is offered a collection of observations and suggestions from researchers who have spent many years of experimenting on a range of animals, including both vertebrates and invertebrates.

The perspectives bring an increasing level of complexity. **Reinhard Blickhan** brings the mechanics of the organism into the picture, and argues that we behave with ease and without being overwhelmed by the complicated task in dynamic situations such as running, hopping or jumping. **Holk Cruse** uses nothing by sensory feedback to control his robots. His ideas have been developed through observations of an insect, the stick insect, that during slow walking are using sensory feedback almost exclusively in the control of their movements. In the overview I offer, I introduce the concept of the central pattern generator (CPG) that provides feedforward control signals to pattern muscle activity during locomotion of all animals. The CPG strongly interacts with sensory feedback. Some of the universal and some of the less universal control principles are offered as potential strategies for robots. **Masafumi Yano** offers a perspective that incorporates sensorimotor integration, mechanics and descending control from the brain. This rich viewpoint illustrates the power of the fully integrated organism to survive in an indefinite environment. Finally, **Shigemi Mori**, demonstrates the flexibility of the sub-human primate control of locomotion. He shows clearly that the sub-human primate, *M fuscata*, are able, with extensive training, to walk bipedally, even though their normal locomotion is quadrupedal. This surprising results shows that the sub-human primate locomotor control system is capable of more plasticity even in such a basic movement as locomotion than had been thought possible.

Robust Behaviour of the Human Leg

Reinhard Blickhan, Andre Seyfarth, Heiko Wagner, Arnd Friedrichs,
Michael Günther and Klaus D. Maier

Dpt. Biomechanics, Institute of Sportscience, D-07740 Jena, Germany
reinhard.blickhan@uni-jena.de

Abstract. The human leg with segments, joints and many muscles is a complicated device. Yet, in dynamic situations such as running, hopping or jumping we behave with ease and without being overwhelmed by the complicated task. We argue that this is possible due to a careful arrangement and fine tuning of all properties from which stability and robustness emerges. Robust and stable systems are easy to control.

1 Introduction

Wheeled vehicles are able to economically cover long distances as long as the substrate is sufficiently convenient. On rough terrain legged systems are of advantage. They can use defined footholds, can jump across obstacles and can orient their bodies. However this results in a much higher degree of freedom of the movement system. Wheeled vehicles have a degree of freedom of two. The frontal movement is powered by the motor, the lateral movement is enabled by the steering movements of the driver. In contrast animals and humans can also raise and rotate their bodies. In addition each of the multisegmented body appendages has additional degrees of freedom (ca. 7). This is the main reason for the enormous difficulty to control legged robots.

Most walking machines are slow. This facilitates control. Another strategy is to reduce degrees of freedom. Examples for this strategy are mixed wheeled and legged systems and pantograph legs [1]. The only fast machines built so far, are the hopping machines and their successors built at the MIT-leg laboratory [2]. Here the construction not only used reduced degrees of freedom but also the inherent dynamics provided by elastic telescope springs. This can also be seen as a way to reduce the complexity of the control system. The control system determines the angle of attack of the leg and the time of telescopic expansion of the pneumatic spring. In fact bouncing is due to the principal roughness of legged locomotion, where the leg is facing an impact at each touch down, the only mode of fast locomotion. A springy leg determines the time course of force generation and thus facilitates leg control. If this is not guaranteed the controller must deliver its decisions within the short contact times (see below). Everybody who observed the walking of artificial quadrupeds knows that this demand is far from present possibilities.

Technical walking and running is per se inspired from natural examples. With respect to the question how to solve the formidable task of locomotion

control it is again worthwhile to examine nature. We are used to talk about central pattern generators, reflex loops, and heterarchic control. However, we have neglected for many years the intimate relationship between the mechanical properties of the system and those of the control. Recently several studies have revealed their relevance and some have even coined the contradicting term "neuromechanics" for a newly emerging field. Let me give some prominent examples. The pendulum mechanism for walking as championed by Hemami [3], Cavagna et al. [4], and Mochon and McMahon [5] has been known for many years. However with respect to robotics the break through came with the studies of McGeer [6] who constructed simple passive walkers to support his calculations. Physical modelling helped him to understand, that the length relation between shank and thigh is not just an accident of evolution but is necessary for swing leg to clear ground. In many studies [7,8] we have put forward that many legged systems in nature such as crabs and cockroaches use the same basic dynamics during locomotion as vertebrates. During fast locomotion the legs interact to operate like a single spring. Recent realisations in different machines confirm the elegance of this approach (Full, pers. comm.). In fact the sprawled posture of the arthropods generally interpreted in terms of static stability has turned out to be a measure to increase stability of locomotion in the horizontal direction. Disturbances at the legs are compensated due to passive features of the system [9,10]. It is important to realise that footing of each leg becomes much less critical. Even small and imprecise neural networks are sufficient for control.

It is well known in mechanics that systems described by coupled nonlinear equations can behave very different depending on initial conditions and selected parameters. They may display unpredictable chaotic behaviour or may converge to stable situations e.g. limiting cycles. Pedal systems are per se nonlinear. In addition, in biological systems the comprising materials have complicated properties. By applying a series of models from very simple lumped-parameter models to multi-body models with many degrees of freedom combined with experimental investigations we try to identify principles of operation of the human leg. Recently, we focus on stability.

2 Results

2.1 The global properties of the human leg during running

Running as a bouncing gait can be described by a simple lumped parameter model: the spring-mass system [11] (Fig.1). The system generates an impact onto the ground depending on landing velocity. Depending on the stiffness of the spring the contact time can be short (stiff spring) or long (compliant spring). The distribution of horizontal force is described by the angle of attack of the system. For the case of symmetric operation deceleration is equal to acceleration and continuous locomotion possible. The point of operation of such a system is partly set by physical physiological conditions. The friction

coefficient limits the angle of attack. The amplitudes of the vertical oscillation should be small to facilitate visual sensation and diminish the cost of locomotion. This is due to the fact that small oscillations reduce the vertical force and enhance contact time which can be generated with slower muscles.

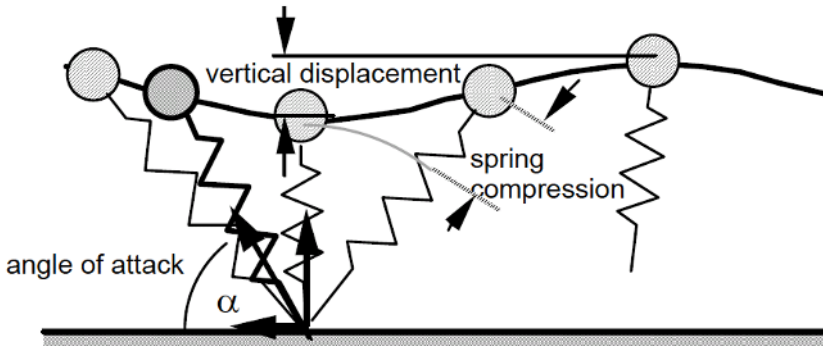


Fig. 1. Simple spring-mass system describing hopping running and jumping

Recent observations (Seyfarth, Geyer, pers. com.) are signalling that other issues may be of similar importance. A small deviation in the angle of attack of the leg spring at touch down results in net acceleration or deceleration of the system. Imagine that the leg would continue the same landing strategy i.e. the same angle of attack at the next step. Due to the acceleration during the previous step there is now an increasing or decreasing mismatch between speed and angle of attack. For close to natural leg stiffness the angles of attack used by the human runner are within a range where running may be stable with respect to speed. Slight mismatches in the motor program are compensated by the behaviour of the system.

2.2 The contribution of the different joints

Due to the degrees of freedom of a system with two joints the quasi-elastic operation of the leg in principle could be realised by compensating inelastic operation of the two joints. Experimental observations [12] have shown, that quasi-elastic operation is a good first approximation. (The deviations will be discussed below.) During hopping knee and ankle joint are operating largely synchronous. During running the knee joint in general reaches the point of maximum bending slightly earlier than the ankle joint. In the long jump the goal of maximum jumping distance results in a similar synchronous operation of the joints. Synchronous operation seems to be of advantage [13].

Copying nature in its essentials one could envision a robot leg built of three segments of equal length with built in rotational springs. Unfortunately, such a system is highly unstable. After a short rotation synchronisation alters.

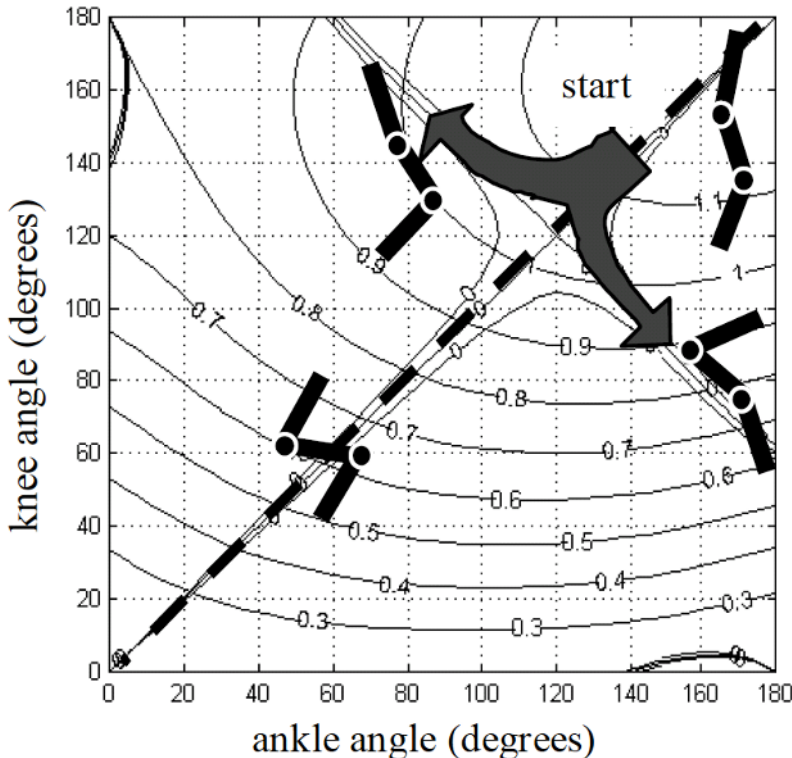


Fig. 2. Starting from a symmetric condition with linear rotational springs at the joints either the knee or the ankle joint over extents.

Flexion in one joint is accompanied by extension in the other (Fig.2). The joints are working against each other. In overextending joints torque changes sign. Such a highly unstable situation would impose serious demands on any control system. A closer look to nature offers a basket with solutions [14]. One answer is geometry: Imitating the arrangement of leg segments of human runners result in a considerable enhancement of the synchronous working range. An additional improvement is possible by introducing slightly nonlinear spring characteristics. Another measure is to introduce springs spanning two joints.

2.3 Coping with losses

Any real mechanical system has to cope with losses due to friction. These might be reduced by improving the joints. However, during running quite different sources of loss must be considered. Running is generated by the cyclic operation of human legs. The horizontal velocity of the foot necessarily oscil-

lates from zero during contact with the substrate to a value of about double running speed during the aerial phase. Similarly, in vertical direction the foot comes to a sudden hold at touch down. The strategy to adapt the velocity of the foot to ground speed at touch down would be highly demanding for control systems. Especially, in axial direction the corresponding demand would require active leg shortening with velocities of about half running speed. In addition, the necessary active accelerations and the decrease in energy storage would increase cost of locomotion.

Instead, the human runner accepts the impact due to the sudden deceleration of the distal masses. The properties of the heel pad, of the sole of the running shoes, the viscoelastic suspension of the muscles (Fig.3), comprising a large part of the distal masses [13] diminish the amplitude and rise-time of the reaction force at touch down. This critically damped impact entails an unavoidable loss. To maintain running speed, the runner is forced to work. The work could be done at different joints. As the main losses occur in axial direction of the leg it is plausible to compensate the losses by active lengthening of the leg. Runners do that by landing with the knees bent, thereby diminishing the impact on all proximal joint surfaces, and by straightening at take off. This lengthening of the leg- and knee-spring can be provided by a drive in series to the spring.

2.4 Muscle properties and attractive legs

The serial arrangement of active and passive elements introduces another complication. Now, the muscle-tendon complex as a whole must guarantee spring-like operation. Muscles have complicated nonlinear behaviour characterised by the force-displacement and force-velocity characteristics. By working at the ascending slope of the force-displacement curve quasi-elastic operation of the muscle could be guaranteed. More complicated to deal with is the force-velocity curve. The force-velocity curve can be understood as an important part of the gears of the locomotor system. While pulling at the drive the forces are high. With shortening speed the muscle's capabilities of force generation diminish. Ideally the muscle-tendon complex takes advantage of energy storage in the tendon and apodemes and simultaneously of the cheap eccentric force generation. This is exactly what happens during long jump [15]. The tendon is stretched immediately after touch down (Fig.4). The rise in force is dominated by muscle recruitment and eccentric force enhancement is easy to maintain due to the eccentric operation of the whole leg. During take off the elastic recoil of the tendon powers straightening of the knee as well as prolonged eccentric loading of the muscle. After the load has fallen below the isometric point of operation muscle shortening dominates. Such a co-operation requires a delicate tuning between muscle properties and properties of the passive tissue. Only technical drives with muscle like characteristics could take advantage of this strategy.

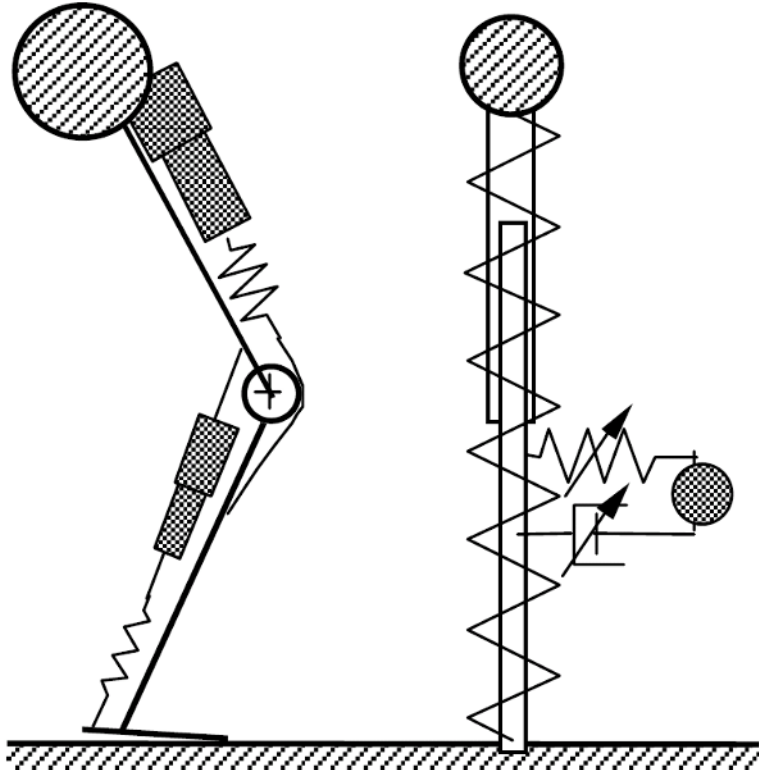


Fig. 3. Viscoelastic suspension of wobbling masses reduce the sharpness of the impact at touch down. Left: anthropomorphic model; lumped-parameter model

We have seen that under certain conditions the spring might help to stabilise locomotion. A springy leg confronted with a rough ground returns automatically to the point of equilibrium. A vertically oscillating spring-mass system without damper would do this infinitely despite of any disturbances. But we have seen, that the human leg entails serial arrangements of elastic elements and musculature (Fig.5). It is by no means obvious how such a system reacts to axial disturbances.

For cyclic systems the Ljapunov-Criteria can be used to examine whether the system asymptotically returns to the prescribed path after disturbance [16]. It assumes an exponential return to the undisturbed condition in the state space. The local slope of this return can be determined from the Eigenvalues of the Jacobian of the equations of motion. In our case with changing conditions during eccentric and concentric periods of the loading cycle these criteria can be taken as a first hint together with numeric simulations. More advanced mathematical methods support our results.

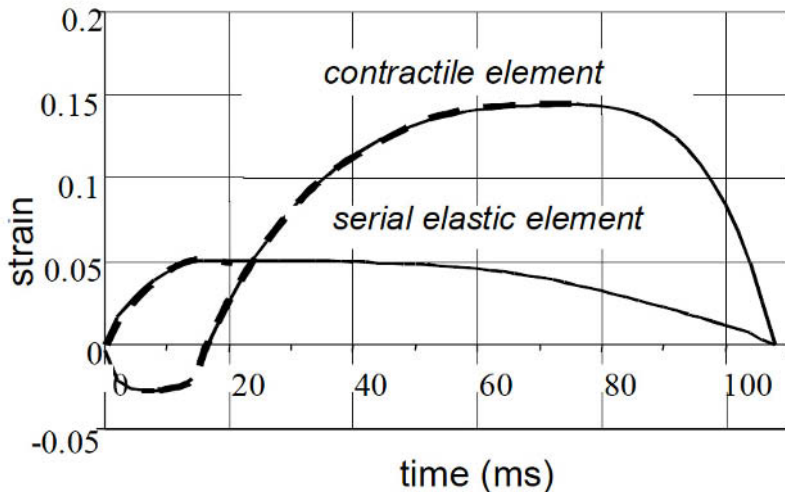


Fig. 4. Time course of strain of the serial elastic element (tendon and apodeme) and the contractile element. dashed line: positive slope or lengthening.(after Seyfarth, et al., 1999)

The results of our calculations show that for a leg model consisting of two massless segments and a knee extensor stabilisation is only possible if the Hill-type muscle with a realistic force length curve is paralleled by a spring and the joint is described realistically including a moving joint axis. In fact stabilisation requires a fine tuning of all these properties (Fig.6).

Especially if the antagonist is spanning two joints antagonistic systems can provide stability with minor requirements with respect to tuning [17]. This is achieved at the cost of co-activation. For the single extensor system described above the activation of the muscle providing a suitable input for the cyclic movement is uniquely determined. For antagonistic systems this is not the case, the system is underdetermined. However, we can calculate activation pattern which provide stability for the system. The stability criterion serves as the necessary additional condition in the system of differential equations. With this approach we find stability for very simple activation patterns. Both muscles are activated simultaneously working against each other in the deflection phase. During the extension phase the flexor is de-activated earlier. New movements can be learned with co-activated muscles providing maximum stability. The neural network controlling the movement then learns to use the fine tuned properties of the system and decreases the co-activation.

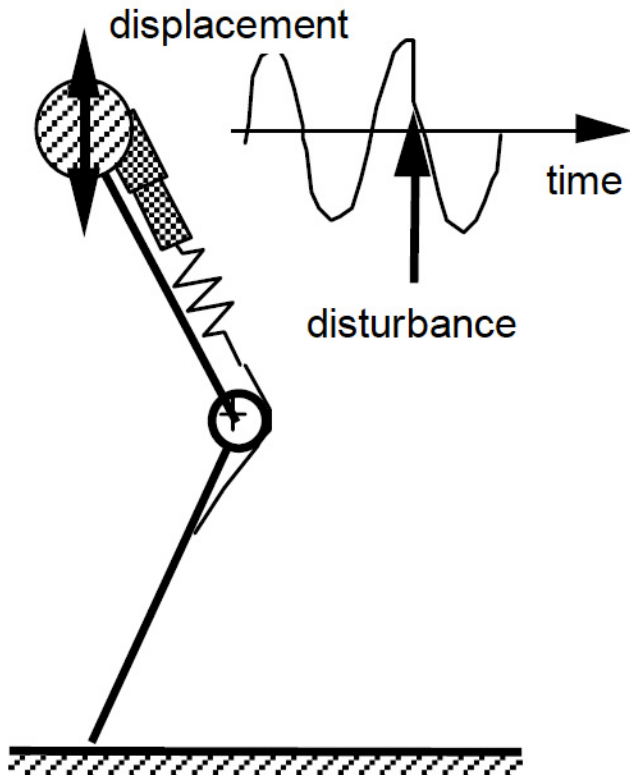


Fig. 5. Two segment model to investigate stability.

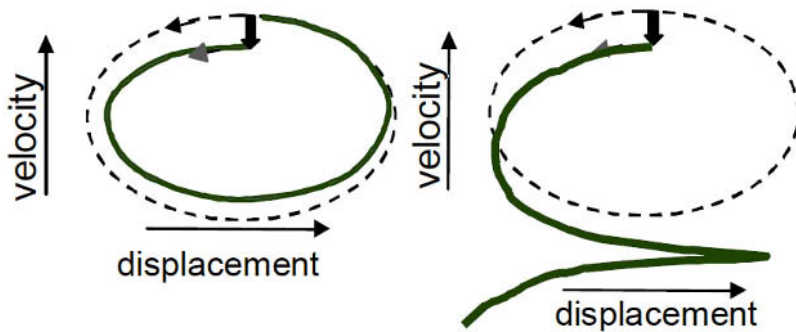


Fig. 6. Phaseplots for a stable(left) and an unstable(right) situation. dashed line: undisturbed; fat line: disturbed

2.5 Robust control

In highly dynamic situations such as running and jumping the delays within the spinal and cortical reflex loops do not allow fine tuned action during the short contact times. These events are largely steered by feed forward control. This requires robust behaviour of the leg as described in the preceding sections. If the leg behaves robust and does not break down in a catastrophic event during ground contact, control, and corrections are possible step by step.

Using the simplest model of a bouncing system, the spring-mass-system, we investigated the suitability of neuronal networks for control [18,19]. Desired speed and angle of attack at next touch down served as input parameters, the take off angles where asked for as output and fed back into the network. It turned out that Multi-Layer-Perceptrons consisting of 7 and 9 neurons in two hidden layers were able to steer such a conservative system to any velocity and along any path (Fig.7). Even though the system learned only to run at various velocities it was able to cover rough ground, i.e. to correct on a step by step basis by adapting the angle of attack. A quite limited number of very simple neurons is sufficient to control such a dynamic behaviour as long as the system properties remain simple and robust.

2.6 Conservative behaviour of the human leg

The human leg has to fulfil many different tasks such as static support during standing, in a hammer like action during a kick, or as a compliant axial strut during running. We investigate to which extent control and properties of the human leg are adapted to certain loading regimes by exposing it to artificial loading situations. An instrumented inclined track allows axial hopping like loading under reduced gravity and with loads from 28 kg to three times body mass.

The results show that the leg adapts to increasing loads by increasing the distance of deceleration. This is achieved by extending the leg to a higher degree at take up and push off. Furthermore the amplitude and the time course of the angular velocity is rather similar in the different tasks. Almost independent of the load and thus of reaction force and muscle recruitment the system is used in a way that presumably allows optimum operation of the participating musculature.

In the machine we could identify similar basic strategies as during hopping: a) quasielastic bouncing where the movement is largely determined by the action of the ankle joint and which is normally used during hopping at the spot; b) compliant bouncing where large excursions are generated by bending of the knee. Whereas in the first case reflexes and material properties seem to be tuned to generate smooth sinusoidal force patterns, the second shows bumpy force-time series. This indicates that during the long contact times

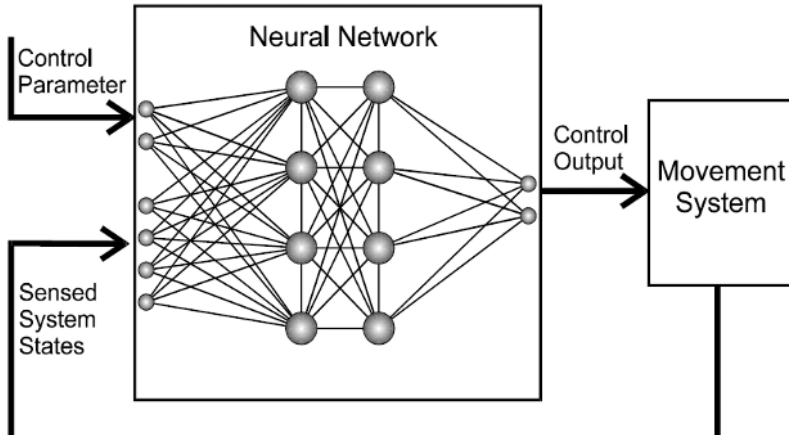


Fig. 7. Neuronal network for robust control of a spring-mass system

involved the quasi-elastic action of the leg is hampered and the suitable reaction force is generated by the concerted action of a series of reflex loops. Similar strategies might be useful in robot legs. With increasing speed and decreasing time for the system to react the contribution of the mechanics of the system should grow.

3 Perspective

We have seen that robust behaviour of the human leg is the result of a very delicate geometrical design twined with intrinsic properties of the muscle tendon complex. Robustness reduces the load on the neuronal control system which is especially important in situations where the time for corrections is limited. In biomechanics legs are considered to be simple. This does not imply that we know all about legs, however, our knowledge about the whole locomotory system including the trunk in dynamic situations is rather limited. Perhaps, simple models which already help to predict operating frequencies may be useful to describe the global behaviour of such complicated arrangements (Fig. 8). In addition like in engineering the design of movement systems is determined by intrinsic boundary conditions given by the limited material properties within the participating structures. Transfer of principles from biology into engineering would be facilitated if the influence of these internal conditions could be identified.

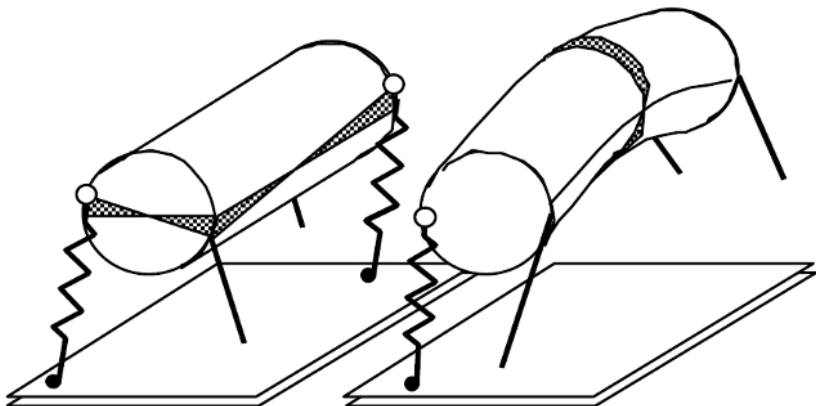


Fig. 8. Elastic beams under torsion and bending describe the action of the trunk of quadruped during trotting and galloping.

Acknowledgements

Supported by grants of the DFG: Innovation College "Motion Systems", INK A22/1-2 TP: B2, C1; Research program "Autonomous Walking", Bl236/8-1, and Bl 236/7.

References

1. Hirose, S., 1984 A study of design and control of a quadruped walking vehicle. Internat. J. Robot. Res. 3, 113-133
2. Raibert, M. H., 1986, Legged robots that balance. MIT Press, Cambridge, MA.
3. Hemami, H., Weimer, F., and Koozekanani, S., 1973 Some aspects of the inverted pendulum problem for modeling of locomotion systems. IEEE Transactions on Automatic Control, pages 658-661
4. Cavagna, G.A., Thys, H., Zamboni, A., 1976, The sources of external work in level walking and running. J. Physiol. Lond. 262:639-657
5. Mochon, S., McMahon, T.A., 1980, Ballistic walking: an improved model. Mathematical Biosciences 52:241-260
6. McGeer, T., 1993, Dynamics and control of bipedal locomotion. Journal of Theoretical Biology, 163:277-314.
7. Blickhan R, Full RJ, 1987, Locomotion energetics of the ghost crab: II Mechanics of the center of mass. J Exp Biol 130:155-174
8. Blickhan, R., Full, R.J., 1993, Similarity in multilegged locomotion: Bouncing like a monopode. J. Comp. Physiol. A-173:509-517
9. Full, R.J., Koditschek, D.E., 1999, Templates and anchors: neuromechanical hypothesis of legged locomotion on land. J. Exp. Biol. 202:3325-3332

10. Kubow, T.M. and Full, R.J., 1999, The role of the mechanical system in control: a hypothesis of self-stabilization in hexapedal runners. *Phil. Trans. Royal Society London B* 354:849-862.
11. Blickhan, R., 1989a, The spring mass model for running and hopping. *J. Biomech.* 22:1217 - 1227
12. Günther, M., Sholukha, V., Blickhan, R., in prep, Joint stiffness of the ankle and the knee in running - an inverse dynamic analysis and forward simulation approach.
13. Seyfarth, A., Friedrichs, A., Wank, V., et. al., 1999, Dynamics of the long jump. *J Biomechanics* 32(12):1259-67
14. Seyfarth, A., Günther, M., Blickhan, R., in prep., A three segmental spring-mass model.
15. Seyfarth, A., Blickhan, R., van Leeuwen, J., 2000, Optimum take-off techniques and muscle design for long jump. *J. exp. Biol.* 203:741-750
16. Wagner, H., Blickhan, R., 1999, Stabilising function of skeletal muscles: an analytical investigation. *J theoret Biol* 199:163-179
17. Wagner H., Blickhan R., 1999, Stabilising function of antagonistic neuromusculoskeletal systems - an analytical investigation-” (*J. biol. Cybernet.* submitted)
18. Maier, K.D., Glauche, V., Blickhan, R., et al. ,2000a, Controlling one-legged three-dimensional hopping movement. *Intern Symp. Adaptive Motion of Animals and machines (AMAM 2000)*
19. Maier, K.D., Glauche, V., Beckstein, et al., in prep, Controlling fast spring-legged locomotion with artificial neural networks. *Soft computing*

Control of Hexapod Walking in Biological Systems

Holk Cruse, Volker Dürr, Josef Schmitz and Axel Schneider

Faculty of Biology, University of Bielefeld, Postfach 100131, D-33501 Bielefeld,
Germany
holk.cruse@uni-bielefeld.de

Abstract. To investigate walking we perform experimental studies on animals in parallel with software and hardware simulations of the control structures and the body to be controlled. In this paper, we will first describe the basic behavioral properties of hexapod walking, as they are known from stick insects. Then we describe a simple neural network called Walknet which exemplifies these properties and also shows some interesting emergent properties. The latter arise mainly from the use of the physical properties to simplify explicit calculations. The model is simple, too, because it uses only static neuronal units. The system is currently tested using an adapted version of the robot TARRY II.

Keywords: walking, stick insect, decentralized control, Walknet, positive feedback

1 Walking: a nontrivial behavior

From a cognitive standpoint, walking seems to be rather uninteresting because it appears to be a fairly automatic behavior. We do not have to think consciously about moving the joints when walking. Nevertheless, we will argue that walking in a natural environment requires considerable „motor intelligence“ and can be regarded as a paradigm for control of behavior in general. First of all, walking, as almost all behavior, has to deal with redundancy. In most biological systems for motor control, particularly those concerned with walking, the number of degrees of freedom is normally larger than that necessary to perform the task. This requires the system to select among different alternatives according to some, often context-dependent optimization criteria, which means that the system usually has to have some autonomy. Therefore, the experimenter does not have direct control of some important inputs to the motor system. Further, such natural systems are physical systems „situated“ in complex, often unpredictable environments, which means that any movement may be modified by the physics of the system and the environment. In turn, adapting to real environments requires the use of sensory information about the environment and the results of the system’s actions. Together, these two factors create a loop through the environment which means that the actual behavior is determined by the properties of the environment as well as those of the walking system. Despite these experimental and theoretical

difficulties, the complexity makes the study of motor mechanisms especially challenging, particularly because they illustrate to a high degree the task of integrating influences from the environment, mediated through peripheral sensory systems, with central processes reflecting the state and needs of the organism. In a walking insect at least 18 joints, three per leg, have to be controlled. Because the environment may change drastically from one step to the next, and even the geometrical properties of the body may change, the control of walking is all but a trivial task. Traditional technical solutions take sensory input into account only to a small degree and usually use hierarchically structured control architectures. In both respects these solutions differ strongly from solutions found by biological systems. Most probably, this difference is the main reason for the failure of traditional solutions when being tested in a realistic environment. Biologically inspired autonomous systems appear to be the solution when one searches for systems being able to act in unpredictable and hostile environments.

The control system explained here consists of a number of distinct modules which are responsible for solving particular subtasks. Some of them might be regarded as being responsible for the control of special „microbehaviors“: for example, a walking leg can be regarded as being in one of two states, namely performing a swing movement or a stance movement. During stance, the leg is on the ground, supports the body and, in the forward walking animal, moves backwards with respect to the body.

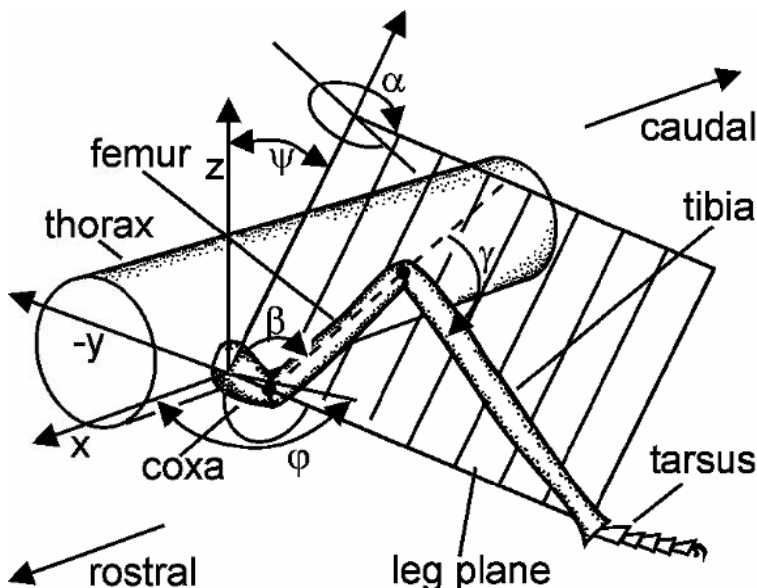


Fig. 1. Sketch of a stick insect leg showing the arrangement of the joints and their axes of rotation.

During swing, the leg is lifted off the ground and moved in the direction of walking to where it can begin a new stance. These two „microbehaviors“ are mutually exclusive. A leg cannot be in swing and in stance at the same time, a situation also holding for many „macrobehaviors“ such as fight or flight, for instance. Therefore, the control structure has to include a mechanism for deciding whether the swing or the stance module is in charge of the motor output. To solve this problem, a simple network, based on positive feedback, is used. This network works like a „two-way“ subsumption system [1], although there is no direct suppression and subsumption influence. Note that no central oscillator is used.

2 Control of the step rhythm of the individual leg

As mentioned, the step cycle of the walking leg can be divided into two functional states, stance and swing. The anterior transition point, i.e., the transition from swing to stance in the forward walking animal, is called the anterior extreme position (AEP) and the posterior transition point is called the posterior extreme position (PEP). Differences in the constraints acting during the two states and in the conditions for their termination suggest that the leg controller consists of three separate control networks. Two low-level networks, a swing network and a stance network, control the movement of the leg during swing and stance, respectively. The transition between swing and stance is controlled by a selector network. The swing network and the stance network are always active, but the selector network determines which of the two networks controls the motor output.

3 Control of the selector network: coordination between legs

The pattern of leg movement in insect walking is usually described as tripod or tetrapod gait (Fig. 2). These terms may suggest a rigid central control structure. However both gaits should rather be considered as extremes of a continuum (e.g. [2]). Actually very different step patterns can be observed e.g. after a brief disturbance of the movement of a single leg or when animals start walking from different leg configurations [3, 4]. Insect gaits may therefore better be described by the term „free gait“ [5]. The usually observed tripod or tetrapod patterns represent limit cycle solutions that are only apparent in undisturbed situations [6]. For insects and crustaceans, it has been shown that a small number of local rules acting between neighboring legs suffice for the emergence of different gaits and the recovery from different disturbances. In the following these rules will be summarized briefly.

In all, six different coupling mechanisms have been found in behavioral experiments with the stick insect (Fig. 5a). One mechanism serves to correct

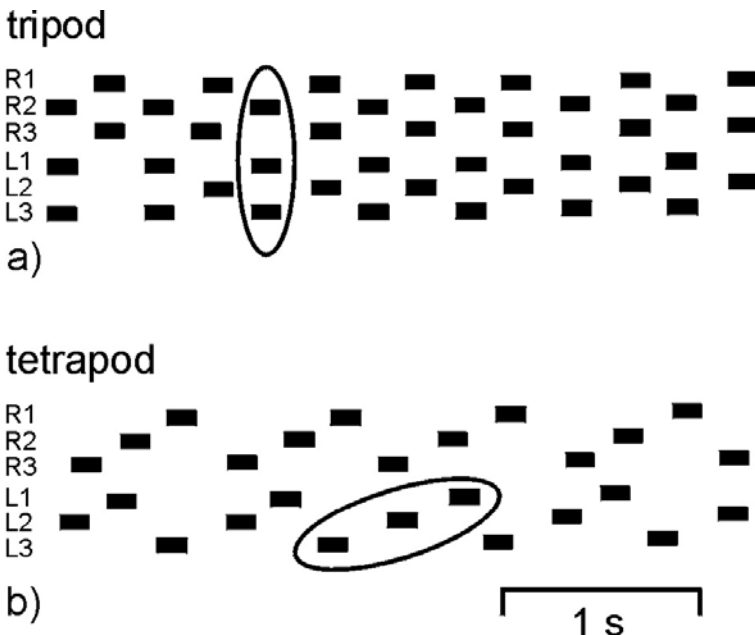


Fig. 2. The step patterns of a tripod (a) and a tetrapod (b) gait as produced by a stick insect. The latter is also referred to as a wave gait. The six traces represent the six legs. Black bars correspond to swing movement. Legs are designated as left (L) or right (R) and numbered from front to rear. Left and right legs on each segment (e.g., L1 and R1) always have a phase value of approximately 0.5. The phase value of adjacent ipsilateral legs (e.g., L1 and L2) is 0.5 in the tripod gait but differs in the tetrapod gait (after [2]).

errors in leg placement; another has to do with distributing propulsive force among the legs. The other four are used in the present model. The beginning of a swing movement, and therefore the end-point of a stance movement (PEP), is modulated by three mechanisms arising from ipsilateral legs: (1) a rostrally directed inhibition during the swing movement of the next caudal leg, (2) a rostrally directed excitation when the next caudal leg begins active retraction, and (3) a caudally directed influence depending upon the position of the next rostral leg. Influences (2) and (3) are also active between contralateral legs. The end of the swing movement (AEP) in the animal is modulated by a single, caudally directed influence (4) depending on the position of the next rostral leg. This mechanism is responsible for the targeting behavior—the placement of the tarsus at the end of a swing close to the tarsus of the adjacent rostral leg. These signals are used by the selector network to decide on swing or stance. Mechanisms (1) to (3) are illustrated in Fig. 3.

4 Control of the swing movement

The task of finding a network that produces a swing movement is simpler than finding a network to control the stance movement because a leg in swing is mechanically uncoupled from the environment and therefore, due to its small mass, essentially uncoupled from the movement of the other legs.

A simple, two-layer feedforward net with three output units and six input units can produce movements (see Fig. 5b, swing net) which closely resemble the swing movements observed in walking stick insects [7]. The inputs correspond to three coordinates defining the actual leg configuration and three defining the target—the configuration desired at the end of the swing. In the simulation, the three outputs, interpreted as the angular velocities of the joints, $d\alpha/dt$, $d\beta/dt$, and $d\gamma/dt$, are used to control the joints. The actual angles (for definition see Fig. 1) are measured and fed back into the net.

Through optimization, the network can be simplified to only 8 (front and middle leg) or 9 (hind leg) non-zero weights (for details see [8]). We believe this represents the simplest possible network for the task; it can be used as a standard of comparison with physiological results from stick insects. Despite its simplicity, the net not only reproduces the trained trajectories, it is able to generalize over a considerable range of untrained situations, demonstrating a further advantage of the network approach. Moreover, the swing net is remarkably tolerant with respect to external disturbances. The learned trajectories create a kind of attractor to which the disturbed trajectory returns. This compensation for disturbances occurs because the system does not compute explicit trajectories, but simply exploits the physical properties of the world. The properties of this swing net can be described by the 3D vector field in which the vectors show the movement produced by the swing net at each tarsus position in the workspace of the leg. Fig. 4 shows the planar projections of one parasagittal section (a), and one horizontal section (b) through the work space.

This ability to compensate for external disturbances permits a simple extension of the swing net in order to simulate an avoidance behavior observed in insects. When a leg strikes an obstacle during its swing, it initially attempts to avoid it by retracting and elevating briefly and then renewing its forward swing from this new position. In the augmented swing net, an additional input similar to a tactile or force sensor signals such mechanical disturbances at the front part of the tibia (Fig. 5b, r1) or the femur (Fig. 5b, r2). These units are connected by fixed weights to the three motor units in such a way as to produce the brief retraction and elevation seen in the avoidance reflex. Other reflexes can be observed when the tibia is mechanically stimulated laterally (r3) or when the femur is touched dorsally (r4). These reflexes have been implemented in an analogous manner (Fig. 5b).

In the model, the targeting influence reaches the leg controller as part of the input to the swing net (Fig. 5b). These signals can be generated by a simple feedforward net with three hidden units and logistic activation functions

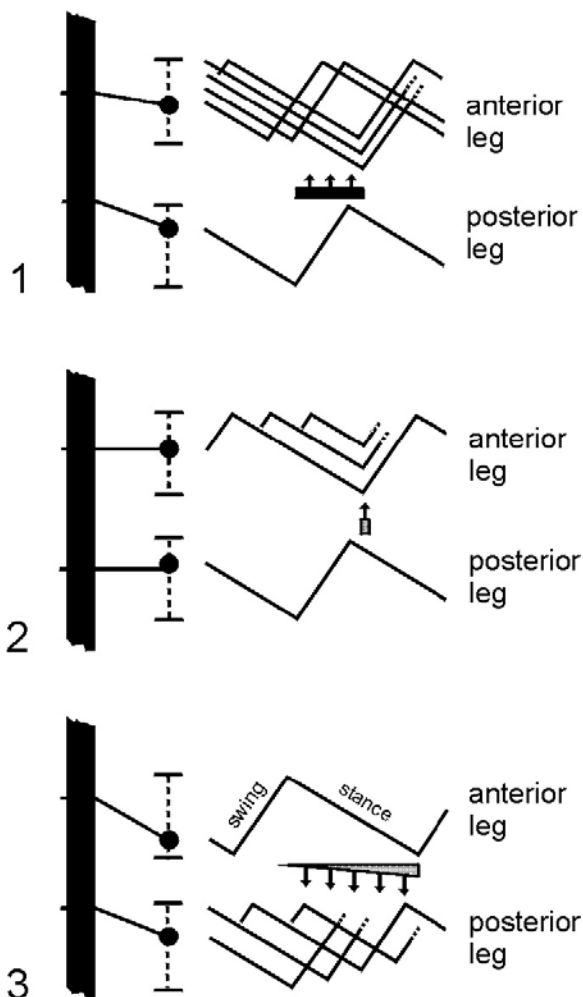


Fig. 3. Illustrations of the mechanisms 1 to 3 (see Fig. 5a) as shown from above to below.

(Fig. 5b, "target net") which directly associates desired final joint angles for the swing to current joint angles of a rostral leg such that the tarsus of the posterior leg is moved in the direction of that of the anterior leg. Compared to a first version [9] the new target net has direct connection between the input and the output layer. There is no explicit calculation of either tarsus position. Physiological recordings from local and intersegmental interneurons [10] support the hypothesis that a similar approximate algorithm is implemented in the nervous system of the stick insect.

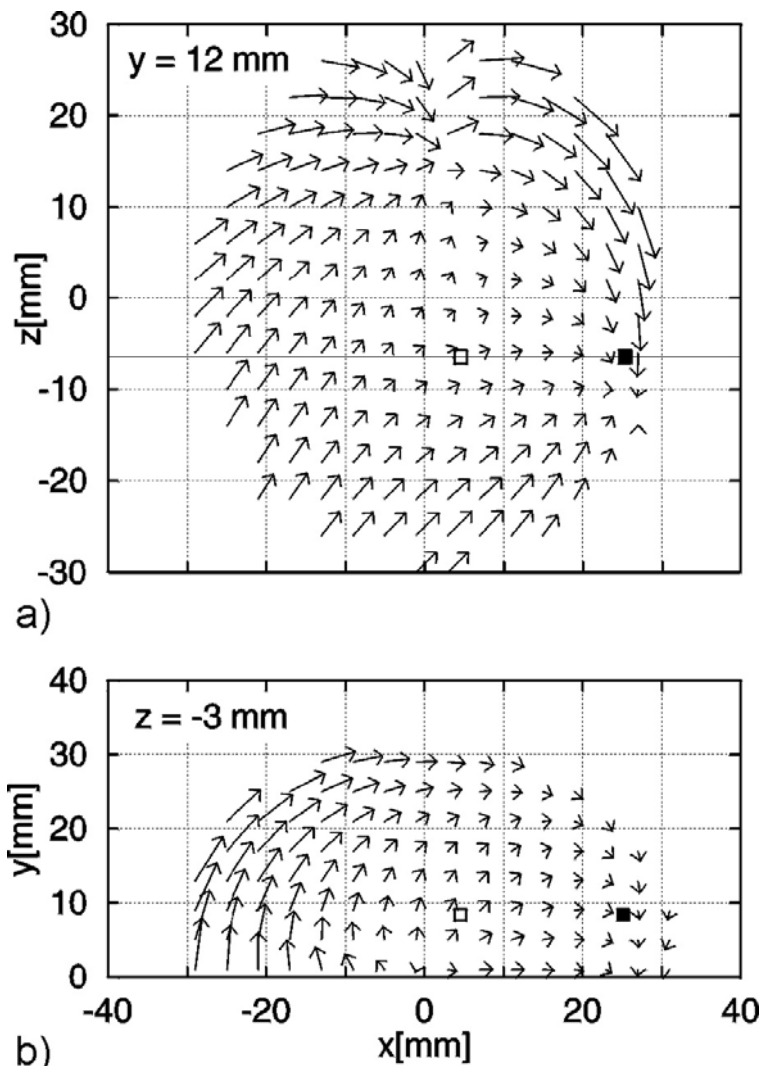


Fig. 4. Vector field representing the movement of the tarsus of a left front leg produced by the swing net. (a) Projection of a parasagittal section ($y = 12 \text{ mm}$, for coordinates see Fig. 1). (b) Projection of a horizontal section slightly below the leg insertion ($z = -3 \text{ mm}$). Left is posterior, right is anterior. The average posterior extreme position (start of swing movement) and of the average anterior extreme position (end of swing movement) are shown by an open square and by a closed square, respectively.

5 Control of the stance movement and coordination of supporting legs

For the stance movement, simple solutions can be found for straight walking on a flat surface [11]. In more natural situations, the task of controlling the stance movements of all the legs on the ground poses several major problems. It is not enough simply to specify a movement for each leg on its own: the mechanical coupling through the substrate means that efficient locomotion requires coordinated movement of all the joints of all the legs in contact with the substrate, that is, a total of 18 joints when all legs of an insect are on the ground. However, the number and combination of mechanically coupled joints varies from one moment to the next, depending on which legs are lifted. The task is quite nonlinear, particularly when the rotational axes of the joints are not orthogonal, as is often the case for insect legs and for the basal leg joint in particular. A further complication occurs when the animal negotiates a curve, which requires the different legs to move at different speeds.

In machines, these problems can be solved using traditional, though computationally costly, methods, which consider the ground reaction forces of all legs in stance and seek to optimize some additional criteria, such as minimizing the tension or compression exerted by the legs on the substrate. Due to the nature of the mechanical interactions and inherent in the search for a globally optimal control strategy, such algorithms require a single, central controller; they do not lend themselves to distributed processing. This makes real-time control difficult, even in the still simple case of walking on a rigid substrate.

Further complexities arise in more complex, natural walking situations, making solution difficult even with high computational power. These occur, for example, when an animal or a machine walks on a slippery surface or on a compliant substrate, such as the leaves and twigs encountered by stick insects. Any flexibility in the suspension of the joints further increases the degrees of freedom that must be considered and the complexity of the computation. Further problems for an exact, analytical solution occur when the length of leg segments changes during growth or their shape changes through injury. In such cases, knowledge of the geometrical situation is incomplete, making an explicit calculation difficult, if not impossible.

Despite the evident complexity of these tasks, they are mastered even by insects with their “simple” nervous systems. Hence, there has to be a solution that is fast enough that on-line computation is possible even for slow neuronal systems. To solve the particular problem at hand, we propose to replace a central controller with distributed control in the form of local positive feedback [8]. Compared to earlier versions [12], this change permits the stance net to be radically simplified. The positive feedback occurs at the level of single joints: the position signal of each is fed back to control the motor output of the same joint. Earlier experiments [13] have shown that body height in the stick insect is controlled by a distributed system in

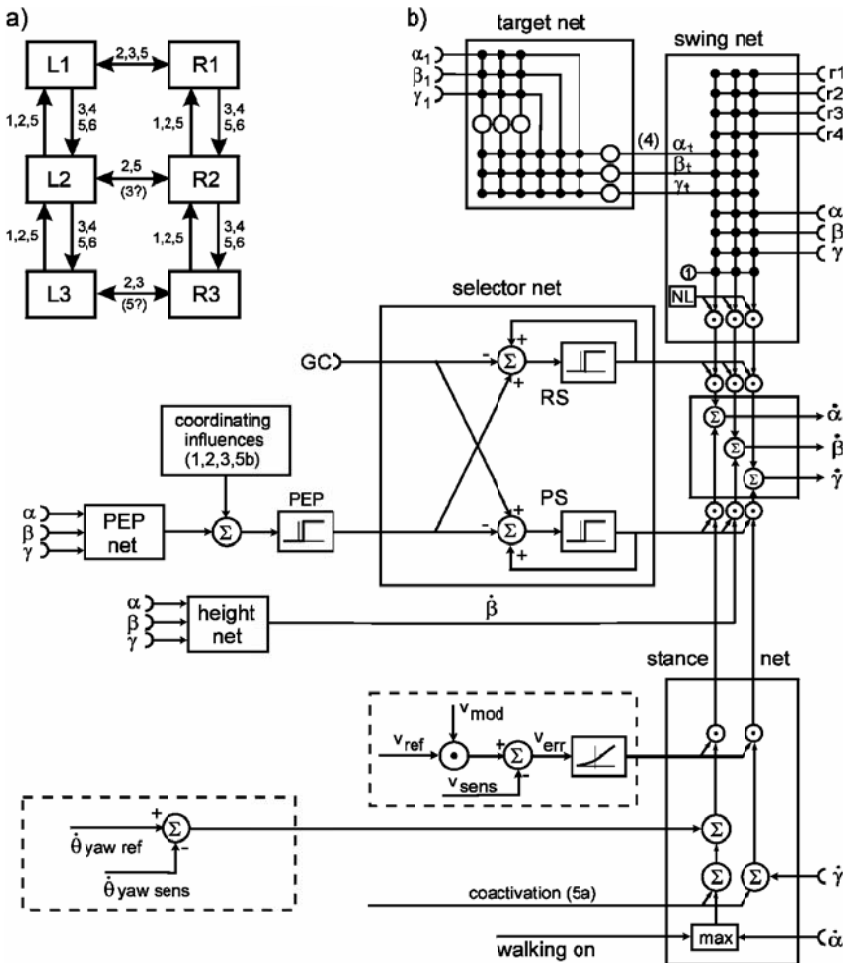


Fig. 5. Fig. 5. (a) Schematic diagram showing the arrangement of the mechanisms coordinating the movements of the different legs. (b) The leg controller consists of three parts: the swing net, the stance net, and the selector net which determines whether the swing or the stance net can control the motor output, i.e., the velocity of the three joints α , β , and γ . The selector net contains four units: the PEP unit signalling posterior extreme position, the GC unit signalling ground contact, the RS unit controlling the return stroke (swing movement), and the PS unit controlling the power stroke (stance movement). The target net transforms information on the configuration of the anterior, target leg, α_1 , β_1 , and γ_1 , into angular values for the next caudal leg which place the two tarsi close together. These desired final values (α_t , β_t , γ_t) and the current values (α , β , and γ) of the leg angles are input to the swing net together with a bias input (1) and four sensory inputs (r1 - r4) which are activated by obstructions blocking the swing and thereby initiate different avoidance movements. A non-linear influence (NL) modulates the velocity profile. For details see Cruse et al. (1998).

which each leg acts like an independent, proportional controller. However, maintaining a given height via negative feedback appears at odds with the proposed local positive feedback for forward movement. To solve this problem we assume that during walking positive feedback is provided for the α joints and the γ joints, but not for the β joints (Fig. 5b, stance net). The β joint is the major determinant of the separation between leg insertion and substrate, which determines body height. The value for the β joint is given by a three layered feedforward network (height net) with three input units (α , β , γ), 5 hidden units and one output unit. This net has been trained using the known leg geometry and approximates data from [14], where force-height characteristics of the standing animal have been measured.

There are, however, several problems to be solved. Only two will be mentioned below. To permit the system to control straight walking and to negotiate curves, a supervisory system was introduced which, in a simple way, simulates optomotor mechanisms for course stabilisation that are well-known from insects and have also been applied in robotics. This supervisory system uses information on the rate of yaw, such as visual movement detectors might provide. Second, we have to address the question of how walking speed is determined in such a positive feedback controller. Again, we assume a central value which represents the desired walking speed v_{ref} . This is compared with the actual speed, which could be measured by visual inputs or by monitoring leg movement (Fig. 5b, boxes marked by broken lines).

One major disadvantage of our simulation is its pure kinematic nature. To test the principle of local positive feedback at least for straight walking, we have performed a dynamic simulation for the six-legged system under positive feedback control during stance. The basic software was kindly provided by F. Pfeiffer, TU Munich. No problems occurred. Nevertheless, a hardware test of the walking situations is necessary. Currently, we are performing such a test by using the robot Tarry IIb, i.e., a reconstructed version of TARRY II [15]. The changes made concern the introduction of passive compliance in each leg joint, a necessary condition for application of positive feedback. For a single leg walking on a treadmill, the test turned out to be successful.

6 Conclusion

As has been shown for the case of straight walking, this network is able to control proper coordination. Steps of ipsilateral legs are organized in triplets forming "metachronal waves", which proceed from back to front, whereas steps of the contralateral legs on each segment step approximately in alternation. With increasing walking speed, the typical change in coordination from the tetrapod to a tripod-like gait is found. For slow and medium velocities the walking pattern corresponds to the tetrapod gait with four or more legs on the ground at any time and diagonal pairs of legs stepping approximately together; for higher velocities the gait approaches the tripod pattern

with front and rear legs on each side stepping together with the contralateral middle leg. The coordination pattern is very stable. For example, when the movement of one leg is interrupted briefly during the power stroke, the normal coordination is regained immediately at the end of the perturbation. Furthermore, the model can cope with obstacles higher than the normal distance between the body and the substrate (see Fig. 6 for an example). It continues walking when a leg has been injured, such that, for example, half of the tibia is removed (see [16]).

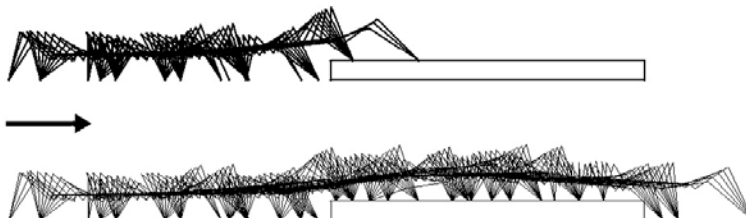


Fig. 6. Simulated walk over an obstacle. Movement direction is from left to right. Leg positions, as viewed from the side, are illustrated only during stance and only for every fifth time interval in the simulation. Upper panel: the first part of the walk until both front legs reach the top of the obstacle. Lower panel: descent from the obstacle until both front legs and one middle leg touch the lower ground.

What about curve walking? The typical engineer's solution is to determine the curve radius and the center of the curve. With these values the trajectories of the different legs are calculated and then, using inverse kinematics, the trajectories for the joint angles are determined. In our case, too, a value is required to determine the tightness of the curve. This, however, does not need to quantitatively correspond to the curve radius. The value is only used as an amplification factor for the positive feedback loop of front and hind legs. This value can deliberately be changed from one moment to the next. No further calculations are necessary.

The introduction of the local band-pass filtered positive feedback in 12 of the 18 leg joints provides a control system which as far as we can see cannot be further simplified, because it is decentralized down to the level of the single joints. This simplification has the side effect that computation time can be minimized. The essential advantage, however, is that, by means of this simplification and the consideration of physical properties of the body and the environment, all problems mentioned above (Sect. 5) can easily be solved, although they, at first sight, seemed to be very difficult.

Unexpectedly, the following interesting behavior was observed. A massive perturbation, for example by clamping the tarsi of three legs to the ground, can make the system fall. Although this can lead to extremely disordered arrangements of the six legs, the system was always able to stand up and resume proper walking without any help. This means that the simple solution

proposed here also eliminates the need for a special supervisory system to rearrange leg positions after such an emergency. Some animations can be found in: <http://www.uni-bielefeld.de/biologie/Kybernetik>

Recent results show that internal "motivational" states are necessary in order to enable the system to react to a given stimulus in different ways depending on the actual internal state. The state itself depends on sensory input, too.

References

1. Brooks, RA (1986) A robust layered control system for a mobile robot. *J. Robotics and Automation* 2, 1423
2. Graham, D. (1985) Pattern and control of walking in insects. *Advances in Insect Physiology*, 18, 31140
3. Graham, D. (1972) A behavioural analysis of the temporal organisation of walking movements in the 1st instar and adult stick insect. *J.comp.Physiol.81*, 2352
4. Dean, J., Wendler, G. (1984) Stick insect locomotion on a wheel: Patterns of stopping and starting. *J. exp. Biol.* 110, 203216
5. McGee, R.B., Iswandhi, G.I. (1979) Adaptive locomotion of a multilegged robot over rough terrain. *IEEE Transactions on Systems, Man, and Cybernetics*, SMC-9, (4), 176-182
6. Cymbalyuk, G.S., Borisuk, R.M., Müller-Wilm,U., Cruse, H. (1998) Oscillatory networks controlling six-legged locomotion. Optimization of model's parameters. *Neural Networks* 11, 1449-1460
7. Cruse, H, and Bartling, C (1995) Movement of joint angles in the legs of a walking insect, *Carausius morosus*. *J. Insect Physiol.* 41, 761-771
8. Cruse, H, Bartling, C, Dean, J, Kindermann, T, Schmitz, J, Schumm, M, and Wagner, H (1996) Coordination in a six-legged walking system: simple solutions to complex problems by exploitation of physical properties. In: P Maes, MJ Mataric, J-A Meyer, J Pollack and SW Wilson (eds.) *From animals to animats 4*. Cambridge MA, MIT Press, pp. 84-93
9. Dean, J. (1990) Coding proprioceptive information to control movement to a target: simulation with a simple neural network. *Biol. Cybern.*, 63, 115120.
10. Brunn, D. and Dean, J. (1994) Intersegmental and local interneurones in the metathorax of the stick insect, *Carausius morosus*. *J. Neurophysiol.*, 72, 1208-1219.
11. Müller-Wilm, U, Dean, J, Cruse, H, Weidemann, HJ, Eltze, J, and Pfeiffer, F (1992) Kinematic model of stick insect as an example of a 6-legged walking system. *Adaptive Behavior* 1, 155-169
12. Cruse, H, Bartling, C, Kindermann, T (1995) High-pass filtered positive feedback for decentralized control of cooperation. In: F Moran, A Moreno, JJ Merelo, P Chacon (eds.), *Advances in Artificial Life*, pp. 668-678. Springer 1995
13. Cruse, H (1976) The control of the body position in the stick insect (*Carausius morosus*), when walking over uneven surfaces. *Biol. Cybern.* 24, 2533
14. Cruse, H, Riemschneider, D, Stammer, W (1989) Control of body position of a stick insect standing on uneven surfaces. *Biol. Cybern.* 61, 7177

15. Frik, M, Guddat, M, Karatas, M, Losch, CD (1999) A novel approach to autonomous control of walking machines. In: G. S. Virk, M. Randall, D. Howard (eds.). Proceedings of the 2nd International Conference on Climbing and Walking Robots CLAWAR 99, 13-15 September, Portsmouth, UK, pp. 333-342, Professional Engineering Publishing Limited, Bury St. Edmunds
16. Cruse, H, Kindermann, T, Schumm, M, Dean, J, Schmitz, J (1998) Walknet - a biologically inspired network to control six-legged walking. Neural Networks 11, 1435- 1447

Purposive Locomotion of Insects in an Indefinite Environment

Masafumi Yano

Research Institute of Electrical Communication, Tohoku University, 2-1-1
Katahira Aoba-Ku, Sendai, 980-8577, Japan
masafumi@riec.tohoku.ac.jp

Abstract. There are many scientific and technological problems that we cannot deal with today. Our current scientific methodology cannot be applied to what is called the real world problem. Because the real world is unpredictably and dynamically changing, it is impossible to objectify it in advance and to apply the traditional methodology to it. This real world problem especially arises in information processing systems such as the recognition and the control systems coping with the real world. The current information systems request in advance the complete information to deal with. In the case of robot in the real world, to attain the purpose a robot is usually required to solve the inverse problem adjusting the changes of the real world. It is always an ill-posed problem. When the robot autonomously solves the ill-posed problem, some proper constraints should be self-organized in the robot. In addition to the self-organization of the constraints, the robot is required to satisfy the constraints in real time. Here we propose a new real-time control mechanism for the purposive movements of a robot under the unpredictably changing environment.

1 Introduction

The real world is by far more complicated than what we up until today have been able to clarify fully through the natural sciences. It contains many phenomena that the methodology of the separation of self and other cannot be applied to. When one isolates something, there is always something left. Therefore, there are always intrinsic problems remaining in the parts left over. There are many problems that we cannot deal with today. Since the real world is unpredictably and dynamically changing, it is impossible to objectify it in advance and to apply the traditional methodology to it. Especially this real world problem is crucial in information processing systems, that is, the recognition and the control systems coping with the real world. Since the current information systems could only deal with explicit and complete information, all problems should be defined and formalized in advance. That is, our current methodology could be applied only to a limited problem, which is rigorously objectified in advance, but the real world is not the case.

This difficulty is arisen from the uncertainties of the real world. There are two kinds of uncertainties in the world. One is a definite uncertainty and the other is an indefinite uncertainty. The former is related to the stochastic

problem. When the stochastic phase space can be defined but it is enormous large, it is possible to find the solution in principle, but actually impossible to find the solution from its very large phase space. In this sense, it is a definite uncertainty. On the contrary, the real world is essentially indefinite, because it is unpredictably and dynamically changing. So it is impossible to prepare the complete information in advance, indicating an indefinite uncertainty. In the cases of indefinite uncertainty, these are always ill-posed problems. It means that the information processing systems coping with the real world should have the ability to self-emerge the information needed for. I will point out the requirements that the emergent systems should satisfy. The system should be indefinite, which is well known as the law of requisite variety proposed by Ashby. It means that the information system interacting with the complex environment should have more complexity than that of environment. Second, the system should be self-referential, because the necessary information could not be added externally. Finally, the emergence of information might be abduction process. The deductive and the inductive logic can be applicable only for the definite problems.

In order to change the ill-posed problem to the well-posed one, it is necessary some appropriate constraints to make up the incompleteness of the information of the problem. In the traditional methodology, it is possible to add some appropriate constraints externally, if we can objectify the problem in advance. If the pre-assumed world is stationary, this methodology will be powerful and useful. For example, in the case of locomotion, the trajectories are usually determined in advance and then the robot walks along the trajectory by feedback control. Or the locomotive patterns are determined kinematically in advance, one of which is selected depending on the condition of the locomotion. On the contrary, in the real world the system itself should incessantly emerge the necessary constraints in a self-referential way in response to the ever-changing environment and satisfy them at every moment. Here we propose a new paradigm for the purposive locomotion in the real world.

2 Motion control system

The motion control systems of animals seem to autonomously create appropriate information depending on the purposes self-organized in the system under the unpredictably changing environment. The motor systems of the animals are generally controlled through three sub-regions in a hierarchical way, the brain, the central pattern generator (CPG) and the effector organs. The flexibility of the movements is generated by the neural network as a control system, indicating that they can organize dynamically their gait patterns quickly in response to the changes of the environment. To coordinate the movements of the muscles in response to the unpredictably changing environments, the control system should be indefinite. Indefinite system means

that the properties of the elements of the system and the relationship of them are not specified in advance. If the control system is definite, it is impossible to adapt to the unpredictably changing environment.

2.1 Higher centers

Since the decision-making mechanism is far complicated and not clarified sufficiently yet, it is assumed that the instruction of behavior is generated in the higher center of cerebrum. So the higher center of cerebrum can be regarded as the highest constraint generator for motor control. The organized program and instructions in the higher center are the sequence of the purposive direction and the velocity. Although the detail of the mechanism of the higher center is not clarified yet, some physiological experiments indicate that the higher center can be considered as coordinating organ between the purposive movement and posture control. There are parallel pathways from the brain stems to the motoneurons, one of which is directly pathway to motoneurons and the other is the descending to the thoracic ganglion known as the CPG. The former might be thought to adjust the muscle tone to maintain its posture and the latter to contribute the coordination of the muscle movements to attain the purposive behavior. To coordinate the functions between the higher center and the thoracic ganglion, neurotmodulators play profound effects on the organization of the behavioral states by switching a neural network from one operating mode to another. The walking patterns are quickly changed depending on the walking velocities and load [1-6]. In the case of stick insect, at high speed the front leg and the hind move simultaneously and the middle antiphasic to the others, forming a tripod to support their body. On the contrary, when they walk slowly, the three legs of each side move metachronally. A pair of legs of the same segment step alternately. As increasing the walking velocity, the insect changes the patterns critically depending on their velocity, resembled to a phase transition. The walking patterns also vary with the load [1,5,6]. In the case of horse, energy consumption during walking does not depend on the walking distance, but almost on the distance.

2.2 Central pattern generator

The thoracic ganglions, as central pattern generators, are an indefinite control system to coordinate between the purposive movements and the unpredictably changing environment, which is well known as the polymorphic circuits or multi-functional circuit [7]. Recently, we have demonstrated that the polymorphic circuits can generate various spatio-temporal patterns using a hard-wired model [8]. But the indefinite control system is only one of necessary conditions. To attain the purpose, the proper constraints should be self-organized and fulfilled by the system itself in response to the changes of

the purpose and the current environment. These motor control organizations are summarized in Fig.1.

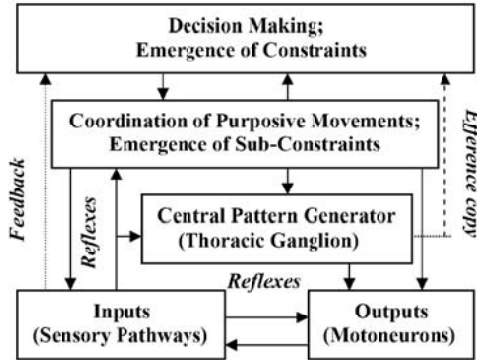


Fig. 1. Hierarchical organization of motor control.

One of the aims of biological motion is to reach its destination. If more complex purpose such as reaching a destination with a required velocity is imposed on the system, the arrival to the destination takes the priority over all other purposes. The velocity of stance phase of right and left side legs is tuned proportional to the angle between the axis of the body and the direction of the destination, which is feed backed until the second time derivative of the angle becomes zero. The velocities of the two sides are given by

$$V_{leg.\text{req}} = V_{body} \pm k_1 \theta \pm k_2 \times f\left(\frac{d^2\theta}{dt^2}\right) \quad (1)$$

Insects walk usually at an optimal stride, indicating that they have an optimal anterior and posterior extreme point. From the viewpoint of the balancing constraints, the frequencies of the two sides should be the same. At lower walking velocity, the frequency of the leg motion is almost constant but minimal, showing that its stride increases with the velocity up to the extreme points. Beyond the velocity determined by the minimal frequency and the maximal stride, they quicken the pace to attain the required velocity. In the turning motion at higher velocity, the frequencies of the two sides tend to be different, but the balancing constraint requires the same frequencies of the two sides. In this case we assume that the lower velocity side increase its frequency to its posture, decreasing the stance duration. The tuning of the frequency of the lower velocity side is given by

$$\begin{aligned} dD_{opt}/dt &= D_{\max} - (D_{opt} + K_b) \\ \Delta k_b &= +k_1 & k_b \geq 0 \\ \Delta k_b &= -k_2 \end{aligned} \quad (2)$$

This quantity is feededback to the rhythmic neuron as follows;

$$\Delta D_R = k_d(D_{opt} - D_{s\tan ce}). \quad (3)$$

So the higher center of brain sends velocities and the frequencies of the two sides to the CPG as the constraints of the purposive movement and posture control.

3 Central pattern generator model

In our model we focus on the walking of insect, so we discuss the control of the motor system after the decision-making, that is, selection of the behavior. The higher center of brain sends the velocities of the both sides of the limbs and their muscle tones as the instructions to CPG after coordinating the purposive movements and the standing posture. In this model the neural network of the control system composed of the higher center of brain and CPG is shown in Fig.2. The CPG send motor outputs to control leg muscles and receive the external afferents as to position, load and force of each muscle. We have already demonstrated in the case of insect walking that the well coordinated motion among the legs is organized not only by the neural system composed of the three ganglion, connected through the inter-segmental connectives, but by the mechanical interaction through the movements of legs. Central pattern generators (CPG) are networks of neurons to control the motor system generating spatio-temporal pattern of neural activities. In this paper, we also construct a coupled nonlinear-oscillator system as the polymorphic network, which can produce various walking pattern by modulating the properties of the composing neurons.

The walking of the insect is controlled by the three thoracic ganglions, prothoracic, mesothoracic and methathoracic ganglions [9]. These ganglions send motor outputs to control leg muscles and receive the external afferents as to position, load and force of each muscle. These ganglions are internally connected each other through a pair of thoracic connectives. It has been clarified that the well coordinated motion among the legs is organized not only by the neural system composed of the three ganglion, connected through the inter-segmental connectives, but by the mechanical interaction through the movements of legs. Central pattern generators (CPGs) are networks of neurons to control the motor system generating spatio-temporal pattern of neural activities. In this paper, we construct a coupled nonlinear-oscillator system as the polymorphic network, which can produce various walking pattern by modulating the properties of the composing neurons.

Inter-segmental inter-neurons in a thoracic ganglion of locust have been extensively investigated by Laurent and Burrows [10,11]. We adopt fundamentally their results as schematically shown in Fig.1. In thoracic ganglion, this signal is transformed into rhythmic wave by rhythmic neuron corresponding to a spiking inter-neuron in the ganglion. The rhythmic neuron makes direct synaptic connection with nonspiking inter-neuron (NS neuron), which is great important to integrate the information on the states of muscles and inter-segmental pathway. NS neuron transforms the output of the rhythmic

neurons to send the motor neuron. We adopt fundamentally their results as schematically shown in Fig.2. In thoracic ganglion, this signal is transformed into rhythmic wave by rhythmic neuron corresponding to a spiking interneuron in the CPG.

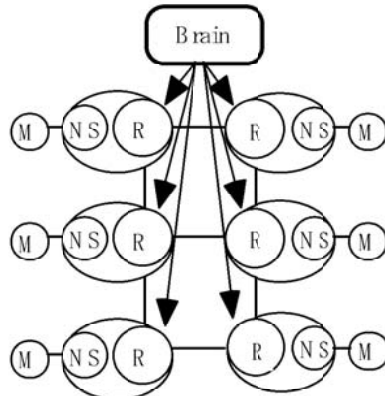


Fig. 2. Inter-segmental connection among CPGs.

The rhythmic neuron makes direct synaptic connection with non-spiking inter-neuron (NS neuron), which is great important to integrate the information on the states of muscles and inter-segmental pathway. NS neuron transforms the output of the rhythmic neurons to send the motor neuron. Inter-segmental connections between rhythmic neurons in the CPG are inhibitive, which produce asynchronous oscillation between neighboring rhythmic neurons. The frequency of the rhythmic neuron determines the temporal patterns of walking, which inhibits each other to appear any phase relationship among the movement of legs. In this sense, the rhythmic neuron is a kind of command neuron that receives the information of walking velocity, that is, purpose of the animal created in the brain. The spatio-temporal patterns of the movement of legs are emerged by integration of the dynamical information of the effector organs in the NS neurons under the constraint driven from the purpose. Under unpredictably changing environment, the system requires some rule to satisfy the constraints, and then walking patterns of the animals should be emerged as the results of the coordination of the movements of the leg muscles. The constraints on the robot should be contented by optimally integrating each objective function of the elements through competition and cooperation among them. The objective function is derived from the energetics of muscle contraction, in which muscle has an optimal shortening velocity to provide the highest efficiency of the energy conversion. So we introduce "the least dissatisfaction for the greatest number of the elements" rule to generate the walking patterns. This rule is quite

similar to the Pareto optimum in the economics and brings forth the cooperation and/or competition among leg movements, resulting in emerging the most efficient walking pattern [12,13].

The equations of rhythmic neuron model are given by

$$\begin{aligned} \frac{dx_{Ri}}{dt} &= -y_{Ri} - f(x_{Ri}) - \sum_j \alpha_{NS_{ij}} (x_{Rj} - x_{Ri}) + \beta_{NS_i} x_{NS_i} \\ \frac{dy_{Ri}}{dt} &= g(x_{Ri}) + D_R \\ f(x) &= (A_1 x^2 + B_1 x + C_1) x \\ g(x) &= (A_2 x^2 + B_2 x + C_2) x \end{aligned} \quad (4)$$

, where x denotes voltage of neuron and DR is the input to the rhythmic neuron, which determines the frequency of the oscillation.

The NS neurons is given by

$$\begin{aligned} \frac{dx_{NS_i}}{dt} &= -y_{NS_i} - f(x_{NS_i}) + \beta_{R_i} x_{R_i} \\ \frac{dy_{NS_i}}{dt} &= g(x_{NS_i}) + D_{NS_i} \\ f(x) &= (A_1 x^2 + B_1 x + C_1) x \\ g(x) &= (A_2 x^2 + B_2 x + C_2) x \end{aligned} \quad (5)$$

where DNs is the input to the rhythmic neuron, which controls the phase relationship among the movement of legs. And the motoneuron is governed by the following equation,

$$\begin{aligned} x_{mi}(t) &= \Lambda \text{ sigmoid}(G_i^{th}(t)H(x_{NS_i}) + G_i^{ag}(t)\bar{F}_{FRF}) \\ G_i^{th}(t) &= k_i^{th}(V_{body,req} - V_{body}) \\ G_i^{ag}(t) &= k_P^{ag}(\theta offset - \theta_i) \end{aligned}, \quad (6)$$

where x_{mi} and \bar{F}_{FRF} are the activity of the motoneuron, which determines the motive force of the leg, and the average repulsive force against the floor, respectively. Each motoneuron is connected to the each corresponding muscle. The outputs of non-spiking neuron are transformed to the excitation with the strength of 1 when above a threshold, otherwise 0. Then they are sent to the corresponding motoneurons.

In order to self-organize the walking pattern according to the circumstance, it is necessary to obtain the information on the surroundings and the state of the legs. At the beginning of the stance phase, only the posterior muscle shortens, but at the end of the stance phase the position sensor of the posterior muscle should strongly inhibit the motoneuron of it, activating the motoneuron of the anterior muscle. In the case of the swing phase, the interaction between the pair of muscles should be reversed. These interactions can be presented by the direct synaptic connection of the position sensor of each muscle with the motoneurons and by the feedback to the connectives between the nonspiking neuron and the motoneuron as shown in Fig.1. The hind leg moves antiphasic to the middle, which also moves antiphasic to the front leg, although there is no strong coupling between the hind and the front legs.

So, the information required to optimize the efficiency of energy conversion is given as follows.

$$\Delta x_{NS_i} = k_\eta \left[\frac{\partial \eta_i / \partial f_i - \left(\sum_{j \neq i} f_j * \partial \eta_j / \partial f_j \right) / \sum_i f_i}{\sum_i f_i} \right]$$

It means that the legs moved synchronously tend to share the load equivalently, where η denote the efficiency curve of the energy conversion of muscle. Each leg requires working more efficiently, so the feedback to NS neuron is

$$\Delta D_{NS_i} = k_{D_{NS_i}} \left[\sum_j \int_0^T f_i * (\partial \eta_i / \partial f_i) dt \right] / \left[\sum_i \int_0^T f_i dt / T \right] \quad (7)$$

This feedback information determines the degree of the synchronization among the legs.

The feedback information from leg to motoneuron is given by

$$\Delta G_i^{th} = k_\eta (V_{i.req} - V_i). \quad (8)$$

4 Results

In case of straight walking, the required velocity is the only purpose of the robot, which is the strong constraint for our model system to attain at any required velocity and any load on the system. Our insect robot can fundamentally generate the two different walking patterns depending on the walking velocities and loads. The walking patterns are characterized by the phase relationship among the six legs, showing the walking pattern of metachronal gait. The phase relationship between the hind and the front drastically changes as the walking velocity increases. As increases the velocity, our robot shows that the front and the hind legs move simultaneously, called tripod gait as reported previously.

In this model, the structure of leg is composed of only two muscles, flexor and extensor muscles, so the movements of legs are limited to move parallel to the axis of the body. When the angle between the axis of the body and the direction of the destination is large, the walking velocity should become slower and the gait pattern is metachronal. When is small, the insect can turn at higher velocity with a tripod gait. At intermediate angle, outer side legs and inner side legs take tripod and metachronal gait, respectively, as shown in Fig.4 a) and b).

5 Discussion

We have simulated an insect robot as an example that can generate appropriate walking patterns to walk efficiently. Since the walking pattern changes

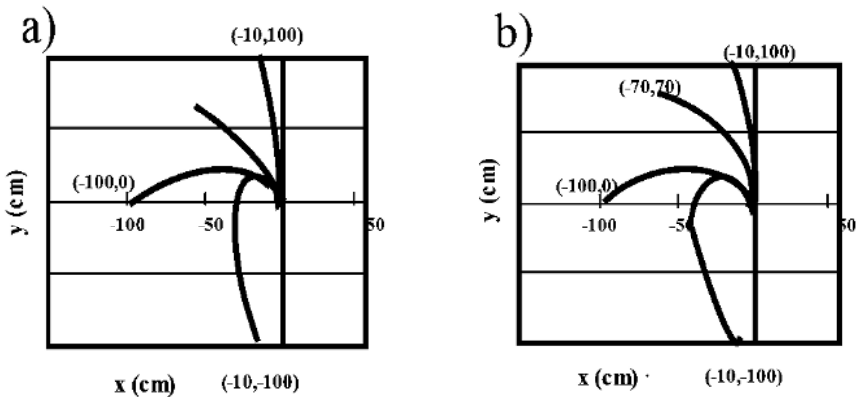


Fig. 3. Trajectories of slow a) and fast b) walk.

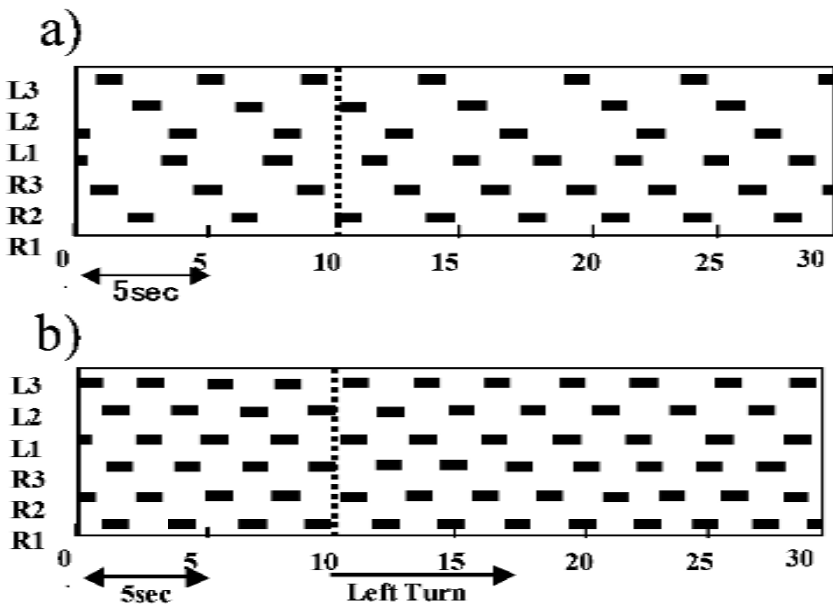


Fig. 4. Gait patterns of turning walk at slow speed a) and high speed b).

crucially depending on their walking velocities and loads, animals could generate a great number of diversities of walking patterns to adapt the unpredictable changes of their surroundings.

We have also showed that a new control mechanism installed in the insect robot, which can walk attaining more complex purposes of the system as possible as it can operate at higher efficiency of energy conversion under unpredictable changes of the environment. This control mechanism is derived

from a metarule to determine the constraints on the motor system. In case of turning walk, the destination takes the priority over all other purposes. So the constraints are self-organized every moment depending on the current state of the system and the environment to attain the purpose. And the constraints may be always fulfilled with more optimal efficiency. As the result the optimal trajectory and the walking patterns emerged.

References

1. Pearson, K.G., (1972). Central programming and reflex control of walking on the cockroach. *J.Exp.Biol.* 56:173-193
2. Pearson, K.G., (1976). The control of walking *Sci. Am.* 235, 72-86
3. Graham, D., (1979). The effects of circumo-esophageal lesion on he behavior of the stick insect *Carausius morosus*. I. Cyclic behavior patterns. *Biol. Cybern.* 32:139-145
4. Graham, D., (1979). The effects of circumo-esophageal lesion on the behavior of the stick insect *Carausius morosus*. II. Change in walking coordination. *Biol. Cybern.* 32,147-152
5. Foth E. and Graham D. (1983a) Influence of loading parallel to the body axis on the walking coordination of an insect. I. Ipsilateral effects. *Biol. Cybern.* 4 7:17-23
6. Foth E. and Graham D. (1983a) Influence of loading parallel to the body axis on the walking coordination of an insect. II.Contralateral effects. *Biol. Cybern.* 48:149-157
7. Getting PA. and Dekin MS. (1985) Tritonia swimming: a model system for integration within rhythmic motor systems. In: Selverston AI(ed) Model neural networks and behavior. Plenum Press. New York, pp 3-20
8. Makino Y., Akiyama M. & Yano M., (2000). Emergent mechanisms in multiple pattern generations of the lobster pyloric network. *Biol. Cybern.* 82:443-454
9. Dean, J., (1989). Leg coordination in the stick insect *Carausius morosus* *J. Exp. Biol.* 145, 103-131
10. Laurent, G., & Burrows, M., (1989a). Distribution of intersegmental inputs to nonspiking local interneurons and motor neurons in the locust. *J. Neurosci.* 8, 3019-3029
11. Laurent, G., & Burrows, M., (1989b). Distribution of intersegmental inputs to nonspiking local interneurons and motor neurons in the locust. *J. Neurosci.* 8, 3030-3039
12. Kimura S., Yano M., & Shimizu, H., (1993). A self-organizing model of walking patterns of insects. *Biol. Cybern.* 69 183-193
13. Kimura S., Yano M., & Shimizu, H., (1994). A self-organizing model of walking patterns of insects II. The loading effect and leg amputation. *Biol. Cybern.* 70 505-512

Control Principles for Locomotion –Looking Toward Biology

Avis H. Cohen

University of Maryland, Biology Department and Institute for Systems Research,
College Park, MD 20742, USA
avis@isr.umd.edu

1 Introduction to Central Pattern Generators and their sensory control

Presented here is an overview of some principles for control of locomotion that are seen in all animals and which offer ideas for robotic design and control. The intention of the overview is to suggest new ways to think about and to perhaps design legged machines taking inspiration and guidance from biology. Some additional potential features of motor control seen in mammalian species are also presented as further examples of concepts that might prove useful for robotic design.

The discussion in this paper will focus on universal principles present in virtually all animals studied, vertebrate and invertebrate. We can have some confidence that the principles that cut across such a wide variety of animals have most likely been heavily selected over evolutionary time to help in that survival, and that the principles are important and highly adaptive control strategies. Two less universal principles are also described for potential robotic design, with some discussion of how they are implemented in the biological system and what they might contribute to artificial systems. Examples of how one might implement the control strategies will be presented from robots of colleagues, H. Kimura, University of Electro-Communications, Tokyo, and A. Lewis, Iguana Robotics. The paper will provide further explanation of the principles as well as pointing to additional material including references, and pedagogical lectures made available in PDF format.

2 CPG and muscle activation

2.1 CPG structure and basic motor pattern

Locomotion in animals could be produced by passive mechanics as the limbs impact the environment (for a passive robot cf. Ref. 1). The muscles and tendons of animal limbs have a remarkable ability to store and release energy (cf. Full, this volume), but, passive mechanics would be inadequate for swimming, uphill locomotion or for locomotion on an absorbent substrate such as sand. It is also known that during locomotion a feedforward excitation to the

muscles exists that can be independent of sensory feedback and brain input [2, 3] (figure1).

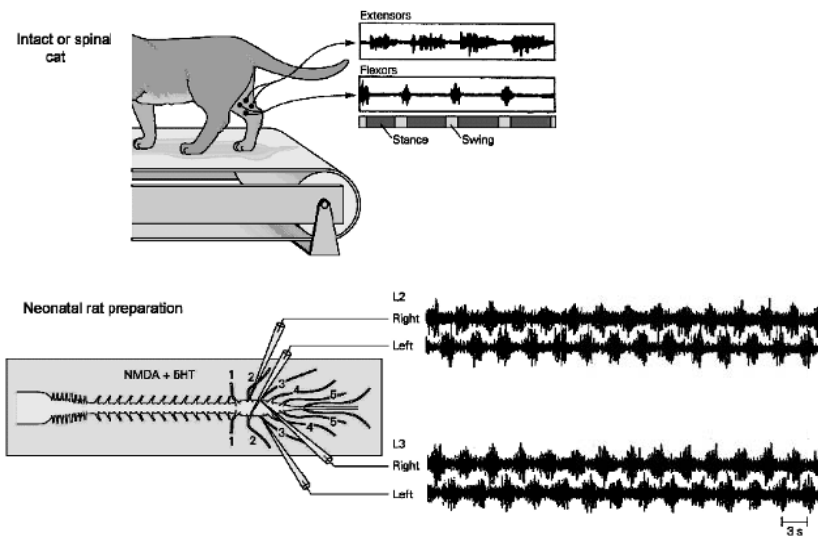


Fig. 1. Demonstration of the existence of CPG in mammals:

Above, the pattern of flexion and extension seen in a cat that is either fully intact or spinalized but with sensory feedback present. Below, a fully isolated spinal cord a neonatal rat is capable of producing a stable alternating pattern of muscle activity similar to that seen during walking. (Adapted from ref 4, data from isolated rat spinal cord from ref 5)

The feedforward muscle activation is generated by a “central pattern generator (CPG)” within the spinal cord. The basic pattern, while not requiring sensory feedback or brain input, does interact with feedback during movement (see below for description of this interaction.)

There is one example of an invertebrate that seems to rely almost entirely on sensory activated reflexes for its locomotion (cf. Cruse presentation), but its walking is so slow that the reflex activation provides perfect ongoing adjustments to environmental conditions.

There is considerable evidence that the spinal CPG of vertebrates is a neural circuit of coupled non-linear oscillators, coordinated by ascending and descending fibers via strong connections. The structure and organization of the spinal CPG is best understood in the lamprey, a fish-like animal that is evolutionarily at the bottom of the vertebrate line. Its spinal cord, while simple, contains all the critical vertebrate components of the nervous system. Furthermore, the outputs of the CPG throughout the vertebrates can be shown to be related to each other by only simple transformations [6]. Thus, the organizational principles found in lamprey are apt to hold for

other vertebrates, even those with limbs. In addition to its anatomical simplicity, the lamprey also has the advantage that it lacks any limbs or paired fins. Its locomotion is a series of traveling waves with the body forming a single wavelength for optimal efficiency [7]. Increases in speed are achieved by increasing the frequency of the traveling waves, but basically preserving the overall shape of the body. The pattern of motor output giving rise to the traveling waves is strict alternation of activity from the left and right sides within a single segment, and a traveling wave of excitation along first one and then the other side of the body. The activation of any two pairs of segments has a constant phase relationship regardless of the speed of propagation of the traveling wave (figure 2).

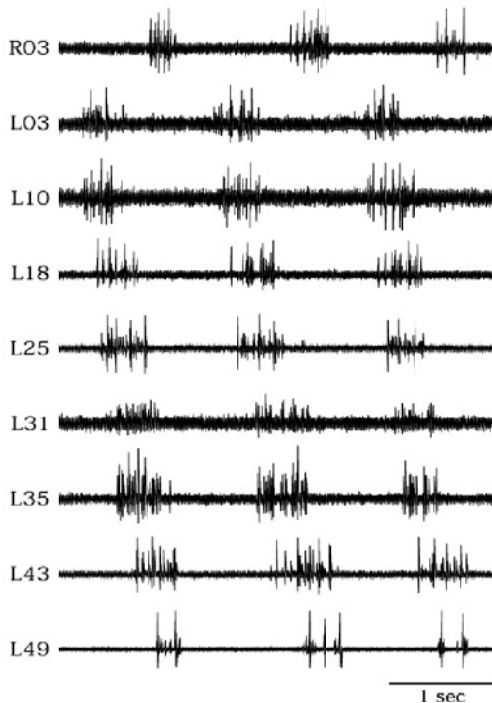


Fig. 2. Lamprey traveling wave observed in isolated spinal cord

The motor outputs recorded from a 50 segments piece of isolated spinal cord bathed in excitatory neural transmitter (adapted from ref 8). The numbers denote the spinal segment in the isolated piece. The output at a single segment alternates (R03-L03), with a wave of activity descending down the spinal cord.

Study of the lamprey CPG has revealed a distributed chain of segmental oscillators, where each oscillator is no more than three spinal segments [9].

Each segmental oscillator has its own intrinsic frequency under any given set of conditions [10]. These intrinsic frequencies differ among each other. The oscillators maintain a single frequency via coupling provided by a system of ascending and descending fibers that apparently make very strong connections overall. There is also evidence that the functional connections of the fibers can be made on segments nearby or upon segments up to more than 20 segments away [11]. The fiber systems are also distributed across the width of the spinal cord [12] (figure 3).

My colleagues and I have modeled the lamprey CPG as a chain of coupled limit cycle oscillators [13]. Coupling has been modeled as a periodic function of the phase difference between any two pairs of oscillators [13, 14]

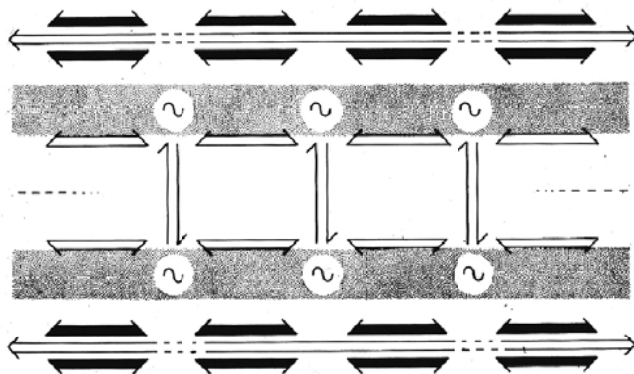


Fig. 3. Functional organization of the lamprey CPG

Each segment or small group of segments consists of a pair of coupled oscillators. The coupling is ascending and descending, and long and short. (adapted from ref 12)

With this view of the CPG in mind, Ralph Etienne-Cummings, Johns Hopkins University, designed an analog VLSI chip to produce periodic bursting to generate the rhythmic output of an actuator for the joint of a limb. The chip diverges in many ways from its biological counterpart, but captures the functional equivalence of the periodicity and strict alternation of a segmental oscillator (figure 4).

When two oscillators are used to control a pair of legs, coupling via mechanisms in keeping with the spirit of the earlier mathematical modeling is effectively works to couple the pair of chips to maintain the limbs phase locked (unpubl. observation). Below, is further discussion of the basic chip and its interaction with sensory feedback from a bipedal limb robot designed by Anthony Lewis, Iguana Robotics.

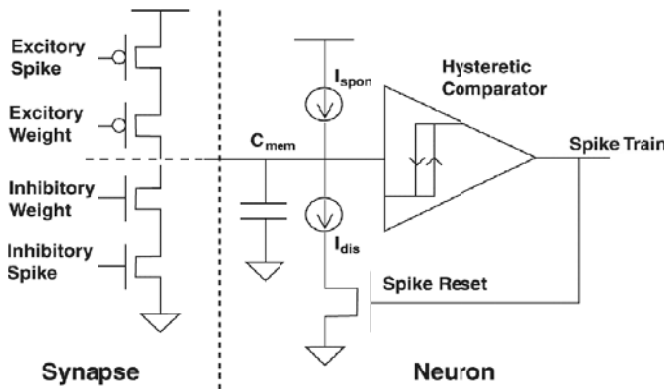


Fig. 4. Circuit for CPG chip (from ref 15)

An example of the use of the CPG to produce stable locomotion in a quadruped is seen in the robot, Tekken, designed by Hiroshi Kimura and his colleagues at University of Electro-Communications, Tokyo. It can generate a range of gait patterns and speeds of locomotion with remarkably smooth action [16].

2.2 Muscle co-activation

By contrast with the lamprey, the muscle activation pattern for limbed animals is not simple alternation, but is often co-activation of antagonistic muscles. Co-activation provides stiffness and stabilization of the joints. For example, during extension of a cat hindlimb, the extensors provide the propulsive force, but flexors are co-active to produce stabilization of the joint (figure 5: data from J-P. Gossard). Similarly, extensors are active during the end of flexion to brace the limb for the impact with the ground [17]. This pattern of co-activation is produced by the CPG of a functionally isolated spinal cord of the cat (figure 5), demonstrating that the pattern is intrinsic to the CPG and does not require sensory feedback or control descending from the brain. David Boothe [18] has shown several neural network models capable of generating this type of co-activation during rhythmic activity of a CPG.

The use of co-activation is also shown in a robotic biped recently developed by Lewis (cf. Presentation by A. Lewis). The use of co-activation damps foot contact and provides increased control of the limb movements generally.

3 Sensory feedback

3.1 Resetting the step cycle

For all CPGs there is one or more critical feedback cue that triggers or resets a cycle period. This mechanism serves to adapt the cycle to the needs of the

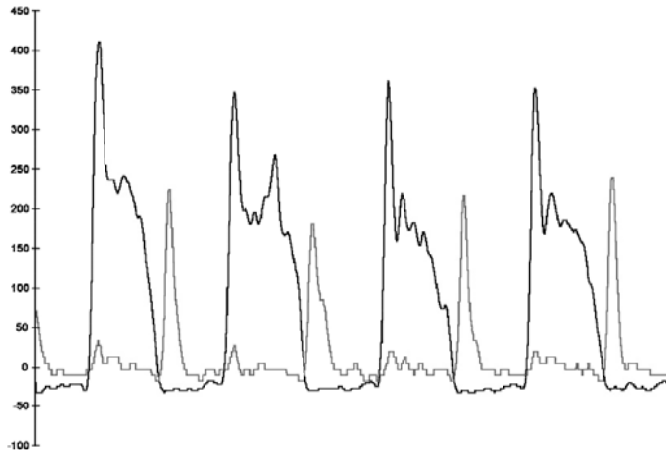


Fig. 5. Co-activation seen in functionally isolated spinal cord of the cat
Recordings from flexor and extensor muscle nerves in a paralyzed cat with its spinal cord cut. Notice the flexors have a low level of activity during the phase of the cycle that extensors are active. Data from J-P. Gossard.

animal under all environmental situations. Phenomenologically, the sensory feedback entrains the locomotor cycle [20]. In cats, it's been shown that several different muscles of the hindlimb can serve this purpose [19] (figure 6). In lampreys, stretch receptors located along the edges of the spinal cord itself serve this purpose. By bending the spinal cord directly, the stretch sensors can entrain the rhythm of the isolated spinal cord [21, 22].

In a biped with passive knees designed by Lewis and controlled by the analog VLSI chip of Etienne-Cummings, an angle sensor of the hip maintained the limbs adaptively while walking on a treadmill. The chip was designed explicitly with a bias to prevent the biped from maintaining itself centered on the moving belt. Thus, with no sensors, the joint angles drift, while with the sensors on, they remain within a relatively stable range of values (figure 7). Through the use of the sensory feedback the biped attained a steady and stable gait [15].

Another example of this form of limb control in a robot is seen in Tekken, the robot developed by H. Kimura and his colleagues [16]. Control of Tekken uses feedback from the limb to create mutual entrainment of the limb and the oscillator that controls it. The success of this kind of dynamic control is seen in the movies of Tekken (cf. H. Kimura presentation), as it walks up and down inclines and over irregular terrain.

3.2 Phase dependent corrections

To guarantee that movement is properly integrated with the environment, all sensory feedback is adaptively gated through the CPG. This means that

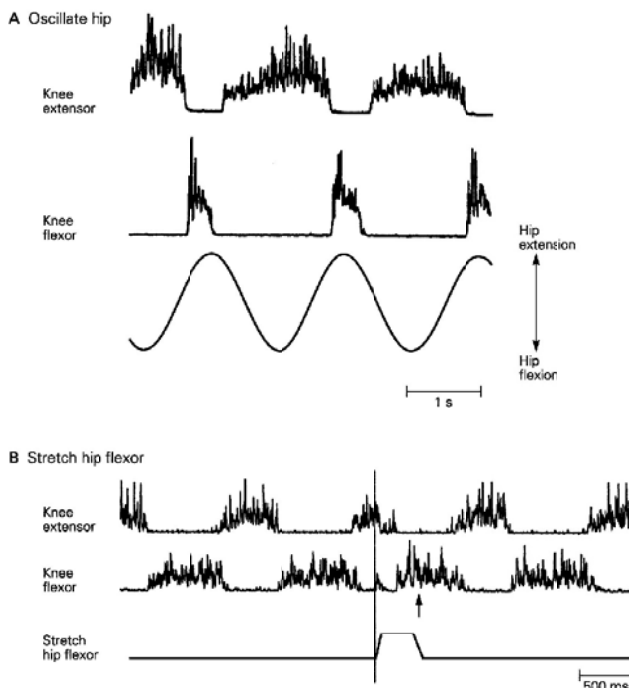


Fig. 6. Hip joint entrains rhythm

Illustration of the entrainment of the CPG with sensory feedback (above) and the resetting of the step cycle (below): the recordings are integrated traces of muscle potentials recorded from a spinal cat. The feedback is stretch of hip muscle. Adapted from ref 4, with data from ref 19.

corrections for perturbations of the limb are gated through the CPG during any form of locomotion. Reflexes that during rest are simple short latency responses of selective muscles, become more complex responses during locomotion. For example, the response to a perturbation to the walking limb will depend on the phase of the cycle during which it occurs. The simple reflex response to a painful stimulus applied to the bottom of the foot is withdrawal through activation of the flexors. However, if one limb is already off the ground when such a stimulus is given to the opposite limb that is in extension, the perturbed limb does not withdraw from the stimulus. Rather, the foot is driven harder onto the stimulus as a result of extensor activity [23], and the opposite limb is moved rapidly down to provide support. However, if the same stimulus is given while the foot is in its flexion phase, the flexors are, indeed, activated. Thus, the response adaptively adjusts to the phase of the step cycle.

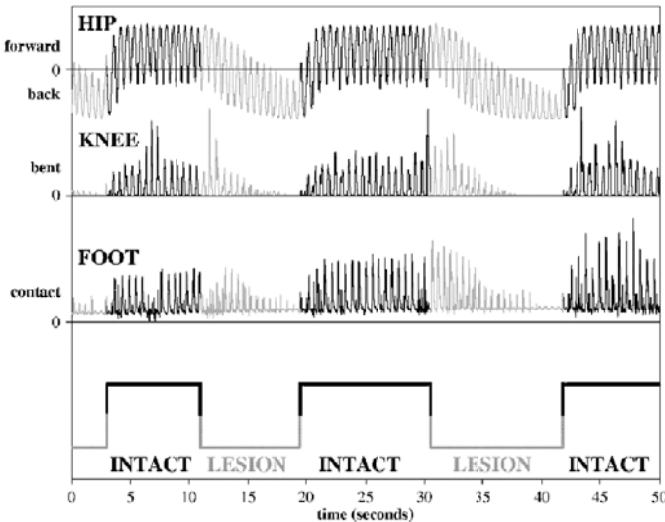


Fig. 7. Biped joint angles with and without feedback

Joint angles with and without sensory feedback to reset the CPG chip: the dark lines indicate the joint angles when the feedback is on; the light lines when the feedback is off. Note how the angles drift away from a steady state when the feedback is off. (from ref 15)

In all CPGs, the same gating of reflexes is seen [24]. The response to a stimulus is adaptively filtered through the CPG to produce a phase dependent response to perturbing stimuli. H. Kimura and his colleagues demonstrate that this principle can effectively be applied to a quadrupedal robot to produce stable walking even when subjected to unexpected perturbations [16]. Cf. Kimura's presentation for dynamic integration of sensory feedback to step over obstacles and over irregular terrain.

3.3 Smart sensors – muscle stretch receptors

The typical stretch receptors for mammalian muscles, also offer potential for robotics. These receptors are part of complex structure called the spindle organ (cf. Ref 4 for overview and references). The stretch receptor itself is embedded in a small muscle fiber that is activated by specialized motor neurons (γ -motor neurons) in the spinal cord that are situated among the motor neurons (α motor neurons) that activate the force producing muscle fibers. The spindle's motor neurons are often separately controlled and serve as part of servo-control system that regulates the excitability of the force producing muscles. Such control produces the unexpected result that the spindle receptors of some muscles are most active when its respective force producing muscle is at its shortest, that is, during contraction. This pattern of activity,

while first shown in decerebrate animals has also been seen during locomotion of intact walking cats [25]. The reason for this counter-intuitive result, is that the activity of the spindle receptor neurons is responsible for activation of the motor neurons to the force producing muscles via synaptic connections of the spindle fibers directly upon the α -motor neurons. Thus, the spindle organs appear to be part of a servo-assist mechanism for the control of the force production in mammalian muscle. The output of the spindle stretch receptors is highly non-linear, as a consequence of the control exerted on the γ -motor neurons. In reference 25, there are mathematical models that can predict the firing pattern of the spindle organs when controlled by γ -motor neurons.

Importantly, a robotic spindle has been implemented and can replicate a great deal of the function of its biological counterpart[26]. Unfortunately, the robotic spindle has not yet been implemented with the activity patterns seen during mammalian locomotion. However, it would appear to contain the necessary structural complexity to produce the full range of behavior that has been documented to date.

It isn't clear that one needs or wants to include a full robotic implementation of the spindle in a robotic limb designed for walking. However, it's possible that one could use the control strategy of a non-linear control of force production for robotic actuators where the stretch receptors, in association with force receptors are used to control the activity of the actuators. Having some kind of complex non-linear control on the force production could potentially provide considerably more flexibility and sophistication in movement. Such a non-linear control strategy would not be the first order strategy, but could be a higher order improvement.

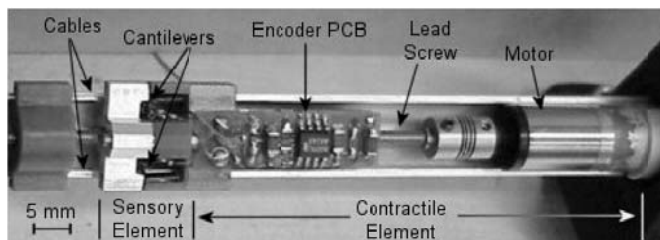


Fig. 8. Spindle implementation by Jaax and Hannaford[26]

4 Summary and conclusions

Presented here is an overview of some principles for control of locomotion that are seen in all animals and which offer ideas for robotic design and control. The intention of the overview is to suggest new ways to think about

and to perhaps design legged machines taking inspiration and guidance from biology. Biological systems have had eons to find and develop optimal methods for control. An animal dies that fails to escape its enemies effectively because of a failure of its locomotor control system. The only control principles for locomotion that are seen universally are those that do allow animals to escape and procreate. Examples are given in which the principles have been applied successfully to limbed robots. The application of the biological principles makes the implementation of the robotic locomotion remarkably smooth and adaptive to most conditions including irregular terrain and random perturbations. Kimura's dynamic integration of sensory input with a limit cycle oscillator provides an example of a robotic system that puts all the pieces together. The movement of Tekken speaks for itself.

Additional suggestions are also provided for potential new approaches that one might consider for legged robots. These suggestions come from less universal features of motor control, but features that nonetheless may offer novel perspectives. The use of co-activation of actuators acting across a single joint, and complex non-linear integration of sensory feedback could offer more flexibility and optimality in both bipedal and quadrupedal machines.

References

1. Garcia, M., Chatterjee, A., Ruina, A., 1998, The simplest walking model: stability, complexity, and scaling, *J. of Biomechanical Eng.*, 120:281-288
2. Grillner S, Wallén P. 1985 Central pattern generators for locomotion, with special reference to vertebrates. *Ann. Rev. Neurosci.* 8:233-61
3. Delcomyn F. 1980 Neural basis of rhythmic behavior in animals. *Science*. 210:492-498.
4. E.R. Kandel, J.H. Schwartz, T.M. Jessell, (Eds.) *Principles of Neural Science*, McGraw-Hill/Appleton & Lange; 4th edition, 2000
5. Cazalets JR, Borde M, Clarac F. 1995 Localization and organization of the central pattern generator for hindlimb locomotion in newborn rat. *J. Neurosci.* 15:4943-4951
6. Cohen, A.H., 1988, Evolution of the vertebrate central pattern generator for locomotion. In: Cohen, AH, Rossignol, S, Grillner, S (eds) *Neural control of rhythmic movements in vertebrates*. Wiley, New York Chichester Brisbane, pp. 129-166.
7. Williams T.L., Bowtell, G., Carling, J.C., Sigvardt, K.A., and Curtin, N.A., 1995, Interactions between muscle activation, body curvature and the water in the swimming lamprey. *Symp Soc Exp Biol* 49:49-59
8. Mellen, N., Kiemel, T, and Cohen A.H. 1995 Correlational analysis of fictive swimming in the lamprey reveals strong functional intersegmental coupling. *J Neurophysiol* 73:1020-30
9. Cohen, A.H., Wallén, P. 1980 The neuronal correlate of locomotion in fish. "Fictive swimming" induced in an *in vitro* preparation of the lamprey spinal cord. *Exp Brain Res.* 41:11-8.
10. Cohen, A. H. 1987a. Effects of oscillator frequency on phase-locking in the lamprey central pattern generator. *J. Neurosci. Meth.* **21**: 113-125.

11. Miller, W.L., Sigvardt, K.A. 2000 Extent and role of multisegmental coupling in the Lamprey spinal locomotor pattern generator. *J Neurophysiol* 83:465-76
12. Cohen, A. H. 1987b. Intersegmental coordinating system of the lamprey central pattern generator for locomotion. *J. Comp. Physiol.* **160**: 181-193.
13. Cohen, A. H., Holmes, P. J. and Rand, R. H. 1982. The nature of the coupling between segmental oscillators of the lamprey spinal generator for locomotion: A mathematical model. *J. Math. Biol.* **13**: 345-369.
14. N. Kopell and G.B. Ermentrout, 1986 Symmetry and phaselocking in chains of weakly coupled oscillators. *Comm. Pure Appl. Math.*, 39:623-660.
15. Lewis, M. A., Etienne-Cummings, R., Hartmann, M.J., Xu, Z. R. and Cohen, A.H. 2003 An in silico central pattern generator: silicon oscillator, coupling, entrainment, and physical computation, *Biol. Cybern.* 88 2, 137-151
16. Fukuoka, Y., Kimura, H., and Cohen, A.H. 2003, Adaptive Dynamic Walking of a Quadruped Robot on Irregular Terrain based on Biological Concepts, *Int. J. Robotics Res.* 22:187-202
17. Engberg, I., Lundberg, A. 1969, An electromyographic analysis of muscular activity in the hindlimb of the cat during unrestrained locomotion. *Acta Physiol Scand* 75:614-630
18. D. Boothe and A.H. Cohen, submitted, Models of the locomotor central pattern generator that achieve coactivation and alternation
19. Hiebert, G.W., Whelan, P.J., Prochazka, A., Pearson, K.G. 1996 Contribution of hind limb flexor muscle afferents to the timing of phase transitions in the cat step cycle. *J Neurophysiol* 75:1126-37
20. Andersson, O., Grillner, S. 1983 Peripheral control of the cat's step cycle. II. Entrainment of the central pattern generators for locomotion by sinusoidal hip movements during "fictive locomotion." . *Acta Physiol Scand* 118:229-39
21. S. Grillner, A. McClellan, and C. Perret. 1981 Entrainment of the spinal pattern generators for swimming by mechanosensitive elements in the lamprey spinal cord in vitro. *Brain Res.*, 217:380-386.
22. McClellan, A.D., Sigvardt, K.A. 1988 Features of entrainment of spinal pattern generators for locomotor activity in the lamprey spinal cord. *J Neurosci*. 8:133-45.
23. Forssberg H. 1979 Stumbling corrective reaction: a phase-dependent compensatory reaction during locomotion. *J. Neurophysiol.* 42:936-53.
24. Rossignol et al. chapter 1988 In: Cohen, AH, Rossignol, S, Grillner, S (eds) Neural control of rhythmic movements in vertebrates. Wiley, New York Chichester Brisbane, pp.
25. Prochazka, A, Gorassini, M. 1998 Ensemble firing of muscle afferents recorded during normal locomotion in cats. *J. Physiol.* 507:293-304
26. K.N. Jaax and B. Hannaford 2002 A Biorobotic Structural Model of the Mammalian Muscle Spindle Primary Afferent Response. *Ann. Biomed. Eng.* Vol. 30, pp. 84-96

Higher Nervous Control of Quadrupedal vs Bipedal Locomotion in Non-human Primates; Common and Specific Properties

Shigemi Mori, Futoshi Mori and Katsumi Nakajima

National Institute for Physiological Sciences, Okazaki, Aichi 444-8585, Japan

Abstract. Bipedal (Bp) terrestrial locomotion is a routine, everyday activity for humans and advanced non-human primates. While its elaboration seems simple, it actually involves much skill and long-term locomotor learning, such that the CNS can achieve a seamless spatial and temporal integration of multiple motor segments. To advance understanding of the CNS control mechanisms that operate during Bp locomotion, it seemed necessary to make use of a non-human primate model. This strategy invites the possibility of employing state-of-the-art interventional recording techniques and cellular-to-systems level of neuroscientific analysis to the study of locomotion. We think that the study of posture and locomotion is fundamental to the understanding of basic brain-behavior relationships from the cellular to the behavioral level of analysis. To this end, we used operant conditioning to train the normally quadrupedal (Qp)-walking juvenile Japanese monkey (*M. fuscata*) to stand upright and walk bipedally on the surface of a moving treadmill belt. Our *M. fuscata* studies have started to reveal brain mechanisms involved in the successful emergence and elaboration of Bp locomotion.

1 Introduction

We acquire the novel capability of walking bipedally according to a genetically designed program. Based on this program, we develop postnatally our musculoskeletal system and its control system so as to elaborate bipedal (Bp) standing and Bp walking [1]. The musculoskeletal system comprises multiple motor or movement segments such as head, neck, trunk, fore- and hind-limbs, each segment having a number of degrees of freedom. The control system is the central nervous system (CNS) comprised of the cerebrum, basal ganglia, cerebellum, brainstem and spinal cord [2]. Neural circuits functionally uniting them also develop postnatally with maturation of individual CNS components. Motor segments are innervated by spinal motoneurons (MNs) which are referred to as the “final common path” because most command motor signals descending from supraspinal structures, and ascending signals arising from the motor segments, converge on them [3]. Thus, the MNs integrate all the descending and ascending signals and send final motor outputs to the skeletal muscles of motor segments.

Previous studies have shown that the brainstem and spinal cord are equipped with neuronal structures that can subserve a variety of postural

reflexes and fundamental movements [2,4]. From a phylogenetical point of view, the motor pathways descending from the brainstem to the spinal cord are the earliest developing ones [5]. In contrast, the motor cortices establish functional connections postnatally first with the cervical MNs innervating the fore-limbs and then the lumbar MNs innervating the hind-limbs. In the macaque monkey, full myelination (maturation) of corticospinal axons in the spinal cord occurs at around 36 months of age [6]. Such a rostrocaudal development of cortico-motoneuronal (CM) connections is well reflected in the postnatal developmental pattern of posture and movements in both the human [1] and non-human primates [7]. In parallel with the growth of the musculoskeletal system and the CNS, locomotor learning from daily practice and experience is necessary for the acquisition of the skill of Bp locomotion. Locomotor practice and experience help the development of CM connections to distally located muscles of the foot, and build up and storage of ‘locomotor memory’ and/or reference centers [2,8].

To advance understanding of CNS control of Bp standing and Bp walking, we have been analyzing the unrestrained normal quadrupedal (Qp) and operantly-trained Bp locomotor behavior of a non-human primate, the Japanese monkey, *M. fuscata* [9-13]. Japanese monkeys are originally Qp, but with long-term locomotor training, they acquire the novel strategy of walking bipedally on the surface of a moving treadmill belt. To describe the functional significance of our findings, the present report addresses four major aspects relating to the elaboration of Bp locomotion: (a) our concept of locomotor control CNS mechanisms including anticipatory and reactive control mechanisms, (b) emergence, acquisition and refinement of Bp locomotion in juvenile Japanese monkeys, and integration of posture and locomotion (c) common and different control properties of Qp and Bp locomotion, and (d) similarity and difference in the kinematics of lower limbs during Bp walking in our monkey model and in the human. The last section addresses a future perspective for understanding “brain-locomotor behavior” relationships.

2 Locomotor control CNS mechanisms including anticipatory and reactive control mechanisms

We have recently proposed a new concept of CNS mechanisms related to locomotor control [2]. As shown conceptually in Figure 1, we hypothesize that descending commands from the cognitive and emotive portions of the higher CNS, and activity of both locomotion evoking centers and posture control centers are constantly compared with that of the reference centers, with their collective output sent to the integration centers. Such a system incorporates both anticipatory and reactive control processes [14]. Critical components of the reference centers are the postural and locomotor memory that is built up by daily walking practice and experience. Its other component includes the postural body scheme or the reference frame of bodily configuration essential

for Bp locomotion [2,15]. The integration centers participate in a comparative function: comparing top-down locomotor command feedforward signals with bottom-up feedback signals revealing the current state of locomotion, and minimizing impairments of posture and locomotion. The integration center's efferent output is distributed by way of executing centers. The latter's concern is that motor signals must be sent to a number of different muscle control systems such that the multiple motor segments they control are activated in a coordinated manner.

Major elements of motor control units are 'interneuronal circuits including the central pattern generator (CPG)', spinal MN columns and motor segments [2,16]. Output signals arising from the execution centers are carried to the spinal cord by the phylogenetically old reticulospinal (RS) and vestibulospinal (VS) pathways, and ensure that appropriate and timely forces are applied to relevant limb joints, the result being a smooth execution of locomotion, with correctly phased limb movements and adequate levels of postural muscle tone [2,4]. Output signals arising from the higher CNS, such as the primary motor area (M1) and supplementary motor area (SMA), are also carried to the MNs of motor control units by way of phylogenetically recent corticospinal and cortico-reticulospinal pathways, and contribute to the refinement of limb movements such as to avoid obstacles on the walking path [2].

During Bp standing and Bp walking, changes in body configuration are first registered by both the labyrinthine and proprioceptive receptors embedded in the motor segments. Changes in the external world are perceived by telereceptors, such as the eyes and ears [3]. By continuous reception and processing of multi-modal interoceptive and exteroceptive afferent inputs, the integration centers can compare the body's moment-to-moment configuration relative to the immediate and distant environment. When both quadrupeds and bipeds encounter unexpected obstacles, they adopt preparatory or anticipatory postures to avoid them. When they fail to clear the obstacles, they take reactive and/or defensive postures to minimize and compensate for the impairments to ongoing locomotion [14]. The central feedback from the integration center combined with peripheral feedback at the cerebral cortical level enables the animal conscious perception of its kinesthetic aspects of volitional (anticipatory) and automatic (reactive) adjustments to locomotion [2]. Anticipatory control mechanisms are probably stored at a high CNS levels such as the visual cortex, SMA and M1 and interconnecting networks, whereas reactive control mechanisms are probably stored at low CNS levels such as the cerebellum, brainstem and spinal cord and interconnecting networks [2].

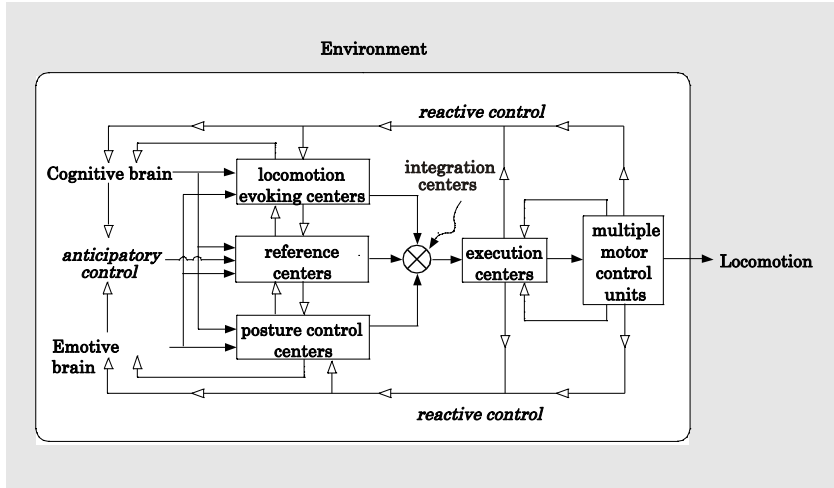


Fig. 1. A conceptualization of the overall integrated control of posture and locomotion including anticipatory and reactive control. From the left to right, the CNS structures and their proposed processes include: cognitive processing, emotive processing, locomotion evoking centers, posture control centers, reference centers, integration centers, execution centers, and multiple motor control units. Open and closed arrowheads represent the ascending and descending flow of signals. Modified from reference [2].

3 Emergence, acquisition and refinement of Bp locomotion in Juvenile Japanese monkeys

Genetically Qp young Japanese monkey, *M. fuscata*, can acquire a novel capability of Bp walking on the surface of a moving treadmill belt [13]. The operant-conditioning methods with which monkey learned to walk quadrupedally and/or bipedally are described in detail elsewhere [10, 12]. After sufficient physical growth and locomotor learning (12 to 24 months), young monkeys (estimated age: 1.6 to 2.4 years) gradually acquired a more upright and a more stable posture, a more stable (less variable) cyclic patterns of joint angles in the lower limbs and coupling among the neighboring joints, and also faster speeds of Bp walking [13]. It was also found that stability of kinematic patterns developed in a rostro-caudal direction, i.e. in the same direction as observed in developing human infants [1]. Our findings demonstrated for the first time the basic principles of the developing monkey to integrate the neural and musculoskeletal mechanisms required for sufficient coordination of upper (head, neck, trunk) and lower (hind-limbs) motor segments so that Bp standing could be maintained and Bp walking elaborated.

Once the monkeys acquired Bp walking capability, they still could walk bipedally even after a few weeks of cessation of locomotor training. This suggests that the monkeys stored a postural body scheme or the reference

frame of bodily configuration necessary for Bp walking. We also found that the Qp walking monkey on the moving treadmill belt could right its posture and continue Bp locomotion [17]. The transition from Qp to Bp walking always began when the left (L) or right (R) hind-limb initiated a stance (ST) phase of the step. For example, at the time when the imaginary position of the monkey's center of body mass (CoM) projected to the supporting L hind-limb, the monkey began an upward excursion of the angle of the weight-bearing hip joint. The L forelimb was then freed from the constraints of weight bearing. With further upward excursion of the hip joint angle, the monkey started to right its posture and initiate reaching and grasping movements, extending the freed fore-limb forward to attain the reward and to eat it ad libitum. This suggests that the monkey's CNS can rapidly select and combine integrated subsets of posture- and locomotor-related neural control mechanisms appropriate for the elaboration of a required task. Our animal model thus provides a unique opportunity to compare the kinematics of Qp and Bp locomotion in a single animal.

During the transitional period from Qp to Bp locomotion, the monkey coordinated sequentially independent movements of multiple motor segments such as eyes, head, neck, trunk, fore and hind-limbs, in order to satisfy the dual purpose of freeing the forelimbs from the constraints of weight-bearing and adopting Bp walking. The locomotion conversion process involved the rapid and smooth succession of targeting, orienting, and righting. Targeting requires the coordinated activity of head, neck, trunk and fore-limbs, and righting that of head, neck, trunk and hind-limb. Kinematics of eye-head position, body axis, and major joint angles of the hind-limbs revealed the significance of a hip maneuver strategy for the monkey's conversion from stable Qp to similarly stable Bp locomotion [17]. Each of these processes includes visuo-motor and vestibulo-motor coordination. The latter is based on interactions of vestibular information with sensory information arising from SW and ST limbs and thus ensuring a good postural stability and postural orientation over a wide range of environmental condition [18]. It is conceivable that spinal reflexes play a crucial role in the coordination of SW and ST limbs. According to Zehr and Stein, generally cutaneous reflexes act to alter SW limb trajectory to avoid stumbling and falling. Stretch reflexes act to stabilize limb trajectory and assist force production during ST. Load receptor reflexes have an effect on both ST phase body weight support and step cycle timing [19].

We have previously proposed that the fastigial nucleus (FN) in the cerebellum is importantly involved in the initiation of Qp locomotion, and in addition in the rapid and smooth succession of targeting, orienting, and righting necessary for the conversion from Qp to Bp walking [2, 17]. In a high decerebrate cat, we have demonstrated that train-pulse microstimulation of the hook bundle of Russell at its midline (cerebellar locomotor region, CLR), through which the crossed fastigiofugal fibers pass, evokes Qp locomotion on

the surface of a moving treadmill belt [20,21]. Descending fastigiofugal fibers projecting contralaterally include fastigio-RS, fastigio-VS, fastigiospinal and fastigio-tecto-RS fibers [2]. In both cats [4,22] and monkeys [23,24], command signals related to righting and walking are mediated to the spinal cord by the RS and VS pathways. Command signals carried by fastigiospinal pathway contribute to the control of neck extensor muscles (targeting), whereas those carried by fastigio-tecto-RS pathway contribute to the coordinated control of head, neck, and body movements (orienting)[2]. Presumably, the command signals descend *in parallel* from a number of interconnected CNS regions, and the weighting function of each CNS site may vary depending on the external and internal requirements for the execution and purpose of locomotion.

It is important to note that the FN is under the control of the cerebellar vermis, to which visual, vestibular, proprioceptive and exteroceptive afferents converge [25,26]. In the FN, there is an additional group of cells, which project to the SMA and M1 via the fastigiothalamic projection [27]. These cells in the FN may conceivably participate even in the volitional control aspect of locomotion [2]. In Sherrington's classic 1906 monograph he described interactions between posture and movements as "*posture follows movements like a shadow*" [3]. *In parallel* command signals arising from the FN will certainly contribute to the control and integration of posture and locomotor-related neuronal subsystems in the CNS.

4 Common and different control properties of Qp and Bp locomotion

During monkey's Qp walking, there were periods in which the CoM was supported by either three or two diagonal limbs. At treadmill speeds of 0.4 and 0.7 m/s, for example, the body mass was supported by the L fore-limb, R hind-limb and R fore-limb when the monkey lifted the L hind-limb from the treadmill belt initiating the 'swing (SW) phase'. At treadmill speeds of 1.0 and 1.3m/s, the body mass was supported mainly by the fore- and hindlimbs on a diagonal axis. During this period, the two other diagonal limbs were often lifted from the treadmill surface and were in 'SW phase'. With an increase in treadmill speed, the period of double support phase (ST phase) by the diagonal limbs was shortened so that these two limbs promptly initiated the next SW phase. In addition, the monkey considerably increased 'stride length' of the fore- and hind-limbs by increasing 'mobile ranges' of hip joint angle. Such changes in the stride length were accompanied by marked dorsi- and plantar flexion of fore- and hind-limb' toes during SW and ST phases, respectively [28].

As during the human Bp walking, *M. fuscata* showed Bp walking characterized by double and/or single support phases of the L and R hind-limbs. During the SW phase of the L hind-limb, the weight of the body mass was fully supported by the R hind-limb alone (single support phase). The stance

R hind-limb soon became the swing limb. However, ‘stride length’ of the Bp hind-limbs was considerably shorter than that of Qp hind-limbs due to kinematic reconfigurations of the hind-limbs, presumably related to biomechanical constraints of Bp standing. These included smaller mobile ranges of the hip and ankle joints, and shorter ST phase. Interestingly, the profile of angular changes of the knee joint was similar for Qp and Bp locomotion, except for a slight change at the ST phase. At faster speed of Bp walking, the monkey inclined its body axis maximally during the period of double support phase. Marked dorsi- and plantar flexion of hind-limb toes were also observed during SW and ST phases, respectively [28].

The SW and ST phases and step cycle frequency are interactive parameters during Bp walking in the human [29]. In two adult monkeys, we compared the changes in these interactive parameters during Qp and Bp walking as the treadmill speeds were increased from 0.4 to 1.5 m/s. As forward speed increased from 0.4 to 1.5 m/s, the average duration of the ST phase for the two animals during Qp locomotion reduced from ~0.9 to ~0.4s, whereas the SW phase remained at ~0.3 s. The associated increase in step cycle frequency was ~0.9 to 1.5 Hz. During Bp locomotion, the corresponding changes were: ST phase, 0.7 to 0.3; SW phase, constant at ~0.2 s; and step cycle frequency, ~1.1 to ~2.0 Hz. These results show that *M. fuscata* increased the speed of its trained Bp locomotion by an increase in the stepping frequency of the hind-limbs whereas it increased the speed of its Qp locomotion by an increase in the total excursion distance of the fore- and hind-limbs. Similar changes in these interactive parameters suggest that our monkeys used the same overall CNS strategy for both Qp and Bp locomotion.

5 Similarity and difference in the kinematics of lower limbs during Bp walking between our monkey model and the human

The bipedal striding gait is uniquely human, and is a most efficient way of moving overground [30]. With Bp walking overground, there is a heel-strike at start of the ST phase and push-off by the big toe at the end. The hip joint extends steadily from approximately 160° at initial foot contact to approximately 180° at the end of the ST phase, whereas the knee joint shows initial flexion (~20°) and extension (~15°) at mid-ST phase followed by major flexion (~45°) at the latter half of this phase. The mobile ranges of the hip and knee joints were estimated to be approximately 50° and 70°, respectively [31]. In five species of non-human primates (chimpanzee, gibbon, baboon, Japanese macaques and spider monkey) walking overground, Okada found that, at foot contact, the joint angles of hip and knee operated in mobile ranges far from a completely stretched position (i.e., 180°) [32]. Hip extension was delayed until the latter half of the ST phase, and the knee joint flexed steadily from the beginning to the end of this phase. All the

non-human primates excepting the spider monkeys walked with a bent-hip, bent-knee posture.

From the above findings, Okada suggested that the propulsive force which carries the CoM forward is contributed largely by the movement of hip joint during human Bp walking, whereas the knee joint has this function in the non-trained, non-human primates [32]. In our trained adult monkey, the Bp walking pattern was quite different from the “bent-hip, bent-knee” walking pattern. We have not observed, however, a heel-strike at the start of ST phase but we found push-off by the toes, probably including the big toe, at the end of this phase. During Bp walking, the mobile ranges of hip and knee joints were approximately 50° ($\sim 120^\circ$ – $\sim 170^\circ$) and 60° ($\sim 95^\circ$ – $\sim 155^\circ$), respectively. The general pattern of hip extension and flexion was comparable to the pattern in Bp walking humans. It was also noteworthy that at mid-ST phase, knee joint angle changed from a decrease (flexion) to an increase (extension). This flexion and extension pattern was also comparable to that in humans. Our results suggest that, for Bp walking, *M. fuscata* acquired a new hip and ankle joint motion appropriate for the generation of propulsive force in a fashion similar to that of the human.

Our suggestion has been reinforced by results related to anticipatory and reactive control of Bp locomotion in the human [33,34]. To study the anticipatory and reactive control capabilities of Bp walking monkey, it was necessary to elicit walking on the treadmill belt on which a rectangular block was attached as an obstacle (block height: 3, 5 or 7 cm) (14 and F Mori et al., in this volume). We have found that the monkey cleared the obstacle with larger than usual flexion of hip and knee joints so that the trailing hind-limb produced enough clearance space over the obstacle while the leading limb alone supported the weight of the body mass. Even before encountering the obstacle, the monkey adopted this “hip and knee flexion strategy” indicating the recruitment of “anticipatory control mechanisms”. The observed “hip and knee flexion strategy” in the monkey was essentially the same as that in the human [33]. When it failed to clear the obstacle, the monkey adopted a defensive posture to compensate for the perturbed posture, indicating the recruitment of “reactive control mechanisms”.

6 Summary and discussion

In the study of Qp and Bp locomotion of non-human primates, most previous studies were by anthropologists and biologists seeking to elucidate their kinematics and the relationships between morphology and species-specific locomotor behavior. Recently, D'Août et al., studied kinesiological features of bonobo (*Pan paniscus*) walking, the extant great apes, because of their phylogenetical and morphological similarities with early hominids [35]. They compared spatio-temporal characteristics of natural Bp and Qp walking over-ground, especially of hind-limb joint movements, and found that they differ

strongly from the human patterns as characterized by “bent-hip, bent-knee” walking. In relation to the heel, they found it was being lifted relative to the toe tips throughout ST phase.

The control mechanisms of Bp human locomotion have been the subject of studies since Marey’s first study in 1894 [36]. A series of photograph was taken of human Bp walking by Muybridge [37]. Bernstein depicted stick figures of body movements from such photographs [38]. Herman et al. measured angular displacement of the hip, knee and ankle joints during human Bp walking and revealed a precise spatio-temporal ordering between them [29]. Nilsson and Thorstensson recorded three orthogonal ground reaction force components in the weight bearing limbs during Bp walking and running, and found complex interaction between the vertical and horizontal forces needed for propulsion and equilibrium [39]. Patla studied and discussed the importance of visual information for “avoidance strategies” and “accommodation strategies” related to planning and execution of changes in gait patterns when safe travel is threatened [34]. For six species of anthropoid primates including the human, Yamazaki calculated muscular forces acting at the joints during Bp walking using computer simulation [40]. Using SPECT (Single Photon Emission Computed Tomography), Fukuyama et al. identified several brain regions where activity increased during Bp walking in human [41].

The change from Qp walking to Bp walking must have required a redesign of the CNS along with reconfiguration of the musculoskeletal system. In Eccles’s 1989 monograph he mentioned that much of the evolution from the simpler mammalian brains had already been accomplished in the higher primates [30]. From an evolutionary point of view, he also summarized several anatomical changes specific to humans. These included elongation of the hind-limb relative to the fore-limb; shortening and broadening of the pelvis; reshaping of the foot; a forward curvature of the vertebral column in the lumbar region (lordosis) with a forward rotation of the iliac portion of the pelvis. The movements of human Bp walking based on such anatomical changes clearly demonstrate that there had been a transformation in the operation of the neural machinery of the brain, but far fewer studies have been undertaken from a movement neuroscience perspective, and our knowledge of the neuronal machinery involved in Bp standing and/or Bp walking, and causal relationships between CNS activity and the control mode of the multiple motor segments is still inadequate.

Our group’s long-term goal is to elucidate CNS mechanisms in the non-human primate that contribute to the control of Bp standing and Bp walking, and especially of the adaptability of locomotor movements to meet the environmental demands. This adaptability is one of the most important characteristics of human Bp walking [34]. In this model animal, non-invasive studies of the CNS and functional inactivation are feasible. Our preliminary study using PET (Positron Emission Tomography) has already revealed that the activity of the M1, SMA, visual cortex and the cerebellum increased in par-

allel, with some intriguing differences noted between Bp and Qp walking [42]. Inactivation of the M1 [43] and SMA by microinjection of muscimol into each area [44] also resulted, respectively, in focal and general impairments of the Bp standing and Bp walking. With the newly developed Bp walking monkey model, we are now at the beginning of a long-term investigation to compare and extrapolate such discovered mechanisms to those that might operate in the human. We plan to continue such investigations on *M. fuscata*, in the hope that our multi-disciplinary approach will help understanding “brain-locomotor behavior” relationships by providing definitive information about the role and operation of higher CNS structure in the integrated control of Bp standing and Bp walking. Within this spectrum of experimental approaches, there is a clear and important role for approaches that feature use of the theory, modeling/simulation and techniques of system neuroscience.

Acknowledgments

The author expresses sincere appreciation to Dr. Edger Garcia-Rill for his critical review and to Dr. D.G. Stuart for his editing of the original version of this manuscript. This study was supported by: a Grant-in Aid for General Scientific Research to S.M., from the Ministry of Education, Science, Sports, Culture and Technology of Japan; and a Grant in Aid on Comprehensive Research on Aging and Health to S.M. from the Ministry of Health and Welfare of Japan.

References

1. McGraw, M. B. 1940. Neuromuscular development of the human infant as exemplified in the achievement of erect locomotion, *J. Pediatrics* 17:747–771.
2. Mori, S., Nakajima, K., Mori, F. 2003. Integration of multiple motor segments for the elaboration of locomotion: the role of fastigial nucleus of the cerebellum. *Brain Mechanisms for the Integration of Posture and Movement*. S. Mori, M. Wiesendanger and D.G. Stuart Eds, Elsevier, Amsterdam, pp. 335–345.
3. Sherrington, C. S. 1906. *The Integrative Action of the Nervous System*, Yale Univ. Press, Yale.
4. Mori, S. 1987. Integration of posture and locomotion in acute decerebrate cats and in awake, freely moving cats. *Prog. Neurobiol.* 26:161–195.
5. Brodal, A. 1981. *Neurological Anatomy in relation to Clinical Medicine*, Oxford Univ. Press, London.
6. Olivier, E., Edgley, S.A., Armand, J., and Lemon, R. 1997. An electrophysiological study of the postnatal development of the corticospinal system in the macaque monkey, *J. Neurosci.* 17:267–276.
7. Hildebrand, M., 1967. Symmetrical gaits of primates, *Am. J. Phys. Anthropol.* 26:119–130.
8. Brooks, V. B. 1986. *The Neural Basis of Motor Control*, Oxford Univ. Press. Oxford.

9. Mori, S., Miyashita, E., Nakajima, K., and Asanome, M. 1996. Quadrupedal locomotor movements in monkeys (*M. fuscata*) on a treadmill: kinematic analyses, *Neuroreport* 7:2277–2285.
10. Mori, S., Matsuyama, K., Miyashita, E., Nakajima, K., and Asanome, M. 1996. Basic neurophysiology of primate locomotion, *Folia Primatol.* 66:192–203.
11. Mori, F., Nakajima, K., Gantchev, N., Matsuyama, K., and Mori, S. 1999. A new model for the study of the neurobiology of bipedal locomotion: The Japanese monkey, *M. fuscata*. *From Basic Motor Control to Functional Recovery*, N. Gantchev and G.N. Gantchev Eds, Academic Publishing House, Sofia, pp. 47–51.
12. Mori, F., Tachibana, A., Takasu, C., Nakajima, K., and Mori, S. 2001. Bipedal locomotion by the normally quadrupedal Japanese monkey, *M. fuscata*: Strategies for obstacle clearance and recovery from stumbling, *Acta Physiol. Pharmacol. Bulg.* 26:147–150.
13. Tachibana, A., Mori, F., Boliek, C. A., Nakajima, K., Takasu, C., and Mori, S. 2003. Acquisition of operant-trained bipedal locomotion in juvenile Japanese monkeys (*Macaca fuscata*): a longitudinal study, *Motor Control* 7: 395–420.
14. Mori, F., Nakajima, K., Tachibana, A., Takasu, C., Mori, M., Tsujimoto, T., Tsukada, H., and Mori, S. 2003. Reactive and anticipatory control of posture and bipedal locomotion in a non-human primate. *Brain Mechanisms for the integration of Posture and Movement*, S. Mori, M. Wiesendanger and D.G. Stuart Eds, Elsevier, Amsterdam, pp. 191–198.
15. Massion, J. 1992. Movement, posture and equilibrium: interaction and coordination, *Prog. Neurobiol.* 38:35–56.
16. Grillner, S. 2003. The motor infrastructure: from ion channels to neuronal network. *Nature Rev. Neurosci.* 4:573–586.
17. Nakajima, K., Mori, F., Takasu, C., Tachibana, A., Okumura, T., Mori, M., and Mori, S. 2001. Integration of upright posture and bipedal locomotion in non-human primates. *Sensorimotor Control*, R. Dengler and A.R. Kossev Eds, IOS Press, Amsterdam, pp. 95–102.
18. Horak, F.B., Mirka, A., and Shupert, C.L. 1989. The role of peripheral vestibular disorders in postural dyscontrol in the elderly. *The Development of posture and gait across the lifespan*, A. Woollacott and A. Shumway-Cook Eds. Univ. of South Carolina Press, Columbia. pp. 253–279.
19. Zehr,E.P., and Stein, R.B. 1999. What functions do reflexes serve during human locomotion? *Prog. Neurobiol.* 58:185–205.
20. Mori, S., Matsui, T., Kuze, B., Asanome, M., Nakajima, K., and Matsuyama, K. 1999. Stimulation of a restricted region in the midline cerebellar white matter evokes coordinated quadrupedal locomotion in the decerebrate cat. *J. Neurophysiol.* 82:290–300.
21. Mori, S., Matsui, T., Mori, F., Nakajima,, K., and Matsuyama, K. 2000. Instigation and control of treadmill locomotion in high decerebrate cats by stimulation of the hook bundle of Russell in the cerebellum, *Can. J. Physiol. Pharmacol.* 78:945–957.
22. Shik, M.L., and Orlovsky, G.N. 1976. Neurophysiology of locomotor automation. *Physiol. Rev.* 56: 465–501.
23. Lawrence, D. G., and Kuypers, H. G. J. M. 1968. The functional organization of the motor system in the monkey. I. The effects of bilateral pyramidal tract lesion. *Brain* 91:1–14.

24. Lawrence, D. G., and Kuypers, H. G. J. M. 1968. The functional organization of the motor system in the monkey. II. The effects of lesions of the descending brain-stem pathways. *Brain* 91:15–36
25. Arshavsky, Y. I., Gelfand, I. M., and Orlovsky, G. N. 1986. *Cerebellum and Rhythmic Movements*. Springer-Verlag. Berlin.
26. Armstrong, D. M. 1986. Supraspinal contribution to the initiation and control of locomotion in the cat. *Prog. Neurobiol.* 26:273–361.
27. Steriade, M. 1995. Two channels in the cerebellothalamicocortical system. *J. Comp. Neurol.* 354:57–70.
28. Nakajima, k., Mori, F., Takasu, C., Mori, M., Matsuyama, K., and Mori, S. 2003 Biomechanical constraints in hindlimb joints during the quadrupedal vs. bipedal locomotion of *M. fuscata*. *Brain Mechanisms for the Integration of Posture and Movement*. S. Mori, M. Wiesendanger and D.G. Stuart Eds, Elsevier, Amsterdam. pp. 183–190.
29. Herman, R. M., Wirta, R., Bampton, S., and Finley, F. R. 1976. Human solutions for locomotion. I. Single limb analysis. *Neural Control of Locomotion, Advances in Behavioral Biology* 18, R.M. Herman, S. Grillner, P.S.G. Stein and D.G. Stuart Eds, Plenum Press, New York, pp.13–49.
30. Eccles, J. C. 1989. *Evolution of the Brain: Creation of the Self*, Routledge, London and New York.
31. Kondo, S. 1985. *Locomotor Analyses and human Bipedalism*, Tokyo Univ. Press, Tokyo.
32. Okada, M. 1985. Primate bipedal walking: Comparative kinematics. *Primate Morphophysiology, Locomotor Analyses and human Bipedalism*, S. Kondo Ed, Tokyo Univ. Press, Tokyo, pp. 47–58.
33. McFadyen, B. J., and Winter, D. A. 1991. Anticipatory locomotor adjustments during obstructed human walking, *Neurosci. Res. Commun.* 9:37–44.
34. Patla, A. E. 1991, Visual control of human locomotion. *Adaptability of Human Gait*, A.E. Patla Ed, Elsevier Science Publishers B.V. North-Holland. pp. 55–97.
35. D'Août, K., Aerts, P., De Clercq, D., De Meester, K., and Van Elsacker, L. 2002. Segment and joint angles of hind limb during bipedal and quadrupedal walking of the Bonobo (*Pan paniscus*). *Am. J. Physical Anthropol.* 119:37–51.
36. Marey, E. J. 1894. *Le Movement*, G. Masson, Paris.
37. Muybridge, E. 1957. *Animals in Motion*, Dover, New York.
38. Bernstein, N. 1967. *The Co-ordination and Regulation of Movements*. Pergamon Press. Oxford.
39. Nilsson, J., and Thorstensson, A. 1989. Ground reaction forces at different speeds of human walking and running, *Acta Physiol. Scan.* 136:217–227.
40. Yamazaki, N. 1985. Primate bipedal walking: Computer simulation. *Primate Morphophysiology, Locomotor Analyses and human Bipedalism*, S. Kondo Ed, Tokyo Univ. Press. Tokyo, pp. 105–130.
41. Fukuyama, H., Ouchi, Y., Matsuzaki, S., Nagahama, Y., Yamauchi, H., Ogawa, M., Kimura, J., and Shibasaki, H. 1997. Brain functional activity during gait in normal subject: a SPECT study. *Neurosci. Lett.* 228:183–186.
42. Mori, F., Nakajima, K., Tachibana, A., et al., 2002. “High-order CNS control mechanisms during bipedal locomotion in the Japanese monkey,” Program No. 854.9, *Abstract Viewer/Itinerary Planner, Washington, DC: Society for Neuroscience, CD-ROM*

43. Nakajima, K., Mori, F., Tachibana, A., Nambu, A., and Mori, S. 2003. Cortical mechanisms for the control of bipedal locomotion in Japanese monkeys: I. Local inactivation of the primary motor cortex (M1). *Neurosci. Res.* 46(suppl. 1):S156.
44. Mori, F., Nakajima, K., Tachibana, A., Nambu, A., and Mori, S. 2003. Cortical mechanisms for the control of bipedal locomotion in Japanese monkeys: II. Local inactivation of the supplementary motor area (SMA). *Neurosci. Res.* 46(suppl. 1):S157.

Part 2

Adaptive Mechanics

Interactions between Motions of the Trunk and the Angle of Attack of the Forelimbs in Synchronous Gaits of the Pika (*Ochotona rufescens*)

Remi Hackert¹, Hartmut Witte^{1,2} and Martin S. Fischer¹

¹ Institut für Spezielle Zoologie und Evolutionsbiologie,
Friedrich-Schiller-Universität Jena, Erbertstraße 1, D-07743 Jena, Germany,
Remi.Hackert@animals-in-motion.com

² Fachgebiet Biomechatronik, Technische Universität Ilmenau, Pf 100565,
D-98684 Ilmenau, Hartmut.Witte@tu-ilmenau.de

Abstract. During half-bound gait on a treadmill pikas (*Ochotona rufescens*: Lagomorpha) show a preference in the choice of the trailing limb (“handedness”). Duration of steps shows significantly higher variation in the trailing limb than in the leading limb. This observation motivated calculations of the position of the center of mass (CoM) in the body frame of the pika during half-bound cycles. CoM is aligned with first of the ulna of the trailing and second of the leading limb during major parts of the forelimbs’ stance phase. Referring to our large cineradiographic data base on the kinematics of the legs we could note that the horizontal motion of the CoM in the body is mainly determined by flexion and extension of the back. This observation underlines the determinant role of the trunk as the main engine for fast locomotion. Using high-speed video films we measured the angle of attack (defined as the angle between the ulna and the ground at touch down). We couldn’t observe any significant change with speed during half-bound, indicating the important role of self-stabilising mechanisms on the choice of kinematics.

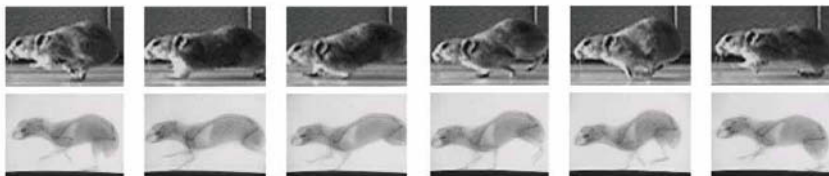


Fig. 1. Pika (*Ochotona rufescens*) in half-bound. Cineradiography with 150 fps. Six events during one motion cycle in time intervals of 25 ms are shown. The hindlimbs move synchronously, while the forelimb show a phase difference (leading vs. trailing limb). Please note especially the flexion of the spine.

1 Introduction

Synchronous gaits, where the feet within a pair of fore- or hindlimbs touch the ground with only slight time differences, gain growing interest in robotics. In comparison to the machines using symmetrical gaits (where feet are placed in diagonals - definition of gaits cf. Hildebrand 1965, 1977), programming work is simplified considerably. In the extreme case, the Buehler hopper shows a pure “bound”, with no phase difference within each pair of legs. Animals are as well able to produce a pure bound (e. g. “bouncing” goats), but the common synchronous locomotor mode of small (and ancestral) mammals is “half-bound”. The hindlimbs are moved synchronously, while the forelimbs show a fluctuating phase lag. The leg which touches the ground first is called “trailing limb”, the other one shows the greater cranial excursion and thus is called the (spatially) “leading limb” (fig. 1).

We performed analyses on four male pikas (*Ochotona rufescens*: Lagomorpha), small tailless mammals living in the steppes of central Asia. They own body weights of 150-200 g, crown-rump-lengths of 140 mm and heights of the CoM over ground of 45 mm. Kinematics have been described in detail in [4]. Pikas are performing half-bound at speeds between 1.2 m/s and 2.4 m/s.

2 Preliminary question: do pikas prefer one forelimb as trailing limb?

We filmed the animals in lateral view with a high speed video system (Micromac® Camsys® + Zoom lenses Fujinon® 2,0/12.5-75.5 mm) at 500 Hz. The duration of each session accounted for about one hour. The pikas ran 30 seconds and were filmed 15 seconds at each sequenc followed by a recreation period of 3 minutes. Speed was staged between 1.2 m/s and 2.2 m/ with a step width of about 0.1 m/s. The effective treadmill speed was controlled via tracking the movements of markers disposed along the treadmill belt. The results of the experiment clearly indicate that pikas systematically prefer one of their forelimbs as the trailing one (fig. 2). With increasing speed this preference becomes more evident but the differences between medium and fast half-bound not always were significant.

The step duration of a pika is described by a decreasing power like function of speed (Fischer and Lehmann, 1998). In the range of half-bound speed, this function may be linearized (cf. fig. 3). At very high speeds (> 1.75 m/sec), in the individuals under study here we noted that the standard deviation of the step duration measured from touch-down of the leading limb to the next touch-down was significantly smaller than the standard deviation of the step duration measured for the trailing limb.

These results indicate that even in animals using their “hands” (fore feet) for running a handedness exists, which even in a small group of animals shows differences between individuals what concerns the preferred side. May

this be an indicator of a body side specific specialization of the extremities (in mechanical performance and/or control), even without profound knowledge about the bases of this effect it indicates that “the” motion scheme of “the” pika does not exist – in so far pikas are real individuals.

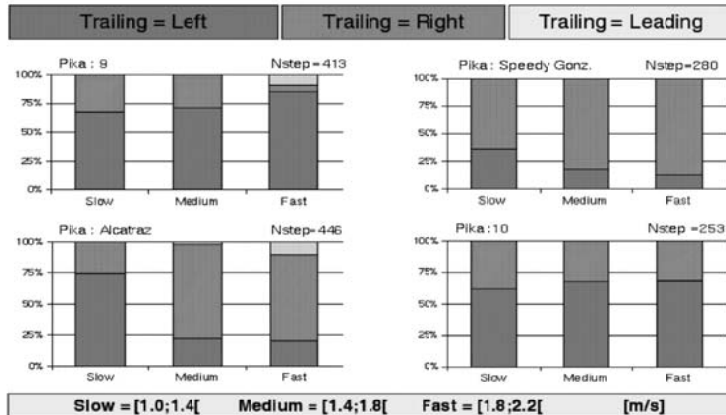


Fig. 2. The four individuals under study systematically preferred one of their forelimbs for the first touch down in a motion cycle of half-bound (trailing forelimb).

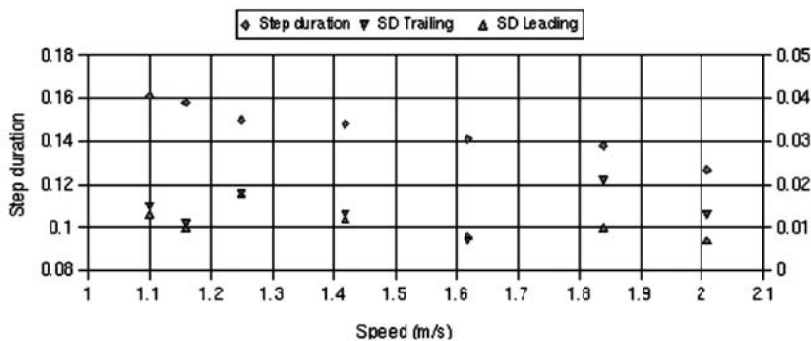


Fig. 3. Step duration of the pika (*Ochotona rufescens*) in half-bound. At speeds > 1.75 m/sec, the S.D. of the step duration is significantly higher ($p < 0.05$) for the leading limb than that for the trailing limb. At each speed $n = 20$ motion cycles were analysed.

3 Trajectories of the centre of mass of pikas in half-bound gait

3.1 Method: Videoradiography.

The animals were filmed at a frequency of 1,000 fps, half-bounding on a treadmill at a speed of 2.0 m/s. At this speed, the step frequency is about 8 cycles per second. At 1,000 fps the high speed cameras provide a resolution of 256 x 64 pixels. The treadmills belt is twice as wide as a pika's body width. One camera was used to film the pikas from the lateral side (the ground appears to be a line on the screen). To control the permanence of speed, this lateral zoom-camera was adjusted with the maximal focus length (75 mm) in such a way that the picture just covered the length of the animal when it was maximally extended. A second camera documented the front view, to ensure that the pika was running straight forward.

3.2 Method: Digitization

To control the effects of optical distortion, a reference grid (mesh width 10 ± 0.05 mm, steel balls of 1 ± 0.01 mm in diameter) was filmed and served as a control for linearization means. The outline of the body was digitised in the global frame with 35 points alternately distributed on the dorsal and on the ventral border of the sagittal projection of the animal. Limb segments were incorporated into the body shape proximally of the elbow and knee joints. The background of the picture (grid of the Faraday's cage of our laboratory) was filled with vertical lines spaced approx. 1 cm. We took advantage from these lines to get an equal distribution of the digitisation points along the body contour. 90% of the animal's mass is included in this digitised area. The number of points used for digitising the body outline arose to be a good compromise between the needs for the binding line between two even following points to stay near to the contour line and the wish to limit the expense for the digitising work.

3.3 Method: Weighing of triangle segments of trunk elements

The distribution of the points on the body outline defined a series of triangles, the areas and centers of which were computed from their corner coordinates. To take account of the mass distribution, we weighed a series of 14 transversal slices of a pika cadaver frozen in its extended position (fig. 4). These values were the base for the computational weight distribution onto the triangles. We thus implicitly neglected the effect of oscillating masses, or seen the other way round, since the thickness of the zone defined by the base of the triangle is about 1 cm, this means that the masses have been considered to oscillate locally in this volume.

3.4 Results

Motion of the center of mass in the body:

- The CoM is located underneath the lung base. It is closer to the ventral outline than to the dorsal one (40:60) (fig. 4).
- The position of the center of mass relatively to the nose (which is a representative for the rather unaccelerated head) is not constant. The horizontal excursion of the CoM is in fixed phase coupling with the motion of the back. During spinal extension, which takes place during the stance phase of the hindlimbs, and at the beginning of the forelimbs' stance phase the CoM moves in the crano-caudal direction. During spinal bending the CoM moves in the caudo-cranaial direction. This excursion equals about 10 % of the animals' length (fig. 5).

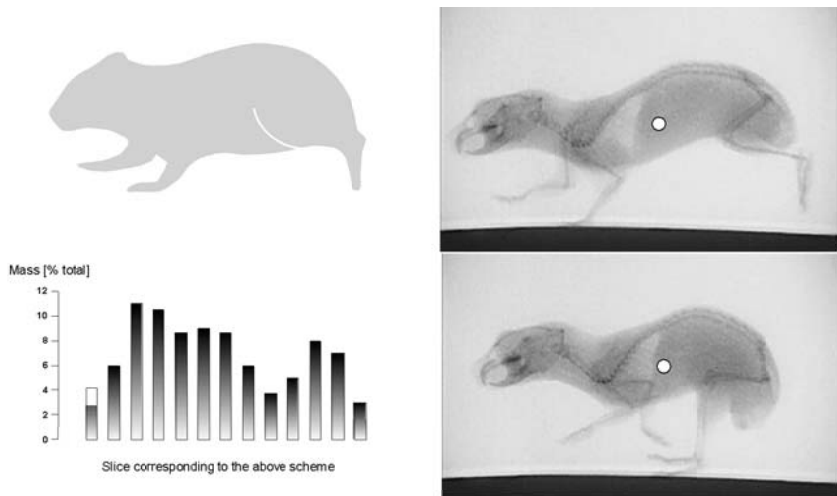


Fig. 4. Left: Mass distribution of the trunk of a pika (*Ochotona rufescens*) including the upper arm (proximally of the elbow joint) and the thigh. Right: position of the center of mass at touch down of the forelimbs (extended back) and of the hindlimbs (bended back). The radius of the circle corresponds to the strength of the interval of confidence.

Vertical motions of the CoM in the global frame:

- The amplitude of the motion of the CoM at 2 m/sec accounts for about 6 mm (10% of the animal's height) (fig. 5).
- During the extension of the back the CoM globally moves down, during the bending of the back it globally moves up (fig. 5).
- The pattern of the CoM vertical motion has more than two extrema.

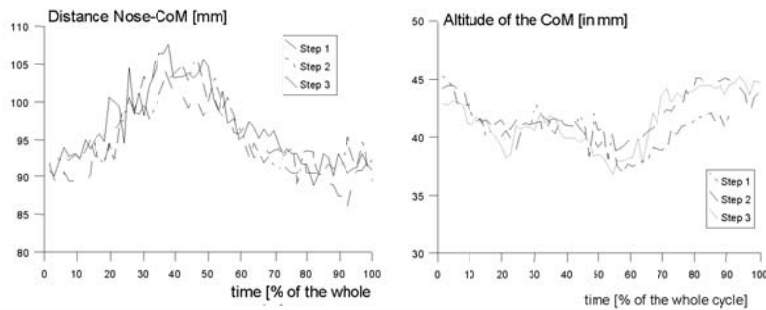


Fig. 5. Motions of the CoM during half-bound of a pika (*Ochotona rufescens*).
Left: horizontal excursions relative to the nose
Right: Vertical excursions with corresponding footfall patterns

Position of the CoM relative to the forelimbs.

- The angle wrist-elbow-CoM of the trailing forelimb is about 180° during that part of its stance phase when no other ground contacts exist (fig. 6).
- After the leading forelimb touches the ground, the weight is transferred to it: the alignment CoM-trailing ulna decreases while the alignment with the leading ulna becomes almost complete.

4 Does the angle of attack couple with speed?

The angle of attack is defined as the angle formed by the connection line of CoM and the ground contact point versus ground. To quantify the variation of the angle of attack with speed we took advantage of the above described effect that at touch down of the trailing limb the ulna points in the direction of the CoM. The orientation of the ulna does not coincide exactly with the direction defined by the connection line of the ground contact point (underneath the metatarso-phalangial joint) and the CoM. This error is systematic and accounts for $+ 5^\circ$.

4.1 Methods

The high speed X-Ray camera accessible to us provided 150 fps. This frame rate is insufficient to determine significant values for the angle of attack, since a pika at observation speed may run up to 8 cycles per second. Consecutively we shaved the forelimbs of a pika and filmed the half-bounding animal on the treadmill with the high speed video system (500 fps, resolution of 256x256 pixels).

The camera field was adjusted to cover one pika length. This enables a rigorous control of pika speed.

4.2 Results

1. The angle of attack does not variate strongly with increasing speed (fig.7).
2. The angle ulna/ground equals about 50° , consecutively the angle of attack is about 45° .

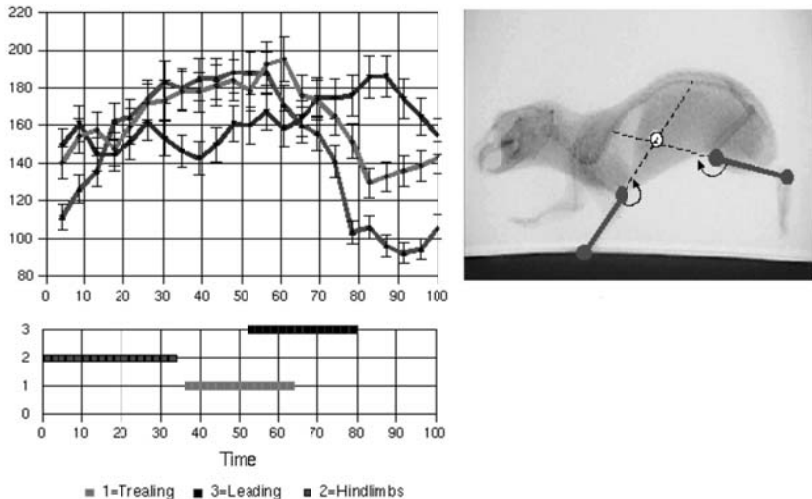


Fig. 6. The angle wrist-elbow-CoM of the trailing forelimb is about 180° during that part of its stance phase when no other ground contacts exist. During late mid stance the leading forelimb takes over and its ulna points to the CoM. Alignment of the shank (kinematically equivalent to the upper arm) mainly occurs during aerial phases.

5 Conclusions

The small mammal's limb is a four segmented flexed structure, which may be compared to a pantograph [5]. It effectively allows for compensation of small irregularities of the ground. It also plays the role of a spring-damper system as the pika runs or trots. The occurrence of elastic phenomena during legged locomotion is commonly accepted in biology (cf. [6], [7], [8] and succeeding publications). The movement of the human CoM during running may be described using spring-mass models [9] [10]. The vertical excursion of the CoM of a half-bounding pika (about 5-6 mm) relatively to the leg length (70 mm) is quite comparable to the excursion of the CoM in human running (about 10 %) [11]. From this point of view (in addition to many others), it also seems promising to extend these templates to quadrupedal locomotion

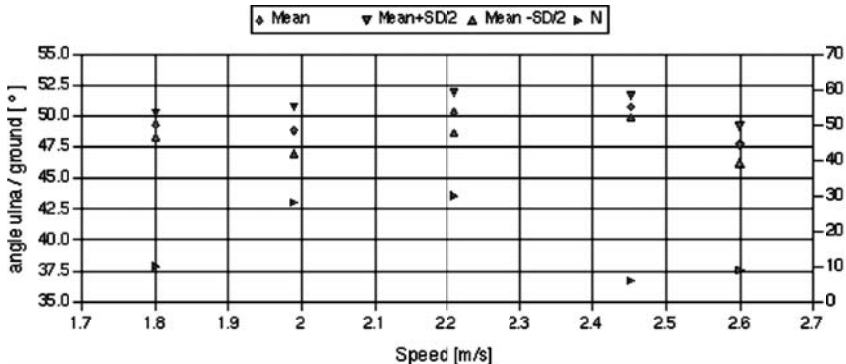


Fig. 7. Variations of the angle ulna/ground with speed are small. The right scale gives the number of steps N used to calculate the mean values and the standard deviations.

[12]. In humans the spring-leg and the mass (CoM) are well aligned. The above described results indicate, that the common linear spring-point mass model may as well be applied to the situation in the pika's forelimbs. In the hindlimbs, the consideration of the mass extension of the trunk seems inevitable. The variation of the CoM height found in this study is very similar to that for the dog derived from numerical integration of ground reaction forces by Cavagna et al. [7]. In that case the vertical displacement of the CoM over time showed more than two extrema. McMahon & Cheng [13] calculated how the angle of attack of a spring-mass system defined as the angle which minimized the maximum of the force during the stance phase variates as a function of the horizontal and vertical velocity. The variation of this angle with horizontal velocity also is small (about 7°). The reasons for an almost constancy of this angle still are poorly understood as far as the dynamics of locomotion is concerned, but perhaps may find an explanation by the results of further studies on the dynamic stability of quadrupedal locomotion.

Our study shows that the motion of the trunk is a determinant factor in the motion of the CoM. The model of a rigid body that jumps from one limb to the other is not able to explain the variety of the pattern of vertical motions of CoM provoked by running locomotor modes. Bending of the back is not a passive bending due to inertia of the back. For robotics the Raibert idea of minimizing dissipative energy flows in combination with the usage of “intelligent”, self-stabilising mechanics with minimal neuronal/computational control effort is attractive. Understanding of motion systems evolutively tested for longer periods in this context may be a promising directive.

Acknowledgments

We thank Prof. R. Blickhan, who kindly provided us access to the high speed camera system. Dr. D. Haarhaus invested his experience in a multitude of cineradiographic experiments.

References

1. Hildebrand M.(1965): Symmetrical gaits of horses. – *Science* 150: 701-708.
2. Hildebrand M.(1977): Analysis of asymmetrical gaits. – *J Mamm* 58(2): 131-156.
3. Jenkins F.A.(1971): Limb posture and locomotion in the Virginia opossum (*Didelphis marsupialis*) and other non-cursorial mammals. *J Zool (Lond)* 165: 303-315.
4. Fischer M.S. & Lehmann R.(1998): Application of cineradiography for the metric and kinematic study of in-phase gaits during locomotion of the pika (*Ochotona rufescens*, Mammalia: Lagomorpha). - *Zoology* 101: 12-37.
5. MS Fischer & H Witte (1998): The functional morphology of the three-segmented limb of mammals and its specialities in small and medium-sized mammals. *Proc Europ Mechanics Coll Euromech 375 Biology and Technology of Walking*: 10–17.
6. Cavagna G.A., Saibene & Margaria (1964) Mechanical work in running - *J Appl Physiol* 19(2) 249-256.
7. Cavagna G.A., Heglund N.C. & Taylor C.R. (1977): Mechanical work in terrestrial locomotion: two basic mechanisms for minimizing energy expenditure. - *Am J Physiol* 233: 243-2.
8. McMahon T.A.(1985): The role of compliance in mammalian running gaits. - *J exp Biol* 115: 263-282.
9. Bernstein N.A.(1967): *The coordination and regulation of movements*. Pergamon, London.
10. Blickhan R.(1989): The spring-mass model for running and hopping. - *J Biomech* 22(11/12): 1217-1227.
11. Lee C.R., Farley C. (1998): Determinant of the center of mass in human walking and running. - *J exp Biol* 201(pt 21): 2935-2944.
12. Full R.J., Koditschek D.E.(1999): Templates and anchors: neuromechanical hypotheses of legged locomotion on land. – *J exp Biol* 202(Pt 23), 3325–3332.
13. McMahon T.A. & Cheng G.C. (1990): The mechanics of running: how does stiffness couple with speed? – *J Biomech* 23 (Suppl. 1): 65-78.

On the Dynamics of Bounding and Extensions: Towards the Half-Bound and Gallop Gaits

Ioannis Poulakakis, James Andrew Smith, and Martin Buehler

Ambulatory Robotics Laboratory, Centre for Intelligent Machines,
McGill University, Montréal QC H3A 2A7, Canada

Abstract. This paper examines how simple control laws stabilize complex running behaviors such as bounding. First, we discuss the unexpectedly different local and global forward speed versus touchdown angle relationships in the self-stabilized Spring Loaded Inverted Pendulum. Then we show that, even for a more complex energy conserving unactuated quadrupedal model, many bounding motions exist, which can be locally open loop stable! The success of simple bounding controllers motivated the use of similar control laws for asymmetric gaits resulting in the first experimental implementations of the half-bound and the rotary gallop on Scout II.

1 Introduction

Many mobile robotic applications might benefit from the improved mobility and versatility of legs. Twenty years ago, Raibert set the stage with his groundbreaking work on dynamically stable legged robots by introducing a simple and highly effective three-part controller for stabilizing running on his one-, two-, and four-legged robots, [9]. Other research showed that even simpler control laws, which do not require task level or body state feedback, can stabilize running as well, [1]. Previous work on the Scout II quadruped (Fig. 1) showed that *open loop* control laws simply positioning the legs at a desired touchdown angle, result in stable running at speeds over 1 m/s, [12].



Fig. 1. Scout II: A simple four-legged robot.

Motivated by experiments on cockroaches (death-head cockroach, *Blaberous discoidalis*), Kubow and Full studied the role of the mechanical system in control by developing a simple two-dimensional hexapedal model, [5]. The model included no equivalent of nervous feedback and it was found to

be inherently stable. This work first revealed the significance of mechanical feedback in simplifying neural control. Full and Koditschek set a foundation for a systematic study of legged locomotion by introducing the concepts of *templates* and *anchors*, [2]. To study the basic properties of sagittal plane running, the *Spring Loaded Inverted Pendulum (SLIP)* template has been proposed, which describes running in animals that differ in skeletal type, leg number and posture, [2]. Seyfarth et al., [11], and Ghigliazza et al., [3], found that for certain leg touchdown angles, the SLIP becomes self-stabilized if the leg stiffness is properly adjusted and a minimum running speed is exceeded.

In this paper, we first describe some interesting aspects of the relationship between forward speed and leg touchdown angles in the self-stabilized SLIP. Next, we attempt to provide an explanation for simple control laws being adequate in stabilizing complex tasks such as bounding, based on a simple sagittal “template” model. Passively generated cyclic bounding motions are identified and a regime where the system is self-stabilized is also found. Furthermore, motivated by the success of simple control laws to generating bounding running, we extended the bounding controller presented in [12] to allow for asymmetric three- and four-beat gaits. The half-bound, [4], and the rotary gallop [4,10], expand our robots’ gait repertoire, by introducing an asymmetry to the bound, in the form of the leading and trailing legs. To the authors’ best knowledge this is the first implementation of both the half-bound and the gallop in a robot.

2 Bounding experiments with Scout II

Scout II (Fig. 1) has been designed for power-autonomous operation. One of its most important features is that it uses a *single* actuator per leg. Thus, each leg has two degrees of freedom (DOF): the actuated revolute hip DOF, and the passive linear compliant leg DOF.

In the bound gait the essential components of the motion take place in the sagittal plane. In [12] we propose a controller, which results in fast and robust bounding running with forward speeds up to 1.3 m/s, without body state feedback. The controller is based on two individual, independent front and back virtual leg controllers. The front and back virtual legs each detect two leg states - stance and flight. During flight, the controller servoed the flight leg to a desired, fixed, touchdown angle. During stance the leg is swept back with a constant commanded torque until a sweep limit is reached. Note that the actual applied torque during stance is determined primarily by the motor’s torque-speed limits, [12]. The sequence of the phases of the resulting bounding gait is given in Fig. 2.

Scout II is an underactuated, highly nonlinear, intermittent dynamic system. The limited ability in applying hip torques due to actuator and friction constraints and due to unilateral ground forces further increases the complexity. Furthermore, as Full and Koditschek state in [2], “locomotion results from

complex high-dimensional, dynamically coupled interaction between an organism and its environment". Thus, the task itself is complex too, and cannot be specified via reference trajectories. Despite this complexity, simple control laws, like the one described above and in [12], can stabilize periodic motions, resulting in robust and fast running without requiring any task level feedback like forward velocity. Moreover, they do not require body state feedback.

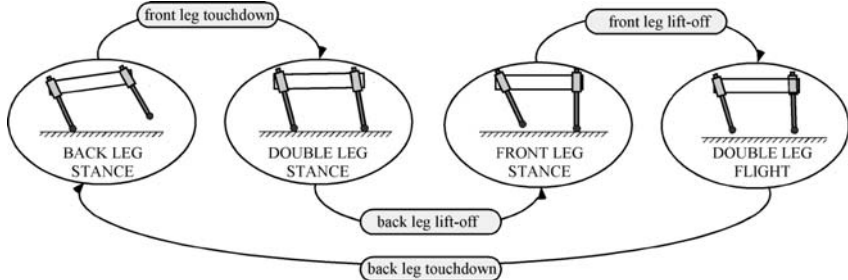


Fig. 2. Bounding phases and events.

It is therefore natural to ask why such a complex system can accomplish such a complex task without intense control action. As outlined in this paper, and in more detail in [7,8], a possible answer is that Scout II's unactuated, conservative dynamics already exhibit stable bounding cycles, and hence a simple controller is all that is needed for keeping the robot bounding.

3 Self-stabilization in the SLIP

The existence of passively stable gaits in the conservative, unactuated SLIP, discussed in [3,11], is a celebrated result that suggests the significance of the mechanical system in control as was first pointed out by Kubow and Full in [5]. However, the mechanism that results in self-stabilization is not yet fully understood, at least in a way that could immediately be applicable to improve existing control algorithms. It is known that for a set of initial conditions (forward speed and apex height), there exists a touchdown angle at which the system maintains its initial forward speed, see Fig. 3 (left). As Raibert noticed, [9], if these conditions are perturbed, for example, by decreasing the touchdown angle, then the system will accelerate in the first step, and, if the touchdown angle is kept constant, it will also accelerate in the subsequent steps and finally fall due to toe stubbing. However, when the parameters are within the self-stabilization regime, the system does not fall! It converges to a periodic motion with symmetric stance phases and higher forward speeds. This fact is not captured in Raibert's linear steady-state argument, [9], based on which one would be unable to predict self-stabilization of the system.

A question we address next is what is the relationship between the forward speed at which the system converges i.e. *the speed at convergence*, and the touchdown angle. To this end, simulation runs have been performed in which

the initial apex height and initial forward velocity are fixed, thus the energy level is fixed, while the touchdown angle changes in a range where cyclic motion is achieved. For a given energy level, this results in a curve relating the speed at convergence to the touchdown angle. Subsequently, the apex height is kept constant, while the initial forward velocity varies between 5 and 7 m/s. This results in a family of constant energy curves, which are plotted in Fig. 3 (right). It is interesting to see in Fig. 3 that in the self-stabilizing regime of the SLIP, an increase in the touchdown angle *at constant energy* results in a lower forward speed at convergence. This means that higher steady state forward speeds can be accommodated by smaller touchdown angles, which, at first glance, is not in agreement with the *global* behavior that higher speeds require bigger (flatter) touchdown angles and is evident in Fig. 3 (right).

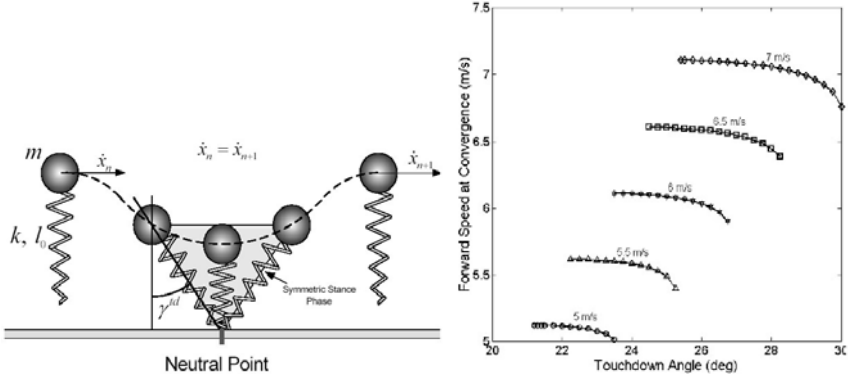


Fig. 3. Left: Symmetric stance phase in the SLIP. Right: Forward speed at convergence versus touchdown angle at fixed points obtained for initial forward speeds 5 to 7 m/s and apex height equal to 1 m ($l_0 = 1$ m, $k = 20$ kN/m and $m = 1$ kg).

The fact that *globally* fixed points at higher speeds require greater (flatter) touchdown angles was reported by Raibert and it was used to control the speed of his robots based on a feedback control law, [9]. However, Fig. 3 (right) suggests that in the *absence* of control and for *constant energy*, reducing the touchdown angle results in an increase of the speed at convergence. Thus, one must be careful not to transfer results from systems actively stabilized to passive systems, because otherwise opposite outcomes from those expected may result. Note also that there might exist parameter values resulting in a local behavior opposite to that in Fig. 3, illustrating that direct application of the above results in designing intuitive controllers is not trivial.

4 Modeling the Bounding Gait

In this section the passive dynamics of Scout II in bounding is studied based on the template model shown in Fig. 4 and conditions allowing steady state cyclic motion are determined.

Assuming that the legs are massless and treating toes in contact with the ground as frictionless pin joints, the equations of motion for each phase are

$$\frac{d}{dt} \begin{bmatrix} \mathbf{q} \\ \dot{\mathbf{q}} \end{bmatrix} = \begin{bmatrix} \dot{\mathbf{q}} \\ -\mathbf{M}^{-1} (\mathbf{F}_{el} + \mathbf{G}) \end{bmatrix}, \quad (1)$$

where $\mathbf{q} = [x \ y \ \theta]^T$ (Fig. 4), \mathbf{M} , is the mass matrix and \mathbf{F}_{el} , \mathbf{G} are the vectors of the elastic and gravitational forces, respectively. The transition conditions between phases corresponding to touchdown and lift-off events are

$$y \pm L \sin \theta \leq l_0 \cos \gamma_i^{td}, \quad l_i \leq l_0, \quad (2)$$

where $i = b, f$ for the back (- in (2)) and front (+ in (2)) leg respectively.

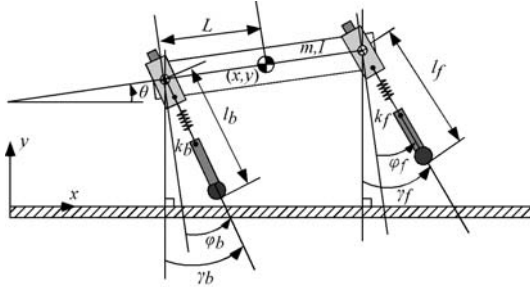


Fig. 4. A template for studying sagittal plane running.

To study the bounding cycle of Fig. 2 a return map is defined using the apex height in the double leg flight phase as a reference point. The states at the n^{th} apex height constitute the initial conditions for the cycle, based on which we integrate successively the dynamic equations of all the phases. This process yields the state vector at the $(n+1)^{th}$ apex height, which is the value of the return map $\mathbf{P} : \mathbb{R}^4 \times \mathbb{R}^2 \rightarrow \mathbb{R}^4$ calculated at the n^{th} apex height, i.e.

$$\mathbf{x}_{n+1} = \mathbf{P}(\mathbf{x}_n, \mathbf{u}_n), \quad (3)$$

with $\mathbf{x} = [y \ \theta \ \dot{x} \ \dot{\theta}]^T$, $\mathbf{u} = [\gamma_b^{td} \ \gamma_f^{td}]^T$; the touchdown angles are control inputs.

We seek conditions that result in cyclic motion and correspond to fixed points $\bar{\mathbf{x}}$ of \mathbf{P} , which can be determined by solving $\mathbf{x} - \mathbf{P}(\mathbf{x}) = \mathbf{0}$ for all the (experimentally) reasonable touchdown angles. The search space is 4-dimensional with two free parameters and the search is conducted using the Newton-Raphson method. An initial guess, $\mathbf{x}_n^{(0)}$, for a fixed point is updated by

$$\mathbf{x}_n^{(k+1)} = \mathbf{x}_n^{(k)} + \left(\mathbf{I} - \nabla \mathbf{P}(\mathbf{x}_n^{(k)}) \right)^{-1} \left[\mathbf{P}(\mathbf{x}_n^{(k)}) - \mathbf{x}_n^{(k)} \right], \quad (4)$$

where n corresponds to the n^{th} apex height and k to the number of iterations. Evaluation of (4) until convergence (the error between $\mathbf{x}_n^{(k)}$ and $\mathbf{x}_n^{(k+1)}$ is smaller than $1e-6$) yields the solution. To calculate \mathbf{P} at $\mathbf{x}_n^{(k)}$, we numerically integrate (1) for each phase using the adaptive step Dormand-Price method with $1e-6$ and $1e-7$ relative and absolute tolerances, respectively.

Implementation of (4) resulted in a large number of fixed points of \mathbf{P} , for different initial guesses and touchdown angles, which exhibited some very useful properties, [7,8]. For instance, the pitch angle was found to be always zero at the apex height. More importantly, the following condition was found to be true for all the fixed points calculated randomly using (4)

$$\gamma_f^{td} = -\gamma_b^{lo}, \quad \gamma_b^{td} = -\gamma_f^{lo}. \quad (5)$$

It is important to mention that this property resembles the case of the SLIP, in which the condition for fixed points is the lift-off angle to be equal to the negative of the touchdown angle (symmetric stance phase), [3].

It is desired to find fixed points at specific forward speeds and apex heights. Therefore, the search scheme described above is modified so that the forward speed and apex height become its input parameters, specified according to running requirements, while the touchdown angles are now considered to be “states” of the search procedure, i.e. variables to be determined from it, [7,8]. Thus, the *search space* states and the “inputs” to the search scheme are $\mathbf{x}^* = [\theta \dot{\theta} \gamma_b^{td} \gamma_f^{td}]^T$ and $\mathbf{u}^* = [y \dot{x}]^T$, respectively.

Fig. 5 illustrates that for 1 m/s forward speed, 0.35 m apex height and varying pitch rate there is a continuum of fixed points, which follows an “eye” pattern accompanied by two external branches. The existence of the external branch implies that there is a range of pitch rates where two *different* fixed points exist for the same forward speed, apex height and pitch rate. This is surprising since the same total energy and the same distribution of that energy among the three modes of the motion -forward, vertical and pitch- can result in two different motions depending on the touchdown angles. Fixed points that lie on the internal branch correspond to a bounding motion where the front leg is brought in front of the torso, while fixed points that lie on the external branch correspond to a motion where the front leg is brought towards the torso’s Center of Mass (COM), see Fig. 5 (right).

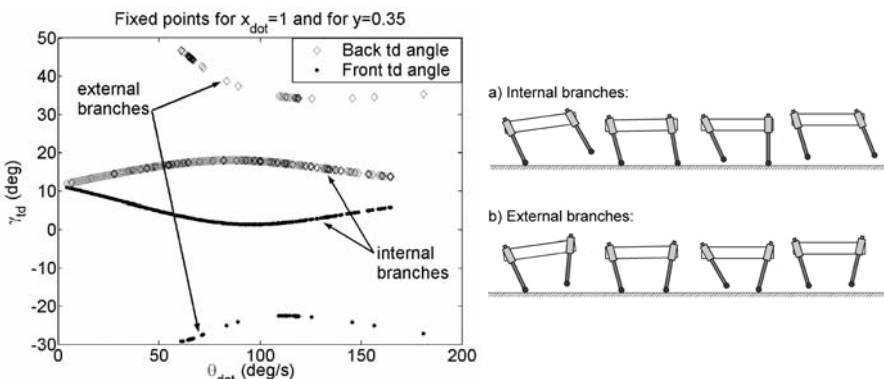


Fig. 5. Left: Fixed points for 1m/s forward speed and 0.35 m apex height. Right: Snapshots showing the corresponding motions.

5 Local stability of passive bounding

The fact that bounding cycles can be generated passively as a response to the appropriate initial conditions may have significant implications for control. Indeed, if the system remains close to its passive behavior, then the actuators have less work to do to maintain the motion and energy efficiency, an important issue to any mobile robot, is improved. Most importantly there might exist operating regimes where the system is passively stable, thus active stabilization will require less control effort and sensing. The local stability of the fixed points found in the previous section is now examined. A periodic solution corresponding to a fixed point $\bar{\mathbf{x}}$ is stable if all the eigenvalues of the matrix $\mathbf{A} = \partial\mathbf{P}(\mathbf{x}, \mathbf{u})/\partial\mathbf{x}|_{\mathbf{x}=\bar{\mathbf{x}}}$ have magnitude less than one.

Fig. 6 (left) shows the eigenvalues of \mathbf{A} for forward speed 1 m/s, apex height 0.35 m and varying pitch rate, $\dot{\theta}$. The four eigenvalues start at dark regions (small $\dot{\theta}$), move along the directions of the arrows and converge to the points marked with “x” located in the brighter regions (large $\dot{\theta}$) of the root locus. One of the eigenvalues (#1) is always located at one, reflecting the conservative nature of the system. Two of the eigenvalues (#2 and #3) start on the real axis and as $\dot{\theta}$ increases they move towards each other, they meet inside the unit circle and then move towards its rim. The fourth eigenvalue (#4) starts at a high value and moves towards the unit circle but it never gets into it, for those specific values of forward speed and apex height. Thus, the system cannot be passively stable for these parameter values.

To illustrate how the forward speed affects stability we present Fig. 6 (right), which shows the magnitude of the larger eigenvalue (#4) at two different forward speeds. For sufficiently high forward speeds and pitch rates, the larger eigenvalue enters the unit circle while the other eigenvalues remain well behaved. Therefore, there exists a regime where the system can be passively stable. This is a very important result since it shows that the system can tolerate perturbations of the nominal conditions without any control action taken! This fact could provide a possible explanation to why Scout II can bound without the need of complex state feedback controllers. It is important to mention that this result is in agreement with recent research from biomechanics, which shows that when animals run at high speeds, passive dynamic self-stabilization from a feed-forward, tuned mechanical system can reject rapid perturbations and simplify control, [2,3,5,11]. Analogous behavior has been discovered by McGeer in his passive bipedal running work, [6].

6 The half-bound and rotary gallop gaits

This section describes the half-bound and rotary gallop extensions to the bound gait. The controllers for both these gaits are generalizations of the original bounding controller, allowing two asymmetric states to be observed in the front lateral leg pair and adding control methods for these new states.

In the half-bound and rotary gallop controllers the lateral leg pair state machine adds two new asymmetric states: the left leg can be in flight while the

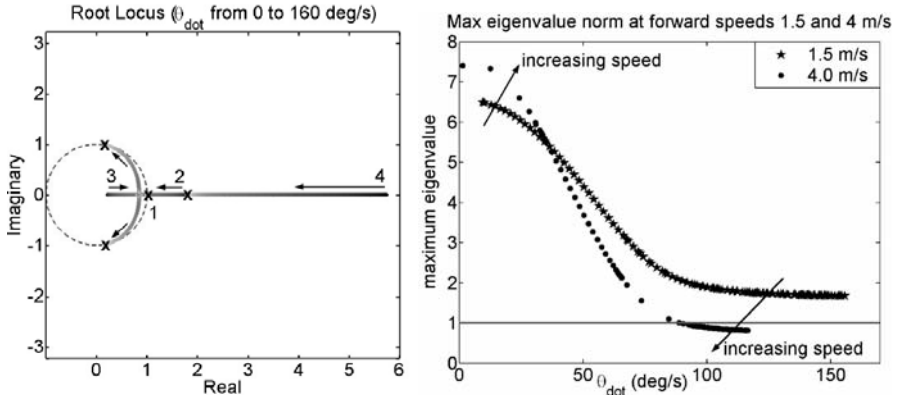


Fig. 6. Left: Root locus showing the paths of the four eigenvalues as the pitch rate, $\dot{\theta}$, increases. Right: Largest eigenvalue norm at various pitch rates and for forward speeds 1.5 and 4m/s. The apex height is 0.35 m.

right leg is in stance, and vice versa. In the regular bounding state machine these asymmetric states are ignored and state transitions only occur when the lateral leg pair is in the same state: either both in stance or both in flight. The control action associated with the asymmetric states enforces a phase difference between the two legs during each leg's flight phase, but is otherwise unchanged from the bounding controller as presented in [12].

The following describes the front leg control actions. Leg 1 (left) touches down before Leg 3 (right):

Case 1: Leg 1 and Leg 3 in flight. Leg 1 is actuated to a touchdown angle (17° , with respect to the body's vertical). Leg 3 is actuated to a larger touchdown angle (32°) to enforce separate touchdown times.

Case 2: Leg 1 and Leg 3 in stance. Constant commanded torques until 0° .

Case 3: Leg 1 in stance, Leg 3 in flight. Leg 1 is commanded as in Case 2 and Leg 3 as in Case 1.

Case 4: Leg 1 in flight, Leg 3 in stance. Leg 1 is commanded as in Case 1 and Leg 3 as in Case 2.

Application of the half-bound controller results in the motion shown in Fig. 7; the front legs are actuated to the two separate touchdown angles and maintain an out-of-phase relationship during stance, while the back two legs have virtually no angular phase difference at any point during the motion. Application of the rotary gallop controller results in the motion in Fig. 8; the front and back leg pairs are actuated to out-of-phase touchdown angles (Leg 1: 17° , Leg 3: 32° , Leg 4: 17° , Leg 2: 32°).

Fig. 9 (left) illustrates the half-bound footfall pattern. The motion stabilizes approximately one second after it begins (at 132 s), without back leg phase difference. Fig. 9 (right) shows the four-beat footfall pattern for the rotary gallop. The major difference between both the bound and the half-

bound controllers and the gallop controller is that a phase difference of 15° (Leg 4: 17° ; Leg 2: 32°) is enforced between the two back legs during the double-flight phase. It must be mentioned here that although the half-bound and the rotary gallop gaits have been studied in biological systems [4], to the authors' best knowledge this is the first implementation on a robot.

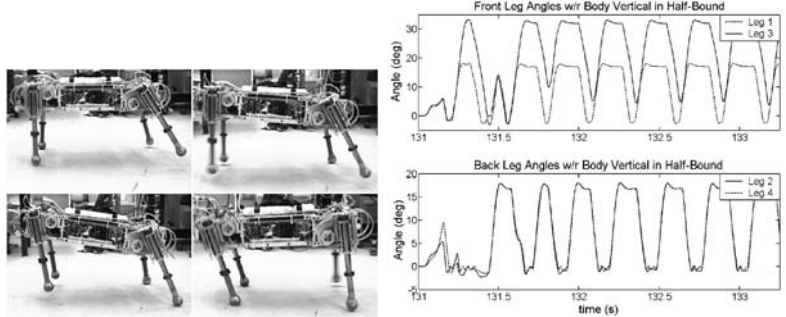


Fig. 7. Left: Snapshots of Scout II during the half bound: back legs (#2,4) in stance, front left leg (#1) touchdown, front right leg (#3) touchdown, and back legs (#2,4) touchdown. Right: Leg angles in the half-bound.

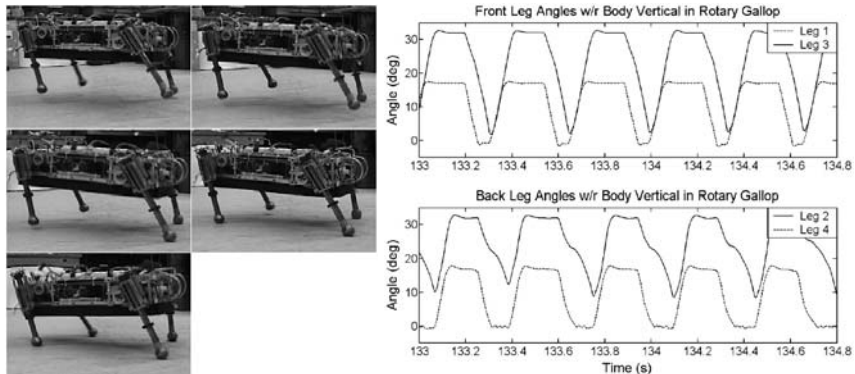


Fig. 8. Snapshots of Scout II during the rotary gallop: All legs in flight, first front leg (#1) touchdown, second front leg (#3) touchdown, first back leg (#4) touchdown and second back leg (#2) touchdown. Right: Leg angles in the rotary gallop.

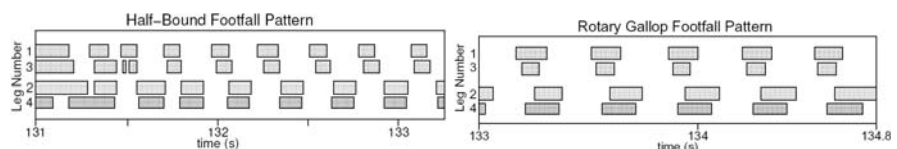


Fig. 9. Stance phases (shaded) for the half-bound (left) and rotary gallop (right).

7 Conclusion

This paper examined the difference between the local and global forward speed versus touchdown angle relationships in the self-stabilized SLIP. It then showed that a more complex model for quadruped sagittal plane running can exhibit passively generated bounding cycles under appropriate initial conditions. Most strikingly, under some initial conditions the model was found to be self-stable! This might explain why simple controllers as those in [12], are adequate in stabilizing a complex dynamic task like running. Self-stabilization can facilitate the control design for dynamic legged robots. Furthermore, preliminary experimental results of the half-bound and rotary gallop running gaits have been presented. Future work includes the application of asymmetric gaits to improving maneuverability on Scout II.

Acknowledgments

Support by IRIS III and by NSERC is gratefully acknowledged. The work of I. Poulakakis has been supported by a R. Tomlinson Doctoral Fellowship and by the Greville Smith McGill Major Scholarship.

References

1. Buehler M. 2002. Dynamic Locomotion with One, Four and Six-Legged Robots. *J. of the Robotics Society of Japan* 20(3):15-20.
2. Full R. J. and Koditschek D. 1999. Templates and Anchors: Neuromechanical Hypotheses of Legged Locomotion on Land. *J. Exp. Biol.* 202:3325-3332.
3. Ghigliazza R. M., Altendorfer R., Holmes P. and Koditschek D. E. 2003. A Simply Stabilized Running Model. *SIAM J. on Applied Dynamical Systems* 2(2):187-218.
4. Hildebrand M. 1977. Analysis of Asymmetrical Gaits. *J. of Mammalogy* 58(31):131-156.
5. Kubow T. and Full R. 1999. The Role of the Mechanical System in Control: A Hypothesis of Self-stabilization in Hexapedal Runners. *Phil. Trans. R. Soc. of Lond. Biological Sciences* 354(1385):854-862.
6. McGeer T. 1989. *Passive Bipedal Running*. Technical Report, CSS-IS TR 89-02, Centre For Systems Science, Burnaby, BC, Canada.
7. Poulakakis I. 2002. *On the Passive Dynamics of Quadrupedal Running*. M. Eng. Thesis, McGill University, Montréal, QC, Canada.
8. Poulakakis I., Papadopoulos E., Buehler M. 2003. On the Stable Passive Dynamics of Quadrupedal Running. *Proc. IEEE Int. Conf. on Robotics and Automation* (1):1368-1373.
9. Raibert M. H. 1986. *Legged Robots That Balance*. MIT Press, Cambridge MA.
10. Schmideler J.P. and Waldron K.J. 1999. The Mechanics of Quadrupedal Galloping and the Future of Legged Vehicles. *Int. J. of Robotics Research* 18(12):1224-1234.
11. Seyfarth A., Geyer H., Guenther M. and Blickhan R. 2002. A Movement Criterion for Running, *J. of Biomechanics* 35:649-655.
12. Talebi S., Poulakakis I., Papadopoulos E. and Buehler M. 2001. Quadruped Robot Running with a Bounding Gait. *Experimental Robotics VII*, D. Rus and S. Singh (Eds.), pp. 281-289, Springer-Verlag.

Part 3

Machine Design and Control

Jumping, Walking, Dancing, Reaching: Moving into the Future. Design Principles for Adaptive Motion

Rolf Pfeifer

Artificial Intelligence Laboratory, Department of Information Technology,
University of Zurich, Andreasstrasse 15, CH-8050 Zurich, Switzerland.
pfeifer@ifi.unizh.ch, phone: +41 1 63 5 4320/31, fax: +41 1 635 68 09,
<http://www.ifi.unizh.ch/~pfeifer>

Abstract. Designing for adaptive motion is still largely considered an art. In recent years, we have been developing a set of heuristics or design principles, that on the one hand capture theoretical insights about adaptive systems, and on the other provide guidance in actually designing and building adaptive systems. In this paper we discuss, in particular, the principle of “ecological balance” which is about the relation between morphology, materials, and control. As we will argue, artificial evolution together with morphogenesis is not only “nice to have” but turns out to be a necessary design tool for adaptive motion.

1 Introduction

The field of adaptive systems, as loosely characterized by conferences such as SAB (Simulation of Adaptive Behavior), AMAM (Adaptive Motion in Animals and Machines), Artificial Life, etc., is very heterogeneous and there is a definite lack of consensus on the theoretical foundations. As a consequence, agent design is – typically – performed in an ad hoc and intuitive way. Although there have been some attempts at elaborating principles, general agreement is still lacking. In addition, much of the work on designing adaptive systems is focused on the programming of the robots. But what we are really interested is in designing entire systems. The research conducted in our laboratory, but also by many others, has demonstrated that often, better, cheaper, more robust and adaptive agents can be developed if the entire agent is the design target rather than the program only. This implies taking embodiment into account and going beyond the programming level proper. Therefore we prefer to use the term “engineering agents for adaptive motion” rather than “programming agents”.

If this idea of engineering agents is the goal, the question arises what form the theory should have, i.e. how the experience gained so far can be captured in a concise scientific way. The obvious candidate is the mathematical theory of dynamical systems, and there seem to be many indications that ultimately this may be the tool of choice for formulating a theory of intelligence. For the time being, it seems that progress over the last few years in the field has been

slow, and we may be well-advised to search for an intermediate solution for the time being. The form of design principles seems well-suited for a number of reasons. First, at least at the moment, there don't seem to be any real alternatives. The information processing paradigm, another potential candidate, has proven ill-suited to come to grips with natural, adaptive forms of intelligence. Second, because of the unfinished status of the theory, a set of principles is flexible and can be dynamically changed and extended. Third, design principles represent heuristics for actually building systems. In this sense, they instantiate the synthetic methodology (see below). And fourth, evolution can also be seen as a designer, a "blind one" perhaps, but an extremely powerful one. We hope to convince the reader that this is a good idea, and that some will take it up, modify the principles, add new ones, and try to make the entire set more comprehensive and coherent. The response so far has been highly encouraging and researchers as well as educated lay people seem to be able to relate to these principles very easily.

A first version of the design principles was published at the 1996 conference on Simulation of Adaptive Behavior (SAB 1996, "From Animals to Animats") (Pfeifer, 1996). A more elaborate version has been published in the book "Understanding Intelligence" (Pfeifer and Scheier, 1999). More recently, some principles have been extended to incorporate ideas on the relation between morphology, materials, and control (Ishiguro et al., this volume; Hara and Pfeifer, 2000a; Pfeifer, 2003).

Although most of the literature is still about programming, some of the research explicitly deals with complete agent design and includes aspects of morphology (e.g. Bongard, 2002; Bongard and Pfeifer, 2001; Hara and Pfeifer, 2000a; Lipson and Pollack, 1999; Pfeifer, 1996; Pfeifer and Scheier, 1999; Pfeifer, 2003). Our own approach over the six years or so has been to try and systematize the insights gained in the fields of adaptive behavior and adaptive motion by incorporating ideas from biology, psychology, neuroscience, engineering, and artificial intelligence into a set of design principles (Pfeifer, 1996; Pfeifer and Scheier, 1999); they form the main topic of this paper.

We start by giving a very short overview of the principles. We then pick out and discuss in detail "ecological balance" and provide a number of examples for illustration. We then show how artificial evolution together with morphogenesis can be employed to design ecologically balanced systems. It is clear that these considerations are only applicable to embodied systems.

This is not a technical paper but a conceptual one. The goal is to provide a framework within which technical research can be conducted that takes into account the most recent insights in the field. In this sense, the paper has somewhat of a tutorial and overview flavor and should be viewed as such.

2 Design principles: overview

There are different types of design principles: Some are concerned with the general “philosophy” of the approach. We call them “design procedure principles”, as they do not directly pertain to the design of the agents but more to the way of proceeding. Another set of principles is concerned more with the actual design of the agent. We use the qualifier “more” to express the fact that we are often not designing the agent directly but rather the initial conditions and the learning and developmental processes or the evolutionary mechanisms and the encoding in the genome as we will elaborate later. The current over will, for reasons of space, be very brief; a more extended version is in preparation (Pfeifer and Glatzeder, in preparation).

Table 1. Overview of the design principles.

Number	Name	Description
<i>Design procedure principles</i>		
P-Princ. 1	Synthetic methodology	Understanding by building
P-Princ 2	Emergence	Systems designed for emergence are more adaptive
P-Princ 3	Diversity-compliance	Tradeoff between exploiting the givens and generating diversity solved in interesting ways
P-Princ 4	Time perspectives	Three perspectives required: “Here and now”, ontogenetic, phylogenetic
P-Princ 5	Frame-of-reference	Three aspects must be distinguished: perspective, behavior vs. mechanisms, complexity
<i>Agent design principles</i>		
A-Princ 1	Three constituents	Task environment (ecological niche, tasks), and agent must always be taken into account
A-Princ 2	Complete agent	Embodied, autonomous, self-sufficient, situated agents are of interest
A-Princ 3	Parallel, loosely coupled processes	Parallel, asynchronous, partly autonomous procs, largely coupled through interaction with environment
A-Princ 4	Sensory-motor coordination	Behavior sensory-motor coordinated with respect to target; self-generated sensory stimulation
A-Princ 5	Cheap design	Exploitation of niche and interaction; parsimony
A-Princ 6	Redundancy	Partial overlap of functionality based on different physical processes
A-Princ 7	Ecological balance	Balance in complexity of sensory, motor, and neural systems: task distribution between morphology, materials, and control
A-Princ 8	Value	Driving forces; developmental mechanisms; self-organization

2.1 P-Princ 1: The synthetic methodology principle.

The synthetic methodology, “understanding by building” implies on the one hand constructing a model of some phenomenon of interest (e.g. how an insect walks, how a monkey is grasping a banana). On the other we want to abstract general principles.

2.2 P-Princ 2: The principle of emergence.

The term emergence is controversial, but we use it in a very pragmatic way, in the sense of not being preprogrammed. When designing for emergence, the final structure of the agent is the result of the history of its interaction with the environment. Strictly speaking, behavior is always emergent; it is always the result of a system-environment interaction. In this sense, emergence is not all or none, but a matter of degree: the further removed from the actual behavior the designer commitments are made, the more we call the resulting behavior emergent.

2.3 P-Princ 3: The diversity-compliance principle.

Intelligent agents are characterized by the fact that they are on the one hand exploiting the specifics of the ecological niche and on the other by behavioral diversity. In a conversation I have to comply with the rules of grammar of the particular language, and then I have to react to what the other individual says, and depending on that, I have to say something different. Always uttering one and the same sentence irrespective of what the other is saying would not demonstrate great behavioral diversity.

2.4 P-Princ 4: The time perspectives principle.

A comprehensive explanation of behavior of any system must incorporate at least three perspectives: (a) state-oriented, the “here and now”, (b) learning and development, the ontogenetic view, and (c) evolutionary, the phylogenetic perspective. The fact that these perspectives are adopted by no means implies that they are separate. On the contrary, they are tightly intertwined, but it is useful to tease them apart for the purpose of scientific investigation.

2.5 P-Princ 5: The frame-of-reference principle.

There are three aspects to distinguish whenever designing an agent: (a) the perspective, i.e. are we talking about the world from the agent’s perspective, the one of the observer, or the designer; (b) behavior is not reducible to internal mechanism; trying to do that would constitute a category error; and (c) apparently complex behavior of an agent does not imply complexity of the underlying mechanism. Although it seems obvious that the world

“looks” very different to a robot than to a human because the robot has completely different sensory systems, this fact is surprisingly often ignored. Second, behavior cannot be completely programmed, but is always the result of a system-environment interaction. Again, it is surprising how often this obvious fact is ignored even by roboticists.

2.6 A-Princ 1: The three-constituents principle.

This very often ignored principle states that whenever designing an agent we have to consider three components. (a) the definition of the ecological niche (the environment), (b) the desired behaviors and tasks, and (c) the agent itself. The main point of this principle is that it would be a fundamental mistake to design the agent in isolation. This is particularly important because much can be gained by exploiting the physical and social environment.

2.7 A-Princ 2: The complete agent principle.

The agents of interest are autonomous, self-sufficient, embodied and situated. This view, although extremely powerful and obvious, is not very often considered explicitly.

2.8 A-Princ 3: The principle of parallel, loosely coupled processes.

Intelligence is emergent from an agent-environment interaction based on a large number of parallel, loosely coupled processes that run asynchronously and are connected to the agent’s sensory-motor apparatus. The term “loosely coupled” is used in contrast to hierarchically coupled processes where there is a program calling a subroutine and the calling program has to wait for the subroutine to complete its task before it can continue. In that sense, this hierarchical control corresponds to very strong coupling.

2.9 A-Princ 4: The principle of sensory-motor coordination

All intelligent behavior (e.g., categorization, memory) is to be conceived as a sensory-motor coordination. This sensory-motor coordination, in addition to enabling the agent to interact efficiently with the environment, serves the purpose of structuring its sensory input. One implication is that the problem of categorization in the real world is greatly simplified through the interaction with the environment because of the generation of “good” (correlated, and stationary) patterns of sensory stimulation.

2.10 A-Princ 5: The principle of cheap design.

Designs must be parsimonious, and exploit the physics and the constraints of the ecological niche. This principle is related to the diversity compliance principle in that it implies, for example, compliance with the laws of physics(e.g., robots with wheels that exploit the fact that the ground is mostly flat).

2.11 A-Princ 6: The redundancy principle.

Agents should be designed such that there is an overlap of functionality of the different subsystems. For example, the visual and the haptic systems both deliver spatial information, but they are based on different physical processes (electromagnetic waves vs. mechanical touch). Merely duplicating components does not lead to very interesting redundancy; the partial overlap of functionality and the different physical processes are essential. If there is a haptic system in addition to the visual one, the system can also function in complete dark, whereas one with 10 cameras ceases to function if the light goes out.

2.12 A-Princ 7: The principle of ecological balance.

This principle consists of two parts, the first one concerns the relation between the sensory system, the motor system, and the neural control. The “complexity” of the agent has to match the complexity of the task environment, in particular: given a certain task environment, there has to be a match in the complexity of the sensory, motor, and neural system. The second is about the relation between morphology, materials, and control: Given a particular task environment, there is a certain balance or task distribution between morphology, materials, and control (for references to both ideas, see, e.g. Hara and Pfeifer, 2000a; Pfeifer, 1996; Pfeifer, 1999, 2000; Pfeifer and Scheier, 1999). Because we are dealing with embodied systems, there will be two dynamics, the physical one or body dynamics and the control or neural dynamics. There is the deep and important question of how the two can be coupled in optimal ways. The research initiated by Ishiguro and his colleagues (e.g. Ishiguro et al., 2003) promises deep and important pertinent insights.

2.13 A-Princ 8: The value principle.

This principle is, in essence, about motivation. It is about why the agent does anything in the first place. Moreover, a value system tells the agent whether an action was good or bad, and depending on the result, the probability of repetition of an action will be increased or decreased. Because of the unknowns in the real world, learning must be based on mechanisms of self-organization. The issue of value systems is central to agent design and

must be somehow resolved. However, it seems that to date no generally accepted solutions have been developed. Research on artificial motivation and emotion, is highly relevant in this context (e.g. Breazeal, 2002; Manzotti, 2000; Picard, 1997; Pfeifer, 2000b).

Although it does capture some of the essential characteristics of adaptive systems, this set is by no means complete. A set of principles for designing evolutionary systems and collective systems, are currently under development. As mentioned earlier, all these principles only hold for embodied systems. In this paper, we focus on the principle of ecological balance which is at the heart of embodiment.

3 Information theoretic implications of embodiment

There is a trivial meaning of embodiment namely that “intelligence requires a body”. In this sense, anyone using robots for his or her research is doing embodied artificial intelligence and have to take into account gravity, friction, torques, inertia, energy dissipation, etc. However, there is a non-trivial meaning, namely that there is a tight interplay between the physical and the information theoretic aspects of an agent. The design principles all directly or indirectly refer to this issue, but some focus on this interplay, i.e. the principle of sensory-motor coordination where through the embodied interaction with the environment sensory-motor patterns are induced, the principle of cheap design where the proper embodiment leads to simpler and more robust control, the redundancy principle which states that proper choice and positioning of sensors leads to robust behavior, and the principle of ecological balance that explicitly capitalizes on the relation between morphology, materials, and neural control. For the purpose of illustration we will capitalize on the latter in this paper. We proceed by presenting a number of case studies illustrating the application of these principles to designing adaptive motion. In previous papers we have investigated in detail the effect of changing sensor morphology on neural processing (e.g. Lichtensteiger and Eggenberger, 1999; Maris and te Boekhorst, 1996; Pfeifer, 2000a, b; Pfeifer and Scheier, 1999). In this paper we focus on the motor system.

3.1 The passive dynamic walker

The passive dynamic walker which goes back to McGeer (1990a, b), illustrated in figure 1a, is a robot (or, if you like, a mechanical device) capable of walking down an incline, there are no motors and there is no microprocessor on the robot; it is brainless, so to speak. In order to achieve this task the passive dynamics of the robot, its body and its limbs, must be exploited (the robot is equipped with wide feet of a particular shape to guide lateral motion, soft heels to reduce instability at heel strike, counter-swinging arms to negate yaw induced by leg swinging, and lateral-swinging arms to stabilize side-to-side

lean (Collins et al., 2001)). This kind of walking is very energy efficient (the robot is – loosely speaking – operated near one of its Eigenfrequencies) and there is an intrinsic naturalness to it (perhaps the natural feel comes from the exploitation of the dynamics, e.g. the passive swing of the leg.). However, its “ecological niche” (i.e. the environment in which the robot is capable of operating) is extremely narrow: it only consists of inclines of certain angles.

A different approach has been taken by the Honda design team. There the goal was to have a robot that could perform a large number of different types of movements. The methodology was to record human movements and then to reproduce them on the robot which leads to a relatively natural behavior of the robot. On the other hand control – or the neural processing, if you like – is extremely complex and there is no exploitation of the intrinsic dynamics as in the case of the passive dynamic walker. The implication is also that the movement is not energy efficient. Of course, the Honda robot can do many things like walking up and down the stairs, pushing a cart, opening a door, etc., whereas the ecological niche of the passive dynamic walker is confined to inclines of a particular angle.

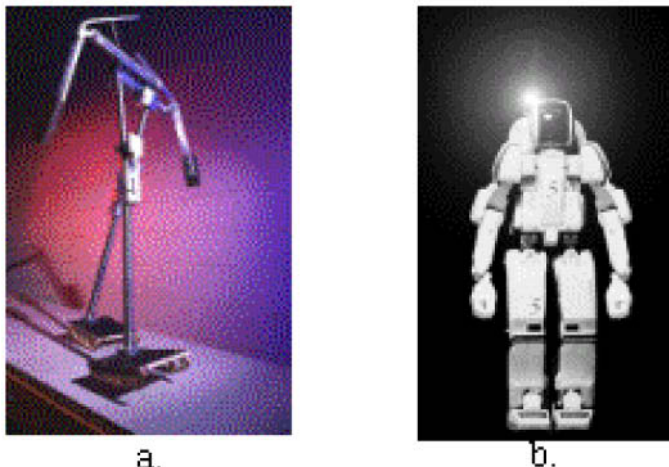


Fig. 1. Two approaches to robot building. (a) The passive dynamic walker (Collins et al., 2001), (b) the Honda robot Asimo.

In term of the design principles, this case study illustrates the principles of cheap design and ecological balance. The passive dynamic walker fully exploits the fact that it is always put on inclines that provide its energy source and generates the proper dynamics for walking. Loosely speaking, we

can also say that the control tasks, the neural processing, is taken over by having the proper morphology and the right materials. In fact, the neural processing reduces to zero. At the same time, energy efficiency is achieved. However, if anything is changed, e.g. the angle of the incline, the agent ceases to function. This is the trade-off of cheap design. In conclusion, as suggested by the principle of ecological balance, there is a kind of trade-off or balance: the better the exploitation of the dynamics, the simpler the control, the less neural processing will be required.

3.2 Muscles – control from materials: reaching and grasping

Let us pursue this idea of exploiting the dynamics a little further and show how it can be taken into account to design actual robots. Most robot arms available today work with rigid materials and electrical motors. Natural arms, by contrast, are built of muscles, tendons, ligaments, and bones, materials that are non-rigid to varying degrees. All these materials have their own intrinsic properties like mass, stiffness, elasticity, viscosity, temporal characteristics, damping, and contraction ratio to mention but a few. These properties are all exploited in interesting ways in natural systems. For example, there is a natural position for a human arm which is determined by its anatomy and by these properties. Reaching for and grasping an object like a cup with the right hand is normally done with the palm facing left, but could also be done – with considerable additional effort – the other way around. Assume now that the palm of your right hand is facing right and you let go. Your arm will immediately turn back into its natural position. This is not achieved by neural control but by the properties of the muscle-tendon system: On the one hand the system acts like a spring – the more you stretch it, the more force you have to apply and if you let go the spring moves back into its resting position. On the other there is intrinsic damping. Normally reaching equilibrium position and damping is conceived of in terms of electronic (or neural) control, whereas in this case, this is achieved (mostly) through the material properties. Or put differently, the morphology (the anatomy), and the materials provide physical constraints that make the control problem much easier. The main task of the brain, if you like, is to set the material properties of the muscles, the spring constants. Once these constraints are given, the control task is much simpler.

These ideas can be transferred to robots. Many researchers have started building artificial muscles (for reviews of the various technologies see, e.g., Kornbluh et al., 1998 and Shahinpoor, 2000) and used them on robots, as illustrated in figure 2.

Facial expressions also provide an interesting illustration for the point to be made here. If the facial tissue has the right sorts of material properties in terms of elasticity, deformability, stiffness, etc., the neural control for the facial expressions becomes much simpler. For example, for smiling, although

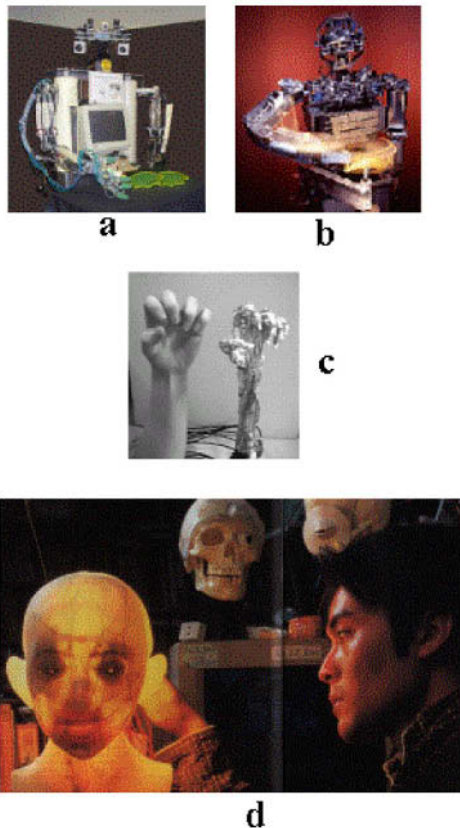


Fig. 2. Robots with artificial muscles. (a) The service robot ISAC by Peters (Vanderbilt University) driven by McKibben pneumatic actuators. (b) The humanoid robot Cog by Rodney Brooks (MIT AI Laboratory), driven by series-elastic actuators. (c) The artificial hand by Lee and Shimoyama (University of Tokyo), driven by pneumatic actuators. (d) The “Face Robot” by Kobayashi, Hara, and Iida (Science University of Tokyo), driven by shape-memory alloys.

it involves the entire face, the actuation is very simple: the “complexity” is added by the tissue properties.

3.3 The dancing robot Stumpy – a synthesis

Figure 3 shows the walking and hopping robot Stumpy which lower body is made of an inverted “T” mounted on wide springy feet. The upper body is an upright “T” connected to the lower body by a rotary joint, the “waist” joint, providing one degree of freedom in the frontal plane. The horizontal beam on the top is weighted on the ends to increase its moment of inertia.

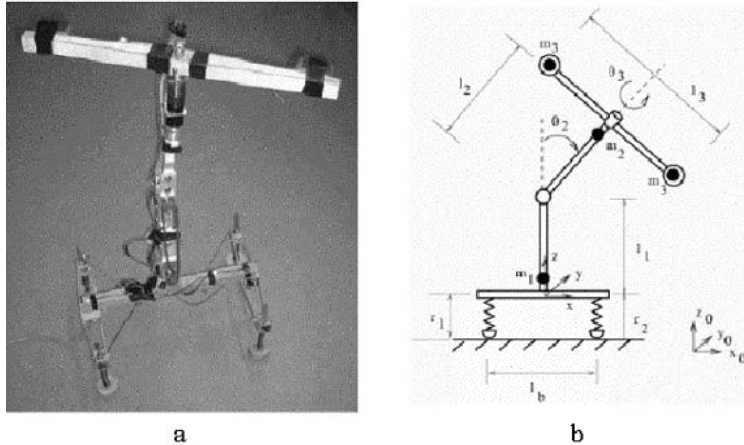


Fig. 3. The dancing, walking, and hopping robot Stumpy. (a) Photograph of the robot. (b) Schematic drawing (details, see text).

It is connected to the vertical beam by a second rotary joint, providing one rotational degree of freedom, in the plane normal to the vertical beam, the “shoulder” joint. Stumpy’s vertical axis is made of aluminum, while both its horizontal axes and feet are made of oak wood. Although Stumpy has no real legs or feet, it can locomote in many interesting ways: it can move forward in a straight or curved line, it has different gait patterns, it can move sideways, and it can turn on the spot. Interestingly, this can all be achieved by actuating only two joints with one degree of freedom – the robot is virtually “brainless”. The reason this works is because the dynamics, given by its morphology and its materials (elastic, spring-like materials, surface properties of the feet), is exploited in clever ways. There is a delicate interplay of momentum exerted on the feet by moving the two joints in particular ways (for more detail, see Paul et al., 2002a, b).

Let us briefly summarize the ideas concerning ecological balance. First, given a particular task environment, the (physical) dynamics of the agent can be exploited which leads not only to a natural behavior of the agent, but also to higher energy-efficiency. Second, by exploiting the dynamics of the agent, often control can be significantly simplified while maintaining a certain level behavioral diversity. Third, materials have intrinsic control properties. And fourth, because ecological balance is exploited, Stumpy displays a surprisingly diverse behavior (dancing walking, and hopping in different ways). In this sense, Stumpy also illustrates the diversity-compliance principle: on the one hand, it exploits the physical dynamics in interesting ways and on the other it displays high diversity.

In section 2 we postulated a set of design principles for adaptive motion. The principle of ecological balance, for example, tells us that given a particu-

lar task environment, there is an optimal task distribution between morphology, materials, and control. The principle of emergence asks the question of how a particular “balance” has emerged, how it has come about. In the study of biological systems, we can speculate about this question. However, there is a possibility of systematically investigating this balance, namely artificial evolution and morphogenesis. Pertinent experiments promise a deeper understanding of these relationships. The remainder of this paper will be devoted to this question.

4 Exploring “ecological balance”—artificial evolution and morphogenesis

The standard approach for using artificial evolution for design is to take a particular robot and use a genetic algorithm to evolve a control architecture for a particular task. The problem with including morphology and materials into our evolutionary algorithms is that the search space which is already very large for control architectures only, literally explodes.

This issue can be approached in various ways, we just mention two. The first is to parameterize the shapes, thus bringing in biases from the designer on the types of shapes that are possible. An example that has stirred a lot of commotion in the media recently is provided by Hod Lipson and Jordan Pollack’s robots that were automatically produced (Lipson and Pollack, 2000). While this example is impressive, it still implies a strong designer bias. If we want to explore different types of morphologies, we want to introduce as little designer bias as possible. This can be done using ideas from biology, i.e. genetic regulatory networks.

4.1 The mechanics of artificial genetic regulatory networks

The basic idea is the following. A genetic algorithm is extended to include ontogenetic development by growing agents from genetic regulatory networks. In the example presented here, agents are tested for how far they can push a large block (which is why they are called “block pushers”). Figure 4a shows the physically realistic virtual environment. The fitness determination is a two-stage process: the agent is first grown and then evaluated in its virtual environment. Figure 4b illustrates how an agent grows from a single cell into a multicellular organism, (for details, see, e.g. Bongard and Pfeifer (2001; in press)).

4.2 Emergence – the achievements of artificial evolution and morphogenesis.

Here are some observations: (1) Organisms early on in evolution are typically smaller than those of later generations: evolution discovers that in order to

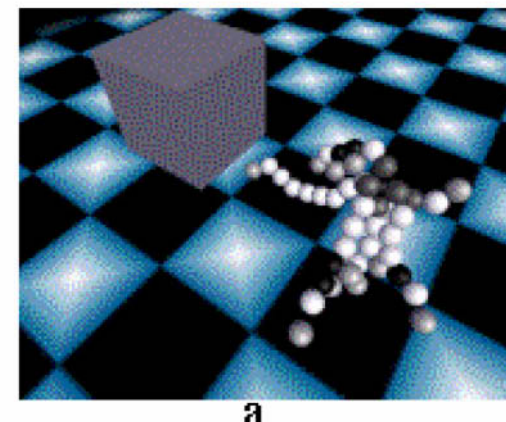
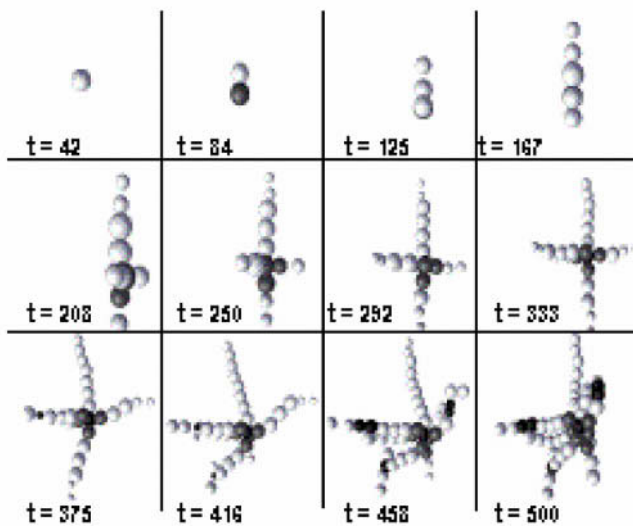
**a****b**

Fig. 4. Examples of Bongard's "block pushers". (a) An evolved agent in its physically realistic virtual environment. (b) growth phase starting from a single cell, showing various intermediate stages (last agent after 500 time steps).

push a block of large size, it is necessary to have a large body. (2) Evolution comes up with means of locomotion. In small creatures, these are very local reflex-like mechanisms distributed through the entire organism. Larger creatures tend to have additional tentacles that can be used to push against the block, which requires a different kind of control. (3) There is no direct

relation between genotype length and phenotypic fitness – the two are largely dissociated. (4) There is functional specialization, i.e. cells differentiate into units containing both sensors and actuators (the white colored cells in figure 4), cells that only contain sensors but no actuators (gray coloring), and cells not containing anything, only providing structural support (black coloring). (5) There is repeated structure, i.e. some combination of cells occur in slightly modified form in various places on the agent. An example from biology are fingers that are similar but differ individually. (6) Some genes specialize to become “master regulatory genes”, i.e. they regulate the activity of other genes. Thus, to an outside observer, it looks as if a hierarchical structure were evolving in the regulatory network. Note that this hierarchy is emergent and results from a “flat” dynamical system. Thus, it can change at a later point in time, unlike “structural” hierarchies. It is important to mention that this has all been “discovered” by simulated evolution and has not been programmed into the system.

5 Discussion and conclusions

By employing the form of design principles we have attempted to make a first step in the direction of providing a coherent framework for design. In the present form we have proposed the principles and argued why they are plausible. The passive dynamic walker and Stumpy provide illustrations of the principles of cheap design and ecological balance.

While this is acceptable and interesting, the design principles would be much more compelling and powerful if they could be demonstrated to emerge from an evolutionary process. Using the principles of genetic regulatory networks, we have worked out methods by which entire agents can be evolved, including their morphology, their material properties, and their control systems.

There are a number of limitations of this approach that we will put on the research agenda for the coming years. One is the incorporation of interaction with the environment during ontogenetic development. Moreover, the “rewrite rules” for neuronal growth will be replaced by more biological mechanisms. Third, instead of defining a fitness function, we will turn to “open-ended evolution” where the survival of the individual is the sole criterion. This requires the definition of pertinent resources that need to be maintained. Fourth, we need to incorporate the variation of material properties into the evolutionary algorithm, so that this aspect can be studied as well. And last but not least, we need to be able to increase the complexity of our task environments which requires much higher computational power.

Let us conclude by raising an issue that is always in the air when working with relatively simple systems (such as block pushers), the one of scalability. By scalability we mean in this context whether the methods proposed (genetic regulatory networks) will be sufficiently powerful to evolve much

more complex creatures capable of many behaviors in very different types of environments. This question, we believe is still open as it is not clear to what extent the real world plays an essential role in evolution, or whether simulated environments can be made sufficiently complex.

Acknowledgements

I would like to thank the members of the Artificial Intelligence Laboratory for many discussions, in particular Josh Bongard for his patience in explaining evolution to me and Gabriel Gómez for discussing the manuscript. Credit also goes to the Swiss National Science Foundation for supporting the research presented in this paper, grant # 20-61372.00.

References

1. Breazeal, C.L. (2002). *Designing Sociable Robots (Intelligent Robotics and Autonomous Agents)*. Cambridge, Mass.: MIT Press.
2. Bongard, J.C. (2002). Evolving modular genetic regulatory networks. In Proc. IEEE 2002 Congress on Evolutionary Computation (CEC2002). MIT Press, 305-311.
3. Bongard, J.C., and Pfeifer, R. (2001). Repeated structure and dissociation of genotypic and phenotypic complexity in artificial ontogeny. In L. Spector et al. (eds.). Proc. of the Sixth European Conference on Artificial Life, 401-412.
4. Collins, S.H., Wisse, M., and Ruina, A. (2001). A three-dimensional passive-dynamic walking robot with two legs and knees. The International Journal of Robotics Research, 20, 607-615.
5. Ishiguro, A., Ishimaru, K., Hayakawa, K., and Kawakatsu, T. (2003). Toward a “well-balanced” design: a robotic case study. How should control and body dynamics be coupled? This volume.
6. Hara, F., and Pfeifer, R. (2000). On the relation among morphology, material and control in morpho-functional machines. In Meyer, Berthoz, Floreano, Roitblat, and Wilson (eds.): From Animals to Animats 6. Proceedings of the sixth International Conference on Simulation of Adaptive Behavior 2000, 33-40.
7. Kornbluh, R. D., Pelrine, R., Eckerle, J., and Joseph, J. (1998). Electrostrictive polymer artificial muscle actuators. Proceedings of the IEEE International Conference on Robotics and Automation 1998. New York, N.Y.: IEEE, 2147-2154.
8. Lipson, H., and Pollack J. B. (2000), Automatic design and manufacture of artificial life forms. Nature, 406, 974-978.
9. Lichtensteiger, L., and Eggenberger, P. (1999). Evolving the morphology of a compound eye on a robot. Proceedings of the third European Workshop on Advanced Mobile Robots (Eurobot'99). IEEE, Piscataway, NJ, USA; 1999; 127-34 .
10. Manzotti, R. (2000). Intentional robots. The design of a goal-seeking environment-driven agent. Unpublished Doctoral Dissertation, University of Genova.

11. Maris, M., and te Boekhorst, R. (1996). Exploiting physical constraints: heap formation through behavioral error in a group of robots. Proceedings of the IROS'96, IEEE/RSJ International Conference on Intelligent Robots and Systems, 1655—1660.
12. McGeer, T. (1990a). Passive dynamic walking. *Int. Journal of Robotics Research*, 9, 62-82.
13. McGeer, T. (1990b). Passive walking with knees. Proc. of the IEEE Conference on Robotics and Automation, 2, 1640-1645.
14. Paul, C., Dravid, R. and F. Iida (2002a) Control of lateral bounding for a pendulum driven hopping robot. to appear in Proceedings of the International Conference of Climbing and Walking Robots , Paris, France (to appear)..
15. Paul, C., Dravid, R. and F. Iida (2002b) Design and Control of a Pendulum Driven Hopping Robot. Proc of the IEEE/RSJ International Conference on Intelligent Robots and Systems, IROS-2002, Lausanne, Switzerland (to appear).
16. Pfeifer, R. (1996). Building “Fungus Eaters”: Design principles of autonomous agents. In P. Maes, M. Mataric, J.-A. Meyer, J. Pollack, and S.W. Wilson (eds.): *From Animals to Animats 4*. Proceedings of the fourth International Conference on Simulation of Adaptive Behavior. Cambridge, Mass.: A Bradford Book, MIT Press, 3-12.
17. Pfeifer, R. (1999). Dynamics, morphology, and materials in the emergence of cognition. In Burgard, W., Christaller, T., Cremers, A. B. (eds.): *KI-99 Advances in Artificial Intelligence*. Proceedings of the 23rd Annual German Conference on Artificial Intelligence, Bonn, Germany, 1999, Lecture Notes in Computer Science, Springer, 1701, 27-44.
18. Pfeifer, R. (2000a). On the role of morphology and materials in adaptive behavior. In Meyer, Berthoz, Floreano, Roitblat, and Wilson (eds.): *From Animals to Animats 6*. Proceedings of the sixth International Conference on Simulation of Adaptive Behavior 2000, 23-32.
19. Pfeifer, R. (2000b). On the role of embodiment in the emergence of cognition and emotion. In H. Hatano, N. Okada, and H. Tanabe (eds.). *Affective minds*. Amsterdam: Elsevier, 43-57.
20. Pfeifer, R. (2001). Embodied Artificial Intelligence: 10 years back, 10 years forward. In: R. Wilhelm (ed.). *Informatics – 10 years back, 10 years ahead*. Lecture Notes in Computer Science. Berlin: Springer, 294-310.
21. Pfeifer, R. (in press). Robots as cognitive tools. *Journal of Cognitive Technology* (to appear).
22. Pfeifer, R. (2003). Morpho-functional machines: basics and research issues. In F. Hara, and R. Pfeifer (eds.). *Morpho-functional machines: the new species*. Tokyo: Springer, 2003.
23. Pfeifer, R., and Glatzeder, B. (in preparation). How the body shapes the way we think: the embodied revolution in artificial intelligence. Cambridge, Mass.: MIT Press.
24. Pfeifer, R., and Scheier, C. (1999). *Understanding intelligence*. Cambridge, Mass.: MIT Press.

Towards a “Well-Balanced” Design: How Should Control and Body Systems be Coupled?

Akio Ishiguro¹, Kazuhisa Ishimaru¹, and Toshihiro Kawakatsu²

¹ Dept. of Computational Science and Engineering, Nagoya University, Nagoya 464-8603, Japan

² Dept. of Physics, Tohoku University, Sendai 980-8578, Japan

Abstract. This study is intended to deal with the interdependency between control and body systems, and to discuss the “relationship as it should be” between these two systems. To this end, a decentralized control of a multi-legged robot is employed as a practical example. The results derived indicate that the convergence of decentralized gait control can be significantly ameliorated by modifying its interaction between the control system and its body system to be implemented.

1 Introduction

In robotics, traditionally, a so-called *hardware first, software last* based design approach has been employed, which seems to be still dominant. Recently, however, it has been widely accepted that the emergence of intelligence is strongly influenced by not only control systems but also their embodiments, that is the physical properties of robots’ body[1]. In other words, the intelligence emerges through the interaction dynamics among the control systems (*i.e.* brain-nervous systems), the embodiments (*i.e.* musculo-skeletal systems), and their environment (*i.e.* ecological niche). In sum, control dynamics and its body (*i.e.* mechanical) dynamics cannot be designed *separately* due to their tight interdependency. This leads to the following conclusions: (1) there should be a “best combination” or a “well-balanced coupling” between control and body dynamics, and (2) one can expect that quite an interesting phenomenon will emerge under such well-balanced coupling.

On the other hand, since the seminal works of Sims[2][3], so far various methods have been intensively investigated in the field of Evolutionary Robotics by exploiting concepts such as *co-evolution*, in the hope that they allow us to simultaneously design control and body systems[4][5]. Most of them, however, have mainly focused on automatically creating both control and body systems, and thus have paid less attention to gain an understanding of well-balanced coupling between the two dynamics. To our knowledge, still very few studies have explicitly investigated this point, *i.e.*, appropriate coupling¹.

¹ Pfeifer introduced several useful design principles for constructing autonomous agents[1]. Among them, *the principle of ecological balance* does closely relate to

In light of these facts, this study is intended to deal with the interaction dynamics between control and body systems, and to analytically and synthetically discuss a well-balanced relationship between the dynamics of these two systems. More specifically, the aim of this study is to clearly answer the following questions:

- How these two dynamics should be coupled?
- What sort of phenomena will emerge under the well-balanced coupling?

Since there are virtually no studies in existence which discuss what the well-balanced coupling is, it is of great worth to accumulate various case studies at present. Based on this consideration, a decentralized control of a multi-legged robot consisting of several body segments is employed as a practical example. The derived result indicates that the convergence of decentralized gait control can be significantly ameliorated by modifying both control dynamics (*e.g.* information pathways among the body segments) and body dynamics (*e.g.* stiffness of the spine) to be implemented.

2 Lessons from biological findings

Before explaining our approach, it is highly worthwhile to look at some biological findings. Beautiful instantiations of well-balanced couplings between nervous and body systems can be found particularly in insects. In what follows, let us briefly illustrate some of these instantiations.

Compound eyes of some insects such as houseflies show special *facet*, *i.e.*, vision segment, distributions; the facets are densely spaced toward the front whilst widely on the side. Franceschini *et al.* demonstrated with a real physical robot² that this non-uniform layout significantly contributes to detect easily and precisely the movement of an object without increasing the complexity of neural circuitry[6].

Another elegant instantiation can be observed in insects' wing design[9][10]. As shown in Fig.1(a), very roughly speaking, insects' wings are composed of hard and soft materials. It should be noted that the hard material is distributed asymmetrically along the moving direction. Due to this material configuration, insects' wings show complicated behavior during each stroke cycle, *i.e.*, twist and oscillation. This allows them to create useful aerodynamic force, and thus they can realize agile flying. If they had symmetrical material configuration as shown in Fig.1(b), the complexity of neural circuitry responsible for flapping control would be significantly increased.

this point, which states that control systems, body systems and their material to be implemented should be balanced. However, there still remains much to be understood about how these systems should be coupled.

² Another interesting robot can be found in [7][8].

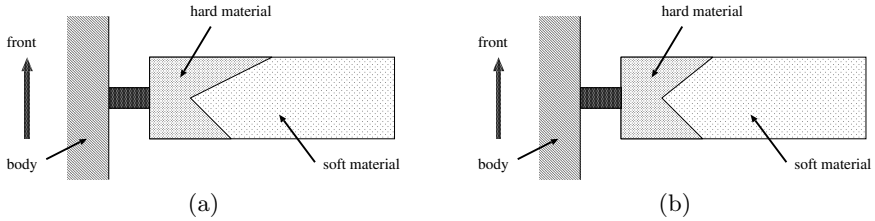


Fig. 1. Material configuration in insects' wings.

3 The model

In order to investigate *well-balanced coupling as it should be* between control and body systems, a decentralized control of a multi-legged robot is taken as a case study. Figure 2 schematically illustrates the structure of the multi-legged robot. As shown in the figure, this robot consists of several identical body segments, each of which has two legs, *i.e.*, right and left legs. For simplicity, the right and left legs of each body segment are allowed to move in phase, and the duty factor and trajectory of all the legs are assumed to be identical, which have to be prespecified before actually moving the robot. For convenience, hereafter the phase of the leg movement of the i th body segment is denoted as θ_i ($i = 1, 2, \dots, n$). Thus, the control parameters in this model end up to be the set of the phases $\theta_1, \theta_2, \dots, \theta_n$.

The task of this robot is to realize rapid gait convergence which leads to a gait with minimum energy consumption rate from arbitrary initial relative-phase conditions. Note that each body segment controls the phase of its own legs in a decentralized manner, which will be explained in more detail in the following section.

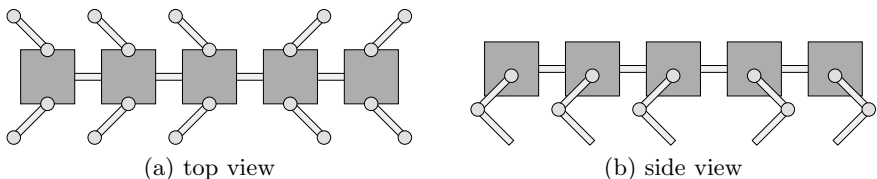


Fig. 2. Structure of the multi-legged robot taken as a practical example.

4 Proposed method

4.1 Analysis of the gait convergence

Based on the above arrangements, this section analytically discusses how the control and body dynamics influence the gait convergence. Let P be the total energy consumption rate of this robot, then P can be expressed as a function of the phases as:

$$P = P(\boldsymbol{\theta}), \quad (1)$$

$$\boldsymbol{\theta} = (\theta_1, \theta_2, \dots, \theta_n)^T. \quad (2)$$

Here, for the purposes of simplified analysis, a simple learning scheme based on a *gradient method* is employed. It is denoted by

$$\Delta\boldsymbol{\theta}^{(k)} = -\boldsymbol{\eta} \frac{\partial P(\boldsymbol{\theta})}{\partial \boldsymbol{\theta}} \Big|_{\boldsymbol{\theta}^{(k)}}, \quad (3)$$

where $\Delta\boldsymbol{\theta}^{(k)}$ is the phase modification at time step k , $\boldsymbol{\eta}$ is an $n \times n$ matrix which specifies how a body segment will exploit the information about phase modification done in other body segments in its determination of the phase modification. Based on Equation (3), the set of the phases at time step k is expressed in the following form:

$$\boldsymbol{\theta}^{(k+1)} = \boldsymbol{\theta}^{(k)} + \Delta\boldsymbol{\theta}^{(k)} = \boldsymbol{\theta}^{(k)} - \boldsymbol{\eta} \frac{\partial P(\boldsymbol{\theta})}{\partial \boldsymbol{\theta}} \Big|_{\boldsymbol{\theta}^{(k)}}. \quad (4)$$

Let $\boldsymbol{\theta}^{(\infty)}$ be a set of converged phases. By performing the Taylor series expansion around $\boldsymbol{\theta}^{(\infty)}$, the partial differentiation of $P(\boldsymbol{\theta})$ with respect to $\boldsymbol{\theta}$ is:

$$\frac{\partial P(\boldsymbol{\theta})}{\partial \boldsymbol{\theta}} \simeq \mathbf{C}(\boldsymbol{\theta} - \boldsymbol{\theta}^{(\infty)}), \quad (5)$$

$$\mathbf{C} = \frac{\partial^2 P(\boldsymbol{\theta})}{\partial \boldsymbol{\theta} \partial \boldsymbol{\theta}} \Big|_{\boldsymbol{\theta}^{(\infty)}}, \quad (6)$$

where \mathbf{C} is an $n \times n$ *Hesse* matrix. Hence, the substitution of Equation (5) into Equation (4) yields:

$$\boldsymbol{\theta}^{(k+1)} = \boldsymbol{\theta}^{(k)} - \boldsymbol{\eta} \mathbf{C}(\boldsymbol{\theta}^{(k)} - \boldsymbol{\theta}^{(\infty)}). \quad (7)$$

For the sake of the following discussion, a *residual vector* $\mathbf{e}^{(k)}$ is introduced, which is equivalent to $\boldsymbol{\theta}^{(k)} - \boldsymbol{\theta}^{(\infty)}$. Then, Equation (7) can be rewritten as:

$$\mathbf{e}^{(k+1)} = \mathbf{A} \mathbf{e}^{(k)}, \quad (8)$$

$$\mathbf{A} = \mathbf{I} - \boldsymbol{\eta} \mathbf{C}, \quad (9)$$

where \mathbf{I} is an $n \times n$ unit matrix.

4.2 Physical meaning of $\boldsymbol{\eta}$ and \mathbf{C}

\mathbf{A} in Equation (8) is a matrix which characterizes the property of gait convergence. This will automatically lead to the following fact: for rapid convergence, the spectral radius of \mathbf{A} should be less than 1.0.

What should be stressed here is the fact that as shown in Equation (9) the matrix \mathbf{A} is composed of the two matrices: $\boldsymbol{\eta}$ and \mathbf{C} . As has been already explained, the matrix $\boldsymbol{\eta}$ specifies the information pathways (or neuronal/axonal interconnectivity) among the body segments, which will be used to calculate the phase modification. This implies that the matrix $\boldsymbol{\eta}$ does relate to the design of the control dynamics.

On the other hand, obviously from the definition (see Equation (6)), \mathbf{C} is a matrix whose nondiagonal elements will be salient as the *long-distance interaction* among the body segments through the physical connections (*i.e.* the spine of the robot) becomes significant. This strongly suggests that the property of this matrix is highly influenced by the design of the body dynamics.

4.3 An effective design of the body dynamics

The design of the control dynamics can be easily done by tuning the elements of the matrix $\boldsymbol{\eta}$. In contrast, much attention has to be paid to the design of the body dynamics. This is simply because one cannot *directly* access the elements of the matrix \mathbf{C} nor tune them unlike the matrix $\boldsymbol{\eta}$.

Before introducing our proposed method, let us briefly conduct a simple yet instructive thought experiment. Imagine a multi-legged robot in which its body segments are tightly connected via a *rigid* spine. In such a case, the phase modification of a certain leg will significantly affect the energy consumption rate of distant legs due to the effect of the *long-distance* interaction.

As has been demonstrated in the thought experiment mentioned above, the *stiffness* of the spine poses serious influence on the property of the matrix \mathbf{C} , particularly the values of its nondiagonal elements. Therefore, it seems to be reasonable to connect the body segments via a *springy* joint. This idea is schematically illustrated in Fig. 3, in which only the two body segments are shown for clarity.

Based on the above consideration, a well-balanced design is investigated by tuning the parameters in the matrix $\boldsymbol{\eta}$ and the ones of the springs inserted between the body segments, which will lead to a reasonable gait convergence.

5 Preliminary simulation results

In order to efficiently investigate well-balanced coupling, a simulator has been developed. The following simulations have been conducted with the use of a

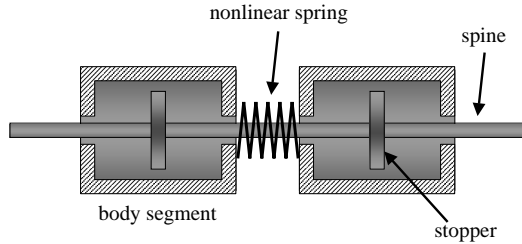


Fig. 3. An effective structure for adjusting the body dynamics.

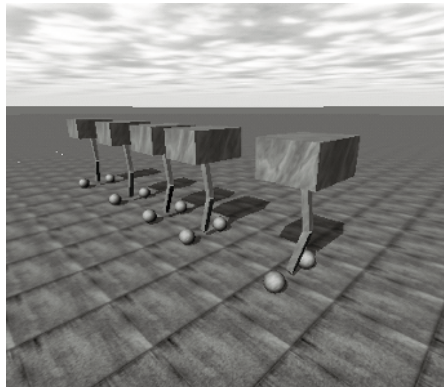


Fig. 4. A view of the developed simulator.

physics-based, three-dimensional simulation environment[11]. A view of the developed simulator is shown in Fig. 4. This environment simulates both the internal and external forces acting on the agent and objects in its environment, as well as various other physical properties such as contact between the agent and the ground, and torque applied by the motors to the joints within an acceptable time limit.

Before carrying out a thorough search of the design parameters, a preliminary experiment has been done to understand the influence of the two dynamics on the gait convergence. In this experiment, the property of the spring inserted between the body segments is assumed to be expressed as:

$$f = -k(\Delta x)^\alpha, \quad (10)$$

where f is the resultant force, k is a spring constant, α controls the degree of the nonlinearity of the spring, and Δx is a displacement.

Shown in Fig. 5 are the resultant data in this experiment; the vertical axis denotes the total energy consumption rate whilst the horizontal axis

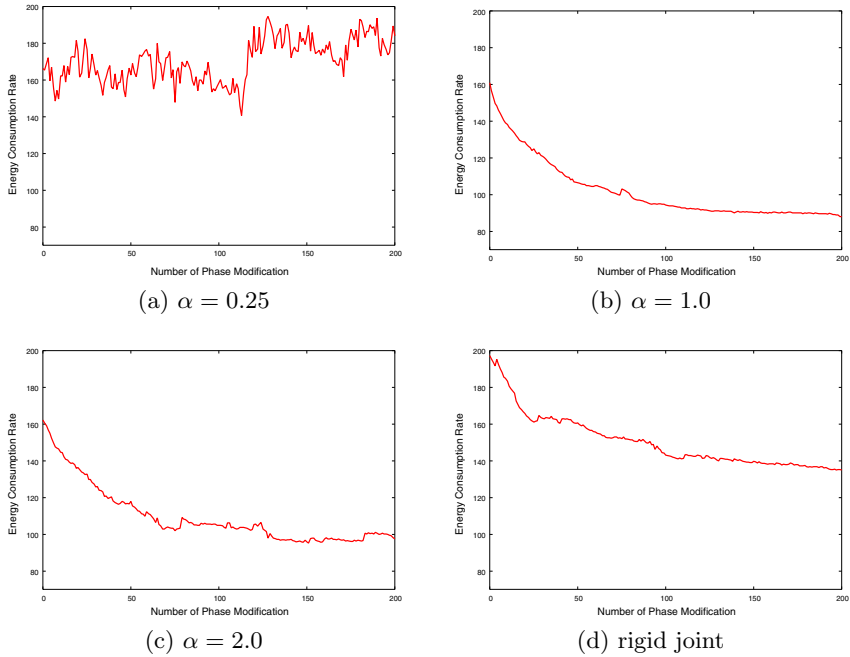


Fig. 5. Preliminary simulation results.

depicts the number of phase modification conducted. Note that each graph was obtained by averaging over 20 different initial relative-phase conditions. As a rudimentary stage of the investigation, only α was varied under the following conditions: the number of the body segments was 5; duty factor 0.5; k 1.0; and η set to $0.04 \times \mathbf{I}$. For the ease of comparison, a representative data under the condition where the body segments were connected via rigid joints is also depicted (see in the figure (d)). As shown in Fig. 5, the gait convergence is highly influenced by the stiffness of the joints, which leads to varying the property of the matrix C .

At present, due to the computationally expensive cost, the parameter optimization for both the control and body systems is totally difficult to be done systematically. Therefore, we took a quite primitive approach; we tried to manually tune these parameters. A best individual obtained in a hand-crafted manner is illustrated in Fig. 6. This data was obtained under the

following conditions: the number of the body segments was 5; duty factor 0.5; k 1.0; α 1.0; and η set to

$$0.04 \times \begin{pmatrix} 1.000 & -0.472 & 0.223 & -0.105 & 0.049 \\ -0.472 & 1.000 & -0.472 & 0.223 & -0.105 \\ 0.223 & -0.472 & 1.000 & -0.472 & 0.223 \\ -0.105 & 0.223 & -0.472 & 1.000 & -0.472 \\ 0.049 & -0.105 & 0.223 & -0.472 & 1.000 \end{pmatrix}.$$

Interestingly, this result outperforms the ones shown in Fig. 5. In spite of the simplicity, these results strongly support the conclusion that the interdependency between the control and body dynamics imposes significant influence on the gait convergence.

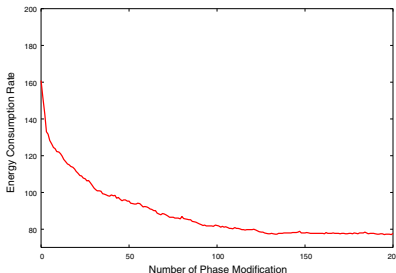


Fig. 6. A representative data obtained by hand-crafted optimization.

6 Conclusion and future work

This paper investigated “well-balanced coupling as it should be” between control and body systems. For this purpose, a decentralized control of a multi-legged robot was employed as a case study. The preliminary experiments conducted in this paper support several conclusions and have clarified some interesting phenomena for further investigation, which can be summarized as: first, control and body dynamics significantly influence the gait convergence; second, well-balanced design in this case study can be analytically discussed in terms of the spectral radius of a matrix which specifies the property of gait convergence; third and finally, as demonstrated in the preliminary experiments, the property of gait convergence can be tuned by varying the dynamics experimentally, which suggests that there should be an appropriate coupling between the two systems.

In order to gain a deep insight into what well-balanced coupling is and should be, an intensive search of the design parameters in the control and body systems is highly indispensable. For this purpose, it seems to be reasonable to implement an *evolutionary computation scheme* such as a genetic

algorithm to efficiently search these parameters. This is currently under investigation. In addition to this simulations, a real physical robot is currently being constructed for experimental verification. A view of this experimental robot is shown in Figure 7. For clarity, the springy joints implemented between the body segments of this robot is also illustrated in the figure.

Another important point to be stressed is closely related to the concept of *emergence*. One of the crucial aspects of intelligence is the *adaptability* under hostile and dynamically changing environments. How can such a remarkable ability be achieved under limited/finite computational resources? One and the only solution would be to exploit *emergence phenomena* created by the interaction dynamics among control systems, body systems, and their environment. This research is a first step to shed some light on this point in terms of balancing control systems with their body systems.

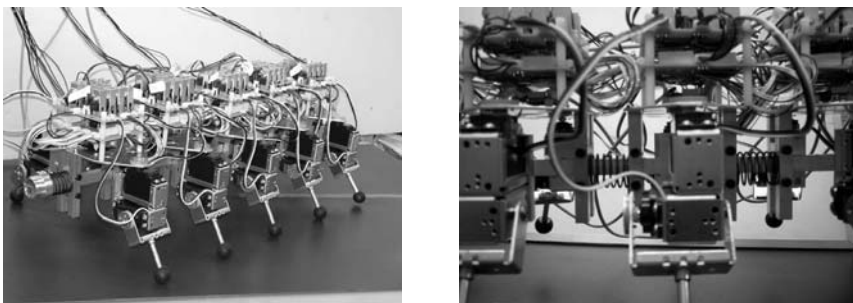


Fig. 7. The experimental multi-legged robot developed. Left: an overall view. Right: Springy joints implemented between the body segments of the experimental robot for the adjustment of its body dynamics.

Acknowledgements

This research was supported in part by a Grant-in-Aid from the Japanese Ministry of Education, Culture, Sports, Science and Technology (No. 14750367) and a Grant-in-Aid from The OKAWA Foundation for Information and Telecommunications (No. 02-22). Many helpful suggestions for the simulator from Yutaka Nakagawa at our laboratory, Josh C. Bongard at Computational Synthesis Lab. of Cornell University, and Martin C. Martin at AI lab. of Massachusetts Institute of Technology were greatly appreciated.

References

1. R. Pfeifer and C. Scheier: Understanding Intelligence, MIT Press (1999)

2. K. Sims: Evolving virtual creatures, *Computer Graphics*, 28, pp.15-34 (1994)
3. K. Sims: Evolving 3D morphology and behavior by competition, *Artificial Life IV Proceedings*, MIT Press, pp.28-39 (1994)
4. W.P. Lee, J. Hallam, and H.H. Lund: A Hybrid GA/GP Approach for Co-evolving Controllers and Robot Bodies to Achieve Fitness-Specified Tasks, *Proc. of The IEEE 3rd International Conference on Evolutionary Computation*, pp.384-389 (1996)
5. C. Paul and J.C. Bongard: The Road Less Traveled: Morphology in the Optimization of Biped Robot Locomotion, *Proc. of The IEEE/RSJ International Conference on Intelligent Robots and Systems* (2001)
6. N. Franceschini, J.M. Pichon, and C. Blanes: From insect vision to robot vision, *Philosophical Transactions of the Royal Society*, London B, 337, pp.283-294 (1992)
7. L. Lichtensteiger and P. Eggenberger: Evolving the Morphology of a Compound Eye on a Robot, *Proc. of The Third European Workshop on Advanced Mobile Robots*, pp.127-134 (1999)
8. L. Lichtensteiger and R. Salomon: The Evolution of an Artificial Compound Eye by Using Adaptive Hardware, *Proc. of The 2000 Congress on Evolutionary Computation*, pp.1144-1151 (2000)
9. R. Wootton: How Flies Fly, *Nature*, Vol.400(8 July), pp.112-113 (1999)
10. R. Wootton: Design, Function and Evolution in the Wings of Holometabolous Insects, *Zoologica Scripta*, Vol.31, No.1, pp.31-40 (2002)
11. <http://www.q12.org/ode/ode.html>

Experimental Study on Control of Redundant 3-D Snake Robot Based on a Kinematic Model

Fumitoshi Matsuno and Kentaro Suenaga

Department of Mechanical Engineering and Intelligent Systems, University of Electro-Communications, 1-5-1 Chofu-ga-oka, Chofu, Tokyo 182-8585, Japan

Abstract. In this paper, we derive a kinematic model and a control law for 3D snake robots which have wheeled link mechanism. We define the redundancy controllable system and find that introduction of links without wheels makes the system redundancy controllable. Using redundancy, it becomes possible to accomplish both main objective of controlling the position and the posture of the snake robot head, and sub-objective of the singular configuration avoidance. Experiments demonstrate the effectiveness of the proposed control law.

1 Introduction

Unique and interesting gait of the snakes makes them able to crawl, climb a hill, climb a tree by winding and move on very slippery floor [1]. Snake does not have hands and legs, however it has many functions. It is useful to consider and understand the mechanism of the gait of the snakes for mechanical design and control law of snake robots.

Snake robots are active code mechanism and useful for search and rescue operation in disaster. Utilization of autonomous intelligent robots in Search and Rescue is a new challenging field of robotics dealing with tasks in extremely hazardous and complex disaster environments. Intelligent, biologically-inspired mobile robots, and, in particular, snake-like robots have turned out to be the widely used robot type, aiming at providing effective, immediate, and reliable response to many strategic planning for search and rescue operations. Design and control of the snake-like robot have recently been receiving much attention, and many locomotion modes for snake-like robot have been proposed [2–5].

Hirose has long investigated snake robots and produced several snake robots, and he models the snake by a wheeled link mechanism with no side slip [2]. Some other snake-like mechanisms are developed in [3–5]. The present research [2,4,5] is looking for other variety of possible locomotion modes "Ring mode", "Inching mode", "Wheeled Locomotion mode" and "Bridge mode" as shown in Fig. 1.

1. Ring mode: The two ends of the robot body are brought together by its own actuation to form a circular shape. The drive to make the uneven circular shape to rotate is expected to be achieved by proper deformation and shifting the center of gravity as necessary.

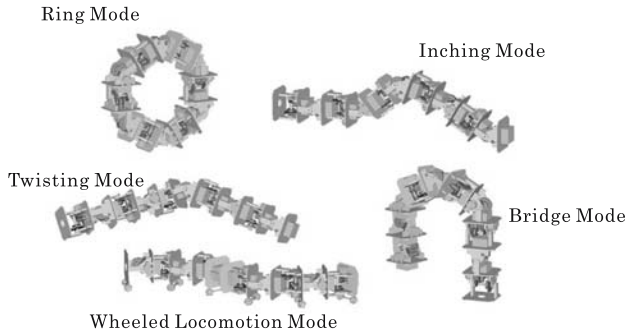


Fig. 1. Variety of possible locomotion of snake robot

2. Inching mode: This is one of the common undulatory movements of serpentine mechanisms. The robot generates a vertical wave-shape using its units from the rear end and propagates the 'wave' along its body - resulting a net advancement in its position.
3. Twisting mode: In this mode the robot mechanism folds certain joints to generate a twisting motion within its body, resulting in a side-wise movement [5].
4. Wheeled locomotion mode: This is one of the common wheeled locomotion mode where the passive wheels (without direct drive) are attached on the units resulting low friction along the tangential direction of the robot body line while increasing the friction in the direction perpendicular to that [2].
5. Bridge mode: In this mode the robot configures itself to "stand" on its two end units in a bridge like shape. This mode has the possibility of implementation of two-legged walking type locomotion. The basic movement consists of left-right swaying of the center of gravity in synchronism with by lifting and forwarding one of the supports, like bipedal locomotion. Motions such as somersaulting may also be some of the possibilities.

The snake robots which have many functions, locomotion modes and 3D motion have been developed, but in the study of controller design for the snake robots the movement is restricted to 2D motion. Construction of a controller which accomplishes 3D motion of 3D snake robots is one of challenging and important problems.

Chirikjian and Burdick discuss the sidewinding locomotion of the snake robots based on the kinematic model [6]. Ostrowski and Burdick analyze the controllability of a class of nonholonomic systems, that the snake robots are included, on the basis of the geometric approach [7]. The feedback control law for the snake head's position using Lyapunov method has been developed by Prautesch et al. on the basis of the wheeled link model [8]. They point out the controller can stabilize the head position of the snake robot to its desired

value, but the configuration of it converges to a singular configuration. We find that introduction of links without wheels and shape controllable points in the snake robot's body makes the system redundancy controllable.

In this paper we consider the singular configuration avoidance of the redundant 3D snake robots. Using redundancy, it becomes possible to accomplish both the main objective of controlling the position and the posture of the snake robot head and the sub-objective of the singular configuration avoidance. Experimental results by using a 13-link snake robot (ACM-R3 [9]) are shown.

2 Redundancy controllable system

In our previous paper we define the redundancy controllable system and propose structure design methodology of redundant snake robots based on the wheeled link model [10].

Let $\mathbf{q} \in R^{\bar{n}}$ be the state vector, $\mathbf{u} \in R^{\bar{p}}$ be the input vector, $\mathbf{w} \equiv S\mathbf{q} \in R^{\bar{q}}$ be the state vector to be controlled, S be a selection matrix whose row vectors are independent unit vectors related to generalized coordinates, $A(\mathbf{q}) \in R^{\bar{m} \times \bar{q}}$, $B(\mathbf{q}) \in R^{\bar{m} \times \bar{p}}$, where \bar{m} is number of equations. We define that the system

$$A(\mathbf{q})\dot{\mathbf{w}} = B(\mathbf{q})\mathbf{u}, \quad \mathbf{u} = \mathbf{u}_1 + \mathbf{u}_2 \quad (1)$$

is redundancy controllable if $\bar{p} > \bar{q}$ (redundancy I), $\bar{p} > \bar{m}$ (redundancy II),¹ the matrix A is full column rank, B is full row rank, and following two conditions are satisfied.

1. There exists an input \mathbf{u}_1 which accomplishes the main objective of the convergence of the vector \mathbf{w} to the desired state \mathbf{w}_d ($\mathbf{w} \rightarrow \mathbf{w}_d$, $\dot{\mathbf{w}} \rightarrow \dot{\mathbf{w}}_d$).
2. There exists an input $\mathbf{u} = \mathbf{u}_1 + \mathbf{u}_2$ which accomplishes the increase (or decrease) of a cost function $V(\mathbf{q})$ related to the sub-objective compared to the input \mathbf{u}_1 and does not disturb the main objective.

For a snake robot based on the wheeled link model we discuss the condition that the system is redundancy controllable [10].

3 Kinematic model of snake robots

Let us consider a redundant n -link snake robot on a flat plane. We introduce a coordinate frame Σ_A which is fixed on the head of the snake robot. The tip point of the snake head is taken as the origin of Σ_A . The reference configuration is set as a straight line configuration on the ground as shown in Fig. 2. The ${}^A x$ axis is set as the central body axis of the snake robot taking the

¹ In the case of $\bar{m} = \bar{p}$, if the state vector to be controlled $\dot{\mathbf{w}}$ in (1) is given, the input \mathbf{u} is determined uniquely. In this sense the system is not redundant, so we introduce the redundancy II.

reference configuration. All joints rotate around y axis or z axis in the reference configuration. Let ${}^A\hat{l}_i = [l_i, 0, 0]^T$ be a link vector from the i -th joint to the $(i - 1)$ -th joint with respect to Σ_A in Fig. 2. Let ϕ_i be the relative

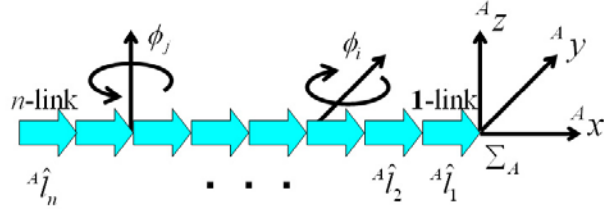


Fig. 2. Reference configuration of 3D snake robot

joint angle between link i and $i + 1$. The link vector ${}^A l_i$ with respect to Σ_A is expressed as

$${}^A l_i = R_{\phi_1} \cdots R_{\phi_{i-1}} {}^A \hat{l}_i \quad (i = 1, \dots, n) \quad (2)$$

where R_{ϕ_i} is $Rot(y, \phi_i) = R^{j\phi_i}$ or $Rot(z, \phi_i) = R^{k\phi_i}$. The 3D snake robot divided two parts. One is the base part and the other is the head part. We define that the first n_h links (head part) are not contact with the ground, and the residual n_b links (base part) are on the same plane which is parallel to the ground. In the base part wheeled links are contact with the ground. Let us introduce inertial Cartesian coordinate frame Σ_W and the coordinate frame Σ_B which is fixed on the end point of the base part (($n_h + 1$)-th link) as shown in Fig. 3. We introduce following three assumptions.

[assumption 1]: All joints of the base part rotate around z axis.

[assumption 2]: Environment is flat.

[assumption 3]: The robot is supported by the wheels of the base part and the head part is not contact with the ground.

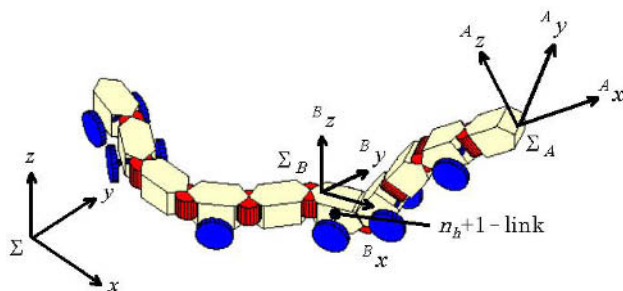


Fig. 3. Coordinate systems of 3D snake robot

The rotation matrix from Σ_B to Σ_A is given as

$${}^A R_B = R_{\phi_1} \cdots R_{\phi_{n_h}}. \quad (3)$$

Let ψ be the absolute attitude angle of the head of the base part about z axis, then the rotation matrix from Σ_B to Σ is expressed as

$${}^W R_B = R^{k\psi} \quad (4)$$

where $R^{k\psi} = \text{Rot}(z, \psi)$. The rotation matrix ${}^W R_A$ from Σ_A to Σ is expressed as

$${}^W R_A = {}^W R_B ({}^A R_B)^{-1} = R^{k\psi} R_{-\phi_{n_h}} \cdots R_{-\phi_1}. \quad (5)$$

Using (5) and (2) gives the link vector \mathbf{l}_i with respect to Σ

$$\begin{aligned} \mathbf{l}_i &= R^{k\psi} R_{-\phi_{n_h}} \cdots R_{-\phi_i} {}^A \hat{\mathbf{l}}_i \quad (i = 1, \dots, n_h) \\ \mathbf{l}_{n_h+1} &= R^{k\psi} {}^A \hat{\mathbf{l}}_{n_h+1} \\ \mathbf{l}_i &= R^{k\psi} R_{\phi_{n_h+1}} \cdots R_{\phi_{i-1}} {}^A \hat{\mathbf{l}}_i \quad (i = n_h + 2, \dots, n). \end{aligned} \quad (6)$$

Let (R, P, Y) be roll, pitch, yaw angles, then we obtain

$$\begin{aligned} R &= \text{atan2}(\pm \tilde{R}_{32}, \pm \tilde{R}_{33}) \\ P &= \text{atan2}(-\tilde{R}_{31}, \pm \sqrt{\tilde{R}_{11}^2 + \tilde{R}_{21}^2}) \\ Y - \psi &= \text{atan2}(\pm \tilde{R}_{21}, \pm \tilde{R}_{11}) \end{aligned} \quad (7)$$

where $\tilde{R} = R_{-\phi_{n_h}} \cdots R_{-\phi_1}$. Using (6) and (7) yields

$$\begin{aligned} \mathbf{l}_i &= R^{k(Y - \text{atan2}(\pm \tilde{R}_{21}, \pm \tilde{R}_{11}))} R_{-\phi_{n_h}} \cdots R_{-\phi_i} {}^A \hat{\mathbf{l}}_i \\ &\quad (i = 1, \dots, n_h) \\ \mathbf{l}_{n_h+1} &= R^{k(Y - \text{atan2}(\pm \tilde{R}_{21}, \pm \tilde{R}_{11}))} {}^A \hat{\mathbf{l}}_{n_h+1} \\ \mathbf{l}_i &= R^{k(Y - \text{atan2}(\pm \tilde{R}_{21}, \pm \tilde{R}_{11}))} R_{\phi_{n_h+1}} \cdots R_{\phi_{i-1}} {}^A \hat{\mathbf{l}}_i \\ &\quad (i = n_h + 2, \dots, n). \end{aligned} \quad (8)$$

The middle position $\mathbf{P}_i = [x_i, y_i, z_i]^T$ of the rotational axis of two wheels attached on the link i is expressed as

$$\mathbf{P}_i = \mathbf{P}_h - \mathbf{l}_1 - \mathbf{l}_2 - \cdots - \mathbf{l}_{i-1} - \frac{l_{wi}}{l_i} \mathbf{l}_i \quad (9)$$

where \mathbf{P}_h is the position vector of the snake head and l_{wi} is the distance between the joint i and the attached position of the wheel of the link i . As the wheel does not slip to the side direction, the velocity constraint condition should be satisfied. If the i -th link is wheeled and contact with the ground, the constraint can be written as

$$\dot{x}_i \sin \theta_i - \dot{y}_i \cos \theta_i = 0 \quad (10)$$

where θ_i is the absolute attitude of the i -th link about z -axis and it is expressed as

$$\begin{aligned}\theta_i &= \psi + \sum_{j=n_h+1}^{i-1} \phi_j \\ &= Y - \text{atan2}(\pm \tilde{R}_{21}, \pm \tilde{R}_{11}) + \sum_{j=n_h+1}^{i-1} \phi_j.\end{aligned}\quad (11)$$

From the assumption 3 z -element of the position vector of the first link of the base part is constant. We set it as h , then we obtain

$$(\mathbf{P}_h - \mathbf{l}_1 - \mathbf{l}_2 - \cdots - \mathbf{l}_{n_h})^T \mathbf{e}_z = h \quad (12)$$

where $\mathbf{l}_z = [0 \ 0 \ 1]^T$. Using time derivative of the geometric relation (7)(9)(12) and the velocity constraint condition (10) yields kinematic model of 3D snake robot.

4 Condition for redundancy controllable system

We consider control of position and posture of the snake head. Let $\mathbf{w} = [x_h \ y_h \ z_h \ R \ P \ Y]^T$ be the vector of the position and the posture of the snake head, $\boldsymbol{\theta} = [\phi_1 \ \cdots \ \phi_{n-1}]^T$ be the vector of relative joint angles, $\mathbf{q} = [\mathbf{w}^T \ \boldsymbol{\theta}^T]^T \in \mathbb{R}^{n+5}$ be the generalized coordinates. The angular velocity of each joint is regarded as the input of the robot system. If a wheel free link is connected to the tail, the movement of the added link does not contribute to the movement of the snake head. So we assume that wheel is attached at the tail link. If all links are wheeled, then we obtain

$$\bar{A}(\mathbf{q})\dot{\mathbf{w}} = \bar{B}(\mathbf{q})\mathbf{u}, \quad \mathbf{u} = \dot{\boldsymbol{\theta}} \quad (13)$$

where

$$\begin{aligned}\bar{A} &= \begin{bmatrix} a_{11} & a_{12} & 0 & 0 & 0 & a_{16} \\ a_{21} & a_{22} & 0 & 0 & 0 & a_{26} \\ \vdots & \vdots & \vdots & \vdots & \vdots & \vdots \\ a_{n_b 1} & a_{n_b 2} & 0 & 0 & 0 & a_{n_b 6} \\ 0 & 0 & 1 & 0 & 0 & 0 \\ 0 & 0 & 0 & 1 & 0 & 0 \\ 0 & 0 & 0 & 0 & 1 & 0 \end{bmatrix} \\ \bar{B} &= \begin{bmatrix} b_{11} & \cdots & b_{1n_h} & 0 & \cdots & 0 \\ b_{21} & \cdots & b_{2n_h} & -l_{w(n_h+2)} & \cdots & 0 \\ \vdots & & \vdots & & \ddots & \vdots \\ b_{n_b 1} & \cdots & b_{n_b n_h} & b_{n_b(n_h+1)} & \cdots & -l_{w_n} \\ b_{(n_b+1)1} & \cdots & b_{(n_b+1)n_h} & 0 & \cdots & 0 \\ b_{(n_b+2)1} & \cdots & b_{(n_b+2)n_h} & 0 & \cdots & 0 \\ b_{(n_b+3)1} & \cdots & b_{(n_b+3)n_h} & 0 & \cdots & 0 \end{bmatrix}\end{aligned}$$

In (13), the first n_b equations are obtained from (9) (10), the $(n_b + 1)$ -th from the derivative of (12), and the $(n_b + 2)$ -th and $(n_b + 3)$ -th equations from derivative of the first two equations of (7).

Let m be the number of wheeled links of the base part. The kinematic model is expressed as

$$A(\boldsymbol{q})\dot{\boldsymbol{w}} = B(\boldsymbol{q})\boldsymbol{u}, \quad \boldsymbol{u} = \dot{\boldsymbol{\theta}} \quad (14)$$

We consider conditions so that the n -link snake robot system can be regarded as the redundancy controllable system which is defined in the section 2. To satisfy the redundancy II the inequality

[condition 1] : $3 \leq m < n - 4$

should be satisfied. To satisfy the full row rankness of the matrix B we should introduce following conditions.

[condition 2] :

In the case that the $(n_h + 1)$ -th link is wheel free : $n_h \geq 3$

In the case that the $(n_h + 1)$ -th link is wheeled : $n_h \geq 4$

[condition 3] :

All joints of the head part do not have same direction of rotational axes.

These three conditions are sufficient condition so that the system is redundancy controllable [10].

The necessary and sufficient condition for the existence of the solution of the system (14) is

$$\text{rank}[A, Bu] = \text{rank}A. \quad (15)$$

5 Controller design for main-objective

Let us define the control input as

$$\begin{aligned} \boldsymbol{u} = \dot{\boldsymbol{\theta}} &= B^+ A \{ \dot{\boldsymbol{w}}_d - K(\boldsymbol{w} - \boldsymbol{w}_d) \} \\ &\quad + (I - B^+ B)\boldsymbol{k} \end{aligned} \quad (16)$$

where B^+ is a pseudo-inverse matrix of B , \boldsymbol{k} is an arbitrary vector and $K > 0$. The first term of the right side of (16) is the control input term to accomplish the main objective of the convergence of the state vector \boldsymbol{w} to the desired value \boldsymbol{w}_d . As the second term $(I - B^+ B)\boldsymbol{k}$ belongs to the null space of the matrix B , we obtain

$$Bu = A \{ \dot{\boldsymbol{w}}_d - K(\boldsymbol{w} - \boldsymbol{w}_d) \}. \quad (17)$$

As the vector $B\mathbf{u}$ can be expressed as a linear combination of column vectors of the matrix A , the condition (14) of the existence of the solution (14) is satisfied. The second term in (16) does not disturb the dynamics of the controlled vector \mathbf{w} . As there is no interaction between \mathbf{w} and $\boldsymbol{\theta}$, we find that the control law (16) accomplishes the sub-objective.

The closed-loop system is expressed as

$$A\{\dot{\mathbf{w}} - \dot{\mathbf{w}}_d + K(\mathbf{w} - \mathbf{w}_d)\} = 0. \quad (18)$$

If the matrix A is full column rank, the uniqueness of the solution is guaranteed. The solution of (18) is given as

$$\dot{\mathbf{w}} - \dot{\mathbf{w}}_d + K(\mathbf{w} - \mathbf{w}_d) = 0$$

and we find that the controller ensures the convergence of the controlled state vector to the desired value ($\mathbf{w} \rightarrow \mathbf{w}_d$). A set of joint angles which satisfies $\text{rank } A < q$ (A is not full column rank) means the singular configuration, for example a straight line ($\phi_i = 0, i = 1, \dots, n-1$).

6 Controller design for sub-objective

We consider the controller design for the sub-objective. In the control law (16), \mathbf{k} is an arbitrary vector. Let us introduce the cost function $V(q)$ which is related to the sub-objective. If we set the vector \mathbf{k} as the gradient \mathbf{k}_1 of the cost function $V(\mathbf{q})$ with respect to the vector $\boldsymbol{\theta}$ related to the input vector \mathbf{u} , we obtain

$$\mathbf{k}_1 = \nabla_{\boldsymbol{\theta}} V(\mathbf{q}) = \left[\frac{\partial V}{\partial \theta_1} \quad \cdots \quad \frac{\partial V}{\partial \theta_{n-1}} \right]$$

and we find that the second term of (16) accomplishes the increase of the cost function V . Actually we can derive

$$\begin{aligned} \dot{V}(\mathbf{q}) &= (\partial V / \partial \mathbf{w}) \dot{\mathbf{w}} + (\partial V / \partial \boldsymbol{\theta}) \dot{\boldsymbol{\theta}} \\ &= (\partial V / \partial \mathbf{w}) \dot{\mathbf{w}} + \mathbf{k}^T B^+ A \{ \dot{\mathbf{w}}_d - K(\mathbf{w} - \mathbf{w}_d) \} \\ &\quad + \mathbf{k}_1^T (I - B^+ B) \mathbf{k}_1. \end{aligned} \quad (19)$$

As $I - B^+ B \geq 0$ [11], we find that the second term of the input (16) accomplishes the increase of the cost function V .

In the case that the sub-objective is the singularity avoidance, we set $B^+ = B^T (BB^T)^{-1}$ and

$$V = \alpha(\det(A^T A)) + \beta(\det(BB^T)) \quad (20)$$

where $\alpha, \beta > 0$. The first term of the right side of (20) implies the measure of the singular configuration. The second term of the right side of (20) is related to the manipulability of the system.

7 Experiments

To demonstrate the validity of the proposed control law experiments have been carried out. The snake robot that we use for the experiments is ACM-R3 [9] as shown in Fig. 4. The snake robot has 13 links and the 2, 6, 8, 9, 10, 12, 13-th links are wheeled. The length $l_i(i = 1, \dots, 13)$ of the links are as follows: $l_1 = l_7 = l_8 = l_9 = l_{10} = l_{11} = l_{12} = 0.16[\text{m}]$, $l_2 = l_3 = l_4 = l_5 = l_6 = l_{13} = 0.08[\text{m}]$. We set $K = I$, $\alpha = 0.2$, $\beta = 2.0 \times 10^6$. The initial position and posture of the head of the snake robot and initial relative joint angles are set as $w(0) = [0, -0.1, 0.142, 0.0715, -0.143, \pi/10]^T$, $\theta(0) = [0, \pi/18, \pi/30, \pi/18, \pi/12, -\pi/9, \pi/6, \pi/6, -\pi/9, -\pi/6, -\pi/10, \pi/30]^T$.



Fig. 4. A research platform robot (ACM-R3)

In experiments, to measure the position and the posture of the snake head we use Quick MAG IV stereo vision system with two fixed CCD cameras. The desired trajectory w_d corresponding to w is represented as the broken lines in Figs. 5 and 6. Fig. 5 shows the transient responses for the controller (16) without using redundancy ($k = 0$). From Fig. 5(a) and (c) we find that the snake robot can not track the desired head trajectory because of the convergence to the singular configuration of a straight line. Fig. 6 shows the transient responses for the controller (16) with using redundancy ($k = k_1$). From Fig. 6 (a) and (c) we find that the snake robot avoids the singular configuration of the straight line. Experimental results show the effectiveness of the proposed controller.

8 Conclusion

We have considered control of redundant 3D snake robot based on kinematic model. We derived conditions so that the snake robot system is redundancy controllable. We propose controller that the snake head tracks the desired trajectory and the robot avoids singular configurations by using redundancy. Experimental results ensure the effectiveness of the proposed control law.

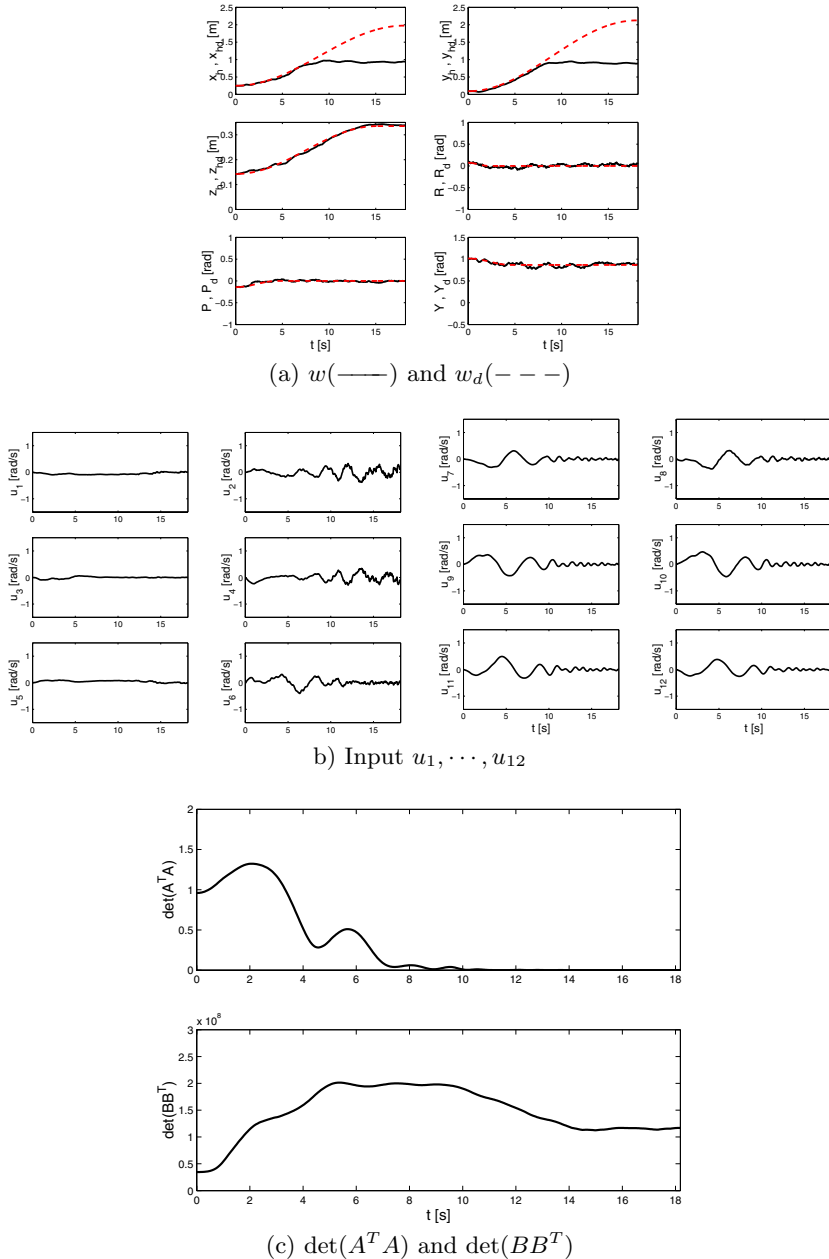


Fig. 5. Transient responses for controller without using redundancy ($k = 0$)

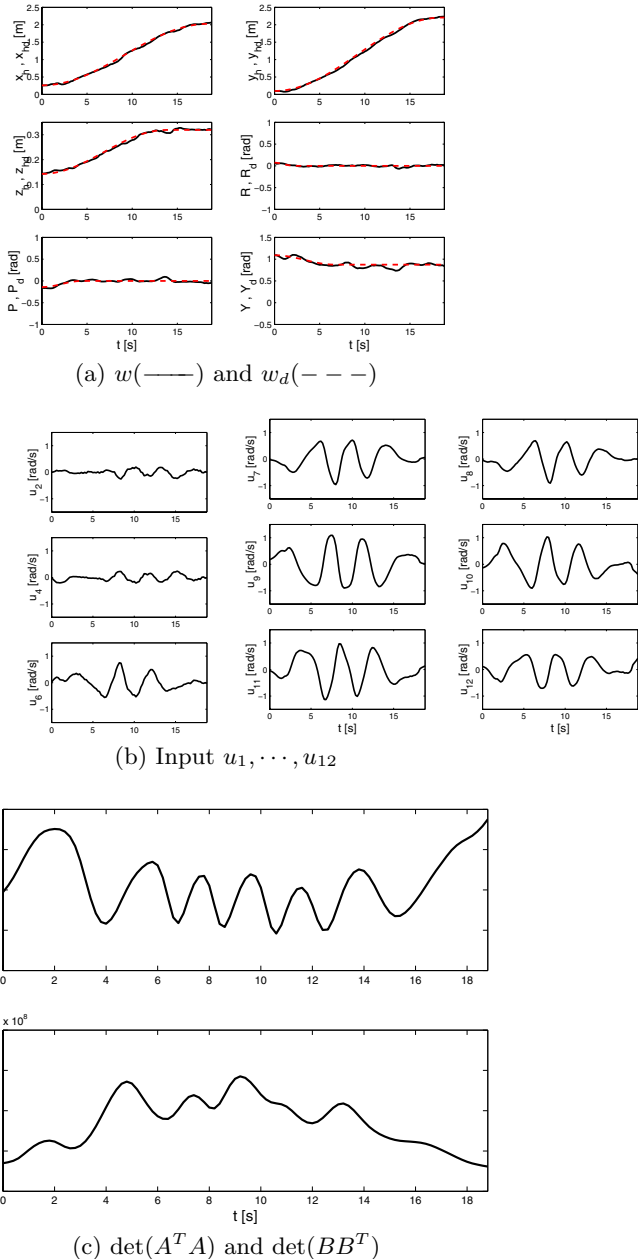


Fig. 6. Transient responses for the controller with using redundancy ($k = k_1$)

References

1. J. Gray, *Animal Locomotion*, pp. 166-193, Norton, 1968
2. S. Hirose, *Biologically Inspired Robots (Snake-like Locomotor and Manipulator)*, Oxford University Press, 1993
3. B. Klaassen and K. Paap, GMD-SNAKE2: A Snake-Like Robot Driven by Wheels and a Method for Motion Control, *Proc. IEEE Int. Conf. on Robotics and Automation*, pp. 3014-3019, 1999.
4. M. Yim, D. Duff and K. Poufas, PolyBot: a Modular Reconfigurable Robot, *Proc. IEEE Int. Conf. on Robotics and Automation*, pp. 514-520, 2000.
5. T. Kamegawa, F. Matsuno and R. Chatterjee, Proposition of Twisting Mode of Locomotion and GA based Motion Planning for Transition of Locomotion Modes of a 3-dimensional Snake-like Robot, *Proc. IEEE Int. Conf. on Robotics and Automation*, pp. 1507-1512, 2002.
6. G. S. Chirikjian and J. W. Burdick, The Kinematics of Hyper-Redundant Robotic Locomotion, *IEEE Trans. on Robotics and Automation*, Vol. 11, No. 6, pp. 781-793, 1995
7. J. Ostrowski and J. Burdick, The Geometric Mechanics of Undulatory Robotic Locomotion, *Int. J. of Robotics Research*, Vol. 17, No. 6, pp. 683-701, 1998
8. P. Prautesch, T. Mita, H. Yamauchi, T. Iwasaki and G. Nishida, Control and Analysis of the Gait of Snake Robots, *Proc. COE Super Mechano-Systems Workshop'99*, pp. 257-265, 1999
9. M. Mori and S. Hirose, Development of Active Cord Mechanism ACM-R3 with Agile 3D Mobility, *Proc. IEEE/RSJ Int. Conf. on Intelligent Robots and Systems*, pp. 1552-1557, 2001.
10. F. Matsuno and K. Mogi, Redundancy Controllable System and Control of Snake Robot with Redundancy based on Kinematic Model, *Proc. IEEE Conf. on Decision and Control*, pp. 4791-4796, 2000.
11. Y. Nakamura, H. Hanafusa and T. Yoshikawa, Task-Priority Based Redundancy Control of Robot Manipulators, *Int. J. of Robotics Research*, Vol. 6, No. 2, pp. 3-15, 1987

Part 4

Bipedal Locomotion Utilizing Natural Dynamics

Simulation Study of Self-Excited Walking of a Biped Mechanism with Bent Knee

Kyosuke Ono and Xiaofeng Yao

Tokyo Institute of Technology, Department of Mechanical and Control Engineering, 2-12-1 Ookayama, Meguro-ku, Tokyo, Japan 152-8552,
ono@mech.titech.ac.jp

Abstract. This paper presents a simulation study of self-excited walking of a four-link biped model whose support leg is holding a bending angle at the knee. We found that the biped model with a bent knee can walk faster than the straight support leg model that has been studied so far. The convergence characteristics of the self-excited walking are shown in relation to the bent knee angle. By using standard link parameter values we investigated the effect of the bent knee angle and foot radius on walking performance. We found that the walking speed of 0.7 m/s can be achieved when the bent knee angle is 15 degrees and the foot radius is 40mm.

1 Introduction

Since a biped robot is the ultimate goal of robotic machines in terms of versatility with environments, friendliness to the human society and sophistication of locomotion, it has been studied by a great number of researchers. In the first age of research of biped mechanisms or humanoid robots from the 1970s to 1995, many control strategies of a biped walking were proposed [1-7]. In addition, dynamic stability of walking locomotion inherent to a biped mechanism on a shallow slope were also studied by a number of researchers [8-10] and passive walking are presented by McGeer [11-13].

At the end of 1995, Honda developed an advanced humanoid robot based on trajectory planning and zero moment point (ZMP) control [14]. Since then, the research of humanoid robots have focused on realizing various kinds of intelligent functions similar to human beings. However, these humanoid robots consume a high power in spite of slow walking compared with human. For this reason it will be important to study a biped mechanism that can perform natural walking in order to improve the walking efficiency.

As a control method of the natural dynamics of the biped mechanism, Ono et al. proposed a self-excitation control of a 2-degree-of-freedom (2-DOF) swing leg and showed that a four-link biped mechanism with and without feet can walk on a level ground by means of only one hip motor in numerical simulation and experiment [15-16]. In this biped model the stance leg is assumed to be kept straight by some rock mechanism. Walking speed can be increased to over 0.4m/s by using a cylindrical foot, but it is still slow compared with human natural walking.

This study aims to find principles of fast biped walking with high efficiency based on self-excitation. Through our understanding of human walking patterns, we know that people always retain some knee flexion during walking [17] when we want to walk fast. Therefore, we try to apply a bent knee angle to the support leg in order to make it walk faster.

In the next section, the analytical model and its basic equations of locomotion will be introduced. In section 3, we show the typical simulated results of stable biped locomotion on level ground with and without a bent knee angle and foot and the convergence characteristics of the self-excited walking in relation to the bent angle. Next, we present the calculated results of the effect of the knee bent angle with and without a foot radius on the walking performance.

2 The analytical model and basic equations

Figure 1 shows the biped mechanism that walks with a bent knee. We consider the biped walking motion on a sagittal plane. The biped model consists of only two legs and does not have a torso. The two legs are connected in a series at the hip joint through a motor. Both legs have a thigh and a shank that are connected at the knee joint. We assume that the biped has knee brakes so that the knee can be locked at any bent angle after the knee collision of the swing leg. The support leg does not extend fully but retains some flexion during the stance phase. Therefore the brake is activated before the swing leg becomes straight and keeps a desired knee angle between the thigh and the shank. The brake is released just when the supporting leg enters the swing phase.

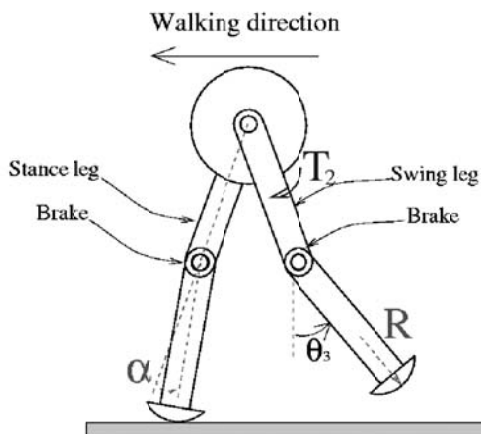


Fig. 1. Self-excited mechanism with bent knee and cylindrical foot

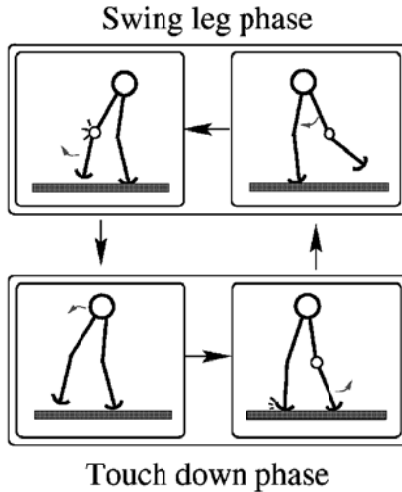


Fig. 2. Two phases of biped walking

Figure 2 shows the algorithm of biped walking. Biped walking can be divided into two phases: the swing leg phase and the touch down phase,

1. From the start of the swinging leg motion to the lock of the knee joint of the swinging leg by the brake. In this phase, only the brake of the supporting leg is activated.
2. From the lock of the knee joint of the swinging leg to the touch down of the bent swinging leg. In this phase, the brakes of both legs are activated.

We assume that the change of the supporting leg to the swinging leg occurs instantly and the friction force between the foot and the ground is large enough to prevent a slip.

To realize stable biped walking on a level ground, the swinging leg should bend at the knee to prevent the tip from touching the ground. In addition, the energy dissipated through knee and foot collisions and joint friction should be supplied by the motor. The swing leg motion can be autonomously generated by the asymmetrical feedback of the form,

$$T_2 = -k\theta_3 \quad (1)$$

If the feedback gain k is increased to a certain value, the swing leg motion begins to be self-excited and the kinetic energy of the swinging leg increases. Since the swing motion has a constant period at any swing amplitude, there is an angular velocity of the support leg whose swing motion as an inverted pendulum can synchronize with the swing leg motion. This velocity determines the walking speed.

In addition, the synchronized motion between the inverted pendulum motion of the supporting leg and the two-DOF pendulum motion of the swinging leg, as well as the balance of the input and the output energy, should have stable characteristics against small deviations from the synchronized motion.

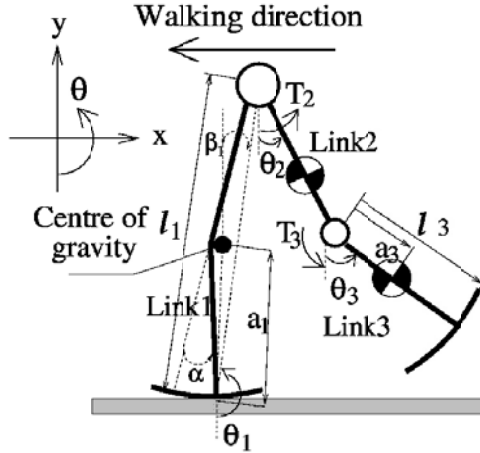


Fig. 3. Analytical model of three degree of freedom walking mechanism

It is also assumed that a small viscous rotary damper with coefficient γ_3 is applied to the knee joint of the swing leg, which produces a torque as:

$$T_3 = -\gamma_3(\dot{\theta}_3 - \dot{\theta}_2) \quad (2)$$

Under the assumption of a fixed bent knee angle of the supporting leg and a free knee joint of the swinging leg, the analytical model during the first phase is treated as a three-DOF link system, as shown in Fig.3. We get the equation of motion in the first phase as:

$$\begin{bmatrix} M_{111} & M_{112} & M_{113} \\ & M_{122} & M_{123} \\ sym & & M_{133} \end{bmatrix} \begin{bmatrix} \ddot{\theta}_1 \\ \ddot{\theta}_2 \\ \ddot{\theta}_3 \end{bmatrix} + \begin{bmatrix} 0 & C_{112} & C_{113} \\ -C_{112} & 0 & C_{123} \\ -C_{113} & -C_{123} & 0 \end{bmatrix} \begin{bmatrix} \dot{\theta}_1^2 \\ \dot{\theta}_2^2 \\ \dot{\theta}_3^2 \end{bmatrix} + \begin{bmatrix} K_{11} \\ K_{12} \\ K_{13} \end{bmatrix} = \begin{bmatrix} -T_2 \\ T_2 - T_3 \\ -T_3 \end{bmatrix} \quad (3)$$

where the elements M_{1ij} , C_{1ij} and K_{1i} of the matrices are shown in Appendix 1. T_2 is the feedback input torque given by Eq.(1) while T_3 is the viscous resistance torque at the knee joint, which is given by Eq.(2).

When the angle between the shank and thigh of the swing leg becomes a certain value, the brake is activated and locks the knee joint. This signifies the end of the first phase. We assume the knee collision occurs plastically at this time. From the assumption of conservation of momentum and angular momentum before and after the knee collision, angular velocities after the knee collision are calculated from the condition $\dot{\theta}_2^+ = \dot{\theta}_3^+$, and the equation is written as:

$$\begin{bmatrix} \dot{\theta}_1^+ \\ \dot{\theta}_2^+ \\ \dot{\theta}_3^+ \end{bmatrix} = [M]^{-1} \begin{bmatrix} f_1(\theta_1, \dot{\theta}_1^-) \\ f_2(\theta_2, \dot{\theta}_2^-) - \tau \\ f_3(\theta_3, \dot{\theta}_3^-) + \tau \end{bmatrix} \quad (4)$$

where the elements of the matrix $[M]$ are the same as M_{1ij} in Eq.(3). f_1, f_2 and f_3 are presented in Appendix 2. τ is the impulse moment at the knee.

During the second phase, the biped system can be regarded as a two-DOF link system. The basic equation becomes

$$\begin{bmatrix} M_{211} & M_{212} \\ M_{212} & M_{222} \end{bmatrix} \begin{bmatrix} \ddot{\theta}_1 \\ \ddot{\theta}_2 \end{bmatrix} + \begin{bmatrix} 0 & C_{212} \\ -C_{212} & 0 \end{bmatrix} \begin{bmatrix} \dot{\theta}_1 \\ \dot{\theta}_2 \end{bmatrix} + \begin{bmatrix} K_{21} \\ K_{22} \end{bmatrix} = 0 \quad (5)$$

where the elements M_{2ij}, C_{2ij} and K_{2ij} of the matrices are shown in Appendix 3.

We assume that the collision of the swinging leg with the ground occurs un-elastically and the friction between the foot and the ground is large enough to prevent slipping. Just like knee collision, the angular velocities of the links after the collision can be derived from conservation laws of momentum and angular momentum. At this time, $\tau = 0$ is put into Eq.(4). After the collision, the supporting leg turn to the swinging leg immediately and the system enter the first phase again.

Table 1. Link parameter values used for simulation

Parameters	Thigh	Shank	Leg
Length $l_i[m]$	0.4	0.4	0.8
Mass $n_i[kg]$	2.0	2.0	4.0
Center of mass $a_i[m]$	0.2	0.2	0.4
Moment of inertia at mass center $I_i[kgm^2]$	0.027	0.027	0.21

3 The results of simulation

The values of the link parameters used in the simulation are shown in Table 1. We use the same values as in our preceding paper [15] because it is easy to find the influence of the bent knee angle by comparing the two results. The fourth order Runge-Kutta method was used to numerically solve the

basic equations. In order to increase the accuracy, the time step is set to be 1ms. Regarding the effect of viscous rotary damper γ_3 , it is found that a proper value will yield the phase delay of the shank. This helps to increase the foot clearance. By considering the efficiency, $\gamma_3 = 0.15 \text{ Nms/rad}$ is used in the simulation. In the numerical simulation, steady walking locomotion is obtained with bent knee angles of less than 17 degrees. When the angle is larger than 17 degrees, the step length decreases suddenly and the biped mechanism falls forward.

Figure 4 illustrates the stick figures of the stable self-excited walking gaits during four steps (two walking cycles) under the conditions of when the model has the bent knee angle and foot or not. For the convenience of comparison, the feedback gain k is set to be 8Nm/rad in all the cases. In Fig.4 (a), the biped has no bent knee angle and no foot. The step length is 0.18 m and the period of one step is 0.64 s, so the walking velocity is 0.28 m/s. In Fig.4 (b), 10 degrees of the bent knee angle is added to the support leg. The step length increases to 0.31 m and the period decreases a little, so that the velocity is increased to 0.5 m/s. The velocity increase is mainly caused by the increase in the moment to drive the supporting leg forward due to the forward shift of the mass center of the leg. In Fig.4 (c), the velocity is increased further to 0.65 m/s by giving the model a foot whose radius R is 0.3 m. From the stick figures, we can clearly observe the increase of the walking speed. We also note that the shank motion of the swing leg delays from the thigh motion that yields a foot clearance (the height of the tip of the swing leg from the ground) for stable walking.

The initial start condition of the supporting leg that can lead to stable walking and the typical converging process of the self-excited walking are shown in Fig. 5 when the knee angle α is zero and the feedback gain k is 6 Nm/rad . Figure 5(a) shows the initial start angle and angular velocity of the supporting leg that can converge to a limit cycle of walking motion and the converging processes from the three different initial conditions of 1 to 3. This graph shows the basin of a limit cycle on a Poincare phase plane at the start of a swing of the supporting leg. The star symbol indicates the start condition of the supporting leg in the steady walking motion (limit cycle). We note that the same unique start condition of the limit cycle can be obtained from three different initial conditions that are far apart from each other. Figure 5(b) shows the change of step length as a function of time in the converging process from the three different initial conditions corresponding to those in Fig.5(a). Since the walking period is 1.3 seconds, as will be shown later, steady walking can be achieved after about ten cycles of walking.

$$\alpha = 0^\circ R = 0m\alpha = 10^\circ R = 0m\alpha = 10^\circ R = 0.3m$$

Figure 6 shows the change of the stable start condition when the bent knee angle is changed to 5, 10 and 15 degrees. We note from these figures that stable walking becomes difficult as the bent knee angle increases when the mass distribution of the biped has not changed. The straight line on the main

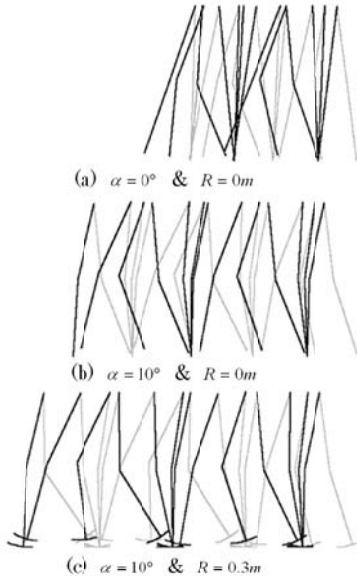


Fig. 4. Stick figures during two walking cycles

trunk of the basin is calculated from the synchronizing condition between the supporting leg and swinging leg based on a physical model, although not explained in detail. A good agreement between the line and calculated point of the stable start condition indicates that stable self-excited walking is generated when the swing leg motion and the support leg motion synchronize with each other..

Figure 7 shows the effect of the bent knee angle on the walking velocity, input power, specific cost, step length and period respectively when $k=8$ Nm/rad and $R=0$ m. The average input power is calculated by:

$$P = \frac{1}{t_{end}} \int_0^{t_{end}} |\dot{\theta}_2 k \theta_3| dt \quad (6)$$

The specific cost is defined as:

$$E = \frac{P}{mgV} \quad (7)$$

From Fig. 7 we note that as the bent angle increases, the step length increases, the period decrease and then the walking velocity increases. It should be noted that the walking velocity at $\alpha = x_6$ increases by 2.3 times that at $\alpha=0$, whereas the increased rate in specific cost is 1.4. The reason for this is considered as follows: As the bent knee angle increases, the position of the mass center of the swing leg approaches the hip joint. Therefore, the swing period will decrease. At the same time, the center of mass is moved

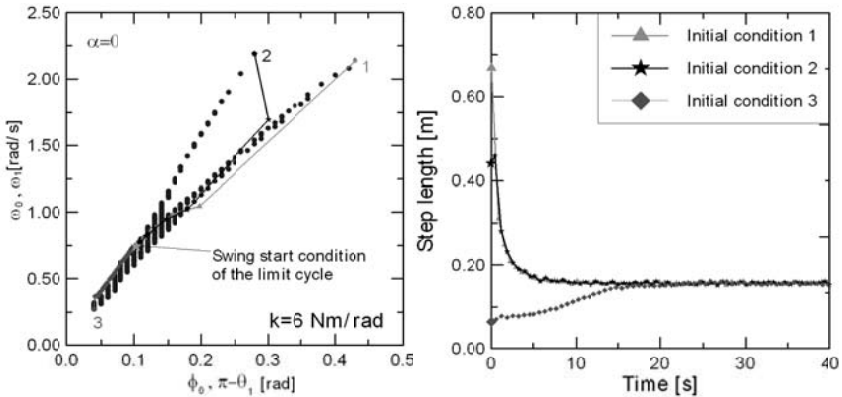


Fig. 5. Start angular position and velocity of support leg that can converge to a limit cycle of walking and converging processes from three different initial conditions($\alpha = 0$). (a) Start angular position and velocity of support leg that result in a limit cycle of walking and converging processes from three different start conditions. (b) Converging processes of step length from three different start conditions.

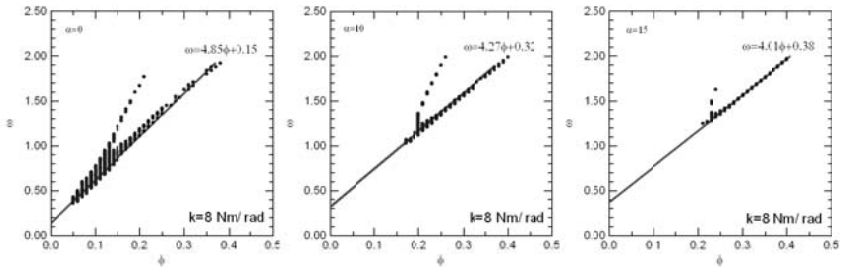


Fig. 6. Start angular position and velocity of support leg that can result in a stable walking for various values of bent knee angles

forward in contrast to that of the straight leg. Therefore, the supporting leg rotates forward faster than in the straight leg model because the offset of mass yields the gravity torque to make the support leg rotate in the forward direction. With a shorter swing period and a longer step length, faster walking is realized in the simulation. However, the specific cost increases until bent knee angle reaches 8 degrees because of the rapid increase of input power. When $\alpha > 8^\circ$ the specific cost stops to increase and even decreases a little because the increase in velocity is faster than the increase in input power. Since the input torque at the hip joint is proportional to the angle of linkage 3 and θ_3 is larger in the bent-knee mode than in the straight-leg mode, the input power increases when the bent angle increases.

Although not shown here, we also found the influence of feedback gain on the walking motion. As the feedback gain increases from 7 Nm/rad to 8 Nm/rad, the step length increases a little but the period increases notably

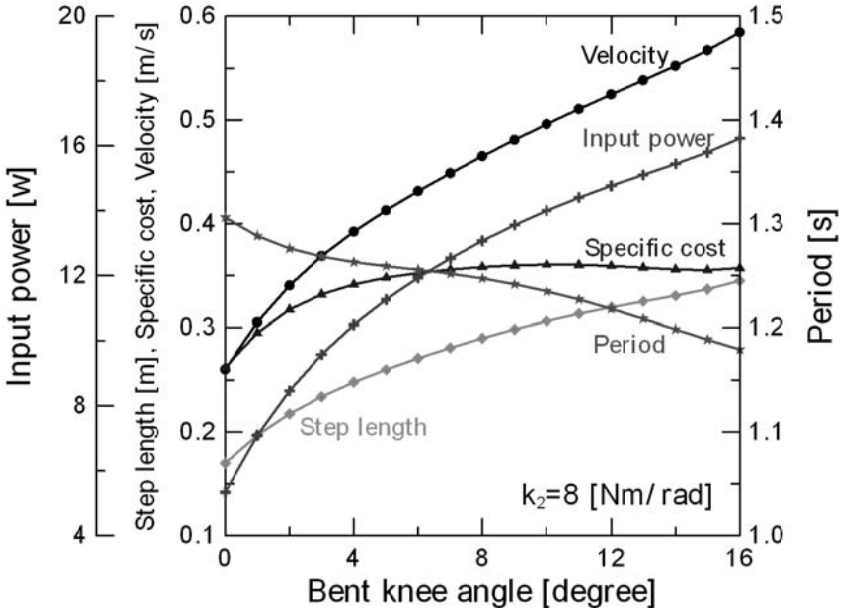


Fig. 7. Walking performance as a function of bent knee angle($R = 0$)

when the bent knee angle is larger than 5 degrees. Therefore, it is not applicable to increase the velocity by increasing the feedback gain only. However, in order to make the biped locomotion enter the limit cycle, we have to increase the feedback gain as the bent knee angle increases. For the straight-leg mode, $k=4.6\text{Nm/rad}$ is enough to obtain a stable walk. But when the bent knee angle increases to 12 degrees, $k=7\text{Nm/rad}$ is indispensable to obtain a stable walk. In addition, the foot clearance is influenced by the feedback gain k . The clearance becomes minimum in the middle of the swing phase. As k increases, the minimum clearance also increases. In the bent-knee walking model, the clearance decreases as the bent angle increases. Since the minimum clearance can be regarded as a margin of stable walking, it is necessary to increase the value of k in order to realize steady walking.

$\alpha = 10^\circ$, $k = 8.0\text{Nm/rad}$ As seen in Fig.4, the walking speed can be further increased by increasing the radius of the cylindrical foot. Figure 7 shows the effect of foot radius on the walking performance when bent knee angle $\alpha \approx 10$ degrees and $k=8\text{Nm/rad}$. Here the mass of the foot is ignored in simulation. From Fig. 7 we can note that as the foot radius increases, the step length and velocity increase almost linearly. This is because the contact point of the support leg is carried by the rolling motion of the cylindrical foot surface in addition to the angular motion as an inverted pendulum. As the radius of the foot reaches 0.4 m, the velocity increases to 0.7 m/s. This means a 40%

increase in contrast to the model without the foot. But we may encounter the problem of losing stability because the foot clearance from the ground will decrease as the radius of the foot increases. When the radius is larger than 0.4 m, the toe of the swing foot may strike the ground. From the simulation, we found that the walking speed of 0.7m/s can also be achieved when $R=0.3\text{m}$ and $\alpha=15$.

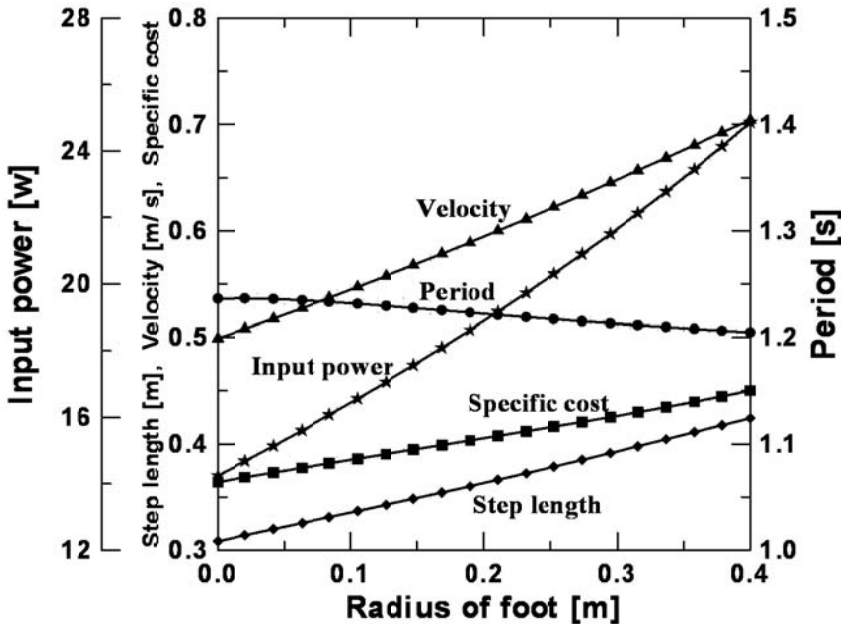


Fig. 8. Effect of foot radius on walking characteristics ($\alpha=10^\circ$ and $k=8.0\text{Nm/rad}$)

4 Conclusion

By giving the supporting leg a bent knee angle, the walking speed of the biped mechanism increases significantly due to the increase in step length and the decrease in period as the knee angle increases. The increasing rate of the bent knee model at 16 bent knee angle from the straight knee model is 2.3 whereas the increasing rate of the specific cost remains 14. The walking speed can be further increased by increasing the foot radius. When $\alpha=10$, the walking velocity increases by 40% whereas the specific cost increases only by 20%. Walking velocity of 0.7 m/s can be obtained when the bent knee angle is 15 and the foot radius is 0.3m or when the bent knee angle is 10 and the foot radius is 0.4m.

References

1. Kato T., Takanishi A., and Naito G., et al, 1981, "The realization of the quasi-dynamic walking by the biped walking machine," Proceedings of the International Symposium on Theory and Practice and Manipulators, POMANSY, pp.341-351.
2. Miyazaki F., and Arimoto S., 1980, "A control theoretic study on dynamical biped locomotion," Journal of Dynamic Systems, Measurement, and Control, 102(4), pp.233-239.
3. Mita T., Yamagaguchi T., Kashiwase T., and Kawase, T., 1984, "Realization of a high speed biped using modern control theory," International Journal of Control, 40(1), pp.107-119.
4. Miura, H., and Shimoyama, I., 1984, "Dynamic Walk of a Biped," Int. J. of Robotics Research, 3(2), pp.60-74.
5. Furusho, j., and Masubuchi, M, 1986, "Control of a Dynamical Biped Locomotion System for Steady Walking," Trans. ASME, J. of Dynamic Systems, Measurement, and Control, 108(2), pp.111-118.
6. Kajita, S. and Kobayashi, A., 1987, "Dynamic Walk Control of a Biped Robot with Potential Energy Conserving Orbit," Journal of SICE, 23(3), pp.281-287.
7. Sano A., Furusho J., 1990, "3D dynamic walking robot by controlling the angular momentum," Journal of the SICE, 26(4), pp.459-466.
8. Goswami, A., Espiau, B., and Keramane, A., 1997, Limit Cycles in a Passive Compass Gait Biped and Passivity-Mimicking Control Laws, J. Autonomous Robots, 4(3), pp.273-286.
9. Garcia, M., Chatterjee, A., Riuna, A., and Coleman, M., J., 1998, The Simplest Walking Model: Stability, Complexity, and Scaling, ASME J. of Biomech. Eng. 120(2), pp.281-288.
10. Goswami,A., Thuiot, B., and Espiau,B., 1998, A Study of the Passive Gait of a Compass-Like Biped Robot: Symmetry and Chaos, Int. J. Robot. Res. 17(12), pp.1282-1301.
11. McGeer T., 1990, "Passive dynamic walking," International Journal of Robotics Research, 9(2), pp.62-81.
12. McGeer, T., 1990, "Passive walking with knees," Proceedings of 1990 IEEE Robotics and Automation Conf., pp.1640-1645.
13. McGeer, T., 1993, "Dynamics and control of bipedal locomotion," Journal of Theoretical Biology, 163, pp.277-314.
14. Hirai, K., Hirose, M., Haikawa, Y., and Takenaka, T., 1998, "The Development of Honda Humanoid Robot, Proc. IEEE Int. Conf. Robotics and Automation," pp.983-985.
15. Ono K., Takahashi R., Shimada T., 2001, "Self-Excited Walking of a Biped Mechanism," Int. J. of Robotics Research, Vol.20, No.12, pp.953-966.
16. Ono K., Furuichi T., and Takahashi, R., 2004, "Self-Excited Walking of a Biped Mechanism with Feet," International Journal of Robotics Research, 23(1), pp.55-68.
17. Jessica Rose and James G. Gamble, 1993, Human Walking (Second Edition), Waverly Company.

Appendix 1

$$M1_{11} = I_1 + m_1 a_1^2 + m_2 l_1^2 + m_3 l_1^2$$

$$M1_{12} = (m_2 a_2 + m_3 l_2) l_1 \cos(\theta_2 - \theta_1)$$

$$M1_{13} = m_3 a_3 l_1 \cos(\theta_3 - \theta_1)$$

$$M1_{22} = I_2 + m_2 a_2^2 + m_3 l_2^2$$

$$M1_{23} = m_3 a_3 l_2 \cos(\theta_3 - \theta_2)$$

$$M1_{33} = I_3 + m_3 a_3^2$$

$$C1_{12} = -(m_2 a_2 + m_3 l_2) l_1 \sin(\theta_2 - \theta_1)$$

$$C1_{13} = -m_3 a_3 l_1 \sin(\theta_3 - \theta_1)$$

$$C1_{23} = -m_3 a_3 l_2 \sin(\theta_3 - \theta_2)$$

$$K1_1 = (m_1 a_1 + m_2 l_1 + m_3 l_1) g \sin(\theta_1 + \beta_1)$$

$$K1_2 = (m_2 a_2 + m_3 l_2) g \sin \theta_2$$

$$K1_3 = m_3 a_3 g \sin \theta_3$$

Appendix 2

$$f_1(\theta_1, \dot{\theta}_1^-) = I_1 \dot{\theta}_1^- + \{a_1 m_1 v_{1x} + l_1(m_2 v_{2x} + m_3 v_{3x})\} \cos \theta_1$$

$$+ \{a_1 m_1 v_{1y} + l_1(m_2 v_{2y} + m_3 v_{3y})\} \sin \theta_1$$

$$f_2(\theta_2, \dot{\theta}_2^-) = I_2 \dot{\theta}_2^- + (a_2 m_2 v_{2x} + l_2 m_3 v_{3x}) \cos \theta_2 + (a_2 m_2 v_{2y} + l_2 m_3 v_{3y}) \sin \theta_2$$

$$f_3(\theta_3, \dot{\theta}_3^-) = I_3 \dot{\theta}_3^- + a_3 m_3 v_{3x} \cos \theta_3 + a_3 m_3 v_{3y} \sin \theta_3$$

Appendix 3

$$M2_{11} = I_1 + m_1 a_1^2 + m_2 l_1^2$$

$$M2_{12} = m_2 a_2 l_1 \cos(\theta_2 - \theta_1)$$

$$M2_{22} = I_2 + m_2 a_2^2$$

$$C2_{12} = -m_2 a_2 l_1 \sin(\theta_2 - \theta_1)$$

$$K2_1 = (m_1 a_1 + m_2 l_1) g \sin \theta_1$$

$$K2_2 = m_2 a_2 g \sin \theta_2$$

Design and Construction of MIKE; a 2-D Autonomous Biped Based on Passive Dynamic Walking

Martijn Wisse and Jan van Frankenhuizen

Delft University of Technology, Dept. of Mechanical Engineering, Mekelweg 2,
NL-2628 CD Delft, The Netherlands

Abstract. For research into bipedal walking machines, autonomous operation is an important issue. The key engineering problem is to keep the weight of the actuation system small enough. For our 2D prototype MIKE, we solve this problem by applying pneumatic McKibben actuators on a passive dynamic biped design. In this paper we present the design and construction of MIKE and elaborate on the most crucial subsystem, the pneumatic system. The result is a fully autonomous biped that can walk on a level floor with the same energy efficiency as a human being. We encourage the reader to view the movies of the walking results at <http://dbl.tudelft.nl/>.

1 Introduction

We are performing research into bipedal walking robots with two long-term goals in mind. First, we expect that it increases our understanding of human walking, which in turn can lead to better rehabilitation of the impaired. Second, autonomous walking robots could greatly enhance the entertainment experience for visitors of theme parks and the like. Both long-term goals impose identical requirements on bipedal robots. They should be anthropomorphic in function and appearance, their locomotion should be robust, natural and energy efficient, and they should be easy to construct and control.

A solution for energetic efficiency is the exploitation of the 'natural dynamics' of the locomotion system. In 1989 McGeer [6] introduced the idea of 'passive dynamic walking'. He showed that a completely unactuated and therefore *uncontrolled* robot can perform a stable walk when walking down a shallow slope. His most advanced prototype (Figure 1A) has knees and a hip joint, which connect in total four thighs and shanks (with rigidly attached circular feet). The inner two legs form a pair and so do the outer legs, so that the machine essentially has 2D behavior.

We believe that passive dynamic walking should be the starting point for successful biped design. For a human-like robot walking on level ground, a necessity of actuation arises for energy input (instead of walking down a slope), and for stabilization against large disturbances. We propose a robot design that can perform a robust motion as a result of the passive dynamics, while the actuators only compensate for friction and impact energy losses.

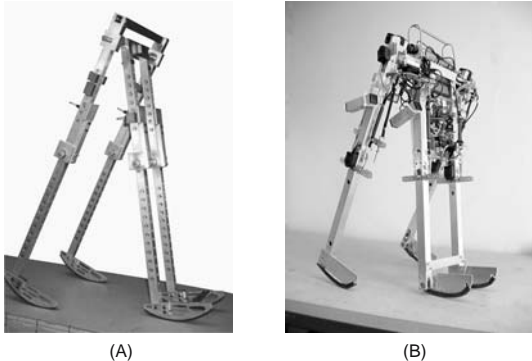


Fig. 1. (A) Close copy of McGeer’s walker by Garcia *et al.*, (B) 2D biped prototype MIKE

We are materializing this combination of passive dynamic walking and actuation in the form of our new prototype MIKE (see Figure 1B). On top of the specifications of McGeer’s machine, MIKE is provided with McKibben muscles (pneumatic actuators) in the hip and knee joints that can provide energy for propulsion and control, thus eliminating the need for a slope and providing an enhanced stability. In this paper we will describe the design and construction of MIKE, focusing in sections II - V on the key construction elements; foot shape, McKibben muscles, pneumatic system, pressure control unit. Section VI presents walking experiments of MIKE walking downhill and on a level floor.

2 Foot shape

2.1 Foot shape in literature

The human foot is shaped so that the center of pressure (the average contact point) travels forward during the progression of a walking step. This effect is known as ‘foot roll-over’. When replicating the human foot for prostheses or for walking robots, many designers apply a curved foot sole with an approximately circular foot roll-over shape. For contemporary foot prostheses, Hansen *et al.* [4] shows the effective foot roll-over shapes of different makes. From his graphs we conclude that they all have a foot radius of 30-35 [cm]. Apparently that was empirically determined to be the best foot shape.

In passive dynamic walking robot research, many computer models and prototypes are equipped with circular feet, following McGeer’s example. McGeer [6] determined the effect of the foot radius on the local stability (i.e. small disturbances) of his walkers and so concluded that a foot radius of about 1/3 of the leg length would be a good choice. However, we argue that a good local stability does not imply a good disturbance rejection for larger disturbances. As an example, we compare the findings of Garcia *et al.* [2] on the simplest walking model with our own. Their simplest walking model was equipped

with point feet (foot radius equal to zero), and showed stable downhill walking for slopes up to 0.015 [rad]. However, when studying the allowable size of the disturbances for that model [10], we found that even a 2% change of the initial stance leg velocity could make the model fall over. In conclusion, more information is needed about the effect of the foot roll-over shape on the allowable size of the disturbances.

2.2 Test machine for foot roll-over shape

We built a test machine (Figure 2) to answer the question: ‘with what foot radius can the largest disturbance be handled?’ The test machine weighs 3 [kg] and is, with a leg length of 38 [cm], approximately half the size of MIKE. It has no knees, the only joint is at the hip. The test machine was placed on a shallow slope with a disturbance half-way. The disturbance was realized by lowering the second half of the walkway. The stability was quantified as the largest amount of lowering that the test machine could still recover from and continue walking to the end of the slope.

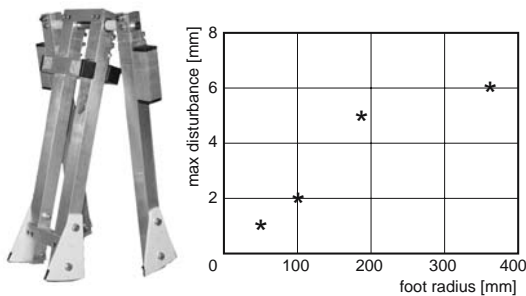


Fig. 2. Stability results of the test machine (left) tested with four different foot radii: 50, 100, 190 and 380 [mm] with a foot length limited to approx. 8 [cm]. Apparently a larger foot radius is always better

We built four different sets of feet with radii from 50 [mm] to 380 [mm], but limited the foot length to about 8 [cm]. The results are plotted in Figure 2. Apparently, the larger the foot radius the better, as coincides with intuition. Of course, when the foot length is limited, there is no gain in increasing the foot radius above a certain value; the walker would just spend more time on the heel and toe.

2.3 Construction

Theoretically, MIKE needs feet with a radius as large as possible. In practice however, there is a limitation to the length of the foot due to the required foot clearance. If the foot is long, bending the knee will not result in enough clearance for the swing leg, but rather in the opposite. Based on the empirically determined prosthetic foot shape and some experimenting with MIKE,

eventually we decided on a foot radius of 25 [cm] and a length of 13 [cm]. This is pretty close to McGeer's recommended 1/3 of the leg length.

Another practical consideration is the place of attachment of the foot to the shank. McGeer shifted the feet somewhat forward from the center, so that the passive reaction torques would keep the knees locked during the stance phase. We don't need this, for we have muscles to actively extend the knees. However, empirical study showed that the best stability results were obtained indeed with the feet shifted forward about 6 [cm], see Figure 3.



Fig. 3. In practice, we obtained the best results with a foot radius of 25 [cm], a foot length of 13 [cm], and a forward displacement of 6 [cm]. The foot switch allows the controller to adapt to the actual step time by registering the exact instant of heel strike

3 McKibben muscles as adjustable springs

3.1 Background and requirements

For autonomous systems, it is crucial to apply lightweight actuators. For a passive dynamic walker, another requirement is that the actuators should not interfere with the passive swinging motions of the legs. McGeer says the following about this matter: "The geared motors or fluidic actuators used on most mechanical bipeds do not satisfy this requirement; lift one of their legs, and it will hang catatonically or, at best, grind slowly to a halt at the bottom of its swing." We chose to use pneumatic McKibben muscles as actuators that fulfill these requirements. In comparison to other alternatives, such as commercially available pneumatic cylinders, McGeer's LITHE [7], Direct Drive torque motors, or MIT Leglab's Series Elastic Actuators [9], the McKibben muscles are very lightweight and simple in construction and application.

Under constant pressure the McKibben muscles behave like a spring with low hysteresis. Because the muscles can only provide tension force, we use them in a pair of antagonists, counteracting on the same passive joint (see Figure 4). Increasing the internal pressure results in a higher spring stiffness, which in turn increases the natural frequency of the limb.

3.2 Operating principle, technical realization and results

A McKibben muscle consists of flexible rubber tube, covered by a weave of flexible yet non-extensible threads, see Figure 5. The operating principle is

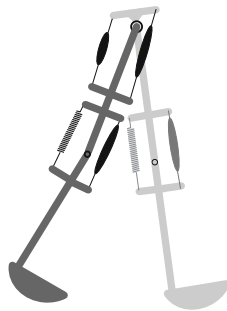


Fig. 4. Overview of the McKibben muscles on MIKE. Each muscle drawn represents two muscles performing the same function in the machine

best explained when starting with a non-attached, pressurized muscle. If from that state the muscle is extended, the non-extensible threads are forced into an orientation with a smaller inter-thread angle, thus decreasing the diameter of the muscle. The cumulative effect of muscle extension and diameter

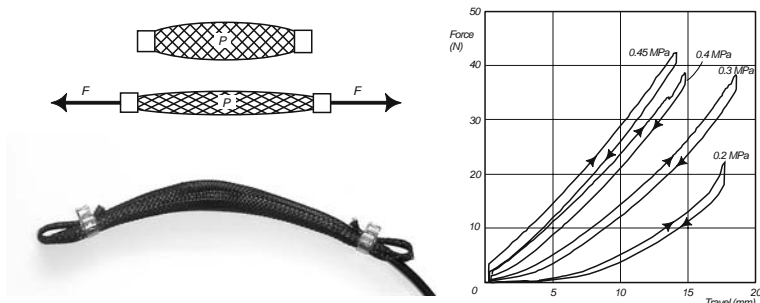


Fig. 5. McKibben muscles; (left top) operating principle, (left bottom) photograph of the Shadow muscle, (right) force-length diagram

reduction is a decrease of muscle volume. Against an assumed constant muscle pressure, reducing the muscle volume costs work. This work can only be supplied by a tension force in the muscle attachments. In other words; muscle extension causes a counteracting force, which makes the muscles act like tension springs. A more detailed study of the McKibben muscle used as an adjustable spring can be found in [11], where the relation between muscle extension and tension force is presented as:

$$F = \frac{b^2 P'}{2\pi n^2 L_0} \Delta L \quad (1)$$

with F = muscle force, b = length of weave threads, P' = relative muscle pressure, n = number of turns of a thread, L_0 = muscle rest length, and ΔL = relative muscle extension. This relation reveals the most important characteristics of a McKibben muscle:

- The muscles behave like linear springs,
- The spring constant is proportional to the muscle pressure.

McKibben muscles are based on a simple concept and are generally easy to construct. However, it is our experience that the choice of materials and connectors is important for the muscle lifetime. Therefore, we use commercially available muscles (Figure 5) made by the Shadow Group [3], which they sell at £6 each. The muscles weigh less than 10 grams and can produce a force of 40 [N] at 0.40 [MPa].

Figure 5 shows the mechanical behavior of one type of Shadow muscle (6 mm diameter, 150 mm length) at different pressure levels. Note that indeed the muscles behave like linear springs (in this range). Also, note that there is a small but noticeable hysteresis-loop, representing losses mainly due to friction between the scissoring threads and the rubber tube.

4 Pneumatic system

4.1 Background and presumptions

Because a McKibben muscle needs pressurized gas for functioning, our autonomous biped MIKE needs to be provided with an efficient, lightweight and properly working pneumatic system. First of all, we have to carry along our own reservoir of pressurized gas. The gas should be stored at saturation pressure in order to keep the necessary container volume as small as possible. Secondly, the high pressure from this container has to be reduced to various operation pressure levels between 0.1 [MPa] and 0.4 [MPa].

Minimizing gas consumption helps to increase the autonomous operation time. Van der Linde [11] developed the so called ‘Actively Variable Passive Stiffness’-system. This system includes a solenoid 3/2 valve that switches the internal muscle pressure between two preset pressure levels. In this way, only a small volume of gas is needed every time the muscle is activated, because the muscle pressure is never completely vented to ambient pressure.

4.2 Requirements

To have time for proper experiments, we need a few minutes of autonomous operation time on one gas container. Measurements on the amount of exhaust gas, during a pressure decrease from 0.35 to 0.15 [MPa] in one muscle, tell us that we need 44 milligrams CO₂ per actuation. During each step 4 muscle activations take place, so that we need 176 milligrams of gas each step. The step time is 0.6 seconds. By choosing an ISI CO₂-bulb [5] with 86 grams of gas, we have an acceptable 5 minutes of continuous experimental time.

Because our goal is to build a transportable and easy to handle biped, we (intuitively) put the maximum total weight on 7 kg. Regarding the amount

(and weight) of the electrical and mechanical sub-systems, a total weight of the pneumatic system of 1 kg seems to be acceptable.

Since the muscle pressure is directly related to the stiffness, it is important to be able to control the pressure levels with high accuracy. A relatively short response time is needed to make it possible to execute control actions during a step time of 0.6 seconds.

4.3 System overview

The pneumatic system provides the actuation for our prototype MIKE. The pneumatic system receives input from the on-board controller in the form of valve control signals. The controller determines when each muscle is activated or de-activated. The two respective muscle pressures are to be preset manually when tuning the prototype. The output of the pneumatic system obviously has the form of joint torques that influence the passive dynamic leg motions.

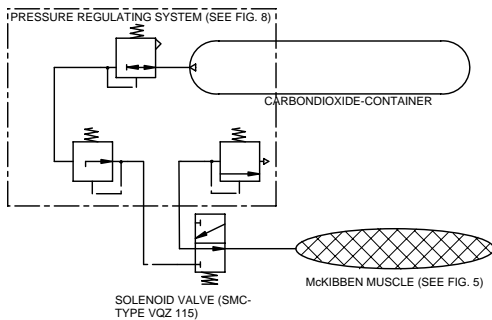


Fig. 6. Overview of the pneumatic system on MIKE

To provide for this desired input-output behavior, the pneumatic system consists of four components (see Figure 6): 1) gas container, 2) manually adjustable pressure reduction valves, 3) electronically controlled 3/2-way switching valves, and 4) McKibben muscles. The pressure reduction system is the most crucial part of the pneumatic system. We developed this system and will present it in the next section. For the valves we use the pilot pressure operated VQZ 115 valves from SMC [8]. Although these are about the most efficient commercially available valves, they still consume 0.5 Watts each. We are encouraging suppliers to develop more efficient valves. The McKibben muscles have been discussed in the previous section.

5 Pressure control unit

5.1 Background and requirements

The pressure control unit must be able to regulate the desired muscle pressures accurately and fast (well within the step time of 0.6 seconds). Second,

application in an autonomous biped requires a compact, lightweight and gas efficient solution.

There are two commercially available regulator principles, each of which can only fulfill part of the above requirements. The indirectly controlled pressure regulators (flapper-nozzle type) provide fast and accurate pressure control at the cost of a high internal gas consumption and relatively large physical dimensions. Directly controlled pressure regulators (piston type) are generally small and lightweight and need no extra gas supply for internal consumption, but are not sensitive and accurate enough for our application. We used the directly controlled principle, as small size and gas efficiency are the most important requirements, and minimized the disadvantages.

5.2 Operating principle

The piston type pressure regulator is drawn in Figure 7. A valve separates the input pressure from the output pressure. The output pressure acts on a spring loaded piston, where the manually adjustable spring load represents the output pressure level. If the output pressure falls below this preset value,

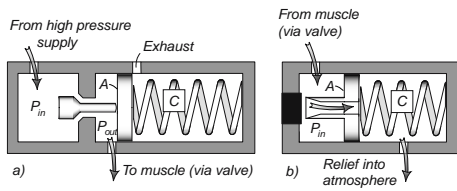


Fig. 7. Working principle of (a) pressure regulator valve and (b) pressure relief valve

the spring loaded piston opens the valve and the output pressure level is restored. To ascertain that the pressure regulator is sensitive, it needs to be constructed with a high ratio of A:C (see Figure 7) and with low internal friction.

The low preset pressure level is realized by integrating a separate pressure relief valve (see Figure 7) in the muscle outlet. The spring loaded piston in the pressure relief valve is open as long as the muscle pressure is higher than the preset level (drawn situation).

5.3 Technical realization and results

The principles discussed above are translated into functioning prototypes. Experiments have convinced us that the required relatively high accuracy cannot be met by a single-stage pressure regulator, due to pressure overshoot and steady state offset. Therefore we have divided the pressure reduction in two stages, see Figure 8.

First, one main pressure regulator directly on the gas bulb brings the pressure from 5.8 [MPa] to about 1.0 [MPa]. Second, a second-stage reduction from 1.0 [MPa] to 0.2 – 0.4 [MPa], with 4 different preset manually adjustable pressure levels, is realized in the input pressure control block ('IN', Figure 8). In these valves, the pistons are equipped with diaphragms to minimize friction effects and to provide the required sensitivity and accuracy. The output pressure control block ('OUT') includes four adjustable pressure relief valves. Basically the same piston construction as in the input pressure reduction valves has been used. The two pressure-control blocks together weigh about 180 gram and have a volume of less than 8 x 5.5 x 1.5 cubic centimeter.

After assembling the complete pneumatic system, it is possible to evaluate the behaviour by measuring the muscle pressure in time, during a switching-action of the described solenoid valve. Figure 8 shows the dynamic response of the complete system (see Figure 6) when pressurized from 0.15 [MPa] to 0.35 [MPa] and back. We obtain an accuracy/repeatability of about 10 [kPa], and a relatively slow response as was to be expected with the choice of pressure regulator type. However, the system is fast enough according to the successful walking results.

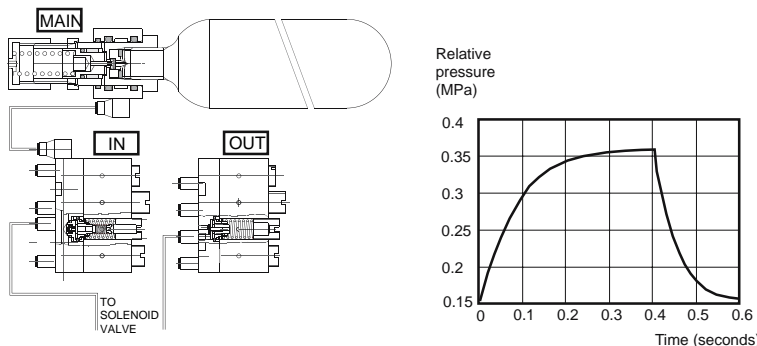


Fig. 8. (left) technical drawings of pressure reduction system, (right) dynamic response of the complete pneumatic system

6 Walking experiments

6.1 Downhill walking

We performed walking experiments with an increasing number of active degrees of freedom, starting with walking down a slope with rigid knees. With rigid knees, foot scuffing is inevitable. To eliminate this problem for our initial experiments, we constructed 'stepping stones' at the expected footfall

locations. Together with the slope angle this required some tuning, eventually resulting in stable walking with steps of 0.24 [m] at a slope angle of 0.06 [rad].

In this setting, we could start with experiments with rigid knees, similar to the testing machine in Figure 2. With the Agilent HEDS-5540 incremental optical encoder on the hip joint, the hip angle was recorded during a successful run as shown in Figure 9. As is apparent from the figure, the gait was not symmetrical. When the middle legs were swinging (positive hip angle), the step was much longer in duration. Heel strike only occurred when they were already far on their way back, noticeable by the small bump (impact shock) in the graph. It is not clear whether this asymmetry resulted from a non-perfect launch or from the machine's natural dynamics. A simulation study in the near future should reveal this. Although not symmetrical, the emergent gait was encouraging enough to continue with experiments with bending knees.

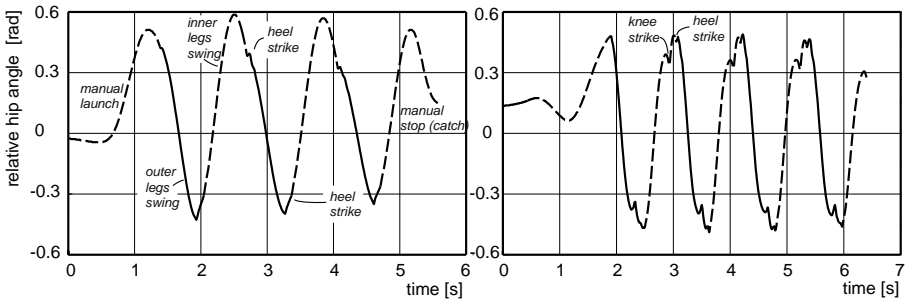


Fig. 9. Walking results (**left**) with stiff knees on a floor with stepping stones on a 0.06 [rad] slope, (**right**) with active knees on a 0.06 [rad] slope. The prototype completes 7 symmetrical steps until the end of the walking surface

By bending the knee for the appropriate time interval during the swing phase of a leg, the prototype can gain just enough foot clearance for continuous walking without stepping stones. As McGeer has shown, it is possible to obtain the appropriate timing with pure passive dynamics by tuning the mechanical properties. In our experience, it is then essential to keep the center of mass of the shank very close below the knee joint. However, we want the ability to actively interfere with the knee motion for future rough terrain walking experiments, so MIKE was provided with knee-stretching muscles. Having these muscles there anyway, we decided to actively control the knee motion rather than completely rely on the passive dynamic motion.

The knee is stretched actively with a McKibben muscle counteracted by a passive spring, see Figure 4. The default knee muscle pressure is 'high' (0.35 [MPa]), which is switched to 'low' (0.08 [MPa]) at the other leg's heel strike, and switched back to 'high' after an empirically determined 400 [ms]. With this activation pattern we obtained steady walking for the entire length

of the slope (5 [m]) with the appearance to be able to continue to walk indefinitely, see Figure 9. It is easy to launch the prototype by hand, so we would call it ‘pretty stable’. We have not yet performed experiments to determine the exact stability of the gait.

In these walking experiments MIKE has about the same specific resistance as a walking human being, using about 10 [W] to pull its 7 [kg] along at a speed of 0.4 [m/s]. The energy consumption consists of three components. First, the propulsion is obtained from gravity by walking down a 0.06 [rad] slope, which counts for 1.6 [W]. Second, the knee muscles use approximately 0.4 [MPa] CO_2 which accounts for 5.3 [W]. Actually, to keep the storage volume small, the CO_2 is stored and supplied at the saturation pressure, 5.8 [MPa]. The inevitable loss of energy in the process of pressure reduction from 5.8 to 0.4 [MPa] is not taken into account. Third, the prototype is equipped with a number of sensors and a a low power (less then 1 [W]) Strong-Arm based Linux machine (the LART [1]), which use together about 3 [W]. Obviously, the bulk of the energy consumption goes to the architecture for improving the stability even when using low-power components. We hope to increase the walking stability without increasing the energy consumption even more by using the timing of the muscle activations as a control parameter [11].

6.2 Walking on level floor

Finally, we activated the hip muscles and leveled out the walking surface. That made the robot lose its natural tendency to tilt and walk forward, so we had to shift the center of mass forward with a few centimeters. The hip muscles are the same as the knee muscles, but operate as antagonistic pairs. When heel strike is detected one muscle is set to high, its antagonist to low, so that the swing leg is pulled forward. We have not yet performed accurate measurements on the torque that the muscles exert on the hip, but it is estimated to be below 2.5 [Nm], approximately the same as the maximal torque from gravity. This simple form of hip control is sufficient to obtain a robust gait, see [12].

Mike performs a steady walk on a level floor, as demonstrated with video’s at <http://dbl.tudelft.nl/>. It can handle irregularities in the terrain, such as the sidewalk in front of our building.

With the ability to walk on level ground, we finally had the opportunity to perform an endurance test. On the 86 grams of CO_2 , MIKE can walk 3.5 minutes. After a continuous walk that long, the main pressure regulator is deeply frozen due to gas expansion; apparently it is a little undersized for the actual gas flow.

7 Conclusion

We started this research with the question: “How to keep the actuators and energy storage device lightweight enough to enable autonomous operation for

a walking biped?" Our solution is provide the biped with a pneumatic actuation system. This form of actuation is successful when applying the following two ideas: 1) use McKibben muscles as adjustable springs and 2) develop a compact and well performing pneumatic system. With these developments we were able to construct a fully autonomous biped. We have succeeded in making it walk in a stable manner on a level floor, see <http://dbl.tudelft.nl/>.

Now that we have concluded the first phase of this project, we are aiming at the following goals: first to add an upper body while maintaining passive dynamic properties, and finally to extend to three dimensions.

Acknowledgements

This research is funded by the Dutch national technology foundation STW. Thanks to Richard van der Linde, Arend Schwab, Dick Plettenburg, Frans van der Helm, Erik Mouw and Jan-Derk Bakker.

References

1. LART board. Strong-arm based low power linux machine, developed at delft university of technology. (<http://www.lart.tudelft.nl/>).
2. M. Garcia, A. Chatterjee, A. Ruina, and M. J. Coleman. The simplest walking model: Stability, complexity, and scaling. *ASME J. Biomech. Eng.*, 120(2):281–288, April 1998.
3. Shadow Group. (<http://www.shadow.org.uk>).
4. A. H. Hansen, D. S. Childress, and E. H. Knox. Prosthetic foot roll-over shapes with implications for alignment of trans-tibial prostheses. *Prosthetics and Orthotics International*, 24:205–215, 2000.
5. ISI. (<http://www.isi-group.com>).
6. T. McGeer. Passive dynamic walking. *Intern. J. Robot. Res.*, 9(2):62–82, April 1990.
7. T. McGeer. Passive dynamic biped catalogue. In R. Chatila and G. Hirzinger, editors, *Experimental Robotics II: The 2nd International Symposium*, pages 465–490, Berlin, 1992. Springer–Verlag.
8. SMC pneumatics. (<http://www.smccusa.com>).
9. G. Pratt and M. Williamson. Series elastic actuators. In *Proceedings of IROS '95*, Pittsburgh, PA, 1995.
10. A. L. Schwab and M. Wisse. Basin of attraction of the simplest walking model. In *Proc., International Conference on Noise and Vibration*, Pennsylvania, 2001. ASME.
11. R. Q. vd. Linde. Design, analysis and control of a low power joint for walking robots, by phasic activation of mckibben muscles. *IEEE Trans. Robotics and Automation*, 15(4):599–604, August 1999.
12. M. Wisse, A. L. Schwab, R. Q. van der Linde, and F. C. T. van der Helm. How to keep from falling forward; elementary swing leg action for passive dynamic walkers. Submitted to IEEE Transactions on Robotics, 2004.

Learning Energy-Efficient Walking with Ballistic Walking

Masaki Ogino¹, Koh Hosoda^{1,2} and Minoru Asada^{1,2}

¹ Dept. of Adaptive Machine Systems, Graduate School of Engineering, Osaka University, 2-1 Yamadaoka, Suita, Osaka, 565-0871, Japan

² HANDAI Frontier Research Center, Osaka University, 2-1 Yamadaoka, Suita, Osaka, 565-0871, Japan

Abstract. This paper presents a method for energy efficient walking of a biped robot with a layered controller. The lower layer controller has a state machine for each leg. The state machine consists of four states: 1) constant torque is applied to hip and knee joints of the swing leg, 2) no torque is applied so that the swing leg can move in a ballistic manner, 3) a PD controller is used so that the certain posture can be realized at the heel contact, which enables a biped robot to walk stably, and 4) as the support leg, hip and knee joints are servoed to go back and the torque to support upper leg is applied. With this lower layer controller, the upper layer controller can search parameters that enable the robot to walk as energy efficiently as human walking without paying any attention to fall down.

1 Introduction

Comparing with human walking, bipedal walking of the current robots is rather rigid since it does not utilize natural dynamics while human walking does. Passive dynamic walking (PDW) is the walking mode in which a robot can go down a shallow incline without any control nor any actuation, only with its own mechanical dynamics [1], and it is one approach to realize natural motion in a robot. This walking looks so similar to human walking that many researchers have intensively studied its characteristic features and the conditions that enable a robot to walk in a PDW manner [2][3][8][9][10][13]. Although PDW teaches us that mechanical dynamics of a robot can reduce control efforts for walking, the structural parameters and initial conditions to realize PDW are strictly limited, and it is not always known how we can apply PDW properties to walking on a level floor. The properties that a controller should have in order to realize both stable and energy efficient walking simultaneously are not known yet.

We suppose that one of such properties is to have a control phase in which no torque is applied to a robot, instead the gravitational and inertial force are utilized for motion. Such kind of walking is called "ballistic walking". Ballistic walking is supposed to be a human walking model suggested by Mochon and McMahon [6]. They got the idea from the observation of human walking data, in which the muscles of the swing leg are activated only at the beginning and the end of the swing phase.

There are a number of methods to realize ballistic walking. Taga proposed a CPG controller that enables a human model to walk very stably with as the same energy efficiency as human walking [14]. The torque profile of his model shows the ballistic properties clearly. His CPG model is, however, very complicated and it is not always necessary to use CPG to realize energy efficient walking in a robot if the same properties are realized with a simpler controller. Actually, Linde shows that the energy efficient walking can be realized by a simple controller in which muscle contraction is activated by sensor information of foot contact [4]. Recently, Pratt demonstrated in simulation and in a real robot that energy efficient walking is possible with a simple state machine controller, in which the knee joint of the swing leg moves passively in the middle of the swing phase [11]. He determined the parameters of walking by hand coding and genetic algorithm, and it is unclear to make the energy efficient walking with learning from non-efficient walking.

In this paper, to utilize mechanical dynamics of a robot structure, we let the hip joint free in the middle of the swing phase, and use torque control instead of a PD controller in the beginning of the swing phase. Moreover, the learning module is added to the state machine controller so that the minimum energy walking can be realized.

The rest of the paper is organized as follows. First, the state machine controller to realize ballistic walking is introduced. Next, the learning module to optimize the parameters of the state machine controller is described. Then, the proposed controller is applied to a biped model that has the same length and mass to a human.

2 Ballistic walking with state machine

Here, we use a robot model consisting of 7 links: a torso, two thighs, two shanks and two foots as shown in Fig.1. The parameters of the robot are shown in Table 1.

The state machine controller at each leg consists of four states, as shown in Fig 2: the beginning of the swing phase (*swing I*), the middle of the swing phase (*swing II*), the end of the swing phase (*swing III*), and the support phase (*support*).

In the support phase, the hip joint is controlled with a proportional derivative (PD) manner so that the torso stands up and the support leg goes back. To the knee joint, torque is applied so that the knee joint becomes straighten during the support phase. Therefore, the torque applied to the hip and waist joint are given by the following equations;

$$\tau_1 = -K_p(\theta_1 - \theta_{1d}) - K_v(\dot{\theta}_1 - \dot{\theta}_{1d}) - K_{wp}\theta_w - K_{wu}\dot{\theta}_w, \quad (1)$$

$$\tau_2 = -K_p(\theta_2 - \theta_{2d}) - K_v(\dot{\theta}_2 - \dot{\theta}_{2d}). \quad (2)$$

The reference trajectory for the above PD controllers are described with the simple sinusoidal functions which connect the angle of the beginning of the

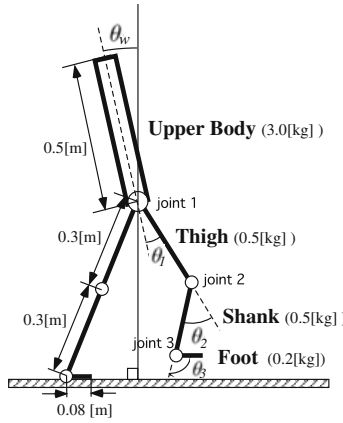


Fig. 1. Robot model

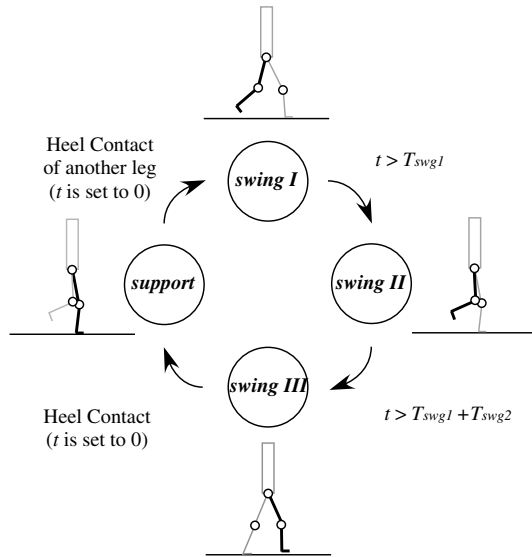


Fig. 2. A state machine controller consisting of four states

state to the desired angle which should be realized at the end of the state,

$$\theta_{1d}(t) = \begin{cases} \frac{(\theta_{1e} - \theta_{1s})}{2} (1 - \cos \frac{\pi t}{T_{spt}}) + \theta_{1s} & (t < T_{spt}) \\ \theta_{1e} & (t \geq T_{spt}) \end{cases}, \quad (3)$$

$$\dot{\theta}_{1d}(t) = \begin{cases} \frac{\pi(\theta_{1e} - \theta_{1s})}{2T_{spt}} \sin \frac{\pi t}{T_{spt}} & (t < T_{spt}) \\ 0 & (t \geq T_{spt}) \end{cases}, \quad (4)$$

$$\theta_{2d}(t) = \begin{cases} \frac{(\theta_{2e} - \theta_{2s})}{2} (1 - \cos \frac{\pi t}{T_{spt}}) + \theta_{2s} & (t < T_{spt}) \\ \theta_{2e} & (t \geq T_{spt}) \end{cases} \quad (5)$$

and

$$\dot{\theta}_{2d}(t) = \begin{cases} \frac{\pi(\theta_{2e} - \theta_{2s})}{2T_{spt}} \sin \frac{\pi t}{T_{spt}} & (t < T_{spt}) \\ 0 & (t \geq T_{spt}) \end{cases} \quad (6)$$

where θ_{*s} indicates the angle at the moment when the controller enters the support phase (the moment of contact of the swing leg with the ground), and θ_{*e} indicates the desired angle that should be realized at the end of the support phase. t is the time since the controller enters to the support phase and T_{spt} is the desired time when the support phase ends. In this simulation, the control gains are set as $K_p = 300.0$ [Nm/rad], $K_v = 3.0$ [Nm sec/rad], $K_{wp} = 300.0$ [Nm/rad] and $K_{wv} = 0.3$ [Nm sec/rad], and the desired angles of the end of the support phase are set as $\theta_{1e} = 20.0$ [deg] and $\theta_{2e} = 0.0$ [deg].

The swing phase is separated to three states; *swing I* (the beginning phase), *swing II* (the middle phase), and *swing III* (the end phase). In *swing I*, the controller applies constant torque to both the hip and knee joint. After the certain time passes, the control state changes to *swing II*, in which no torque is applied to the hip and knee joints. Therefore, in *swing II*, the swing leg moves in a fully passive manner. After the swing time passes T_{swg2} , the control state changes to *swing III*, in which the joints are servoed using PD controllers so that the desired posture at the end of the swing phase can be realized. By taking a certain posture at the moment of ground contact, a certain degree of walking stability can be assured. The state of the controller transits to the state *support* when the swing leg contacts with the ground. The output torque can be summarized as the following equations,

$$\tau_1 = \begin{cases} A & (t < T_{swg1}) \\ 0 & (T_{swg1} \leq t < T_{swg1} + T_{swg2}) \\ -K_p(\theta_1 - \theta_{1d}) - K_v(\dot{\theta}_1 - \dot{\theta}_{1d}) & (T_{swg1} + T_{swg2} \leq t) \end{cases} \quad (7)$$

and

$$\tau_2 = \begin{cases} -B & (t < T_{swg1}) \\ 0 & (T_{swg1} \leq t < T_{swg1} + T_{swg2}) \\ -K_p(\theta_2 - \theta_{2d}) - K_v(\dot{\theta}_2 - \dot{\theta}_{2d}) & (T_{swg1} + T_{swg2} \leq t) \end{cases}, \quad (8)$$

where the reference trajectory in *swing III* is given in the same manner as the support phase, eqs.(4)-(7). In our study, the desired angles of the hip and knee joints at the end of the swing phase are set as $\theta_{1e} = -20$ [deg] and $\theta_{2e} = 0$ [deg], respectively. T_{swg1} and T_{swg2} are set to 0.2 [sec], and 0.05 [sec].

Throughout walking, a PD controller with the weak gains ($K'_p = 3.0$ [Nm/rad] and $K'_v = 0.3$ [Nm sec/rad]) is used to the ankle joints,

$$\tau_3 = -K'_p(\theta_3 - \theta_{3d}) - K'_v(\dot{\theta}_3 - \dot{\theta}_{3d}) \quad (9)$$

The desired angle of the ankle joint is always fixed to 90 [deg]. Therefore, the ankle joint works as a spring is attached.

The simulation result of the controller is shown in Fig. 3, in which the resultant torque curves are shown with control mode during one period (two steps). In this figure, the control modes 1, 2, 3 and 4 correspond to *swing I*, *swing II*, *swing III* and *support*, respectively. In Fig. 3, large torque is

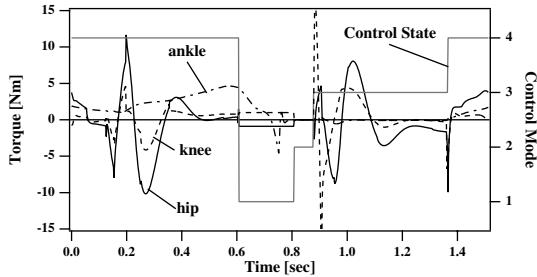


Fig. 3. State machine mode and torque during one period

observed at the end of the swing phase and the beginning of the support phase. This torque might be caused by too large or too small torque applied at the beginning of the swing phase. If the appropriate torque is applied in *swing I* (at the beginning of the swing phase), this feedback torque might be lessen and the more energy-efficient walking could be realized. In the next section, the optimization of this torque is attempted by adding a learning module.

3 Energy minimization by a learning module

To realize the energy efficient walking, a learning module which searches appropriate output torque in *swing I* is added to the controller described in the previous section (Fig.4). Besides torque, the learning module searches the appropriate value of control parameters which determine the end of the duration of passive movement, T_{swg2} . It is noted that these parameters are not related to the PD controller which stabilizes walking. For the evaluation of energy efficiency, we use the average of all the torque which is applied during one walking period (two steps),

$$Eval = \frac{1}{T_{step}} \int_0^{T_{step}} \sum_{i=1}^3 \tau_i dt \quad (10)$$

Using this performance function, the appropriate values of the parameters are searched in the probabilistic ascent algorithm as follows.

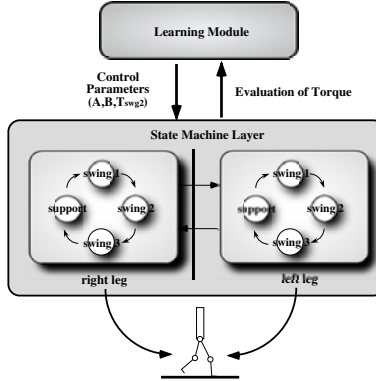


Fig. 4. Ballistic walking with learning module

- 1 $if(Eval < Eval_{min})$
- 2 $A_{min} = A$
- 3 $B_{min} = B$
- 4 $T_{swg2min} = T_{swg2}$
- 5 $A = A + \text{random perturbation}$
- 6 $B = B + \text{random perturbation}$
- 7 $T_{swg2} = T_{swg2} + \text{random perturbation}$

The simulation results are shown in Fig. 5. Figures 5 (a), (b) and (c) show the time courses of the output torque applied to the hip and knee joints in *swing I*, A, B, and the passive time, T_{swg2} , and the average of total torque, $Eval$, respectively. Even though the input torque changes variously, the PD controller in *swing III* which keeps the posture at ground contact constant realizes a stable walking.

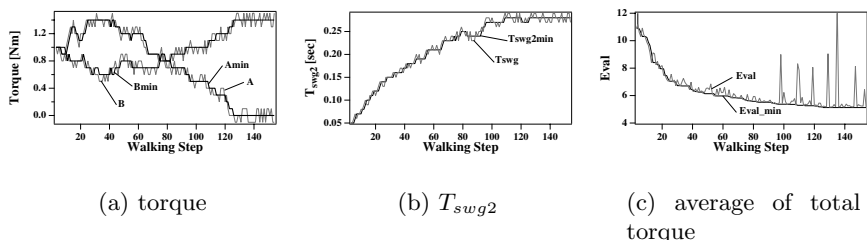


Fig. 5. Learning curve of control parameters and total torque

Comparing the first step with the 80th the average of total torque decreases (Fig. 5(c)), even though the output torque of the beginning of the

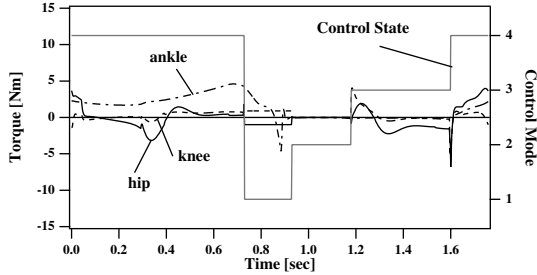


Fig. 6. State machine mode and torque by a state machine controller with a learning module

swing phase at the 80th step is almost the same as the first step (Fig. 5(a)), whereas the passive time, T_{swg2} , increases (Fig. 5(b)). The total torque of walking, therefore, depends more on the passive time than the magnitude of the feed forward torque that is given in the beginning of the swing phase.

Furthermore, in the final stage of learning, after the 120th step, the output torque of the hip joint at the beginning in the swing phase becomes zero while the torque of the knee joint increases. This result might be strange because many researchers have applied torque to hip joint in swing phase. In this stage, the large energy output appears among weak ones (Fig. 5(c)). This may be because a robot walks on a wing and a prayer on the subtle balance between dynamics and energy. Once the balance is lost, the PD controller compensates stability with large torque.

Fig. 6 is the time-course of the torque around the 80th step. Comparing the torque appeared in Fig. 6 with those in Fig. 3, the total torque are reduced about 1/10 in the hip and knee joints, whereas the torque profile at the ankle joint is almost the same.

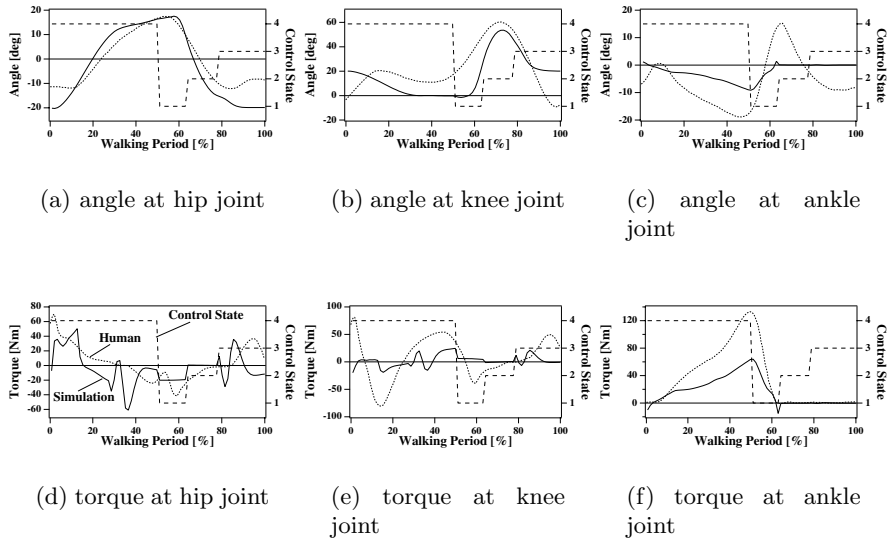
4 Comparing with human data

In this section, we apply the proposed controller to the model that has the same mass and length of links as human, and the torque and angle of each link are compared with the observed data in human walking.

For parameters of human model, we use the same model as that of Oghara and Yamazaki [7], which is shown in Table 1. The control gains at hip and knee joints are set as $K_p = 6000.0$ [Nm/rad], $K_v = 300.0$ [Nm sec/rad], $K_{wp} = 6000.0$ [Nm/rad] and $K_{wv} = 100.0$ [Nm sec/rad]. The desired angles at the end of the swing and support phases are the same as in Section 2.

The time course of angle and torque of the simulation results are shown in Figs. 7 with human walking data (from [15]). The horizontal axis is normalized by the walking period.

	Mass [kg]	Length [m]	Inertia [kg m ²]
HAT	46.48	0.542	3.359
Tigh	6.86	0.383	0.133
Shank	2.76	0.407	0.048
Foot	0.89	0.148	0.004

Table 1. Mass and length of human model links**Fig. 7.** Comparing with human walking data

	Human	Simulation
Support : Swing [%:%]	60:40	60:40
Walking Rate [steps/sec]	1.9	1.3
Walking Speed [m/sec]	1.46	0.46
Walking Step [m]	0.76	0.36
Energy Consumption [cal/m kg]	0.78	0.36

Table 2. Characteristics of simulation and human walking

At the hip joint, while the time course of joint angle is almost same as human, torque curve is quite different, especially in around 80% and 30% walking periods in which strong effects of PD controllers appears (Fig. 7(b)). At the knee joint, the pattern of the time course of joint angle roughly resembles human data in shape except at around the end of the swing phase

and the beginning of the support phase, in which the knee joint of human data becomes straighten but that of simulation data does not. Moreover, the torque pattern is quite different from human data. At the ankle joint, it is surprised that the torque pattern shares common traits with human data, even though the ankle joint is modeled as simple spring joint. Fig. 7(f) shows that, although the control state after the support phase is named "*swing I*", it works as double support phase. The rate of swing phase to support phase is the same as human data (40:60).

Table 2 compares characteristics of walking in the simulation result with that in human data ([12]). It shows that the simulation algorithm succeeds in finding the parameters which enable the human model to walk with 45% less energy consumption. But this walk may not necessarily mean the energy efficient walking because the walking speed (and the walking rate) is much slower than human walking. This may be because the proposed controller uses the ankle joint only passively, and only the energy consumption is taken into consideration in the evaluation function (eq. 10). Acquiring fast walking is our future issue.

5 Discussion

Our controller has a state machine on each leg, which affects each other by sensor signals. Even this simple controller enables a biped robot to walk stably. There are two reasons. First, PD controllers at the end of the swing phase ensure that a biped touches down on the ground with the same posture. This prevents a swing leg from contacting with too shorter or too longer step length because of inadequate forward torque given at the beginning of the swing phase. But this stabilization does not always work well. It mainly depends on the posture at ground contact. How this posture is determined is the issue we should attack next.

The second reason for stable walking is that the controller has some common features to CPG (Central Pattern Generator). In the CPG model, the activities of neurons are affected by sensor signals (or environment), and as a result global entrainment between a neural system and the environment takes place [14]. Our proposed controller doesn't have a walking period explicitly. The period of the controller is strongly affected by the information from touch sensors, which determine the state transition of a state machine in each leg. It can be said that our controller has some properties like global entrainment between the state machine controller and the environment.

Walking mode realized in this paper is much slower than human walking as shown in Table 2. We suppose that the reason of this slow walking owes to the passive use of the ankle joint. To realize fast walking, it is necessary to shorten the walking period and to make the step length longer. They are closely related to the ankle joint setting because the speed of falling forward of the support leg is largely affected by the stiffness of the ankle joint, and the

step length can be longer if the support leg rotates around the toe. Controlling the walking speed is another issue to be attacked.

Acknowledgments

This study was performed through the Advanced and Innovational Research program in Life Sciences from the Ministry of Education, Culture, Sports, Science and Technology, the Japanese Government.

References

1. Asano, F. Yamakita, M. and Furuta, K., 2000, "Virtual passive dynamic walking and energy-based control laws", *Proceedings of the 2000 IEEE/RSJ Int. Conf. on Intelligent Robots and Systems*, pp. 1149-1154.
2. Garcia, M. Chatterjee, A. Ruina, A. and Coleman, M., 1998, "The simplest walking model: stability, complexity, and scaling", *J. Biomechanical Engineering*, Vol. 120, pp. 281-288.
3. Goswami, A. Thuiilot, B. and Espiau, B., 1998, "A Study of the Passive Gait of a Compass-Like Biped Robot: symmetry and Chaos", *Int. J. Robotics Research*, Vol. 17, No. 12, pp.1282-1301.
4. Van der Linde, R. Q., 2000, "Actively controlled ballistic walking", *Proceedings of the IASTED Int. Conf. Robotics and Applications 2000*, August 14-16, Honolulu, Hawaii, USA.
5. McGeer, T., 1990, "Passive walking with knees", *1990 IEEE Int. Conf. on Robotics and Automation*, 3, Cincinnati, pp.1640-1645.
6. Mochon, S. and McMahon, T.A., 1980, "Ballistic walking", *J. Biomech.*, 13, pp. 49-57.
7. Ogihara, N. and Yamazaki, N., 2001, "Generation of human bipedal locomotion by a bio-mimetic neuro-musculo-skeletal model", *Biol. Cybern.*, 84, pp. 1-11.
8. Ogino, M. Hosoda, K. and M. Asada., 2002, "Acquiring passive dynamic walking based on ballistic walking", *5th Int. Conf. on Climbing and Walking Robots*, pp.139-146.
9. Ono, K. Takahashi, R. Imadu, A. and Shimada, T., 2000, "Self-excitation control for biped walking mechanism", *Proceedings of the 2000 IEEE/RSJ Int. Conf. on Intelligent Robots and Systems*, pp. 1149-1154.
10. Osuka, K. and Kirihara, K., 2000, "Development and control of new legged robot quartet III - from active walking to passive walking-", *Proceedings of the 2000 IEEE/RSJ Int. Conf. on Intelligent Robots and Systems*, pp. 991-995.
11. Pratt, J., 2000, "Exploiting Inherent Robustness and Natural Dynamics in the Control of Bipedal Walking Robots", Doctor thesis, MIT, June.
12. Shumway-Cook, A. Woollacott, M., 1995, "Motor Control : Theory and Practical Applications", Williams and Wilkins.
13. Sugimoto, Y. and Osuka, K., 2002: "Walking control of quasi-passive-dynamic-walking robot 'Quartet III' based on delayed feedback control", *Proceedings of the Fifth Int. Conf. on Climbing and Walking Robots*, pp. 123-130.
14. Taga, G., 1995, "A model of the neuro-musculo-skeletal system for human locomotion: I. Emergence of basic gait", *Biol. Cybern.*, 73, pp. 97-111.
15. Winter, DA., 1984, "Kinematic and kinetic patterns of human gait; variability and compensating effects", *Human Movement Science*, 3, pp. 51-76.

Motion Generation and Control of Quasi Passive Dynamic Walking Based on the Concept of Delayed Feedback Control

Yasuhiro Sugimoto and Koichi Osuka

Dept. of Systems Science, Graduate School of Informatics, Kyoto University, Uji, Kyoto, 611-0011, JAPAN

Abstract. Recently, Passive-Dynamic-Walking (PDW) has been noticed in the research of biped walking robots. In this paper, focusing on the entrainment phenomena which is the one of character of PDW, we provide a new control method of Quasi-Passive-Dynamic-Walking. Concretely, at first, for the sake of the continuous walking of robot and taking place of the entrainment phenomenon, we adopt a kind of PD control which gains are regulated by the state of the contact phase of swing leg. And, considering the making use of the concept of DFC, we use $(k-1)$ -th trajectory of the walking robot as the reference trajectory of the k -th step. As a result, it can be expected that the robot itself generates the optimum stable trajectory and the walking is stabilized by using this trajectory.

1 Introduction

Recently a lot of researches of humanoid robots or biped locomotion have been carried out. ASIMO(HONDA) and HRP-series(AIST) are very famous examples. In such researches of walking robots, recently, Passive Dynamic Walking(PDW) which was studied by McGeer[1] at first, has been noticed. As the features of this motion, the following are raised: This walking is very smooth and similar to human's walking. Secondly, it can be realized only by the dynamics of robot without any input torques if the robot walks on smooth slope. Moreover, by using the effect of gravitational field skillfully, the robot walks with high energy efficiency. From these features, the various studies of applications of PDW have been made expecting a realization of a high-efficient and smooth walking of robot [2][3][4][5][6].

Especially, in the application of PDW, some control methods of Quasi-Passive-Dynamic-Walking(Quasi-PDW) have been proposed [4][5][6]. Quasi-PDW means that the robot usually does PDW without any torque inputs, and just only when the walking begins or disturbances come in, the actuators of the robot are used for stabilization of walking. As one of this control method, focusing the contact phase of the swing leg with the ground (we call it's state Impact point), we proposed a control method which based on Delayed Feedback Control(DFC) [5][6]. This control method is very simple and does not require making any reference trajectory. But, it can not stabilize the walking without a proper set of initial conditions. (especially it requires

proper initial velocities) And since it focuses just only on impact point, the performance of stabilization is relatively small.

Then, referring to the one of the control method of Quasi-PDW[4], we consider both following two: one is to make use of the concept of the DFC and the second one is to provide some reference trajectory for continuous walking. From the above, in this paper, we will propose a new control method in which $(k-1)$ -th step's trajectory of the walking robot are used as k -th reference trajectory and the PD gains in this control law are regulated in each steps depending on the state of the impact point. By doing so, it is expected that the robot walks continuously and the entrainment phenomena of PDW will occur, and then, its walking will converge to the stable trajectory. This trajectory is equivalent to the trajectory which the robot in PDW generates. This means that the robot walking finally becomes to be stabilized by using PDW trajectory which is made by the robot itself.

2 Model of the walking robot

A model of the biped robot which we consider is shown in Fig.1.

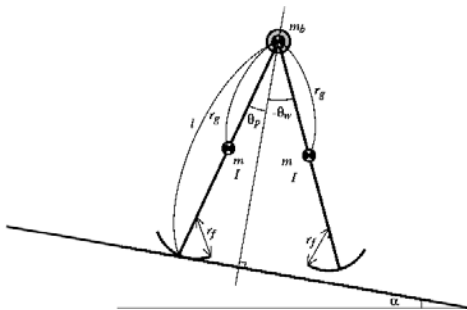


Fig. 1. Compass model of Walking robot

Let the support leg angle be θ_p , the swing (non-supported) leg angle be θ_w , a slope angle be parameter α , and a torque vector which is supplied to the support leg and the swing leg be $\tau(t) = [\tau_p, \tau_w]^T$. And β is the support leg angle at the collision of the swing leg with the ground. Then, the dynamic equation of the robot can be derived using the well known Euler-Lagrange approach:

$$M(\theta)\ddot{\theta} + N(\theta, \dot{\theta})\dot{\theta} + g(\theta, \alpha) = \tau(t), \quad (1)$$

where $M(\theta)$ is the inertia matrix, $N(\theta, \dot{\theta})\dot{\theta}$ is the centrifugal and Colioris term, and $g(\theta, \alpha)$ is the gravity term. See [4] or [6] in detail. If we assume that a transition of the support leg and the swing leg occurs instantaneously and

the impact of the swing leg with the ground is inelastic and occurs without sliding, the equation of transition at the collision can be derived by using the conditions of conservation of angular momentum:

$$P_b(\beta)\dot{\theta}^- = P_a(\beta)\dot{\theta}^+, \quad (2)$$

where $\dot{\theta}^-$, $\dot{\theta}^+$ are the pre-impact and the post-impact angular velocities respectively. The details of $P_b(\beta)$, $P_a(\beta)$ are provided in [4] or [6].

And we difine an vector p as:

$$p(k) = (\beta_k, \dot{\theta}_{p,k}^-, \dot{\theta}_{w,k}^-)^T, \quad (3)$$

where β_k is β at the k -th collision, $\dot{\theta}_{p,k}^-$ and $\dot{\theta}_{w,k}^-$ are the k -th pre-impact angular velocities of the support leg and the swing leg respectively. And we call this p as **Impact point**.

3 Stability of passive dynamic walking

If the input torques are assumed to be constant over each k -th step and some assumptions will be hold, it can be stated that the discrete dynamic system of impact point: $p(k+1) = \mathcal{P}(p(k), \tau(k))$ can be well defined and the stability of the equilibrium point of this system is equivalent to the stability of PDW [5]. Here, expanding this statement, we show that the stability of the equilibrium point of this system is equivalent to the stability of PDW even if the input torques are not constant but continue and differentiable between each k -th step.

Theorem 1 Let the input torques $\tau(t)$ be continue and differentiable between each k -th step. Then, with regard to impact point $p(k)$ and input torques $\tau(t)$, a following map \mathcal{P}_{cl}

$$p(k+1) = \mathcal{P}_{cl}(p(k), \tau) \quad (4)$$

can be defined. And, p^* is a stable equilibrium point of this map Eq.(4) with $\tau(t) = 0$ for $T_p(k-1) \leq t^V < T_p(k)$, if and only if, the continuous trajectory of the motion of the robot that passes through p^* is stable in the sense of Lyapunov, where $T_p(k)$ is a time when the k -th impact occurs.

Proof Basically, it can be proved by similar way of the proof of lemma 1 and 2 in [5]. At first, let the set of the states of the robot just before impact be \mathcal{S} , then the target system of the robot can be denoted as follows:

$$\Sigma : \begin{cases} \dot{x}(t) = f_{cl}(x(t)) & (x^-(t) \notin \mathcal{S}) \\ x^+(t) = \Delta(x^-(t)) & (x^-(t) \in \mathcal{S}), \end{cases} \quad (5)$$

where,

$$x(t) := (\theta_p, \theta_w, \dot{\theta}_p, \dot{\theta}_w)^T, f_{cl} := f(x(t)) + g(x(t))\tau(t),$$

$$f(x(t)) = \begin{bmatrix} (\dot{\theta}_p, \dot{\theta}_w)^T \\ -M^{-1}(\theta)(N(\theta, \dot{\theta})\dot{\theta} + g(\theta, \alpha)) \end{bmatrix}, g(x(t)) = \begin{bmatrix} 0 \\ M^{-1}(\theta) \end{bmatrix}.$$

Because of the condition of $\tau(t)$, it can be said that $f_{cl}(t)$ can have a unique solution which depends continuously on the initial condition between the each k -th step, and then, the map $\mathcal{P}_{cl,x}(x, \tau)$ can be well-defined [7]. This map means that the state just before the k -th collision x_k^- is mapped to the state just before the $(k+1)$ -th collision x_{k+1}^- when input torques τ are used. Then, using the following matrixes:

$$E = \begin{pmatrix} 1 & 0 & 0 \\ -1 & 0 & 0 \\ 0 & 1 & 0 \\ 0 & 0 & 1 \end{pmatrix}, F = \begin{pmatrix} 1 & 0 & 0 & 0 \\ 0 & 0 & 1 & 0 \\ 0 & 0 & 0 & 1 \end{pmatrix},$$

we can defined a map $\mathcal{P}_{cl}(p(k), \tau)$ as follows:

$$p(k+1) = F\mathcal{P}_{cl,x}(Ep(k), \tau(k)) := \mathcal{P}_{cl}(p(k), \tau). \quad (6)$$

Secondly, because the existence of the map $\mathcal{P}_{cl,x}(x, \tau)$ can be shown, using the same way of proof of lemma 2 in [5], we can say that p^* is a stable equilibrium point of the system: $p(k+1) = \mathcal{P}_{cl}(p(k), \tau)$ with $\tau(t) = 0$ for $T_p(k-1) \leq t^v < T_p(k)$, if and only if, the continuous trajectory of the robot that passes through p^* is stable in the sense of Lyapunov.

From this theorem, it can be said that even if the input torques are not constant but continue and differentiable between each k -th step, the stability of impact point $p(k)$ on the discrete dynamical system is greatly related to the stability of PDW.

4 DFC-based control method

To propose a new control method of Quasi-Passive-Dynamic-Walking, we particularly consider the following two key ideas. The first one is making use of the concept of DFC so as not to design the reference trajectory which the robot in PDW generates correctly. The second one is providing roughly designed reference trajectory and stabilizing the walking by using this reference trajectory so as to be possible to start its walking without a proper initial condition or to continuous walking even if some disturbances come in.

To construct new controller with the above ideas, in this paper, we focus on the entrainment phenomena which is one of the properties of PDW. The entrainment phenomena of PDW means that even if the robot starts walking with different initial conditions, its walking converges to a specific trajectory which is agree with the trajectory of PDW. However, the states of robot which can cause the entrainment phenomena will exist in narrow region because the initial conditions which can cause PDW exist in very narrow region and PDW is very sensitive to disturbance. So, it seems that it is difficult to stabilize Quasi-Passive-Dynamic-Walking only by using the entrainment phenomena.

Then, we construct a new control method which has the next two properties, that is, “*generation of PDW using the entrainment phenomena and the*

concept of DFC so as to be needless of correctly design of the reference trajectory of PDW" and "stabilization the walking for the sake of its continuous walking and taking place of the entrainment phenomena".

4.1 Our previous control method of quasi-PDW

Discrete-DFC based control method As an example of the control method of Quasi-PDW, the discrete-DFC based control method [5] or [6] can be given. This control method is that, since it can be proved that the stability of PDW is equivalent to the stability of the equilibrium impact point on the discrete dynamical system:

$$p(k+1) = \mathcal{P}(p(k), \tau), \quad (7)$$

Quasi-Passive-Dynamic-Walking can be stabilized by using the input torques $\tau(k)$ which stabilize $p(k)$ of the system Eq.(7):

$$\tau(k) = K(y(k) - y(k-1)) = K \begin{bmatrix} P_p(k) - P_p(k-1) \\ P_w(k) - P_w(k-1) \end{bmatrix}, \quad (8)$$

where $P_p(k), P_w(k)$ are the kinetic energy of the support and swing leg at impact point respectively. From Eq.(8), we can see that this control method is very simple and does not need any information of the equilibrium point p^* of Eq.(7), that is, it can stabilize Quasi-PDW without making any reference trajectory. However, focusing only on impact point, the performance of this control method is relatively not so good. So, this can not stabilize the walking when big disturbances come in. Furthermore, this can not stabilize the walking without proper initial conditions especially initial velocities of the legs.

Weekly guidance control method On the contrary, as one of the control method which utilizes the entrainment phenomena, Osuka and Saruta proposed the following control method [4] (we call it "weekly guidance control method"):

$$\begin{aligned} \tau &= K_f(\delta(k))[M(\theta)s + N(\theta)\dot{\theta}^2 + g(\theta, \alpha)], \\ \delta(k) &= \beta(k) - \beta(k-1), \\ s &= \ddot{\theta}_d + K_v(\dot{\theta}_d - \dot{\theta}) + K_p(\theta_d - \theta), \end{aligned} \quad (9)$$

where, $K_f(x)$ is defined by

$$K_f(x) = \begin{cases} 1 & \|x\| \geq \gamma \\ (-\cos(\frac{x\pi}{\gamma}) + 1)/2 & \|x\| \leq \gamma, \end{cases} \quad (10)$$

and an example of $K_f(x)$ is shown in Fig.2.

As the features of this control method, the following can be given: $|\beta_k - \beta_{k-1}|$ is adopted as an evaluate function of the stability of walking and it is

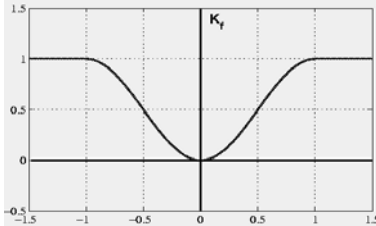


Fig. 2. Example of function K_f at $\gamma = 1.0$

used as the weight of trajectory tracking controller. According to the features, even if there is an error between the reference trajectory $r_d = [\theta_d, \dot{\theta}_d]$ used in this control method and the trajectory $r_{id} = [\theta_{id}, \dot{\theta}_{id}]$ which the robot in PDW generates, the trajectory of robot converges to r_{id} and $|\beta_k - \beta_{k-1}|$ becomes small gradually during the robot walks continuously, owing to the entrainment phenomena. And finally, $|\beta_k - \beta_{k-1}|$ becomes zero and then the robot becomes to do PDW. Therefore, it can be expected that Quasi-PDW, will be realized by using this control method.

However, we think that there are the following problems in this control method (9).

- In case that the robot's walking is disordered by some disturbances after its walking converges to r_{id} , that is, after robot come to do PDW, is it unreasonable to make the walking to converge to PDW using the r_d once again ? Since the ideal trajectory r_{id} will be made already by robot itself, are there some method of making use of r_{id} for stabilization of its walking ?
- How on earth do we make the reference trajectory r_d ?
- From Section 3, is it better to use the data of impact point $p(k)$ than β_k when the stability of walking is evaluated ?

Especially, with regard to r_d , even if there would be some differences between r_d and r_{id} , we could expect the walking would converge to r_{id} owing to the entrainment phenomena. But, it is desired that the difference between r_d and r_{id} is as small as possible to improve the efficiency of this control method. Therefore, it is needed to make a sufficient proper reference trajectory r_d in advance, and then, it can not be said any more that this control method fully makes use of the entrainment phenomena of PDW.

4.2 The propose control method

From 4.1, 4.1 and the consequence of Section 3 which means that the impact point $p(k)$ is greatly related to the stability of robot's walking, we propose the following control method.

Updating reference trajectory control method based on DFC

$$\begin{aligned}\tau_k &= K_f(\delta_k)[K_v(\dot{\theta}_{k-1} - \dot{\theta}_k) + K_p(\theta_{k-1} - \theta_k)] \\ \delta_k &= \|p(k) - p(k-1)\|_\phi,\end{aligned}\quad (11)$$

where θ_k is k -th step's $\theta = (\theta_p, \theta_w)^T$, $K_f(\cdot)$ is defined by Eq.(10), ϕ is a constant matrix $\phi \in \mathcal{R}^{3 \times 3}$ and $\|\cdot\|_M$ is a norm defined by $\|x\|_M = \sqrt{x^T M x}$ and a constant matrix $M \in \mathcal{R}^{m \times n}$.

As one of the features of this control method(11), the following can be given: at first, it evaluates the stability of walking by using the data of impact point $p(k)$ and $p(k-1)$. And secondly, it realizes tracking control not with r_d which is made in advance but with r_{k-1} which is the $(k-1)$ -th trajectory of robot. As a result, the reference trajectory is updated in each steps.

Since the walking is stabilized by PD-control whose gains are regulated depending on the stability of walking, it can be said that this proposed control method (11) satisfies the specification which is “*stabilization of the walking for the sake of its continuous walking and taking place of the entrainment phenomena*”.

And, since updating the reference trajectory using the $(k-1)$ -th step trajectory in each steps is equivalent to doing *continuous*-DFC and the entrainment phenomena will cause because walking will continue, we can expect that its walking will converge to r_{id} without making correctly design of the trajectory r_{id} during the robot walks continuously. Therefore, the proposed control method can satisfy the secondary specification which is “*to generate of PDW using the entrainment phenomena and the concept of DFC so as to be needless of correctly design of the reference trajectory of PDW*”. Moreover, if once the walking of robot converges to PDW, it holds true that $r_k = r_{k-1} = r_{id}$. So, it is also the advantage of this control method that it can use r_{id} as the reference trajectory after the convergence to PDW.

Furthermore, with regard to initial reference trajectory r_0 , since it can expected that the robot itself makes the ideal trajectory r_{id} during the walking, it is enough to design r_0 roughly with which walking can be occur without falling down.

Remark In case of using the proposed method Eq.(11) with a real robot, it is more reasonable that we obtain r_{id-sim} by some simulation using the proposed method with an roughly designed r_0 at first, then we use this r_{id-sim} as r_0 when we actually apply the proposed method to the real robot.

5 Computer simulation

In this section, we investigate the validity of the proposed control method (11) by several simulations. We use same physical parameters of robot as Quartet III [4]. The initial conditions of the robot are set as $\theta_0(0) = [-0.34, 0.34, 0, 0]^T$ and

$$K_p = \begin{pmatrix} 30 & 0 \\ 0 & 30 \end{pmatrix}, \quad K_v = \begin{pmatrix} 25 & 0 \\ 0 & 25 \end{pmatrix}, \quad \phi = \begin{pmatrix} 5 & 0 & 0 \\ 0 & 0.1 & 0 \\ 0 & 0 & 0.1 \end{pmatrix}, \quad \gamma = 1.0.$$

The initial reference trajectory $r_0(t)$ is set as,

$$\theta_{p,0}(t) = 2.2667t^2 + 0.79333t - 0.34000,$$

$$\dot{\theta}_{p,0}(t) = 4.4894t + 0.79333,$$

$$\theta_{w,0}(t) = 8.4524t^2 - 5.0810t - 0.34000,$$

$$\dot{\theta}_{w,0}(t) = 16.905t - 5.0810.$$

These are obtained as following. At first, $\theta_p(t)$ and $\theta_w(t)$ are given as quadratic equations which pass $[(0,-0.34),(0.25,0),(0.4,0.34)]$ and $[(0,0.34),(0.3,-0.4),(0.4,-0.34)]$ respectively. Then, $\dot{\theta}_p(t)$ and $\dot{\theta}_w(t)$ are obtained by differentiating $\theta_p(t)$ and $\theta_w(t)$ respectively. Furthermore, since it can be that k -th step's walking period is bigger than $(k-1)$ -th step's walking period, we use a 7th polynomial which is approximated to $(k-1)$ -th step's trajectory as k -th step's reference trajectory.

Simulation results are shown in Fig.3-Fig.5. Fig.3 shows the support leg angle and swing leg angle $\theta_p(t)$ and $\theta_w(t)$. Fig.4 shows the input torques $\tau(t)$, where the solid line means the support leg and the dotted line means the swing leg respectively. Fig.5 shows the 1,2,3,7 and 24th step's reference trajectory respectively. To compare with our previous control method, the simulation results with weekly guidance control method Eq.(9) in which the same r_0 is used as the reference trajectory, are shown in Fig.6 and 7.

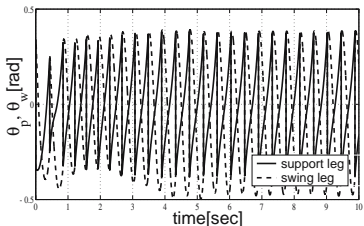


Fig. 3. Trajectory of θ_p, θ_w by Eq.(11)

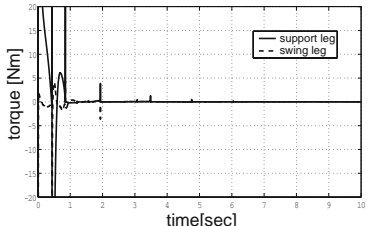


Fig. 4. Input torque by Eq.(11)

From these figures, though the robot's walking is not uniformly and the input torques are needed to continue walking at the beginning of walking, the input torques τ and K_f are decreasing gradually during some steps. And finally, r_k becomes equivalent to r_{k-1} and the robot becomes to walk via PDW. On the contrary, the robot's walking with the weekly guidance control can not converge to PDW though the robot can continue walking. This is because it does not use the proper reference trajectory r_d . So, we can say that the proposed control method Eq.(11) works well.

Secondly, we investigate the robustness of the proposed control method against disturbance. Simulation results in which the slope angle α is set as

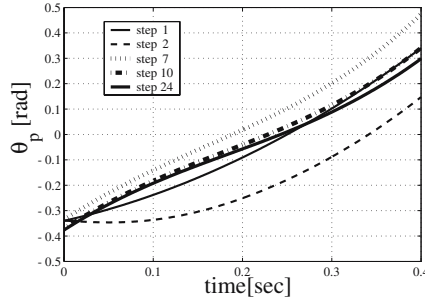


Fig. 5. Reference trajectory of θ_p

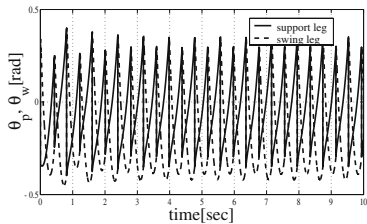


Fig. 6. Trajectory of θ_p, θ_w by Eq.(9)

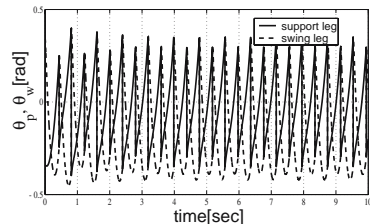


Fig. 7. Input torque by Eq.(9)

6[deg] (nominal value of α is 3[deg]) between 5[sec] and 6[sec], are shown in Fig.8 and 9. To compare with our previous control methods, simulation results when Eq.(8) and Eq.(9) are used are also shown in the same figures. Here, there is a problem how we set the reference trajectory r_d in Eq.(9). In this simulation, for easily convergence to PDW, we make the reference trajectory which is very close to the trajectory of PDW but is not agree perfectly and use it.

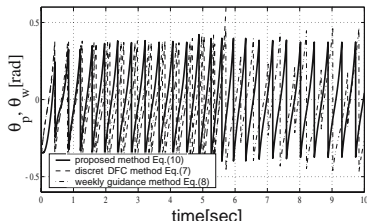


Fig. 8. Trajectory of θ_p, θ_w

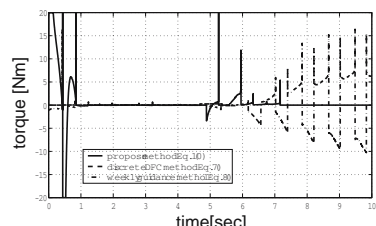


Fig. 9. Input torque

From these figures, we can see that the robot with the discrete-DFC based control Eq.(8) can not continue walking after the disturbance is added, and the robot with the weekly guidance control Eq. (9) can not converge to PDW again. On the contrary, the robot with the proposed method Eq.(11) can walk down continually after the disturbance is added and becomes to walk via PDW again. So we can say that the proposed method works well.

6 Conclusion and future work

In this paper, making use of the concept of DFC and the entrainment phenomena of PDW, we proposed a new control method of Quasi-PDW. Concretely, the proposed method uses $(k-1)$ -th step's trajectory of the walking as the reference trajectory of the k -th step and regulates the gain according to Impact Point. And the effectiveness of the proposed control method was shown through several simulations.

As a problem yet to be solved in the future is to prove the effectiveness of the proposed control method and obtain the systematic derivation methods of K_p , K_v and ϕ in Eq.(11). Furthermore, we should carry out experiments with a real robot.

References

1. T.McGeer: "Passive Dynamic Walking", *Int.J.of Rob.Res.*, Vol.9, No.2, 1990
2. A. Goswami, B. Thuilot and B. Espiau: "A Study of the Passive Gait of a Compass-Like Biped Robot: Sysmmetry and Chaos", *Int. J.of Rob. Res.* pp.1282–1301,2000
3. F. Asano, M. Yamakita, N. Kamamichi, Z. LUO, "A Novel Gait Generation for Biped Walking Robots Based on Mechanical Energy Constraint", *Proc. of the IEEE/RSJ Int. Conf. on Intellignet Robots and Systems(IROS)*, pp.2637–2644, 2002
4. K.Osuka,Y.Saruta: "Gait Control of Legged Robot Quartet III via Passive Walking", *Proc. of the 8 th Symposium on Control Technology8th*, pp.355–360,2000 (in Japanese)
5. Y. Sugimoto, K. Osuka, "Stabilization of semi passive dynamic walking based on delayed feedback control", *Proc. of the 7 th Robotics Symposia*, pp89–94, 2002 (in Japanese)
6. Y. Sugimoto, K. Osuka, "Walking Control of Quasi-Passive-Dynamic-Walking Robot "Quartet III" based on Delayed Feedback Control", *Proc. of the 5th Int. Conf. on Climbing and Walking Robots(CLAWAR)*, pp.123–130, 2002
7. J. W. Grizzle, F. Plestan and G. Abba: "Poincare's Method for Systems with Impulse Effects: Application to Mechanical Biped Locomotion", *Proc. of the 38th Conference on Decision & Control*, pp. 3869–3876,1999
8. K.Pyragas, "Continuous control of chaos by selfcontrolling feedback", *Phys.Lett.A*,vol 170,pp.421–428,1992

Part 5

**Neuro-Mechanics
& CPG and/or Reflexes**

Gait Transition from Swimming to Walking: Investigation of Salamander Locomotion Control Using Nonlinear Oscillators

Auke Jan Ijspeert¹ and Jean-Marie Cabelguen²

¹ Swiss Federal Institute of Technology, CH-1015 Lausanne, Switzerland

² Inserm EPI9914, Inst. Magendie 1 rue C. St-Saëns, F-33077 Bordeaux, France

Abstract. This article presents a model of the salamander’s locomotion controller based on nonlinear oscillators. Using numerical simulations of both the controller and of the body, we investigated different systems of coupled oscillators that can produce the typical swimming and walking gaits of the salamander. Since the exact organization of the salamander’s locomotor circuits is currently unknown, we used the numerical simulations to investigate which type of coupled-oscillator configurations could best reproduce some key aspects of salamander locomotion. We were in particular interested in (1) the ability of the controller to produce a traveling wave along the body for swimming and a standing wave for walking, and (2) the role of sensory feedback in shaping the patterns. Results show that configurations which combine global couplings from limb oscillators to body oscillators, as well as inter-limb couplings between fore- and hind-limbs come closest to salamander locomotion data. It is also demonstrated that sensory feedback could potentially play a significant role in the generation of standing waves during walking.

1 Introduction

The salamander, a tetrapod capable of both swimming and walking, offers a remarkable opportunity to investigate vertebrate locomotion. It represents, among vertebrates, a key element in the evolution from aquatic to terrestrial habitats.

This article investigates the mechanisms underlying locomotion and gait transition in the salamander. We develop computational models of the spinal circuits controlling the axial and limb musculature, and investigate how these circuits are coupled to generate, and switch between, the aquatic and terrestrial gaits. In previous work, one of us developed neural network models of the salamander’s locomotor circuit based on the hypothesis that the circuit is constructed from a lamprey-like central pattern generator (CPG) extended by two limb CPGs [2]. In that work, a genetic algorithm was used to instantiate synaptic weights in the models such as to optimize the ability of the CPG to generate salamander-like swimming and walking patterns. Here, we develop models based on coupled nonlinear oscillators, and extend that work by systematically investigating different types of couplings between the oscillators capable of producing the patterns of activity observed in salamander

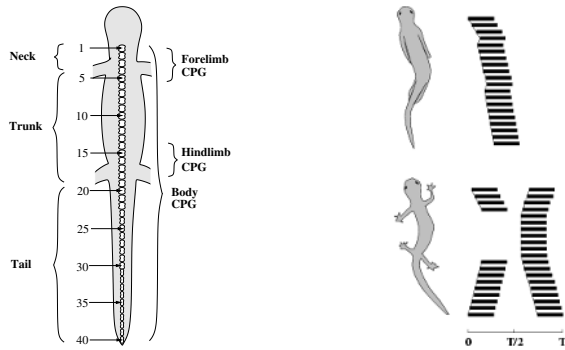


Fig. 1. Left: Schematic dorsal view of the salamander's body. Right: Patterns of EMG activity recorded from the axial musculature during swimming (top) and walking (bottom), adapted from Delvolv   et al. 1997.

locomotion. The use of nonlinear oscillators instead of neural network oscillators allows us to reduce the number of state variables and parameters in the models, and to focus on a systematic study of the inter-oscillator couplings.

We address the following questions: (1) how are body and limb CPGs coupled to produce traveling waves of lateral displacement of the body during swimming and standing waves during walking? (2) how is sensory feedback integrated into the CPGs? (3) does sensory feedback play a major role in the transition from traveling waves to standing waves? (4) to what extent is the inter-limb coordination between fore and hind limbs due to inter-limb coupling and/or the coupling with the body CPG? Clearly most of these questions are relevant to tetrapods in general.

2 Neural control of salamander locomotion

The salamander uses an anguilliform swimming gait very similar to the lamprey. The swimming is based on axial undulations in which rostrocaudal waves with a piece-wise constant wavelength are propagated along the whole body with limbs folded backwards (Figure 1, right). As in the lamprey, the average wavelength usually corresponds to the length of the body (i.e. the body produces one complete wave) and does not vary with the frequency of oscillation [3]. On ground, the salamander switches to a stepping gait, with the body making S-shaped standing waves with nodes at the girdles [3]. The stepping gait has the phase relation of a trot, in which laterally opposed limbs are out of phase, while diagonally opposed limbs are in phase. The limbs are coordinated with the bending of the body such as to increase the stride length in this sprawling gait. EMG recordings [3] have confirmed the bimodal nature of salamander locomotion, with axial traveling waves along

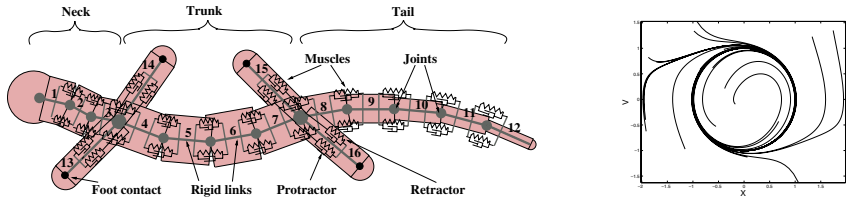


Fig. 2. Left: Mechanical model of the salamander's body. The two-dimensional body is made of 16 rigid links connected by one-degree-of-freedom joints. Each joint is actuated by a pair of antagonist muscles simulated as spring and dampers. Right: Limit cycle behavior of the nonlinear oscillator, time evolution with different random initial conditions.

the body for swimming, and mainly standing waves coordinated with the limbs for walking (Figure 1).

The CPG underlying axial motion—the body CPG—is located all along the spinal cord. Similarly to the lamprey [1], it spontaneously propagates traveling waves corresponding to fictive swimming when induced by NMDA excitatory baths in isolated spinal cord preparations [4]. Small isolated parts of 2 to 3 segments can be made to oscillate suggesting that rhythmogenesis is similarly distributed in salamander as in the lamprey. The neural centers for the limb movements are located within the cervical segments C1 to C5 (Figure 1 left) for the forelimbs and within the thoracic segments 14 to 18 for the hindlimbs [5–7]. These regions can be decomposed into left and right neural centers which independently coordinate each limb [5,7].

3 Mechanical simulation

The two-dimensional mechanical simulation of the salamander is an extension of Ekeberg's simulation of the lamprey [8]. The 25 cm long body is made of twelve rigid links representing the neck, trunk and tail, and four links representing the limbs (Figure 2). The links are connected by one-degree-of-freedom joints, and the torques on each joint are determined by pairs of antagonist muscles simulated as springs and dampers. The signals sent by the motoneurons contract muscles by modifying (increasing) their spring constant. The accelerations of the links are due to four types of forces: the torques due to the muscles, inner forces linked with the mechanical constraints due to the joints, contact forces between body and limbs, and the forces due to the environment (friction on ground, and inertial hydrodynamic forces in water). The dynamics equations underlying the simulation are described in more detail in [2].

4 Locomotion controller

4.1 Nonlinear oscillator

We construct our models of the CPGs by using the following nonlinear oscillator to represent a local oscillatory center:

$$\begin{aligned}\tau \dot{v} &= -\alpha \frac{x^2 + v^2 - E}{E} v - x \\ \tau \dot{x} &= v\end{aligned}$$

where τ , α , and E are positive constants. This oscillator has the interesting property that its limit cycle behavior is a sinusoidal signal with amplitude \sqrt{E} and period $2\pi\tau$ ($x(t)$ indeed converges to $\tilde{x}(t) = \sqrt{E} \sin(t/\tau + \phi)$, where ϕ depends on the initial conditions, see also Figure 2, right).

We assume that the different oscillators of the CPG are coupled together by projecting to each other signals proportional to their x and v states in the following manner

$$\begin{aligned}\tau \dot{v}_i &= -\alpha \frac{x_i^2 + v_i^2 - E_i}{E_i} v_i - x_i + \sum_j (a_{ij}x_j + b_{ij}v_j) + \sum_j c_{ij}s_j \\ \tau \dot{x}_i &= v_i\end{aligned}$$

where a_{ij} and b_{ij} are constants (positive or negative) determining how oscillator j influences oscillator i . In these equations, the influence from sensory inputs s_j weighted by a constant c_{ij} is also added, see next sections for further explanations.

4.2 Body CPG

We assume that the body CPG is composed of a double chain of oscillators all along the 40 segments of spinal cord. The type of connections investigated in this article are illustrated in Figure 3 (left). For simplicity, we assume that only nearest neighbor connections exist between oscillators. In our first investigation, the oscillators are assumed to be identical along the chain (with identical projections), as well as between each side of the body. The connectivity of the chain is therefore defined by 6 parameters, two (the a_{ij} and b_{ij} parameters) for each projection from one oscillator to the other (i.e. the rostral, caudal, and contralateral projections). Of these 6 parameters, we fixed the couplings between contralateral oscillators to $a_{ij} = 0$ and $b_{ij} = -0.5$ in order to force them to oscillate in anti-phase. We systematically investigated the different combinations of the four remaining parameters (the rostral and caudal projections) with values ranging from -1.0 to 1.0, with a 0.1 step.

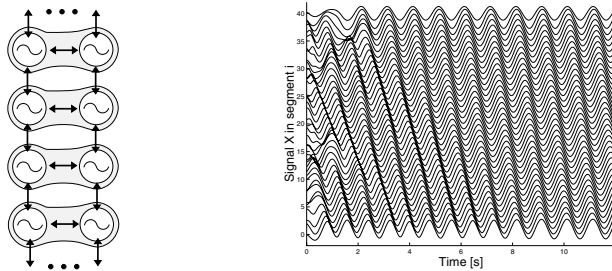


Fig. 3. Left: Configuration of the body CPG. Right: oscillations in a 40-segment chain (only the activity in a single side is shown).

Traveling wave Experiments on isolated spinal cords of the salamander suggest that, similarly to the lamprey, the body CPG tends to propagate rostro-caudal (from head to tail) traveling waves of neural activity. During (intact) swimming, the wavelength of the wave corresponds approximately to a bodylength. We therefore systematically investigated the parameter space of the body CPG configuration to identify sets of parameters leading to stable oscillations with phase lags between consecutive segments approximately equal to 2.5% of the period (in order to obtain a 100% phase lag between head and tail). The goal is to obtain traveling waves which are due to asymmetries of interoscillator coupling, while maintaining the same intrinsic period (the same τ) for all oscillators.

We found that several coupling schemes could lead to such traveling waves. The coupling schemes can qualitatively be grouped in three different categories: dominantly caudal couplings, balanced caudal and rostral couplings, and dominantly rostral couplings.¹ By dominant, we mean that the sum of the absolute values of the weights in one direction are significantly larger than in the other direction. While all groups can produce traveling waves corresponding to salamander swimming, solutions which have balanced caudal and rostral couplings need significantly more cycles to stabilize into the traveling wave (starting from random initial conditions) than the solutions in which one type of coupling is dominant. It is therefore likely that the salamander has one type of coupling which is dominant compared to the other. A very similar conclusion has been made concerning the lamprey swimming controller [9].

Figure 3 (right) illustrates the traveling waves generated by one of the dominantly caudal chains. As can be observed, starting from random initial

¹ Dominantly caudal and rostral couplings are essentially equivalent since each coupling type which is dominant in one direction has an equivalent in the other direction by inverting the sign of some weights. However, that equivalence is lost when the intrinsic frequencies of some oscillators are varied, see the “Piece-wise constant wavelength” paragraph.

states, the oscillations rapidly evolve to a traveling wave. Since the period of the oscillations explicitly depend on the parameter τ , the period can be modified independently of the wavelength. The wavelength of one-body length is therefore maintained for any period, when all oscillators have the same value of τ (i.e. the same intrinsic period). This allows one to modify the speed of swimming by only changing the period of oscillation, as observed in normal lamprey and salamander swimming.

Interestingly, while the connectivity of the oscillators favors a one-body length wavelength, it is possible to vary the wavelength by modifying the intrinsic period of some oscillators, the oscillators closest to the head, for instance. Reducing the period of these oscillators leads to an increase of the phase lag between consecutive oscillators (a reduction of the wavelength), while increasing their period leads to a decrease of the phase lag, and can even change the direction of the wave (i.e. generate a caudo-rostral wave). This type of behavior is typical of chains of oscillators [9].

Piece-wise constant wavelength We identify at least four potential causes for the small changes of wavelength observed along the body at the level of the girdles: (1) differences of intrinsic frequencies between the oscillators at the girdles and the other body oscillators, (2) differences in intersegmental coupling along the body CPG (with three regions: neck, trunk, and tail), (3) effect of the coupling from the limb CPG, (4) effect of sensory feedback. Recent in-vitro recordings on isolated spinal cords showed that a change of wavelength is also obtained during fictive swimming. It therefore seems that the phenomenon is mainly due to the CPG configuration rather than to sensory feedback (explanation number four is therefore the less likely). We tested these different hypotheses with the numerical simulations. For the hypothesis 2, it meant adding 8 parameters for differentiating the intersegmental couplings in the neck, trunk and tail regions.

The results suggest that, in our framework, the most likely cause of the three-wave pattern is a combination of differences in intersegmental coupling and of intrinsic frequencies of the oscillators at the girdles. The differences in intersegmental coupling lead to variations in the wavelength of the undulation along the spinal cord. But they do not explain the abrupt changes of phases at the level of the girdles. These are best explained by small differences in intrinsic frequencies of the oscillators of the body CPGs at the two girdles (these could also potentially be due to the projections from the limb CPG, see next sections).

We can furthermore tell that the effect of variations of the intrinsic frequencies depend on which coupling is dominant in the body CPG. The patterns observed in the salamander are best explained with either a combination of dominantly caudal coupling and higher intrinsic frequency at the girdles, or dominantly rostral coupling and lower intrinsic frequencies at the girdles. The resulting activity in the latter configuration is illustrated in Figure 5 (left).

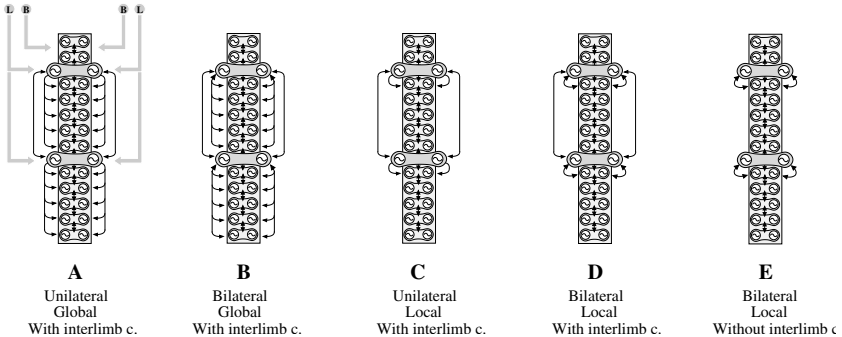


Fig. 4. Different potential CPG configurations.

Swimming We tested the body CPG in the mechanical simulation for controlling swimming. Since the mechanical simulation has only 11 joints along the body, 11 pairs of equally-spaced oscillators were picked from the body CPG to drive the muscle models, such that the oscillators in one pair project to the muscle on their respective side. A “motoneuron” m_i signal is obtained from the states x_i with the following equation $m_i = \beta \max(x_i, 0)$, where β is a positive constant gain. This motoneuron signal controls how much a muscle contracts by essentially changing the spring constant of the spring-and-damper muscle model (see [2]). An example of the swimming gait is shown in Figure 5 (left). The speed of swimming can be modulated by changing the frequency of all oscillators (through the parameter τ), while the direction of swimming can be modulated by applying an asymmetry of the amplitude parameter E between left and right sides of the chain. The salamander will then turn toward the side which receives the highest amplitude parameter.

4.3 Different body-limb CPG configurations for gait transition

One of the goals of this article is to investigate different types of couplings between the body and limb CPGs, and how these couplings affect the gait transitions between swimming and walking. There are currently too few biological data available to indicate how the different neural oscillators in the body and limb CPGs are interconnected. Our aim is to investigate which of these configurations can best reproduce some key characteristics of salamander locomotion.

We tested five different types of coupling (Figure 4). These couplings differ in three characteristics: *unilateral/bilateral* couplings, in which the limb CPGs are either unilaterally or bilaterally (i.e. in both directions) coupled to the body CPG, *global/local* couplings, in which the limb CPGs project either to many body CPG oscillators, or only those close to the girdles, and *with/without* interlimb couplings between fore- and hindlimbs. In our previous work [2], we tested configuration A (unilateral, global, with interlimb

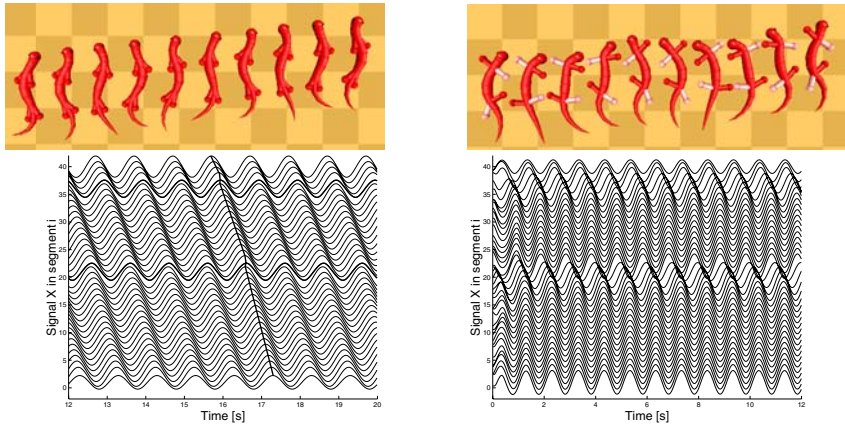


Fig. 5. Left, top: Swimming gait. Left, bottom: corresponding activity in the the body CPG (only the activity in a single side is shown). Note the piece-wise constant wavelength. The oscillations at the level of the girdles are drawn with thicker lines. Right top: walking gait. Right bottom: corresponding oscillations along the body in a CPG of type A.

coupling) using neural network oscillators. The unilateral projections from limb to body CPG essentially means a hierarchical structure in the CPG for that configuration.

In all configurations, we assume that two different control pathways exist for the body and the limb CPGs, in order words, that the control parameters τ and E can be modulated independently for the body and limb oscillators. In particular, we make the hypothesis that the gait transition is obtained as follows: swimming is generated when *only* the body CPG is activated ($E_{body} = 1.0$ and $E_{limb} = 0.005$), and walking is generated when *both* body *and* limb CPGs are activated ($E_{body} = 1.0$ and $E_{limb} = 1.0$).

The simulation results show that only configurations A and B, i.e. those with global coupling between limb and body CPG can produce standing waves (in the absence of sensory feedback). For these configurations, the global coupling from limb oscillators to body oscillators ensures that the body CPG oscillates approximately in synchrony in the trunk and in the tail when the limb CPG is activated (Figure 5, right). For the other configurations (C, D, and E) the fact that the couplings between limb and body CPGs are only local means that traveling waves are still propagated in the trunk and the tail, despite the influence from the limb oscillators. Configurations E, which lacks interlimb couplings can still produce walking gaits very similar to those of configurations C and D, because the coupling with the body CPG gives a phase relation between fore- and hindlimbs of approximately 50% of the period (because fore and hindlimbs are separated by approximately the half of one body-length).

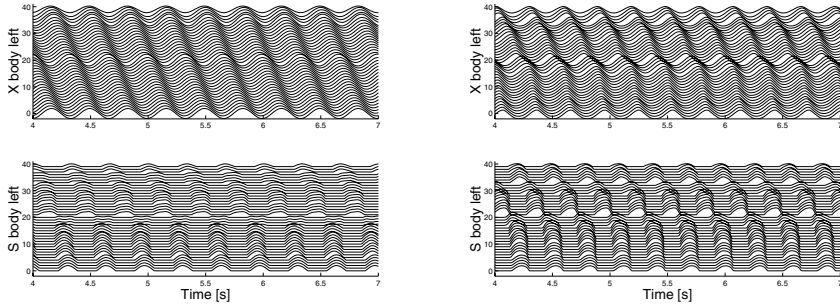


Fig. 6. Left: Walking gait produced by configuration D, **without** sensory feedback. Right: Walking gait produced by configuration D, **with** sensory feedback. Top: output of the body CPG, Bottom: output of the stretch sensors.

Having bilateral couplings between limb and body CPGs does not affect the walking pattern in a significant way. However, if the coupling from body CPG to limb CPG is strong, it will affect the swimming gait. In that case, even if the amplitude of the limb oscillators is set to a negligible value ($E_{limb} = 0.005$), the inputs from the body CPG will be sufficient to drive the limb oscillators which in return will force the body CPG to generate a wave which is a mix between a traveling wave and standing wave. It is therefore likely that the couplings between limb and body CPG are stronger from limb to body CPG than in the opposite direction.

Note that the fact that CPG configurations B, C and D can not produce standing waves, does however not exclude the possibility that these configurations produce standing waves when sensory feedback is added to the controller. This will be investigated in the next section.

Effect of sensory feedback When a lamprey is taken out of the water and placed on ground, it tends to make undulations which look almost like standing waves because the lateral displacements do not increase along the body but form quasi-nodes (i.e. points with very little lateral displacements) at some points along the body [10].

Interestingly, the same is true in our simulation. When the swimming gait is used on ground (without sensory feedback), the body makes a S-shaped standing wave undulation instead of the traveling wave undulation generated in water. This is due to the differences between hydrodynamic forces in water (which have strongly different components between directions parallel and perpendicular to the body) and the friction forces on ground (which are more uniform). The sensory signals from such a gait are then reflecting this S-shaped standing wave, despite the traveling waves sent to the muscles.

Sensory feedback is therefore a potential explanation for the transition from a traveling wave for swimming to a standing wave for walking. We therefore tested the effect of incorporating sensory feedback in the different

CPG configurations described above. Sensory feedback to the salamander's CPG is provided by sensory receptors in joints and muscles. We designed an abstract model of sensory feedback by including sensory units located on both sides of each joint which produce a signal proportional to how much that side is stretched: $s_i = \max(\phi_i, 0)$ where ϕ_i is the angle of joint i measured positively away from the sensory unit. For simplicity, we only consider sensory feedback in the body segments (i.e. not in the limbs), and assume that a sensory unit for a specific joint is coupled only locally to the two (antagonist) oscillators activating that joint.

Figure 6 shows the activity of the body CPG and the sensor units produced during a stepping gait with a controller with configuration D. Without sensory feedback (Figure 6, left), this controller produces a traveling wave during walking because the limb oscillators have only local projections to the body CPG. Despite this traveling wave of muscular activity, the body (in contact with the ground) makes essentially an S-shaped standing wave as illustrated by the sensory signals (synchrony in the trunk and in the tail, with an abrupt change of phase in between). When these sensory signals are fed back into the CPG (Figure 6, right), the body CPG activity is modified to approach the standing wave (i.e. the phase lag between segments decrease in the trunk and in particular in the tail). Note that if the sensory feedback signals are too strong, the stepping gait becomes irregular. Interestingly, the sensory feedback leads to an increase of the oscillation's frequency, something which has also been observed in a comparison between swimming with and without sensory feedback in the lamprey [11].

5 Discussion

The primary goal of this article was to investigate which of different CPG configurations was most likely to control salamander locomotion. To the best of our knowledge, only three previous modeling studies investigated which type of neural circuits could produce the typical swimming and walking gaits of the salamander. In [12], the production of S-shaped standing waves was mathematically investigated in a chain of coupled non-linear oscillators with long range couplings. In that model, the oscillators are coupled with closest neighbor couplings which tend to make oscillators oscillate in synchrony, and with long range couplings from the extremity oscillators to the middle oscillators which tend to make these coupled oscillators oscillate in anti-phase. It is found that for a range of strengths of the long range inhibitory coupling, a S-shaped standing wave is a stable solution. Traveling waves can also be obtained but only by changing the parameters of the coupling. In [2], one of us demonstrated that a leaky-integrator neural network model of configuration A could produce stable swimming and walking gaits. Finally, in [13], it was similarly demonstrated that a neural network model of the lamprey swimming controller could produce the piece-wise constant swimming of salamander and the S-shaped standing of walking depending on how phasic input

drives (representing signals from the limb CPGs and/or sensory feedback) are applied to the body CPG. The current paper extends these previous studies by investigating more systematically different potential body-limb CPGs configurations underlying salamander locomotion.

The simulation results presented in this article suggest that CPG configurations which have global couplings from limb to body CPGs, and interlimb couplings (configurations A or B) are the most likely in the salamander. These configurations can indeed produce stable swimming and walking gaits with all the characteristics of salamander locomotion. Our investigation does not exclude the other configurations, but suggest that these would need a significant input from sensory feedback to force the body CPG to produce the S-shaped standing wave along the body. These results suggest new neurophysiological experiments. It would, for instance, be interesting to make new EMG recordings during walking without sensory feedback (e.g. by lesion of the dorsal roots). If the EMG recordings remain a standing wave, it would suggest that configurations A or B are most likely, while if they correspond to a standing wave it would suggest that configurations C, D, or E are most likely.

To make our investigation tractable, we made several simplifying assumptions. First of all, we based our investigation on nonlinear oscillators. Clearly, these are only very abstract models of oscillatory neural networks. In particular, they have only few state variables, and fail to encapsulate all the rich dynamics produced by cellular and network properties of real neural networks. We however believe they are well suited for investigating the general structure of the locomotion controller. To some extent, some properties of interoscillator couplings are universal, and do not depend on the exact implementation of the oscillators. This is observed for instance in chains [9], as well as rings of oscillators [14]. Our goal was therefore to analyze these general properties of systems of coupled oscillators.

An interesting aspect of this work was to combine a model of the controller and of the body, since this allowed us to investigate the mechanisms of entrainment between the CPG, the body and the environment. We believe such an approach is essential to get a complete understanding of locomotion control, since the complete loop can generate dynamics that are difficult to predict by investigating the controller (the central nervous system) in isolation of the body. The transformation of traveling waves of muscular activity into standing waves of movements when the salamander is placed on ground is an illustration of the complex dynamics which can result from the complete loop.

Finally, this work has also direct links with robotics, since the controllers could equally well be used to control a swimming and walking robot. Especially interesting is the ability of the controller to coordinate multiple degrees of freedom while receiving very simple input signals for controlling the speed, direction, and type of gait.

Acknowledgements

We would like to acknowledge support from the french “Ministère de la Recherche et de la Technologie” (program “ACI Neurosciences Intégratives et Computationnelles”) and from a Swiss National Science Foundation Young Professorship grant to Auke Ijspeert.

References

1. A.H. Cohen and P. Wallen. The neural correlate of locomotion in fish. "fictive swimming" induced in a in vitro preparation of the lamprey spinal cord. *Exp. Brain Res.*, 41:11–18, 1980.
2. A.J. Ijspeert. A connectionist central pattern generator for the aquatic and terrestrial gaits of a simulated salamander. *Biological Cybernetics*, 85(5):331–348, 2001.
3. I. Delvolvé, T. Bem, and J.-M. Cabelguen. Epaxial and limb muscle activity during swimming and terrestrial stepping in the adult newt, *Pleurodeles Waltl. Journal of Neurophysiology*, 78:638–650, 1997.
4. I. Delvolvé, P. Branchereau, R. Dubuc, and J.-M. Cabelguen. Fictive rhythmic motor patterns induced by NMDA in an in vitro brain stem-spinal cord preparation from an adult urodele. *Journal of Neurophysiology*, 82:1074–1077, 1999.
5. G. Székely and G. Czéh. Organization of locomotion. In *Frog Neurobiology, a Handbook*, pages 765–792. Springer Verlag, Berlin, 1976.
6. M. Wheatley, M. Edamura, and R.B. Stein. A comparison of intact and in-vitro locomotion in an adult amphibian. *Experimental Brain Research*, 88:609–614, 1992.
7. J. Cheng, R.B. Stein, K. Jovanovic, K. Yoshida, D.J. Bennett, and Y. Han. Identification, localization, and modulation of neural networks for walking in the mudpuppy (*necturus maculatus*) spinal cord. *The Journal of Neuroscience*, 18(11):4295–4304, 1998.
8. Ö. Ekeberg. A combined neuronal and mechanical model of fish swimming. *Biological Cybernetics*, 69:363–374, 1993.
9. N. Kopell. Chains of coupled oscillators. In M.A. Arbib, editor, *The handbook of brain theory and neural networks*, pages 178–183. MIT Press, 1995.
10. G. Bowtell and T.L. Williams. Anguiform body dynamics: modelling the interaction between muscle activation and body curvature. *Phil. Trans. R. Soc. Lond. B*, 334:385–390, 1991.
11. Li Guan, T. Kiemel, and A.H. Cohen. Impact of movement and movement-related feedback on the lamprey central pattern generator for locomotion. *The Journal of Experimental Biology*, 204:2361–2370, 2001.
12. B. Ermentrout and N. Kopell. Inhibition-produced patterning in chains of coupled nonlinear oscillators. *SIAM Journal of Applied Mathematics*, 54(2):478–507, 1994.
13. T. Bem, J.-M. Cabelguen, O. Ekeberg, and S. Grillner. From swimming to walking: a single basic network for two different behaviors. *Biological Cybernetics*, page In press, 2002.
14. J. Collins and Richmond. Hard-wired central pattern generators for quadrupedal locomotion. *Biological Cybernetics*, 71:375–385, 1994.

Nonlinear Dynamics of Human Locomotion: from Real-Time Adaptation to Development

Gentaro Taga

Graduate School of Education, University of Tokyo
7-3-1 Hongo, Bunkyo-ku, Tokyo 113-0033, Japan

Abstract. The nonlinear dynamics of the neuro-musculo-skeletal system and the environment play central roles for the control of human bipedal locomotion. Our neuro-musculo-skeletal model demonstrates that walking movements emerge from a global entrainment between oscillatory activity of a neural system composed of neural oscillators and a musculo-skeletal system. The attractor dynamics are responsible for the stability of locomotion when the environment changes. By linking the self-organizing mechanism for the generation of movements to the optical flow information that indicates the relationship between a moving actor and the environment, visuo-motor coordination is achieved. Our model can also be used to simulate pathological gaits due to brain disorders. Finally, a model of the development of bipedal locomotion in infants demonstrates that independent walking is acquired through a mechanism of freezing and freeing degrees of freedom.

1 Introduction

The theory of nonlinear dynamics, which claims that spatio-temporal patterns arise spontaneously from the dynamic interaction between components with many degrees of freedom [1,2], is progressively attracting more attention in the field of motor control. The concept of self-organization in movement was initially applied to describe motor actions such as rhythmic arm movements [3]. In the meantime, neurophysiological studies of animals have revealed that the neural system contains a central pattern generator (CPG), which generates spatio-temporal patterns of activity for the control of rhythmic movements through the interaction of coupled neural oscillators [4]. Moreover, it has been reported that the centrally generated rhythm of the CPG is entrained by the rhythm of sensory signals at rates above and below the intrinsic frequency of the rhythmic activity [4]. This phenomenon is typical for a nonlinear oscillator that is externally driven by a sinusoidal signal.

Inspired by the theoretical and experimental approaches to self-organized motor control, we proposed that human bipedal locomotion emerges from a global entrainment between the neural system's CPG and the musculo-skeletal system's interactions with a changing environment [5]. A growing number of simulation studies have focused on the dynamic interaction of neural oscillators and mechanical systems in order to understand the mechanisms of generation of adaptive movements in insects [6], fish [7] and quadruped

animals [8-10]. In the field of robotics, an increasing number of studies have implemented neural oscillators to control movements of real robots [11-13].

The concept of self-organization argues that movements are generated as a result of dynamic interaction between the neural system, the musculo-skeletal system and the environment. If this is the case, the implicit assumption that the neural system is a controller and that the body is a controlled system needs to be revised. This paper presents a series of our models of human bipedal locomotion, all of which demonstrate the nonlinear properties of the neuro-musculo-skeletal system. The aim of this paper is to provide a framework for understanding the generation of bipedal locomotion [5, 14], real-time flexibility in an unpredictable environment [15], anticipatory adaptation of locomotion when confronted with an obstacle [16], visuo-motor coordination using optical flow information [17], the generation of pathological gaits and the acquisition of locomotion during development [18].

2 Real-time adaptation of locomotion through global entrainment

2.1 A model of the neuro-musculo-skeletal system for human locomotion

In principle, bipedal walking of humanoid robots can be controlled if the specific trajectory of each joint and of the zero moment point (ZMP) are planned in advance and feedback mechanisms are incorporated [19]. However, it is obvious that this method of control is not robust against unpredictable changes in the environment.

Is it possible to generate bipedal locomotion by using a neural model of the CPG in a self-organized manner? Let us assume that the entire system is composed of two dynamical systems: a neural system that is responsible for generating locomotion and a musculo-skeletal system that generates forces and moves in an environment. The neural system is described by differential equations for coupled neural oscillators, which produce motor signals to induce muscle torques and which receive sensory signals indicating the current state of the musculo-skeletal system and the environment. The musculo-skeletal system is described by Newtonian equations for multiple segments of the body. The input torque is generated by the output of the neural system. Using computer simulation we proved that a global entrainment between the neural system and the musculo-skeletal system is responsible for generating a stable walking movement [5].

Here I will present a model of [14]. As shown in Fig.1, the musculo-skeletal system consists of eight segments in the sagittal plane. The triangular foot interacts with the ground at its heel and/or toe. According to the output of the neural system, each of twenty "muscles" generates torque at specific joints. It is important to note that a number of studies have produced examples of walking robots, such as the passive dynamic walkers [20, 21] and the

dynamic running machines [22], which exploit the natural dynamics of the body. The oscillatory property of the musculo-skeletal system is an important determinant to establishing a walking pattern.

Our simulated neural system was designed based on the following assumptions:

(1) The neural rhythm generator (RG) is composed of neural oscillators, each of which controls the movement of a corresponding joint. As a model neural oscillator, we adopt the half-center model, which is composed of two reciprocally inhibiting neurons and which generates alternative activities between the two neurons [23].

(2) All of the relevant information about the body and the environment is taken into account. The angles of the body segments in an earth-fixed frame of reference and ground reaction forces are available to the sensory system. Global information on the position of the center of gravity (COG) with respect to the position of the center of pressure (COP) is also available. We assume that a gait is represented as a cyclic sequence of what we call global states: the double-support phase, the first half of the single-support phase, and the second half of the single-support phase. The global states are defined by the sensory information on the alternation of the foot contacting the ground and the orientation of the vector from the COP to the COG.

(3) Reciprocal inhibitions are incorporated between the neural oscillators on the contralateral side, which generates the anti-phase rhythm of muscles between the two limbs. Connections between the neural oscillators on the ipsilateral side change in a phase-dependent manner, using the global state to generate complex phase relationships of activity among the muscles within a limb.

(4) Both the local information on the angles of the body segments and the global information on the entire body are sent to the neural oscillators in a manner similar to the functional stretch reflex, so that neural oscillation and body movement are synchronized. Sensory information is sent only during the relevant phase of the gait cycle by modulating the gains of the sensory pathways in a phase-dependent manner, which is determined by the global state.

(5) All of the neural oscillators share tonic input from the higher center, which is represented by a single parameter. By changing the value of this parameter, the excitability of each oscillator can be controlled so that different speeds of locomotion are generated.

(6) While the neural rhythm generator induces the rhythmic movement of a limb, a posture controller (PC) is responsible for maintaining the static posture of the stance limb by producing phase-dependent changes in the impedance of specific joints. The final motor command is a summation of the signals from the neural rhythm generator and the posture controller.

The computer simulation demonstrated that, given a set of initial conditions and values of various parameters, a stable pattern of walking emerged

as an attractor formed in the state space of both the neural and musculoskeletal system. Figure 2 shows neural activities, muscle torques and a stick picture of walking within one gait cycle. The attractor was generated by the global entrainment between the oscillatory activity of the neural system and rhythmic movements of the musculo-skeletal system.

When we first proposed the model of bipedal locomotion [5], there were few studies to suggest the existence of a spinal CPG in humans. More recently, several studies have shown evidence for a spinal CPG in human subjects with spinal cord injury [24-26]. Our model is likely to capture the essential mechanism for the generation of human bipedal locomotion.

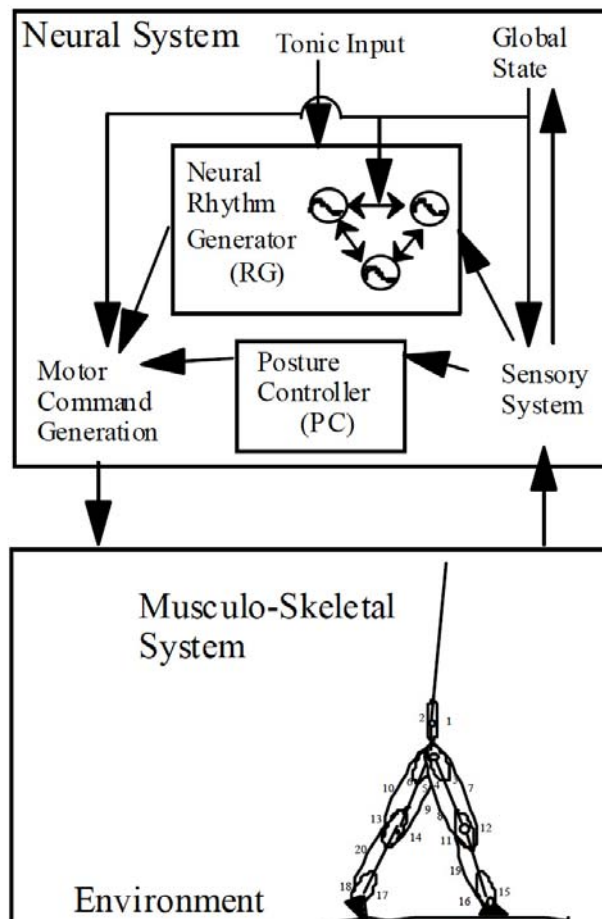


Fig. 1. A model of the neuro-musculo-skeletal system for human locomotion [14].

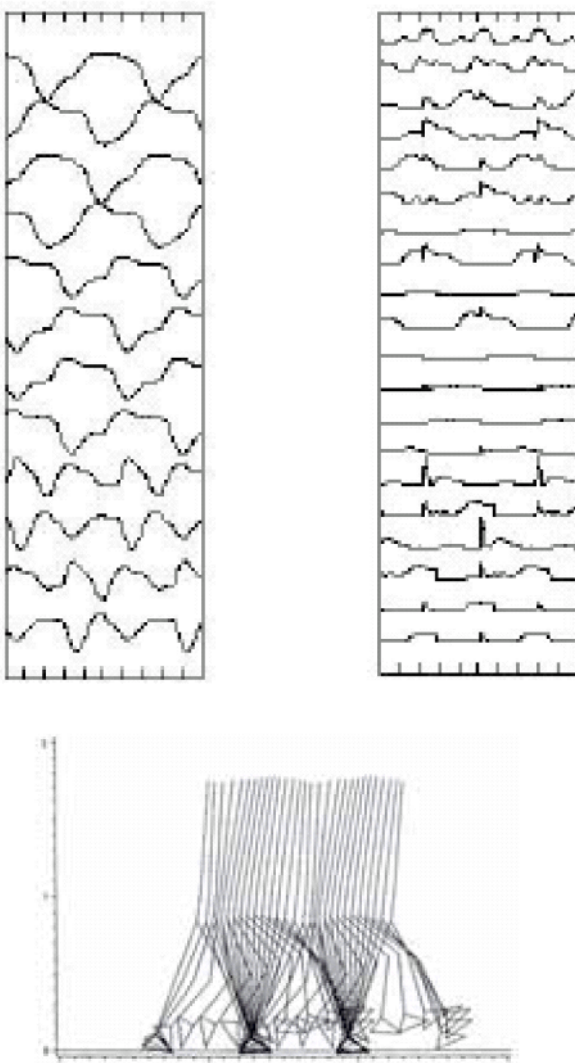


Fig. 2. The results of computer simulation of emergence of neural activity, muscle torque and walking movements generated in a self-organized manner.

2.2 Real-time flexibility of bipedal locomotion in an unpredictable environment

When the solution of the differential equations representing the neural and musculo-skeletal systems converged to a limit cycle that was structurally stable, walking movement was maintained even with small changes in the initial conditions and parameter values [15]. For example, when part of the body was disturbed by a mechanical force, walking was maintained and the steady state was recovered due to the orbital stability of the limit cycle attractor. When part of the body was loaded by a mass, which can be applied by changing the inertial parameters of the musculo-skeletal system, the gait pattern did not change qualitatively but converged to a new steady state, where the speed of walking clearly decreased. When the walking path suddenly changed from level to uneven terrain, the stability of walking was maintained but the speed and the step length spontaneously changed as shown in Fig. 3. Naturally, the stability of walking was broken for a heavy load and over a steep and irregular terrain.

This real-time adaptability is attributed not only to the afferent control based on the proprioceptive information generated by the interaction between the body and the mechanical environment, but also to the efferent control of movements based on intention and planning. In this model, a wide range of walking speeds was available using the nonspecific input from the higher center to the neural oscillators, which was represented by a single parameter. Changes in the parameter can produce bifurcations of attractors, which correspond to different motor patterns [5,15].

It is open to question whether a 3D model of the body with a similar model of the neural system will perform dynamic walking with stability and flexibility. Designing such a model is a crucial step toward constructing a humanoid robot that walks in a real environment [27].

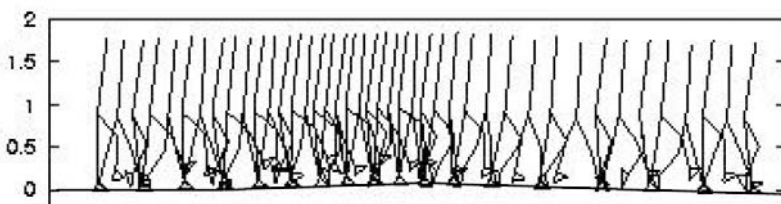


Fig. 3. Walking over uneven terrain.

3 Anticipatory adjustment of locomotion through visuo-motor coordination

3.1 Anticipatory adjustment of locomotion during obstacle avoidance

As long as the stability of the attractor is maintained, the locomotor system can produce adaptive movements even in an unpredictable environment. However, this way of generating motor patterns is not sufficient when the attractor loses stability due to drastic changes in the environment. For example, when we step over an obstacle during walking, the path of limb motion must be quickly and precisely controlled using visual information that is available in advance. Given the emergent properties of the neuro-musculo-skeletal system for producing the basic pattern of walking, how is this anticipatory adaptation to the environment realized? Neurophysiological studies in cats have shown that the motor cortex is involved in visuo-motor coordination during anticipatory modification of the gait pattern [28].

It was examined whether modifications of the basic gait pattern could produce rapid enough changes so as to clear an obstacle placed in its path. As shown in Fig. 4, the neural rhythm generator was combined with a system referred to as a discrete movement generator, which receives both the output of the neural oscillators and visual information regarding the obstacle and generates discrete signals for modification of the basic gait pattern [16].

By computer simulation, avoidance of obstacles of varying heights and proximity was demonstrated, as shown in Fig. 5. An obstacle placed at an arbitrary position can be cleared by sequential modifications of gait, namely by modulating the step length when approaching the obstacle and modifying the trajectory of the swinging limbs while stepping over it. An essential point is that a dynamic interplay between advance information about the obstacle and the on-going dynamics of the neural system produces anticipatory movements. This implies that the planning of limb trajectory is not free from the on-going dynamics of the lower levels of the neural system, body dynamics, and environmental dynamics.

3.2 A model of the neuro-musculo-skeletal system for human locomotion

The maintenance of gait when changes in the environment occur quickly relative to the walking rhythm was possible with the addition of a neural processing component. A further question is what mechanism would be responsible for adaptation through the action perception cycle of the visuo-motor coordination. For example, how can the precise positioning of a foot on a visible target on the floor during walking be achieved? The ecological approach of perception and action argues that adaptation to the complex environment is achieved not by the construction and the use of internal representations

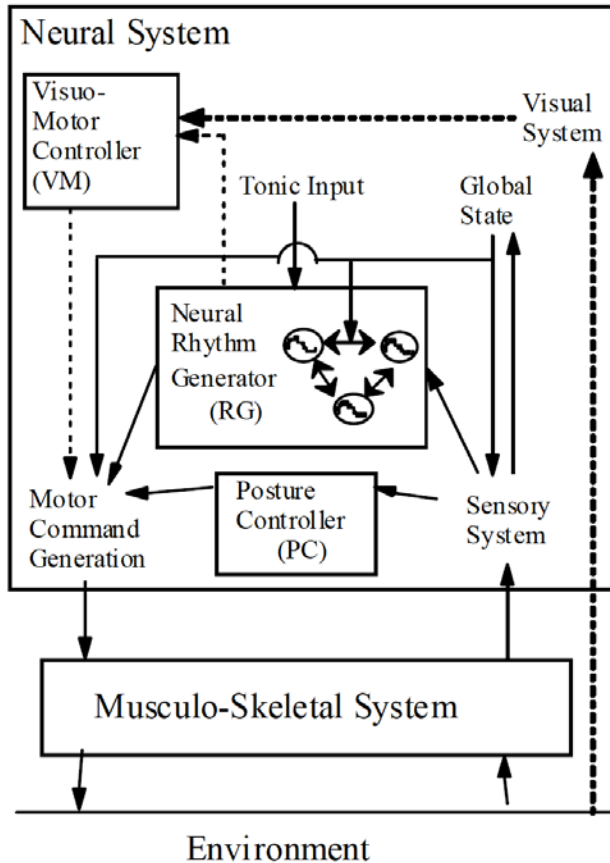


Fig. 4. A model of obstacle avoidance via anticipatory adaptation during walking [16].

of the world but rather by the use of real time information available in the optical flow [29]. Time to contact an obstacle or a target, which information can be obtained directly from a set of invariants present in the optical flow, has been studied as a key element in the visual control of locomotion [30].

We assumed that the step length modulation command, which was modelled in [a] previous study, was continuously related to optical information about the time remaining before one reached the target with the current eye-foot axis [17]. This optical variable in relation to the subject's own movement was labelled as time-to-foot (TTF) as shown in Fig. 6. We further assumed that the current step period was available and that it could be used with TTF to determine whether the step length must be shortened or lengthened to position the foot on the target.

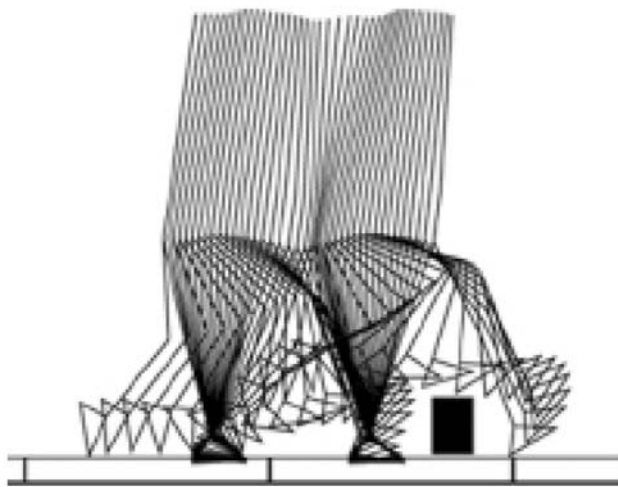


Fig. 5. Result of computer simulation of [16].

Results of computer simulation gave rise to successful pointing behavior as shown in Fig. 7. The generated behaviors for regulating step length were similar to those observed in human subjects performing a locomotor pointing task: namely, the time course of the inter-trial variability of the toe-target distance and the relationship between the step number at which the regulation is initiated and the total amount of adjustments involved. An important point of this model was that the adaptation of locomotion emerged from a perception-action coupling type of control based on temporal information rather than on the representation of the target. This is the first attempt to bridge the gap between the ecological approach to perception and the self-organized control of locomotion based on global entrainment.

4 Computational “lesion” experiments in gait pathology

It is well known that specific damage to the brain or the peripheral nervous system leads to locomotor disorders. Although the musculo-skeletal dynamics during walking have been intensively studied in clinical applications of orthopaedic issues [31], very few studies have taken a modelling approach to understanding pathological gaits due to brain dysfunctions. A question to be asked here is whether the generic model for the emergence of a basic gait can be used to reproduce pathological patterns of gait by changing model parameters.

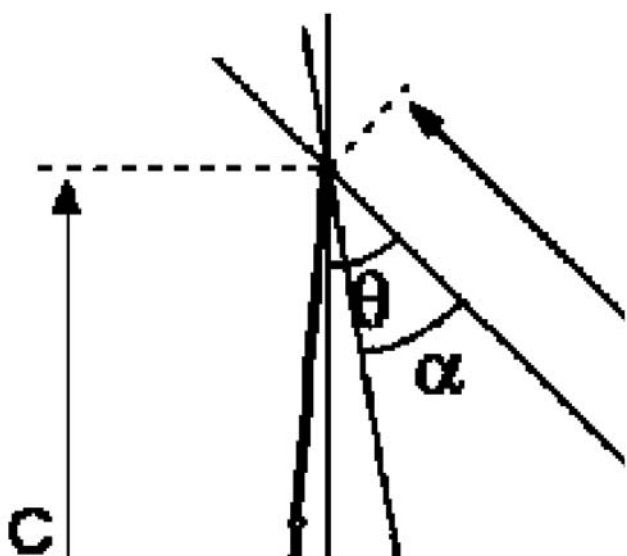


Fig. 6. Time-to-foot information [17].

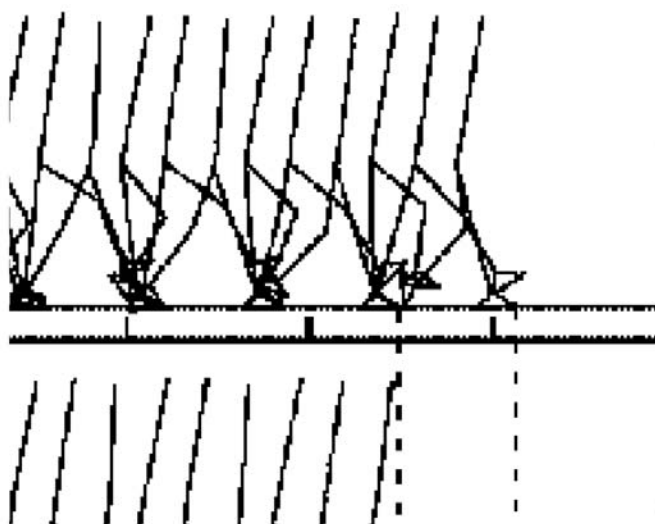


Fig. 7. Result of computer simulation of locomotor pointing tasks [17]. **a.** steady state walking. **b.** adjustment of step by shortening of step length. **c.** adjustment of step by lengthening of step length.

As shown in Fig. 8, asymmetric gaits, irregular gaits with changing step lengths and shuffling gaits with very small step lengths were generated by changing the values of the parameters of the motor or sensory pathways asymmetrically, decreasing the strength of the connections between the neural oscillators and decreasing the tonic input to the rhythm generator, respectively. These patterns of gaits were similar to those of patients with hemiplegia, cerebellar disease, and Parkinson's disease. The results demonstrated that qualitative changes in gait patterns were produced by the computational "legion" study. This inferred that the generation of pathological gaits can be viewed as a self-organizing process, where dynamic interactions between remaining parts of the system spontaneously produce specific patterns of activity.

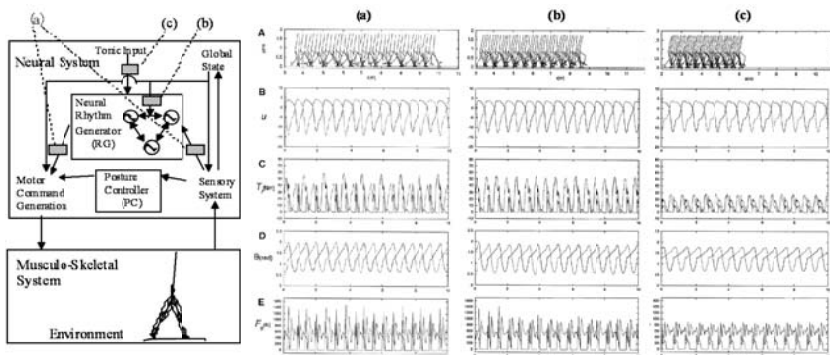


Fig. 8. Generation of pathological gaits. (a), (b) and (c) in the model show the area affected by the changes, and the gaits generated by these changes are presented in the three columns on the right-hand side.

5 Freezing and freeing degrees of freedom in the development of locomotion

Once we had chosen a structure of the neural system and a set of parameter values that produced a walking movement as a stable attractor, the model exhibited flexibility against various changes in the environmental conditions. However, it was difficult to determine the structure of the model and to tune the parameters, since the entire system was highly nonlinear. A number of studies have used a genetic algorithm [32,33] and reinforcement learning [34] to obtain good locomotor performance in animals and in humans. Another approach to overcoming the difficulty of parameter tuning of locomotor systems is to explore the motor development of infants and to unravel a developmental principle of the neuro-musculo-skeletal system. Here I show that

freezing and freeing degrees of freedom is one of the key mechanisms for the acquisition of bipedal locomotion during development.

A prominent feature of locomotor development is that newborn infants who are held erect under their arms perform locomotor-like activity [35]. The existence of newborn stepping behavior implies that the neural system already contains a CPG for rhythmic movements of the lower limbs. Interestingly, this behavior disappears after the first few months. Then, around one year of age, infants start walking independently. Why are the successive appearance, disappearance and reappearance of stepping observed in the development of locomotion? According to traditional neurology, the disappearance of motor patterns is due to the maturation of the cerebral cortex, which inhibits the generation of movements on the spinal level. However, it was reported that the stepping of infants of a few months of age can be easily induced on a treadmill [35]. It is likely that the spinal CPG is used for the generation of independent walking.

I hypothesized that this change reflects the freezing and freeing degrees of freedom of the neuro-musculo-skeletal system, which may be produced by the interaction between a neural rhythm generator (RG) composed of neural oscillators and a posture controller (PC). A computational model was constructed to reproduce qualitative changes in motor patterns during development of locomotion by the following sequence of changes in the structure and parameters of the model, as shown in Fig. 9 [18].

(1) It was assumed that the RG of newborn infants consists of six neural oscillators which interact through simple excitatory connections and that the PC is not yet functioning. When the body was mechanically supported and the RG was activated, the model produced a stepping movement, which was similar to newborn stepping. Tightly synchronized movements of the joints were generated by highly synchronized activities of the neural oscillators on the ipsilateral side of the RG, which we called "dynamic freezing" of the neuro-muscular degrees of freedom.

(2) When the PC was recruited and its parameters were adjusted, the model became able to maintain static posture by "static freezing" of degrees of freedom of the joints. The disappearance of the stepping was caused by interference between the RG and the PC.

(3) When inhibitory interaction between the RG and the PC was decreased, independent stepping appeared. This movement was unable to produce forward motion. We called this mechanism as "static freeing," since the frozen degrees of freedom of the musculo-skeletal system by the PC were freed.

(4) By decreasing the output of the PC and increasing the input of the sensory information on the segment displacements to the RG, forward walking was gradually stabilized. The simply synchronized pattern of neural activity in the RG changed into a complex pattern with each neural oscillator generating rhythmic activity asynchronously with respect to one another. By this

mechanism, called "dynamic freeing," gait patterns became more similar to those of adults.

This model suggests that the u-shaped changes in performance of stepping movements can be understood as the sequence of dynamic freezing, static freezing, static freeing and dynamic freeing of degrees of freedom of the neuro-musculo-skeletal system. This mechanism is considered to be important for the acquisition of stable and complex movements during development. In particular, parameter tuning for dynamic walking becomes easier after the control of a static posture is established.

6 Concluding comments

To understand human locomotion, we need a multidisciplinary approach that includes different types of studies such as biomechanics, neurophysiology, ecological psychology, developmental psychology, theoretical physics, computer science and robotics. The purpose of the present paper was to present a general framework capable of integrating different types of observations. We have shown that the neuro-musculo-skeletal model can reproduce varieties of behaviours concerning human locomotion on a basis of nonlinear dynamics.

A lot of questions remained to be solved with regard to the development of locomotion. In early infancy, we can observe spontaneous movements of the head, trunk, arms and legs. The patterns of movements are not random and are more complex than simply rhythmic movements [36]. It is not clear whether the spontaneous movements are manifestations of activity by the spinal central pattern generator or not. This is an extremely important point to clarify in understanding the mechanism of the development of walking and other voluntary movements. Another interesting issue is that young infants can perceive the human walking pattern long before they start to walk. Do they use some form of representation of the walking pattern when they practise independent walking? If so, is the mechanism the same as the one for learning a new movement in adults? Brain imaging techniques in infants progressively reveal the status of brain development in early infancy [37]. The advancement of this type of technique may provide deeper insight into the design principle of human locomotion in the near future.

References

1. Nicolis, G., Prigogine, I., 1977, *Self-organization in Nonequilibrium Systems*, John Wiley and Son..
2. Haken, H., 1976, *Synergetics - An Introduction*, Springer-Verlag.
3. Sch()ner, G., Kelso, J.A.S., 1988, Dynamic pattern generation in behavioral and neural systems, *Science*, 239, 1513-1520.
4. Grillner, S., 1985, Neurobiological bases of rhythmic motor acts in vertebrates, *Science*, 228, 143-149.

(1) Newborn Stepping

Neural System

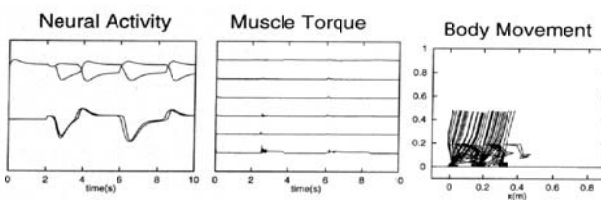
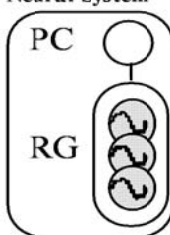
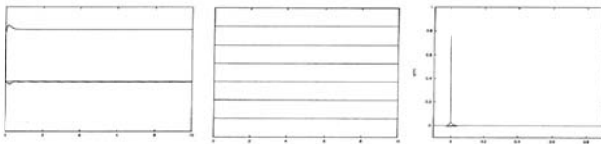
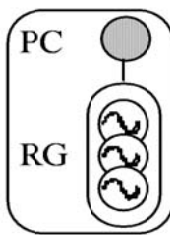
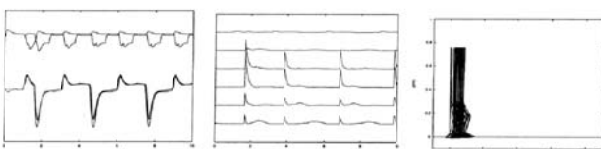
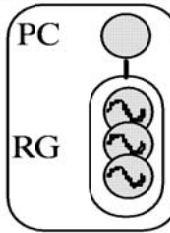
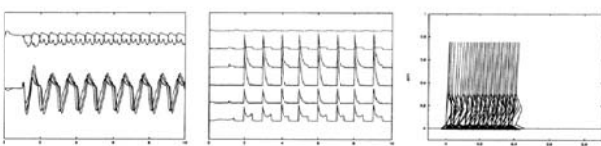
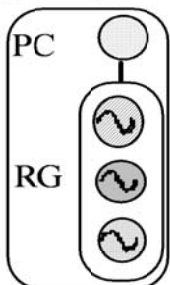
**(2) Acquisition of Standing****(3) Acquisition of Walking****(4) Change to Adult-like Pattern of Walking**

Fig. 9. A model of the development of bipedal locomotion of infants and results of computer simulation.

5. Taga, G., Yamaguchi, Y., and Shimizu, H., 1991, Self-organized control of bipedal locomotion by neural oscillators in unpredictable environment, *Biol. Cybern.*, 65, 147-159.
6. Kimura, S., Yano, M., Shimizu, H., 1993, A self-organizing model of walking patterns of insects, *Biol. Cybern.*, 69, 183-193.
7. Ekeberg, O., 1993, A combined neuronal and mechanical model of fish swimming, *Biol. Cybern.*, 69, 363-374.
8. Wadden, T., Ekeberg, O., 1998, A neuro-mechanical model of legged locomotion: single leg control. *Biol. Cybern.*, 79, 161-173.
9. Ijspeert, A.J. 2001. A connectionist central pattern generator for the aquatic and terrestrial gaits of a simulated salamander. *Biol. Cybern.* 84, 331-348.
10. Lewis, M. A., Etienne-Cummings, Hartmann, M. J., Xu, Z. R., and Cohen, A. H. 2003. An in silico central pattern generator: silicon oscillator, coupling, entrainment, and physical computation. *Biol. Cybern.* 88:137-151.
11. Miyakoshi, S., Yamakita, M., Furata, K., 1994, Juggling control using neural oscillators, *Proc. IEEE/RSJ IROS*, 2, 1186-1193.
12. Kimura, H., Sakurama, K., Akiyama, S., 1998, Dynamic walking and running of the quadruped using neural oscillators, *Proc. IEEE/RSJ, IROS*, 1, 50-57.
13. Williamson, M., M., 1998, Neural control of rhythmic arm movements, *Neural Networks*, 11, 1379-1394.
14. Taga, G., 1995, A model of the neuro-musculo-skeletal system for human locomotion. I. Emergence of basic gait, *Biol. Cybern.*, 73, 97-111.
15. Taga, G., 1995, A model of the neuro-musculo-skeletal system for human locomotion. II. Real-time adaptability under various constraints, *Biol. Cybern.*, 73, 113-121.
16. Taga, G., 1998, A model of the neuro-musculo-skeletal system for anticipatory adjustment of human locomotion during obstacle avoidance. *Biol. Cybern.*, 78, 9-17.
17. de Rugy A., Taga, G., Montagne, G., Buekers, M., J., Laurent M., 2002, Perception-action coupling model for human locomotor pointing, *Biol. Cybern.* 87, 141-150.
18. Taga, G., 1997, Freezing and freeing degrees of freedom in a model neuro-musculo-skeletal system for development of locomotion, *Proc. XVIth Int. Soc. Biomech. Cong.*, 47.
19. Vukobratovic, M., Stokic, D., 1975, Dynamic control of unstable locomotion robots, *Math. Biosci.* 24, 129-157.
20. McGeer, T., 1993, Dynamics and control of bipedal locomotion, *J. Theor. Biol.* 163, 277-314.
21. van der Linde, R. Q., 1999, Passive bipedal walking with phasic muscle contraction, *Biol. Cybern.* 81, 227-237.
22. Raibert, M., H., 1984, Hopping in legged systems - modeling and simulation for the two-dimensional one-legged case, *IEEE Trans. SMC*, 14, 451-463.
23. Matsuoka, K., 1985, Sustained oscillations generated by mutually inhibiting neurons with adaptation, *Biol. Cybern.* 52, 367-376.
24. Calancie, B., Needham-Shropshire, B., Jacobs, et al., 1994, Involuntary stepping after chronic spinal cord injury, Evidence for a central rhythm generator for locomotion in man, *Brain*, 117, 1143-1159.
25. Dimitrijevic, M., R., Gerasimenko, Y., Pinter, M., M., 1998, Evidence for a spinal central pattern generator in humans, *Ann NY Acad Sci*, 860, 360-376.

26. Dietz V., 2002, Proprioception and locomotor disorders, *Nature Rev. Neurosci.* 3, 781-790
27. Miyakoshi, S., Taga, G., Kuniyoshi, Y. et al., 1998, Three dimensional bipedal stepping motion using neural oscillators - towards humanoid motion in the real world. *Proc. IEEE/RSJ*, 1, 84-89.
28. Drew, T., 1988, Motor cortical cell discharge during voluntary gait modification, *Brain Res.*, 457, 181-187.
29. Gibson, J. J., 1979, *An ecological approach to visual perception*. Houghton-Mifflin, Boston.
30. Lee, D. N., 1976, A theory of visual control of braking based on information about time-to-collision. *Perception* 5, 437-459.
31. Zajac F. E., Neptune, R. R., Kautz, S. A., 2003, Biomechanics and muscle coordination of human walking Part II: Lessons from dynamical simulations and clinical implications. *Gait and Posture*, 17, 1-17.
32. Lewis, M., A., Fagg, A., H., Bekey, G. A., 1994, Genetic Algorithms for Gait Synthesis in a Hexapod Robot, In Zheng, Y., F., ed. *Recent Trends in Mobile Robots*, World Scientific, New Jersey, 317-331.
33. Yamazaki, N., Hase, K., Ogiwara, N., et al. 1996, Biomechanical analysis of the development of human bipedal walking by a neuro-musculo-skeletal model, *Folia Primatologica*, 66, 253-271.
34. Sato, M., Nakamura, Y., Ishii, S., 2002, Reinforcement learning for biped locomotion. *Lect. Notes Comput. Sc.* 2415, 777-782.
35. Thelen, E., Smith, L., B., 1994, *A Dynamic Systems Approaches to the Development of Cognition and Action*, MIT Press.
36. Taga, G., Takaya, R., Konishi, Y., 1999, Analysis of general movements of infants towards understanding of developmental principle for motor control. *Proc. IEEE SMC*, V678-683
37. Taga,G., Asakawa, K., Maki, A., Konishi, Y., Koizumi, H., 2003, Brain imaging in awake infants by near infrared optical topography, *PNAS* 100-19, 10722-10727

Towards Emulating Adaptive Locomotion of a Quadrupedal Primate by a Neuro-musculo-skeletal Model

Naomichi Ogihara¹ and Nobutoshi Yamazaki²

¹ Department of Zoology, Graduate School of Science, Kyoto University
Kitashirakawa-Oiwakecho, Sakyo, Kyoto 606-8502, Japan

² Department of Mechanical Engineering, Faculty of Science and Technology,
Keio University, 3-14-1, Hiyoshi, Kohoku, Yokohama 223-8522, Japan

Abstract. A neuro-musuculo-skeletal model of a quadrupedal primate is constructed in order to elucidate the adaptive nature of primate locomotion by the means of simulation. The model is designed so as to spontaneously induce locomotion adaptive to environment and to its body structure, due to dynamic interaction between convergent dynamics of a recurrent neural network and passive dynamics of a body system. The simulation results show that the proposed model can generate a stepping motion natural to its body structure while maintaining its posture against an external perturbation. The proposed framework for the integrated neuro-control of posture and locomotion may be extended for understanding the adaptive mechanism of primate locomotion.

1 Introduction

Variations in osteological and muscular anatomy in primates are well correlated with differences in their primary locomotor habits [1]. Modifications in limb length and body proportion are also connected to their locomotion since these parameters determine the natural oscillation pattern of a body system [2,3,4]. These findings imply that primate locomotion is basically generated in such a way that they utilize the structures of body system, which are rationally acquired through their evolutional process. Locomotion of animals, including that of primates, is often regarded adaptive in terms of robustness against environmental changes and unknown perturbations. However, there are actually two sides in adaptive mechanism of primate locomotion - adaptivity to the environment, and to the body structure.

Such a twofold adaptivity found in the primate locomotion can be hypothesized to be emerged by dynamic interaction between the nervous system and the musculo-skeletal system. A network of neurons recurrently connecting to the others can be viewed as a dynamical system, which autonomously behaves based on a minimization principle; it behaves convergently to decrease an energy function defined in it [5]. Moreover, a body is also a dynamical system that has passive properties due to its physical characteristics such as segment inertial parameters and joint mobilities [6]. If these dynamical systems are

mutually connected as they are in actuality, appropriate constraints may be self-organized because of the convergent characteristics of the systems, and the adaptive nature of the primate locomotion could be spontaneously emulated. In the present study, a neuro-musculo-skeletal model of a quadrupedal primate is constructed based on the above-mentioned idea.

2 Model

2.1 Mechanical model

A quadrupedal primate is modeled as a 16-segment, three-dimensional rigid body kinematic chain as shown in Fig. 1. The equation of motion of the model is derived as

$$\mathbf{M}\ddot{\mathbf{q}} + \mathbf{h}(\dot{\mathbf{q}}, \mathbf{q}) + \mathbf{g} - \boldsymbol{\alpha}(\mathbf{q}) + \boldsymbol{\beta}(\dot{\mathbf{q}}) = \mathbf{T} + \boldsymbol{\Phi} \quad (1)$$

where \mathbf{q} is a (51 x 1) vector of translational and angular displacement of the middle trunk segment and 45 joint angles, \mathbf{T} is a vector of joint torques, \mathbf{M} is an inertia matrix, \mathbf{h} is a vector of torque component depending on Coriolis and centrifugal force, \mathbf{g} is a vector of torque component depending on gravity, $\boldsymbol{\alpha}$ and $\boldsymbol{\beta}$ are vectors of elastic and viscous elements due to joint capsules and ligaments (passive joint structure) which restrict ranges of joint motions, $\boldsymbol{\Phi}$ is a vector of torque component depending of the ground reaction forces acting on the limbs, respectively. The primate model is constructed after a female Japanese macaque cadaver. Each segment is approximated by a truncated elliptical cone in order to calculate its inertial parameters.

All joints are modeled as three degree-of-freedom gimbal joints. However, here we restrict abduction-adduction and medial-lateral rotation of limb joints by visco-elastic elements. Joints connecting trunk segments are also restricted, so that the head and the trunk segments can be treated as one segment. The other joint elastic elements are represented by the double-exponential function [7]:

$$\begin{aligned} \alpha_j &= k_{j1} \exp(-k_{j2}(q_j - k_{j3})) - k_{j4} \exp(-k_{j5}(k_{j6} - q_j)) \\ \beta_j &= c_j \dot{q}_j \end{aligned} \quad (2)$$

where α_j and β_j the torque exerted by elastic and viscous element around the j th joint, q_j is the j th joint angle, and $k_{j1\sim 6}$ and c_j are coefficients defining the passive joint properties, respectively. In this study, the coefficients $k_{j1\sim 6}$ are determined so as to roughly imitate actual joint properties. The ground is also modeled by visco-elastic elements. The hand and the foot are modeled with four points that can contact the ground. The actual center of pressure (COP) is calculated using the points. The global coordinate system and the body (trunk) coordinate system are defined as illustrated in Fig. 1.

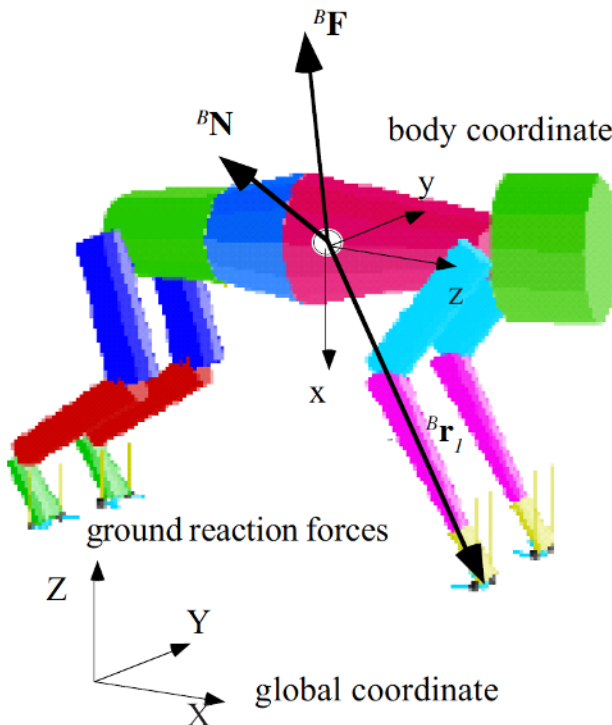


Fig. 1. Mechanical model of a quadrupedal primate.

2.2 Nervous model

Integrated control of posture and locomotion It is generally accepted that locomotion is generated by alternating the activities of the extensor and flexor muscles under the control of rhythm-generating neural circuits in the spinal cord known as the central pattern generator (CPG) [8,9]. However, previous research on decerebellated cats shows that coordination of limbs is greatly disturbed and balance of the trunk is lost in these animals [10]; whereas decerebrate cats, whose cerebellums are left intact, can balance themselves and walk in more coordinated ways [11]. The cerebellum is a region where various sensory information, such as the vestibular organ and the afferent signals from proprioceptors and exteroceptors, is all integrated. Thus, the integration of multimodal afferent information in the cerebello-spinal systems is suggested indispensable for integrated control of posture and locomotion [12].

From biomechanical and kinesiological viewpoint, both posture and locomotion can be seen as being controlled by adjusting ground reaction forces acting on the limbs. To sustain the trunk segment at a certain position and

orientation in three-dimensional space, appropriate force and moment have to be applied to the center of the mass (COM) of the trunk. In case of locomotion, they must be applied in a traveling direction to displace the body. In primates, such a force and a moment can only be applied by generating the reaction forces acting on the limbs from the ground, and the nervous system somehow needs to adjust them in an integrative manner. Here we assume that activities of the neurons in the nervous system represent ground reaction forces necessary to maintain the posture and locomotion, and appropriate forces are spontaneously generated based on the various sensory inputs.

Recurrent neural network model In this study, an array of 12 neurons is expressed as $\mathbf{u} = [\mathbf{u}_1 \ \mathbf{u}_2 \ \mathbf{u}_3 \ \mathbf{u}_4]^T$, where \mathbf{u}_L is the (3×1) vector of the state variables corresponding to three components of the ground reaction force vector of the L th limb ($L=1,2,3,4$; 1=right fore, 2=left fore, 3=right hind, 4=left hind). In order to sustain the trunk posture, the nervous system consisting of the neurons is assumed to behave so as to spontaneously fulfill the following equations of equilibrium:

$$\begin{aligned} {}^B\mathbf{F} &= \sum_{L=1}^4 \gamma_L \mathbf{u}_L \\ {}^B\mathbf{N} &= \sum_{L=1}^4 ({}^B\mathbf{r}_L) \times (\gamma_L \mathbf{u}_L) = \sum_{L=1}^4 \mathbf{S}({}^B\mathbf{r}_L) \cdot \gamma_L \mathbf{u}_L \end{aligned} \quad (3)$$

where ${}^B\mathbf{F}$ and ${}^B\mathbf{N}$ are the (3×1) vectors corresponding to the neuronal representation of force and moment should be applied at the COM of the trunk segment, ${}^B\mathbf{r}_L$ is the position vector from the COM to the COP of the L th limb, γ_L is the signal from the cutaneous receptor of the palm/sole of the L th limb (=1 when the limb touches the ground, and 0 otherwise), $\mathbf{S}(\mathbf{r})$ is a matrix representing skew operation on the vector \mathbf{r} , respectively. The left superscript B indicates that the vectors are represented in the body (trunk) coordinate frame. Such a nervous system can be modeled by a recurrent neural network [5] as follows:

$$\frac{d\mathbf{u}_L}{dt} = -\gamma_L \mathbf{A} \cdot \mathbf{Q}_L^T \cdot \mathbf{W} \cdot \left(\sum_L \mathbf{Q}_L \gamma_L \mathbf{u}_L - \begin{bmatrix} {}^B\mathbf{F} \\ {}^B\mathbf{N} \end{bmatrix} \right) - \mathbf{B} \mathbf{u}_L, \quad \mathbf{Q}_L = \begin{bmatrix} \mathbf{I} \\ \mathbf{S}({}^B\mathbf{r}_L) \end{bmatrix} \quad (4)$$

where \mathbf{Q}_L is the (6×3) matrix, \mathbf{I} is the (3×3) unit matrix, \mathbf{W} is the (6×6) diagonal weight matrix, \mathbf{A} is the (3×3) diagonal matrix of reciprocals of time constants, \mathbf{B} is the (3×3) diagonal matrix, respectively. The neural states \mathbf{u} autonomously behave so as to decrease the following potential function:

$$E = \frac{1}{2} \left(\sum_L \mathbf{Q}_L \gamma_L \mathbf{u}_L - \begin{bmatrix} {}^B\mathbf{F} \\ {}^B\mathbf{N} \end{bmatrix} \right)^T \cdot \mathbf{W} \cdot \left(\sum_L \mathbf{Q}_L \gamma_L \mathbf{u}_L - \begin{bmatrix} {}^B\mathbf{F} \\ {}^B\mathbf{N} \end{bmatrix} \right) + \frac{1}{2} \mathbf{u}_L^T \mathbf{B} \mathbf{u}_L \quad (5)$$

where E is the potential function representing the weighted summation of square errors of Eq. (3). Therefore, the proposed neural network, given the input ${}^B\mathbf{F}$ and ${}^B\mathbf{N}$, can autonomously estimate the ground reaction forces necessary to sustain the balance of the posture while minimizing the force.

${}^B\mathbf{F}$ and ${}^B\mathbf{N}$, are assumed to be determined by the intention (motivation) to keep the trunk stable at an appropriate position and orientation, and the input from the vestibular organ, which works as the sensor of the translational and rotational velocities of the head (trunk) segment, as

$${}^B\mathbf{F} = \mathbf{K}_F({}^B\mathbf{p}^d) - \kappa(\delta - \zeta){}^B\mathbf{n}_g - \mathbf{C}_F {}^B\dot{\mathbf{p}} \quad (6)$$

$${}^B\mathbf{N} = \mathbf{K}_N {}^B\Theta^d - \mathbf{C}_N {}^B\omega \quad (7)$$

$${}^B\mathbf{p}^d = \sum_L \gamma_L {}^B\mathbf{r}_L \left/ \sum_L \gamma_L \right. \quad (8)$$

where ${}^B\mathbf{p}^d$ is the position vector from the COM to the centroid of the polygon formed by the COP's of the limbs, ${}^B\mathbf{n}_g$ is the unit vector showing the direction of the gravitational force, ${}^B\dot{\mathbf{p}}$ is the velocity of the COM of the trunk segment, δ is the distance between the COM and the ground along the vector ${}^B\mathbf{n}_g$, ${}^B\Theta^d$ is the Eulerian angles between the present and the desired orientation of the body, ${}^B\omega$ is the angular velocity vector of the trunk segment, κ and ζ are coefficients, \mathbf{K}_F , \mathbf{K}_N , \mathbf{C}_F , \mathbf{C}_N are (3 x 3) diagonal matrices of coefficients, respectively. The third term in the right side in Eq. (6) and the second term in Eq. (7) show the input from the vestibular organ, while others show the intention of motion, which is to keep the body position at some distance apart from the ground.

Since ${}^B\mathbf{p}^d$, ${}^B\mathbf{n}_g$, ${}^B\dot{\mathbf{p}}$, and ${}^B\omega$ are all represented in the body reference frame, the nervous system is assumed to be able to sense these quantities; ${}^B\mathbf{p}^d$ by the cutaneous receptors on the palm/sole and the muscle spindles (joint angle sensors), and ${}^B\mathbf{n}_g$, ${}^B\dot{\mathbf{p}}$, and ${}^B\omega$ by the vestibular system. The sensory-motor map, \mathbf{Q} and \mathbf{J} , are assumed to be correctly represented in the nervous system.

Rhythm pattern generator The rhythm pattern generator, which coordinates sequential limb movement in a quadrupedal animal, exists in primates as well [14]. Here it is modeled by the equations proposed by Matsuoka [15,16]:

$$\begin{aligned} \tau \dot{U}_L &= -U_L + \sum_i z_{Li} y_i + s_0 - h_L V_L \\ \tau' \dot{V}_L &= -V_L + y_L \quad y_L = \max(U_L, 0) \end{aligned} \quad (9)$$

where U_L is the inner state of the L th CPG neuron whose activation corresponds to the stance-swing phase of the L th limb, V_L is a variable representing self-inhibition of the U_L , τ and τ' are time constants, y_L is the

output of the L th CPG neuron, z_{Li} is the weight of neural connections, h_L is the weight of self-inhibition, s_0 is the constant input, respectively. The CPG is assumed to represent swing phase of the L th limb if $(y_L - \eta) > 0$ and stance phase if otherwise (η is a constant). To command the limb motion in a swing phase according to the CPG signal, we assume another neural variables \mathbf{v}_L which correspond to three components of the ground reaction force vector of the L th limb:

$$\mathbf{v}_L = (y_L - \eta)\mathbf{m}_L \quad (10)$$

where \mathbf{m}_L is a (3×1) vector of coefficients determining the uplift motion of limb in swing phase. \mathbf{m}_L is assumed to be zero when in stance phase. In order for the nervous system not to depend on the swing limb for supporting the body against gravity, the CPG signal is assumed to be inputted in Eq. (4) as

$$\frac{d\mathbf{u}_L}{dt} = -\gamma_L \mathbf{A} \cdot \mathbf{Q}_L^T \cdot \mathbf{W} \cdot \left(\sum_L \mathbf{Q}_L \gamma_L \mathbf{u}_L - \begin{bmatrix} {}^B\mathbf{F} \\ {}^B\mathbf{N} \end{bmatrix} \right) - \mathbf{B}\mathbf{u}_L + \lambda \varepsilon \cdot [\max(-\varepsilon u_{L,x}, 0), 0, 0]^T \quad (11)$$

where $\varepsilon = \text{sgn}(y_L - \eta)$, and $u_{L,x}$ is the x component of \mathbf{u}_L . The third term represents that $u_{L,x}$ should be positive when the CPG commands the L th limb to be in swing phase, and negative when in stance phase.

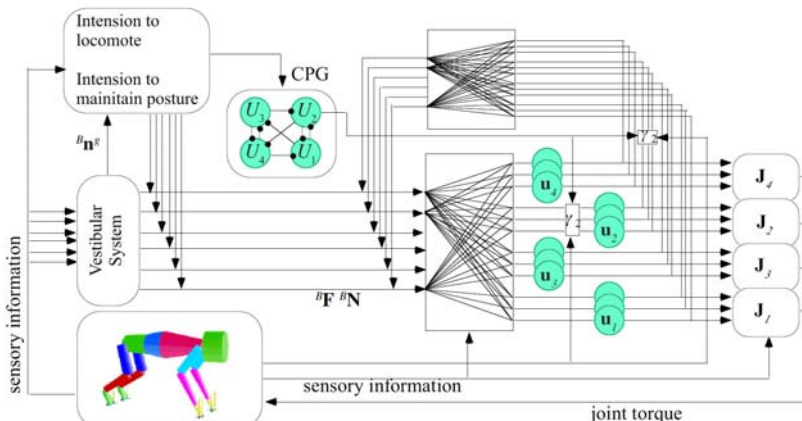


Fig. 2. Schematic diagram of the neural network. The CPG output and the cutaneous signal are drawn only for $L=2$.

Joint torque The joint torques are generated according to the signals from the nervous system, \mathbf{u}_L and \mathbf{v}_L , as

$$\mathbf{n}_L = -\mathbf{J}_L^T(\mathbf{u}_L + \mathbf{v}_L) \quad (12)$$

where \mathbf{n}_L is the (9×1) vector of the joint torques of the L th limb, \mathbf{J}_L is the (9×3) Jacobian matrix. Another recurrent neural network can be added which produces the joint torques based on the anatomical constraints of the musculo-skeletal systems [13]. However, for simplicity, here we compute the torques by the principle of virtual work.

2.3 Mutual interaction between neuro-mechanical systems

Fig. 2 shows a schematic diagram of the interaction between the neuro-mechanical systems. Given the intention to keep the posture, the nervous system can autonomously generate the signal \mathbf{u} , which corresponds to the ground reaction forces, such as to decrease the potential function defined in Eq. (5). In addition, the CPG generates the rhythmic signal \mathbf{v} . \mathbf{u} and \mathbf{v} are then transformed by the sensory-motor map \mathbf{J} to produce the joint torque \mathbf{n} . On the other hand, the sensory information of resultant motion is returned to the nervous system by the vestibular systems (${}^B\mathbf{n}_g$, ${}^B\dot{\mathbf{p}}$, and ${}^B\omega$), the cutaneous receptor (γ_L), and the proprioceptor (\mathbf{q}), so that the entire systems are mutually integrated.

If the CPG is not activated, a stationary posture is generated. When the model intends to locomote, the CPG is activated and the limbs start to move sequentially. The rhythmic signals can be regarded as a perturbation interfering maintenance of the posture. But because of the inherent convergent properties of the nervous system and the body system, adaptive locomotion may be self-organized.

2.4 Calculation Method

The model is expressed as simultaneous differential equations. They are numerically integrated using the variable time-step Runge-Kutta method with Merson error estimator. It is difficult to estimate a steady states of the entire systems because the touches to the ground at many points. Therefore, the model is initially placed apart from the ground. The neural parameters which define the behavior of the system, such as \mathbf{W} , \mathbf{A} , \mathbf{B} , \mathbf{K} , and \mathbf{C} are arbitrarily chosen. The neurons in the rhythm pattern generator are so connected that the limbs move in diagonal sequence.

3 Results

3.1 Generation of stationary postures

In order for a quadrupedal animal to sustain its posture, of course, appropriate joint torques has to be generated by the nervous system. Fig. 3A shows that the primate model with the proposed neural network can autonomously generate appropriate joint torques and successfully sustain its body. Furthermore, the model can alter inclination of the trunk segment and its axial

rotation without falling down, as illustrated in Fig. 3B and C. The model can change its intended posture autonomously by coordinating joint torques, just by altering one signal input from the cortex, ${}^B\Theta^d$. It should be noted that the model stands without any prior knowledge about the environment. Therefore, the same model should be able to stand on an uneven terrain.

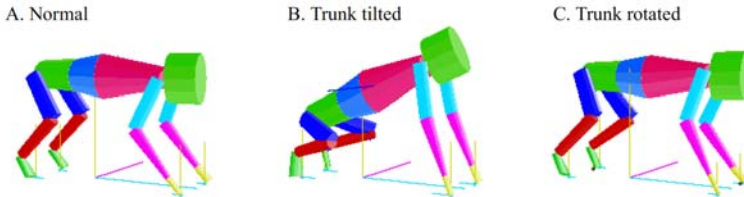


Fig. 3. Generated stationary postures. A Normal posture. B The trunk segment is inclined. C The trunk is rotated.

3.2 Generation of stepping motion

Fig. 4 illustrates the stick picture of a generated stepping behavior of the model (A), and changes in vertical ground reaction force (B) and joint angles (C, D) over time. The stick diagram is traced every 0.3 sec for 1.5 sec (approximately equal to its stepping cycle). In this study, soon after the calculation is started, the impulsive reaction force due to foot-ground contact is applied to the model, and the model comes to a steady position. After that, according to the activation of the CPG, the model starts to generate a stepping motion; thus the ground reaction forces are sequentially altered. However, the joint angle profiles show that, while ranges of forelimb joint motions are large, those of hindlimb become small, and the hindlimb is actually not lifted up from the ground here, although the model tries to, as seen in the Fig. 4B. Because the tuning of the parameters in the nervous system is not optimized, the model has not succeeded in generating locomotion pattern that is comparable to that of actual monkeys. But the model autonomously reacts to keep its balance while continuously jiggling the body.

To examine the adaptivity of the stepping motion, a perturbation is applied (10N in the forward direction plus 10N in the lateral direction for 0.1sec) to the trunk segment. Fig. 5 shows changes in the ground reaction force and the joint angles over time, and the arrows in the figure indicate the time when the perturbation is applied. As the graphs show, the body is swayed and the joint motions are disturbed because of the perturbation, but it can spontaneously coordinate its joint torques to balance itself due to the combined dynamics of the neural and the body systems.

In this study, no mechanism is implemented for precisely controlling the swing phase. In addition, an intention to move forward is not given to the

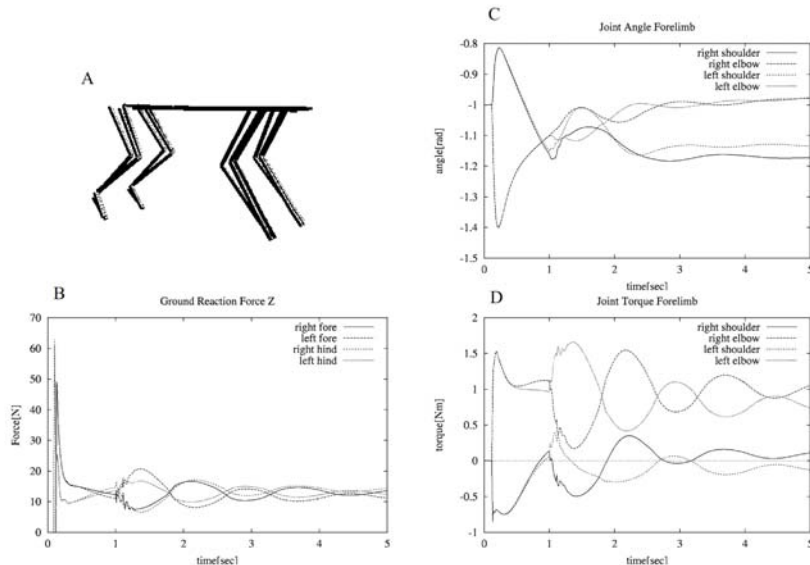


Fig. 4. Generated stepping motion

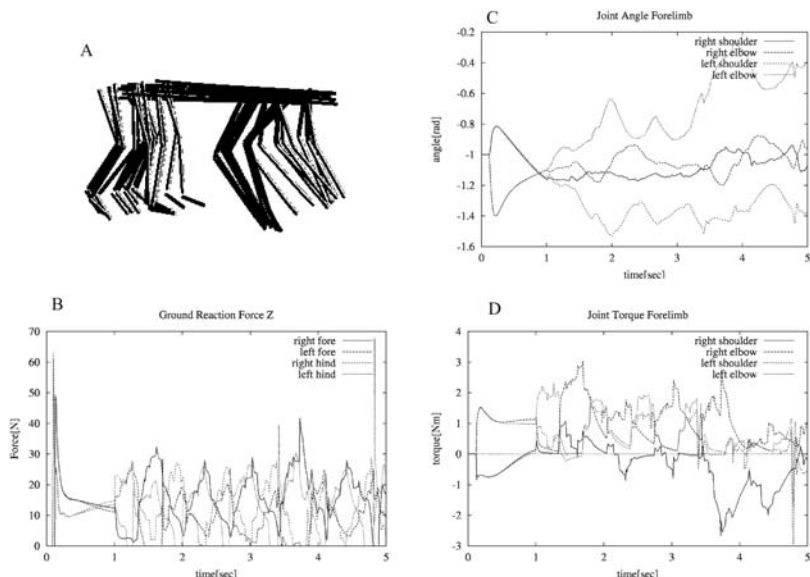


Fig. 5. Reaction to an external perturbation. The arrows indicate when the perturbation is applied.

model; thus it dose not walk but jiggle. If proper constraints are additionally considered in the nervous system as we did previously [17], and the intention to walk is set, locomotion may hopefully be generated.

4 Discussion

The results show that the proposed model generates an adaptive stepping motion. Here, the joint torques are not preplanned like a humanoid robot [18] at all, but they are spontaneously yielded by the natural behavior of the combined dynamics of the body and the neural circuit. As in Eq. (4), the neural network is implicitly designed to generate ground reaction forces as if a virtual visco-elastic element is attached between the body and the space [19,20]. Therefore, the enormous number of joint degree of freedom is spontaneously coordinated to produce appropriate reaction forces, and at the same time, motions are naturally generated in terms of the body structure. The model also shows robustness to changes in body parameters and noises on the neural activities. Even though the mass of a segment or a parameter defining a joint property is altered, the model can still maintain its posture. Local reflex mechanism, such as righting reflexes, could also be added in this model coordinately, since the proposed neural system can adapt the resultant effect of the added reflex.

Although there is no direct evidence showing such a proposed network actually exists, however, recently, the fastigial nucleus in the cerebellum is found to be a new locomotion inducing site [21,22], indicating that the integration of multimodal sensory information and the rhythmic signals at this level is important for generation of coordinated limb movements. It is also noted that load receptors take very important roles in generation of locomotion [23,24], suggesting that reaction forces may be computed by the neurons, and the posture and locomotion is functionally integrated by them. The framework of the proposed model may be biologically feasible and similar representation and integration of the neural information may be implemented in the actual nervous system.

We believe this kind of synthetic approach is important for elucidating adaptive nature of primate locomotion. It is because physiological study by itself does not illuminate how the actual nervous system functions as a dynamical system. Certainly, advances in physiology and neuroscience have revealed to where each of neurons is connected and how it functions. Newly developed instrumentations also successfully visualize functional localization of activity in the brain in various tasks or functions including human walking [25]. However, these findings alone do not indicate how the nervous system controls the timing and magnitude of activity of each of muscles to generate adaptive locomotion in various environments. Whereas the proposed synthetic approach can qualitatively predict the interactive dynamics of the entire neuro-musculo-skeletal system, so that the underlying hypothesis can

be tested, and insights on the adaptive mechanism can be gained through the simulation, as insisted in the systems biology approach [26].

Yet, the adaptive nature of primate locomotion does not emerge in the nervous system by itself. In biological systems, the body dynamics becomes a part of the neural dynamics and vice versa, as mimicked in this simulation. Therefore, the physical characteristics of the body system determined by its anatomy and morphology greatly affects the integrated dynamics. Understanding of inherent reasonability of the primate body structure is thus also essential, and it should be incorporated into the model as well.

Acknowledgements

The authors are grateful to Prof. H. Ishida and Dr. M. Nakatsukasa for their continuous supports and encouragement. This work is supported by the grant-in-aid from the Japan Society for the Promotion of Science (#13740496) and the grant-in-aid for the 21st Century COE Research (A2).

References

1. Gebo DL (ed) (1993) Postcranial Adaptation in Nonhuman Primates. Northern Illinois University Press, DeKalb
2. Mochon S, McMahon TA (1980) Ballistic walking. *J Biomech* 13: 49-57
3. Yamazaki N (1990) The effect of gravity on the interrelationship between body proportions and brachiation in the gibbon. *Hum Evol* 5: 543-558
4. Yamazaki N (1992) Biomechanical interrelationship among body proportions, posture, and bipedal walking. In: Matano S, Tuttle RH, Ishida H, Goodman M (eds) Topics in Primatology Vol. 3. University of Tokyo Press, Tokyo, pp.243-257
5. Hopfield JJ, Tank DW (1986) Computing with neural circuits: A model. *Science* 233: 625-633
6. McGeer T (1992) Principles of walking and running. In: Alexander M (ed) Mechanics of Animal Locomotion (Advances in Comparative and Environmental Physiology Vol.11). Springer-Verlag, Berlin, pp.113-139
7. Davy DT, Audu ML (1987) A dynamic optimization technique for predicting muscle forces in the swing phase of gait. *J Biomech* 20: 187-201
8. Grillner S (1975) Locomotion in vertebrates: central mechanisms and reflex interaction. *Physiol Rev* 55: 274-304
9. Shik ML, Orlovsky GN (1976) Neurophysiology of locomotor automatism. *Physiol Rev* 56: 465-501
10. Orlovsky GN (1970) Influence of the cerebellum on the reticulo-spinal neurones during locomotion. *Biophysics* 15: 928-936
11. Mori S (1987) Integration of posture and locomotion in acute decerebrate cats and in awake, freely moving cats. *Progress in Neurobiology* 28: 161-195
12. Armstrong DM, Apps R, Marple-Horvat DE (1997) Aspects of cerebellar function in relation to locomotor movements. In: de Zeeuw CI, Strata P, Voogd J (eds) *Progress in Brain Research*. The Cerebellum: From Structure to Control. Elsevier, Amsterdam, pp.401-421

13. Ogihara N, Yamazaki N (2001) Generation of spontaneous reaching movement based on human anatomical constraints (in Japanese with English abstract). *Transactions of the Japan Society of Mechanical Engineers C-67*: 2314-2320
14. Eidelberg E, Walden JG, Nguyen LH (1981) Locomotor control in macaque monkeys. *Brain* 104: 647-663
15. Matsuoka K (1985) Sustained oscillations generated by mutually inhibiting neurons with adaptation. *Biol Cybern* 52: 367-376
16. Matsuoka K (1987) Mechanisms of frequency and pattern control in the neural rhythm generators. *Biol Cybern* 56: 345-353
17. Ogihara N, Yamazaki N (2001) Generation of human bipedal locomotion by a bio-mimetic neuro-musculo-skeletal model. *Biol Cybern* 84: 1-11
18. Hirai K, Hirose M, Haikawa Y, Takenaka T (1998) The development of Honda humanoid robot. *Proc IEEE Intl Conf Robotics and Automations* 1321-1326
19. Pratt J, Chew CM, Torres A, Dilworth P, Pratt G (2001) Virtual model control: An intuitive approach for bipedal locomotion. *Int J Robot Res* 20: 129-143
20. Sari K, Nelson G, Quinn R (2000) Dynamics and control of a simulated 3-D humanoid biped. *Proc Intl Symp Adaptive Motion of Animals and Machines 1: ThP-I-2*
21. Mori S, Matsui T, Kuze B, Asanome M, Nakajima K, Matsuyama K (1999) Stimulation of a restricted region in the midline cerebellar white matter evokes coordinated quadrupedal locomotion in the decerebrate cat. *J Neurophysiol* 82: 290-300
22. Mori S, Matsui T, Mori F, Nakajima K, Matsuyama K (2000) Instigation and control of treadmill locomotion in high decerebrate cats by stimulation of the hook bundle of Russell in the cerebellum. *Can J Physiol Pharmacol* 78: 945-957
23. Dietz V, Muller R, Colombo G (2002) Locomotor activity in spinal man: significance of afferent input from joint and load receptors. *Brain* 125: 2626-2634
24. DuySENS J, Van de Crommert HWAA, Smits-Engelsman BCM, Van der Helm FCT (2002) A walking robot called human: lessons to be learned from neural control of locomotion. *J Biomech* 35: 447-453
25. Miyai I, Tanabe CT, Sase I, Eda H, Oda I, Konishi I, Tsunazawa Y, Suzuki T, Yanagida T, Kubota K (2001) Cortical mapping of gait in humans: A Near-Infrared spectroscopic topography study. *Neuroimage* 14: 1186-1192
26. Kitano H (2002) Computational systems biology. *Nature* 420: 206-210

Dynamics-Based Motion Adaptation for a Quadruped Robot

Hiroshi Kimura and Yasuhiro Fukuoka

Graduate School of Information Systems, University of Electro-Communications,
1-5-1 Chofu-ga-oka, Chofu, Tokyo 182-8585, Japan

Abstract. In this paper, we propose the necessary conditions for stable dynamic walking on irregular terrain in general, and we design the mechanical system and the neural system by comparing biological concepts with those necessary conditions described in physical terms. PD-controller at joints can construct the virtual spring-damper system as the visco-elasticity model of a muscle. The neural system model consists of a CPG (central pattern generator) and reflexes. A CPG receives sensory input and changes the period of its own active phase. CPGs, the motion of the virtual spring-damper system of each leg and the rolling motion of the body are mutually entrained through the rolling motion feedback to CPGs, and can generate adaptive walking. We report our experimental results of dynamic walking on terrains of medium degrees of irregularity in order to verify the effectiveness of the designed neuro-mechanical system. The motion adaptation can be integrated based on the dynamics of the coupled system constructed by the mechanical system and the neural system. MPEG footage of these experiments can be seen at: <http://www.kimura.is.uec.ac.jp>.

1 Introduction

Many previous studies of legged robots have been performed, including studies on running and dynamic walking on irregular terrain. However, studies of autonomous dynamic adaptation allowing a robot to cope with an infinite variety of terrain irregularities have been started only recently and by only a few research groups. One example is the recent achievement of high-speed mobility of a hexapod over irregular terrain, with appropriate mechanical compliance of the legs[1,2]. The purpose of this study is to realize high-speed mobility on irregular terrain using a mammal-like quadruped robot, the dynamic walking of which is less stable than that of hexapod robots, by referring to the marvelous abilities of animals to autonomously adapt to their environment.

As many biological studies of motion control progressed, it has become generally accepted that animals' walking is mainly generated at the spinal cord by a combination of a CPG (central pattern generator) and reflexes receiving adjustment signals from a cerebrum, cerebellum and brain stem[3,4]. A great deal of the previous research on this attempted to generate walking using a neural system model, including studies on dynamic walking in simulation[5–8], and real robots[9–13]. But autonomously adaptable dynamic

Table 1. Biological concepts of legged locomotion control.

	ZMP based	Limit Cycle based	
		by Neural System (CPG and reflexes)	by Mechanism (spring and damper)
good for control of	posture and low speed walking	medium speed walking	high speed running
main controller	upper neural system acquired by learning	lower neural system (at spinal cord, brain stem, etc.)	musculoskeletal system through self stabilization

walking on irregular terrain was rarely realized in those earlier studies. This paper reports on our progress in the past couple of years using a newly developed quadruped called “Tekken,” which contains a mechanism designed for 3D space walking (pitch, roll and yaw planes) on irregular terrain[14].

2 Adaptive dynamic walking based on biological concepts

Methods for legged locomotion control are classified into ZMP-based control and limit-cycle-based control (Table.1). ZMP (zero moment point) is the extension of the center of gravity considering inertia force and so on. It was shown that ZMP-based control is effective for controlling posture and low-speed walking of a biped and a quadruped. However, ZMP-based control is not good for medium or high-speed walking from the standpoint of energy consumption, since a body with a large mass needs to be accelerated and decelerated by actuators in every step cycle.

In contrast, motion generated by the limit-cycle-based control has superior energy efficiency. But there exists the upper bound of the period of the walking cycle, in which stable dynamic walking can be realized[15]. It should be noted that control by a neural system consisting of CPGs and reflexes is dominant for various kinds of adjustments in medium-speed walking of animals[3]. Full et al.[16] also pointed out that, in high-speed running, kinetic energy is dominant, and self-stabilization by a mechanism with a spring and a damper is more important than adjustments by the neural system. Our study is aimed at medium-speed walking controlled by CPGs and reflexes (Table.1).

2.1 The quadruped “Tekken”

We designed Tekken to solve the mechanical problems which occurred in our past study using a planar quadruped “Patrush”[13]. The length of the body and a leg in standing are 23 and 20 [cm]. The weight of the whole robot is 3.1 [Kg]. Each leg has a hip pitch joint, a hip yaw joint, a knee pitch joint,

and an ankle pitch joint. The hip pitch joint, knee pitch joint and hip yaw joint are activated by DC motors of 20, 20 and 5 [W] through gear ratio of 15.6, 18.8 and 84, respectively. The ankle joint can be passively rotated in the direction if the toe contacts with an obstacle in a swing phase, and is locked while the leg is in a stance phase.

Two rate gyro sensors and two inclinometers for pitch and roll axes are mounted on the body in order to measure the body pitch and roll angles. The direction in which Tekken moves while walking can be changed by using the hip yaw joints.

2.2 Virtual spring-damper system

Full et al.[16,17] pointed out the importance of the mechanical visco-elasticity of muscles and tendons independent of sensory input under the concepts of “SLIP(Spring Loaded Inverted Pendulum)” and the “preflex”. Those biological concepts were applied for the development of hexapods with high-speed mobility over irregular terrain[1,2]. Although we are referring to the concept of SLIP, we employ the model of the muscle stiffness, which is generated by the stretch reflex and variable according to the stance/swing phases, aiming at medium-speed walking on irregular terrain adjusted by the neural system

All joints of Tekken are PD controlled to move to their desired angles in each of three states (A, B, C) in Fig.1 in order to generate each motion such as swinging up (A), swinging forward (B) and pulling down/back of a supporting leg (C). The constant desired angles and constant P-gain of each joint in each state were determined through experiments.

Since Tekken has high backdrivability with small gear ratio in each joint, PD-controller can construct the virtual spring-damper system with relatively low stiffness coupled with the mechanical system. Such compliant joints of legs can improve the passive adaptability on irregular terrain.

2.3 Rhythmic motion by CPG

Although actual neurons as a CPG in higher animals have not yet become well known, features of a CPG have been actively studied in biology, physiology, and so on. Several mathematical models were also proposed, and it was pointed out that a CPG has the capability to generate and modulate walking patterns and to be mutually entrained with a rhythmic joint motion[3–6].

As a model of a CPG, we used a neural oscillator: N.O. proposed by Matsuoka[18], and applied to the biped simulation by Taga[5,6]. In Fig.4, the output of a CPG is a phase signal: y_i . The positive or negative value of y_i corresponds to activity of a flexor or extensor neuron, respectively. We use the hip joint angle feedback as a basic sensory input to a CPG called a “tonic stretch response” in all experiments of this study[14]. This negative feedback makes a CPG be entrained with a rhythmic hip joint motion.

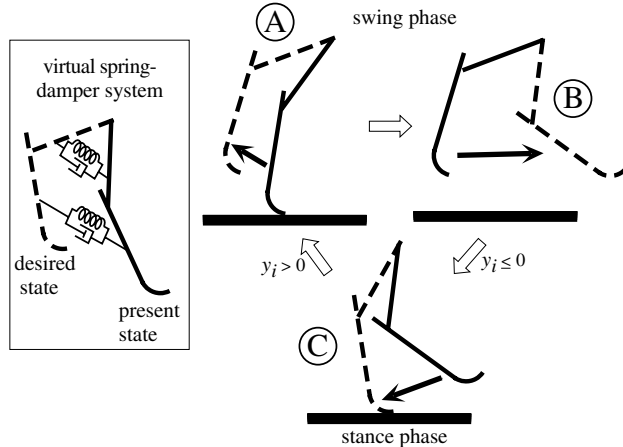


Fig. 1. State transition in the virtual spring-damper system, where y_i is the output phase signal of a CPG.

By connecting the CPG of each leg (Fig.4), CPGs are mutually entrained and oscillate in the same period and with a fixed phase difference. This mutual entrainment between the CPGs of the legs results in a gait. We newly propose an asymmetric CPG network shown in Fig.4 in order to generate an arbitrary gait from a trot to a pace via a walk with a single network configuration of CPGs. In Fig.4, a CPG of a foreleg is inhibited by a CPG of a hindleg with a connecting weight, and a CPG of a hindleg is not inhibited by a CPG of a foreleg.

2.4 Necessary conditions for stable dynamic walking on irregular terrain

We propose the necessary conditions for stable dynamic walking on irregular terrain, which can be itemized in physical terms:

- the swinging legs should be free to move forward during the first period of the swing phase,
- the swinging legs should land reliably on the ground during the second period of the swing phase,
- the angular velocity of the supporting legs relative to the ground should be kept constant during their pitching motion around the contact points at the moment of landing or leaving,
- the phase difference between rolling motion of the body and pitching motion of legs should be maintained regardless of a disturbance from irregular terrain, and
- the phase differences between the legs should be maintained regardless of delay in the pitching motion of a leg receiving a disturbance from irregular terrain.

2.5 Reflexes and responses

It is well known in physiology that

- some sensory stimuli modify CPG activity and reflexive responses to sensory stimuli are phase dependent under CPG activity[4].

Such interaction between CPG activity and a sensory stimulus is very important for adaptation and corresponds to the necessary conditions described in physical terms in Section 2.4.. In this paper, we define a “reflex” as joint torque generation based on sensor information and a “response” as CPG phase modulation through sensory feedback to a CPG.

The flexor and extensor reflexes contribute to satisfy the conditions (a) and (b), respectively. The flexor reflex is implemented as the passive ankle joint mechanism in Tekken. The extensor reflex has not yet been implemented in Tekken.

In addition, the following biological concepts are known[19]:

- when the vestibule in a head detects an inclination in pitch or roll plane, a downward-inclined leg is extended while an upward-inclined leg is flexed.

We call the reflex/response for an inclination in the pitch plane a “vestibulospinal reflex/response”, the role of which corresponds to the condition (c) and (e). In Tekken, hip joint torque in the stance phase is adjusted by the vestibulospinal reflex, since the body pitch angle is added to pitch hip joint angle. For the vestibulospinal response, the body pitch angle is feedbacked to the CPGs.

On the other hand, we call the response for an inclination in the roll plane a “tonic labyrinthine response for rolling”, the role of which corresponds to the condition (b) and (d). The tonic labyrinthine response is employed as rolling motion feedback to CPGs in Section 3..

The necessary condition (e) can be satisfied by the mutual entrainments between CPGs and the pitching motion of legs and the mutual entrainments among CPGs[13].

3 Entrainment between pitching and rolling motions

3.1 Rolling motion feedback to CPGs

Since a dynamic system similar to an inverted pendulum appears in the two-legged stance phase, a rolling motion is naturally generated in most of the gaits as a result. The amplitude of the rolling motion generated in walking on flat terrain is determined mainly by the gait, duty factor, and the period of the pitching motion cycle. As described as the condition (d) in Section 2.4.,

the change of the phase difference between rolling motion of the body and pitching motion of legs disturbs stable walking.

Therefore, we made the body angle around the roll axis be input to the CPGs as a feedback signal in order to synchronize rolling motion and pitching motion (upper left part of Fig.4)[14]. In Fig.2, CPGs, the pitching motion of the legs and the rolling motion of the body are mutually entrained through the rolling motion feedback to CPGs. This means that the rolling motion can be the standard oscillation for whole oscillations, in order to compensate for the weak connection between the fore and hind legs in the CPG network (Fig.4). As a result, the phase difference between the fore and hind legs is fixed, and the gait becomes stable.

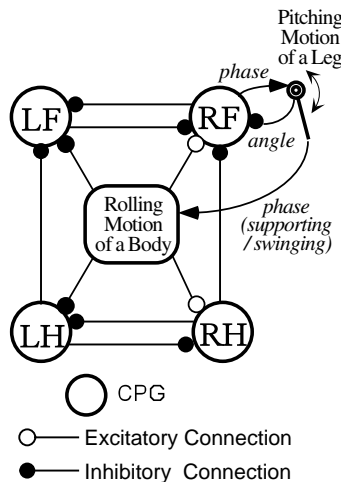


Fig. 2. Relationship among the CPGs, the pitching motion of a leg, and the rolling motion of the body in walking with rolling motion feedback to CPGs.

3.2 Tonic labyrinthine response for rolling

When a leg lands on a bump while walking on irregular terrain, the disturbance of the rolling motion to the pitching motion becomes larger. Therefore, the periods of the current phases of the CPGs in the pitching motion should be adjusted according to the rolling motion, in order to satisfy the condition (b) and (d) described in Section 2.4..

The rolling motion feedback to CPGs contributes to an appropriate adjustment of the periods of the stance and swing phases while walking on irregular terrain (Fig.3), as a tonic labyrinthine response for rolling (TLRR) described in Section 2.5.. In Fig.3, the right foreleg lands on a bump in a trot gait, and the body is inclined in a roll plane. Extending the stance phase of the left hindleg (E+), and shortening the stance phase of the right foreleg (E-) and the swing phase of the left foreleg (F-), prevent the body from the

excess inclination in a roll plane and help the condition (d) be satisfied. Extending the swing phase of the right hindleg ($F+$) enables the reliable landing of the leg on the ground and helps the condition (b) be satisfied..

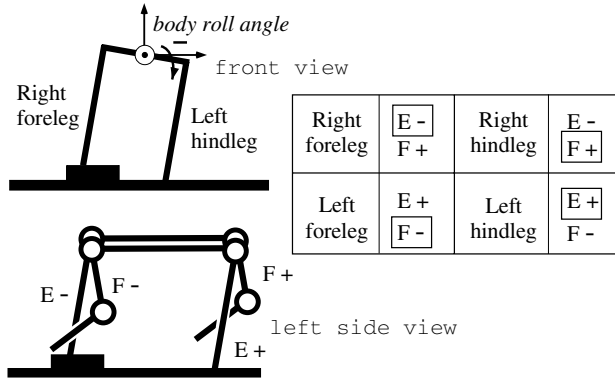


Fig. 3. A tonic labyrinthine response for rolling. E or F means the extensor or flexor neuron of a CPG, respectively. '+' or '-' means the activity of the neuron is increased or decreased by rolling motion feedback to CPGs, respectively.

3.3 Walking on flat terrain

The desired angle of the hip joint in the stance phase: θ_{stance} , the time constant of N.O.: τ are variables to change the indexes of walking such as the walking speed and the cyclic period of walking, respectively. For examples, when we shorten the cyclic period of walking by decreasing τ , the stride becomes short since the period of the state (B) in Fig.1 becomes short. As a result, the walking speed is kept almost constant. However, we cannot change the single index independent of other indexes in general, since those variables influence each other and walking is generated through interaction with floor.

Values of all parameters in the neural system including the virtual spring-damper system except for θ_{stance} and τ were determined experimentally. But it should be noted that those values were constant in the following experiments independent of terrain.

4 Adaptive walking on irregular terrain

4.1 Experiments on terrain of medium degree of irregularity

Since the phase difference between rolling motion of the body and pitching motion of legs is largely changed in walking on irregular terrain, a tonic labyrinthine response for rolling (TLRR) is essential.

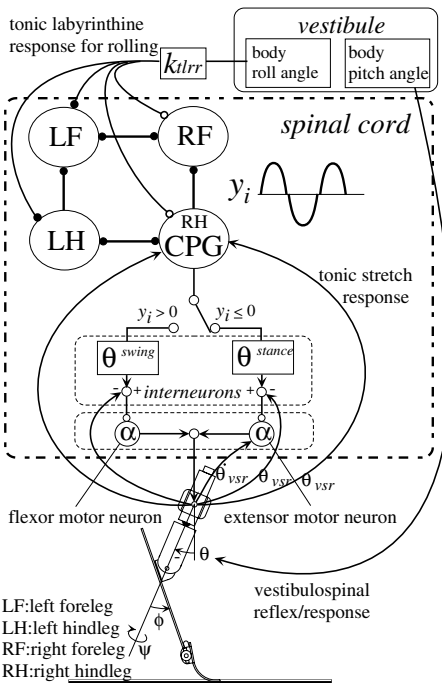


Fig. 4. Control diagram for Tekken.

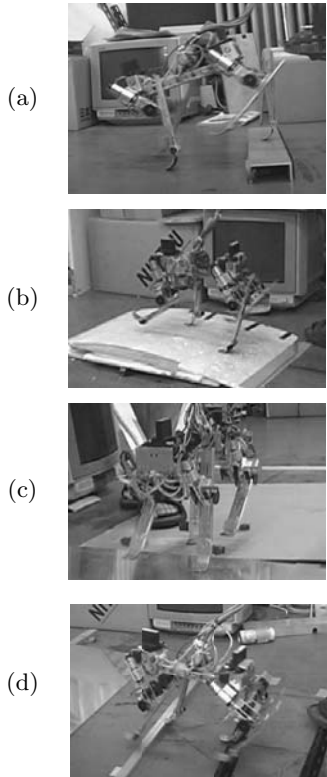


Fig. 5. Walking over irregular terrain.

We made Tekken walk on several irregular terrains with the fixed values of parameters. Tekken walked over an obstacle 4 [cm] in height while stumbling and landing on the obstacle (Fig.5-(a)). Tekken walked up and down a slope of 10 [deg] in the forward direction (Fig.5-(b)), and walked over slopes of 3 and 5 [deg] in a side ways direction (Fig.5-(c)) with an appropriate adjustment of periods of the stance and swing phases. Tekken also walked over terrains consisting of several boards 1.5 [cm] in height, and series of obstacles (Fig.5-(d)) with speed 0.7 [m/s]. Without a TLRR, the gait was greatly disturbed, even if Tekken didn't fall down.

Consequently, it was shown that method proposed in this study gives Tekken autonomous adaptation ability, since walking over unknown terrain of medium degree of irregularity was realized with fixed values of parameters.

4.2 Trade-off of stability and energy consumption

We have to solve the trade-off problem between the stability and the energy consumption[14] in order to determine the value of the time constant of

N.O.: τ . In this study, we employ the following Eq.(1) in order to change τ according to the wide stability margin (WSM)¹ measured using joint angle sensors. Eq.(1) means that we choose the large value of τ while WSM is high in order to decrease the energy consumption, and choose the small value of τ while WSM is low in order to increase WSM.

$$\tau = 0.12(\text{wide stability margin})/w \quad (1)$$

where WSM is normalized by the body width of Tekken ($w = 120$ [mm]).

As a result of experiments[14], it was shown that stable walking on irregular terrain with the lower energy consumption was obtained using Eq.(1).

4.3 Visual adaptation

By detecting the height and the distance to obstacles using vision, the robot can adjust the time constant of N.O.: τ for increasing the stability on terrain of high irregularity while keeping energy consumption low on terrain of low irregularity. In addition, the robot can change the leg length in the swinging phase based on vision in order to prevent the leg from stumbling on obstacles. As a result, Tekken can walk over an obstacle 5.5 [cm] in height (28% of the leg length) with vision.

5 Conclusion

In the neural system model proposed in this study, the relationships among CPGs, sensory input, reflexes and the mechanical system are simply defined. The physical oscillations such as the motion of the virtual spring-damper system of each leg and the rolling motion of the body are mutually entrained with CPGs as the neural oscillations. A CPG receives sensory input and changes the period of its own active phase as responses. The virtual spring-damper system also receives sensory input and outputs torque as reflexes. The states in the virtual spring-damper system are switched based on the phase signal of the CPG. Consequently, the adaptive walking is generated through the interaction with environment.

The motion adaptation can be integrated based on the dynamics of the coupled system constructed by the mechanical system and the neural system. The neural system centering the CPGs can afford autonomous adaptation at the several levels from the lower virtual spring-damper system to the higher vision system.

¹ The WSM is defined as the shortest distance from the projected point of the center of gravity to the edges of the polygon constructed by the projected points of legs independent of their stance or swing phases.

References

1. Saranli, U., Buehler, M., and Koditschek, D. E. 2001. RHex: a simple and highly mobile hexapod robot. *Int. J. Robotics Research* 20(7):616–631.
2. Cham, J. G., Bailey, S. A., Clark J. E., Full, R. J., Cutkosky, M. R. 2002. Fast and Robust: Hexapedal Robots via Shape Deposition Manufacturing. *Int. J. Robotics Research* 21(10-11):869–882.
3. Grillner, S. 1981. Control of locomotion in bipeds, tetrapods and fish. *Handbook of Physiology II* American Physiol. Society, Bethesda, MD. 1179–1236.
4. Cohen, A. H., and Boothe, D. L. 1999. Sensorimotor interactions during locomotion: principles derived from biological systems. *Autonomous Robots* 7(3):239–245.
5. Taga, G., Yamaguchi, Y., and Shimizu, H. 1991. Self-organized control of bipedal locomotion by neural oscillators. *Biolog. Cybern.* 65:147–159.
6. Taga, G. 1995. A model of the neuro-musculo-skeletal system for human locomotion II. - real-time adaptability under various constraints. *Biolog. Cybern.* 73:113–121.
7. Miyakoshi, S., Taga, G., Kuniyoshi, Y., and Nagakubo, A. 1998. Three dimensional bipedal stepping motion using neural oscillators - towards humanoid motion in the real world. *Proc. of IRSO1998*, pp. 84–89.
8. Ijspeert, A.J. 2001. A connectionist central pattern generator for the aquatic and terrestrial gaits of a simulated salamander. *Biolog. Cybern.* 84(5):331–348.
9. Kimura, H., Akiyama, S., and Sakurama, K. 1999. Realization of dynamic walking and running of the quadruped using neural oscillator. *Autonomous Robots* 7(3):247–258.
10. Ilg, W., Albiez, J., Jedele, H., Berns, K., and Dillmann, R. 1999. Adaptive periodic movement control for the four legged walking machine BISAM. *Proc. of ICRA1999*, pp. 2354–2359.
11. Lewis, M. A., Etienne-Cummings, Hartmann, M. J., Xu, Z. R., and Cohen, A. H. 2003. An in silico central pattern generator: silicon oscillator, coupling, entrainment, and physical computation. *Biolog. Cybern.* 88:137–151.
12. Tsujita, K., Tsuchiya, K., and Onat, A. 2001. Adaptive Gait Pattern Control of a QuadrupedLocomotion Robot, *Proc. of IROS2001*, pp. 2318–2325.
13. Kimura, H., Fukuoka, Y., and Konaga, K. 2001. Adaptive dynamic walking of a quadruped robot using neural system model. *Advanced Robotics* 15(8):859–876.
14. Fukuoka, Y., Kimura, H., Cohen, A.H. 2003. Adaptive Dynamic Walking of a Quadruped Robot on Irregular Terrain based on Biological Concepts. *Int. J. Robotics Research*, 22(3-4):187–202.
15. Kimura, H., Shimoyama, I., and Miura, H. 1990. Dynamics in the dynamic walk of a quadruped robot. *Advanced Robotics* 4(3):283–301.
16. Full, R. J., and Koditschek, D. E. 1999. Templates and anchors: neuromechanical hypotheses of legged locomotion on land. *J. Exp. Biol.* 202:3325–3332.
17. Full, R. J. 2000. Biological inspiration: lessons from many-legged locomotors. *Robotics Research 9*, J.M.Hollerbach and D.E.Koditschek Eds, Springer London. pp. 337–341.
18. Matsuoka, K. 1987. Mechanisms of frequency and pattern control in the neural rhythm generators. *Biolog. Cybern.* 56:345–353.
19. Nanzando's Medical Dictionary 18th Ed. 1998. Nanzando, Tokyo. 1211. (in Japanese)

A Turning Strategy of a Multi-legged Locomotion Robot

Kazuo Tsuchiya, Shinya Aoi and Katsuyoshi Tsujita

Dept. of Aeronautics and Astronautics, Graduate School of Engineering, Kyoto University, Yoshida-honmachi, Sakyo-ku, Kyoto 606-8501, Japan

Abstract. In this paper, we analyze the walking stability of a multi-legged locomotion robot. Based on dynamic characteristics, we propose a strategy for turning whose effectiveness is verified by numerical simulations. The robot can turn more efficiently with fewer slips after decreasing walking stability. That is, the maneuverability of the robot increases by changing the dynamic properties of the robot.

1 Introduction

The locomotion of a robot with many legs has the advantage of stability, since it is supported by many legs. However, this design lacks maneuverability since the robot is constrained to the ground by many legs. An established method of controlling a robot consists of motion planning and motion control. Motion planning computes the movement of the joints to realize a given motion, and motion control manipulates the joints to achieve a designed motion. This method is not efficient, and solutions cannot adapt to changes in environment. From a practical viewpoint, it is important to improve the maneuverability of multi-legged locomotion robots.

In ethology, research on arthropod locomotion has advanced. Arthropod locomotion is very stable and can maneuver on rough terrain, climb over obstacles, and turn quickly. Research is trying to elucidate how the arthropod produces stable locomotion and maneuverability. Dean *et al.* [2] and Schmitz *et al.* [8] examined the locomotion of the stick insect, *Carausius morosus*, and proposed a control system for a hexapod robot that achieves straight and curve walking and straight walking over obstacles by numerical simulations. Watson *et al.* [9], [10] studied the kinematics and neural legged locomotion control of the obstacle climbing of the cockroach, *Blaberus discoidalis*. Based on the results, Quinn *et al.* [5] developed locomotion controllers for hexapod robots. Jindrich and Full [3] and Kubow and Full [4] investigated the dynamic properties of the turning motions of the cockroach. Schmitt and Holmes [6], [7] analyzed the dynamics of turning behavior based on a simplified mathematical model, which revealed that the cockroach decreases walking stability by moving the points on its body where the intermittent forces from the ground act, enabling it to turn quickly.

This paper deals with the turning motion of a multi-legged locomotion robot. First, we analyze the walking stability of the robot. The analysis reveals that by changing control parameters, walking stability decreases, and

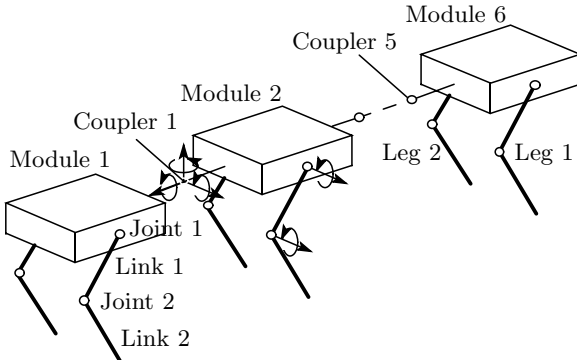


Fig. 1. Schematic 3-D model of the multi-legged locomotion robot

beyond a critical point, a meandering motion appears. Based on dynamic properties, we propose a control strategy for the robot that realizes an efficient turning motion by decreasing walking stability; in other words, increasing the maneuverability of the robot by changing its dynamic characteristics.

2 Model

2.1 3-D dynamics model

We considered the multi-legged locomotion robot shown in Fig. 1. It has six modules, each with one body and two legs. Each leg consists of two links that are connected to each other through a one degree of freedom (DOF) rotational joint. They are connected to the body by a one DOF rotational joint. Each module is connected to each other through a coupler composed of roll, pitch, and yaw joints. The modules are enumerated from Module 1 to Module 6, and the coupler between Module i and Module $(i+1)$ is numbered as Coupler i ($i = 1, \dots, 5$). The left and right legs are numbered as Legs 1 and 2, respectively. The joints and the links of each leg are numbered from the side of the body as Joints 1 and 2 and Links 1 and 2. The coordinate axes $\{\mathbf{a}_i\} = \{\mathbf{a}_{i1}, \mathbf{a}_{i2}, \mathbf{a}_{i3}\}$ ($i = 0, \dots, 6$) are fixed on the ground ($i = 0$) or on the body of Module i ($i = 1, \dots, 6$), where axis \mathbf{a}_{i1} is toward the nominal direction of locomotion and axis \mathbf{a}_{i3} is toward the vertical direction. The position vector of the body of Module 1 is given by vector \mathbf{r}_0 expressed as $r_0 = [r_{01}, r_{02}, r_{03}]$ in $\{\mathbf{a}_0\}$. The posture of the body of Module 1 is expressed as Euler angles $\theta_0 = [\theta_{01}, \theta_{02}, \theta_{03}]$, where θ_{01} , θ_{02} , and θ_{03} are the rotation angles around axes \mathbf{a}_{01} , \mathbf{a}_{02} , and \mathbf{a}_{03} , respectively. Similarly, we define θ_{im} ($i = 1, \dots, 5$, $m = 1, 2, 3$) as the components of Euler angles from $\{\mathbf{a}_i\}$ to $\{\mathbf{a}_{i+1}\}$, and $\theta_{ik}^{(j)}$ ($i = 1, \dots, 6$, $j = 1, 2$, $k = 1, 2$) as the relative angle of Joint k of Leg j of Module i .

The state variable is defined as $q^T = [r_{0m}, \theta_{i-1m}, \theta_{ik}^{(j)}](i = 1, \dots, 6, j = 1, 2, k = 1, 2, m = 1, 2, 3)$. An equation of motion for state variable q is derived using Lagrangian formulation by

$$M\ddot{q} + H(q, \dot{q}) = G + \sum_{i,j} \tau_{ij} + \sum_{i,j,k} \tau_{ik}^{(j)} + \Lambda \quad (1)$$

where M is the inertia matrix, $H(q, \dot{q})$ is the nonlinear term that includes Coriolis and centrifugal forces, G is the gravity term, $\tau_{ij}(i = 1, \dots, 5, j = 1, 2, 3)$ and $\tau_{ik}^{(j)}(i = 1, \dots, 6, j = 1, 2, k = 1, 2)$ are the input torques of the actuators at the joints ($j = 1$: roll, $j = 2$: pitch, $j = 3$: yaw) of Coupler i and Joint k of Leg j of Module i , and Λ is the reaction force from the ground. The reaction force is modeled using a spring and damper model.

2.2 Clock-driven leg controller

Here, we explain a locomotion control system. The robot has a simple clock-driven, open-loop gait. All the joints have motors and are controlled by a proportional-derivative (PD) controller. The leg joints are controlled by incorporation of the periodic desired angles, while the joints of the couplers are passively controlled without incorporating the desired angles. To design the desired angles of the leg joints, first we introduce Oscillator $i, j(i = 1, \dots, 6, j = 1, 2)$ for Leg j of Module i . Oscillator i, j has phase $\phi_i^{(j)}$ whose angular velocity is constant. Second, we design the nominal trajectory $\hat{\eta}_i^{(j)}(i = 1, \dots, 6, j = 1, 2)$ of the tip of Leg j of Module i in the sagittal plane of $\{a_i\}$ as a function of phase $\phi_i^{(j)}$, that is, $\hat{\eta}_i^{(j)} = \hat{\eta}_i^{(j)}(\phi_i^{(j)})$. Trajectory $\hat{\eta}_i^{(j)}$ consists of the trajectories of swinging stage $\hat{\eta}_{iSw}^{(j)}$ and supporting stage $\hat{\eta}_{iSp}^{(j)}(i = 1, \dots, 6, j = 1, 2)$, which are also the functions of phase $\phi_i^{(j)}$ and change at the anterior extreme position (AEP) and the posterior extreme position (PEP) as shown in Fig. 2.

$$\hat{\eta}_i^{(j)}(\phi_i^{(j)}) = \begin{cases} \hat{\eta}_{iSw}^{(j)}(\phi_i^{(j)}) & 0 \leq \phi_i^{(j)} < \phi_A \\ \hat{\eta}_{iSp}^{(j)}(\phi_i^{(j)}) & \phi_A \leq \phi_i^{(j)} < 2\pi \end{cases} \quad i = 1, \dots, 6, j = 1, 2 \quad (2)$$

where $\phi_A = 2\pi(1 - \beta)$ that indicates the phase value at AEP, and β is a duty ratio that indicates the ratio between the time interval for the supporting stage and the period of one step of locomotion. Finally, from inverse kinematics, we obtained the desired angle $\hat{\theta}_{ik}^{(j)}(i = 1, \dots, 6, j = 1, 2, k = 1, 2)$ of Joint k of Leg j of Module i as the function of phase $\phi_i^{(j)}$.

3 Stability analysis of walking

In this section, we simplified the actual 3-D model of the multi-legged locomotion robot to a 2-D model and then analyze the walking stability based on

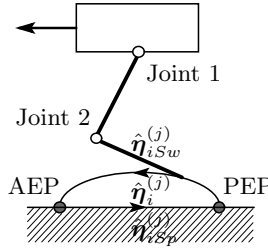


Fig. 2. Nominal trajectory of the leg

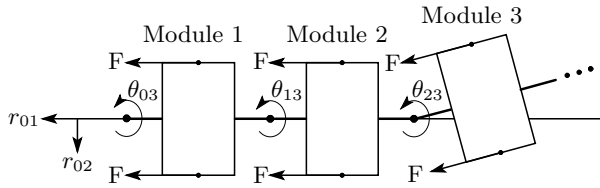


Fig. 3. Simplified 2-D model of the multi-legged locomotion robot

the simplified 2-D model. Next, we verified that walking changes naturally into meandering by comparing the analysis results based on the 2-D model with the numerical simulation results of the actual 3-D model.

3.1 Simplified 2-D dynamics model

We assumed that many of the robot legs always touch the ground when it walks, and so the vertical motion of the robot can be ignored. Next, using the numerical simulations of the actual 3-D model, we found that the periodic meandering motion is longer than the period of the cyclic motion of the legs. We assumed that intermittent forces from the ground can be modeled as constant forces. We also assumed that the locomotion speed of the robot is constant.

Based on these assumptions, the 3-D model shown in Fig. 1 is simplified to the 2-D model shown in Fig. 3. This simplified 2-D model consists of rigid bodies that are connected to each other through a one DOF rotational joint and constrained on a plane. As propulsive forces, the constant follower forces, F , parallel to each module act on both sides of each module. As friction forces, the forces tangential to each module whose magnitudes are proportional to the velocities of these directions act on both sides of each module. In light of the assumptions, we contracted the state variables by $\bar{q}^T = [r_{02}, \theta_{03}, \dots, \theta_{53}]$. Note that state variable r_{01} is also contracted since it is outside of our interest, and its equation can be separated from the other equations. By putting $\dot{\xi}^T = [\dot{q}^T, \ddot{q}^T]$, (1) is written simply as

$$\dot{\xi} = f(\xi) \quad (3)$$

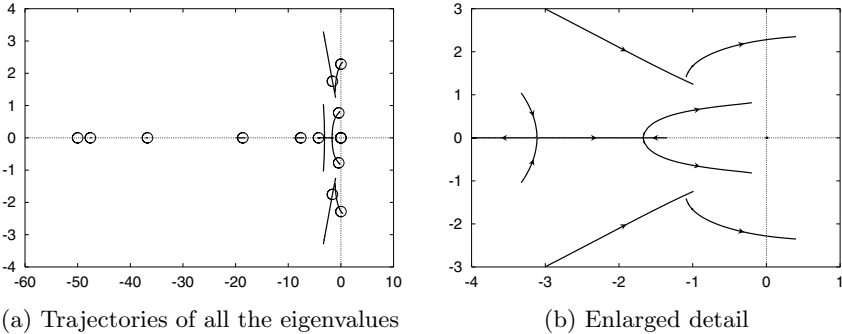


Fig. 4. Trajectories of the eigenvalues of the linearized equation while chaning the compliances of the yaw joints of the couplers

3.2 Stability analysis

We define $\xi_0 (= [0, \dots, 0]^T)$ as the equilibrium solution of (3) and $\delta\xi$ as a perturbation from the equilibrium solution and then define $\xi = \xi_0 + \delta\xi$. By substituting ξ into (3), we obtain a linearized equation by

$$\dot{\delta\xi} = D_\xi f(\xi_0)\delta\xi \quad (4)$$

where $D_\xi \equiv \frac{\partial}{\partial\xi}$. From (4), we investigated the walking stability, while the compliances of the yaw joints of the couplers are increased. To increase the compliances, the corresponding PD feedback gains K_{i3} and $D_{i3}(i = 1, \dots, 5)$ are decreased by using parameter f as follows:

$$\begin{cases} K_{i3} = K_0(2\pi f)^2 \\ D_{i3} = 2K_0\zeta(2\pi f) \end{cases} \quad i = 1, \dots, 5 \quad (5)$$

where ζ and K_0 are set as 0.8 and 0.01, respectively. The physical parameters of the 2-D model are given as follows: The mass of each module is 0.8 [kg], $F = 3.32$ [N], and $\dot{r}_{01} = 0.167$ [m/s]. Figures 4a and b show the trajectories of the eigenvalues of the linearized equation (4). These figures show that when parameter f decreases and reaches a critical point, a pair of eigenvalues cross the imaginary axis and become unstable. That is, Hopf bifurcation occurs. Note that this system has two zero eigenvalues and that in Fig. 4a the points enclosed by circles correspond to the eigenvalues when bifurcation occurs. From these results, it is revealed that when the compliances are small, walking is stable, but when the compliances increase beyond a bifurcation point, walking becomes unstable through Hopf bifurcation.

3.3 Numerical simulation

Here, we validated that walking actually becomes unstable through Hopf bifurcation when the compliances of the yaw joints of the couplers are increased

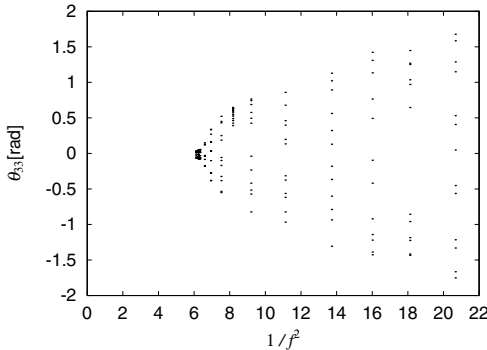


Fig. 5. Plot of the yaw angle θ_{33} of Coupler 3 at $\phi_6^{(1)}=0$ versus parameter $1/f^2$



Fig. 6. Meandering motion obtained by 3-D numerical simulation

beyond a critical point, based on the numerical simulation of the 3-D model. Second, we verified that the stability analysis based on the 2-D model is valid by comparing the results of numerical simulation and stability analysis. The physical parameters of the 3-D model are given as follows: The mass of each body is 0.6 [kg], the mass of Links 1 and 2 of each leg are 0.05 [kg], the length of Links 1 and 2 of each leg are 0.05 [m], the period of each leg motion is 0.5 [s], the stride of each leg is 0.05 [m], and $\beta = 0.6$. The nominal gait pattern of the robot is set so that Legs 1 and 2 of each module and the unilateral legs on adjacent modules move out of phase with each other. That is, the phases of the oscillators have relationships such that $\phi_i^{(1)} - \phi_i^{(2)} = \pi$ ($i = 1, \dots, 6$) and $\phi_i^{(j)} - \phi_{i+1}^{(j)} = \pi$ ($i = 1, \dots, 5$, $j = 1, 2$).

First, we carried out numerical simulations of the 3-D model, while the compliances of the yaw joints of the couplers are increased by using a parameter f that is similar to (5). Fig. 5 shows the plot of the yaw angle θ_{33} of Coupler 3 on the Poincaré sections with respect to parameter $1/f^2$ that corresponds to the compliances. In this paper, the Poincaré section is assumed to be $\phi_6^{(1)} = 0$. Since $\phi_i^{(j)}$ is 2π -periodic, the sampling interval is equal to the period of the leg motion. This figure indicates that there is a critical point beyond which the robot begins to meander (Fig. 6). Thus, it is verified that walking becomes unstable through Hopf bifurcation and then smoothly becomes meandering. But note that the vertical line of each Poincaré section with respect to parameter $1/f^2$ is filled, since the motion of the legs and

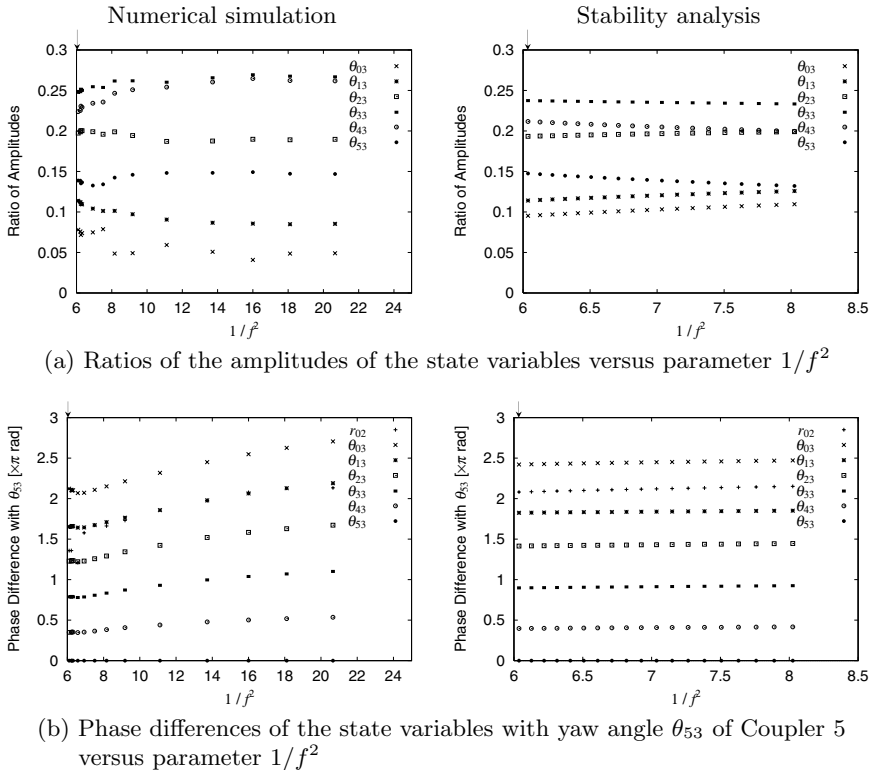


Fig. 7. Comparison between numerical simulation and stability analysis

the meandering motion are not synchronized. As expected from the analysis of the 2-D model, this bifurcation does not depend on the gait pattern. For example, a similar bifurcation exists, even if Legs 1 and 2 of each module move in phase and the legs on adjacent modules move out of phase (i.e. $\phi_i^{(1)} = \phi_i^{(2)}$ ($i = 1, \dots, 6$), $\phi_i^{(j)} - \phi_{i+1}^{(j)} = \pi$ ($i = 1, \dots, 5$, $j = 1, 2$)). Furthermore, the simulation results verified that the meandering period is about 14 times longer than the period of the leg movements.

Next, to verify the validity of the stability analysis based on the 2-D model, we compared the unstable eigenvectors obtained by stability analysis with the state variables of the meandering motion obtained by numerical simulations. In Figures 7a and b, we compared the ratios of the amplitudes and the phase differences with yaw angle θ_{53} of Coupler 5 of the state variables with respect to parameter $1/f^2$ between numerical simulation and stability analysis. From these figures, we found that the results of the numerical simulations and the stability analyses resemble each other, especially near the bifurcation point which is indicated by arrows. These results verified that the stability analysis based on the 2-D model is valid.

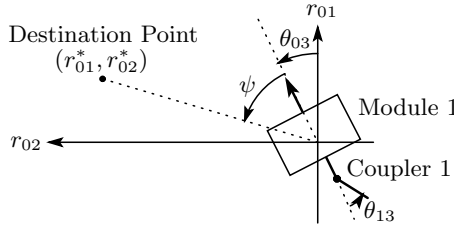


Fig. 8. Turning walk control

4 Turning walk control

In this section, based on the dynamic properties of walking analyzed in the previous section, we propose a turning strategy for the robot.

4.1 Turning strategy

1. When the robot starts to turn, the compliances of the yaw joints of all the couplers except for Coupler 1 are increased.
2. The input torque at the yaw joint of Coupler 1 is activated by incorporating the desired angle that directs the first module in a turning direction.

To turn the robot, this strategy attempts to direct the first module to the turning direction and then make the other modules follow the first module, since they are passively connected to each other. Note that, now, the robot can turn with less constraint forces, since it has less walking stability.

4.2 Numerical analysis

Here, we verify the effectiveness of the proposed turning strategy by numerical simulations. We consider a task in which the robot approaches a destination point (r_{01}^*, r_{02}^*) while walking and turning. We assume that the robot can get information about the angle ψ between the walking direction and the direction of the destination point (Fig. 8). Then, input torque τ_{13} at the yaw joint of Coupler 1 is given by

$$\tau_{13} = -K_{13}(\theta_{13} + \psi) - D_{13}\dot{\theta}_{13} \quad (6)$$

Numerical simulations were carried out as follows: First, the robot starts to walk in the direction of the r_{01} -axis by setting the compliances of the yaw joints of the couplers low enough; when the first module reaches point $(r_{01}, r_{02}) = (0, 0)[\text{m}]$, the robot begins to turn almost perpendicularly by setting the destination point as $(r_{01}^*, r_{02}^*) = (0, 50)[\text{m}]$. Note that we consider

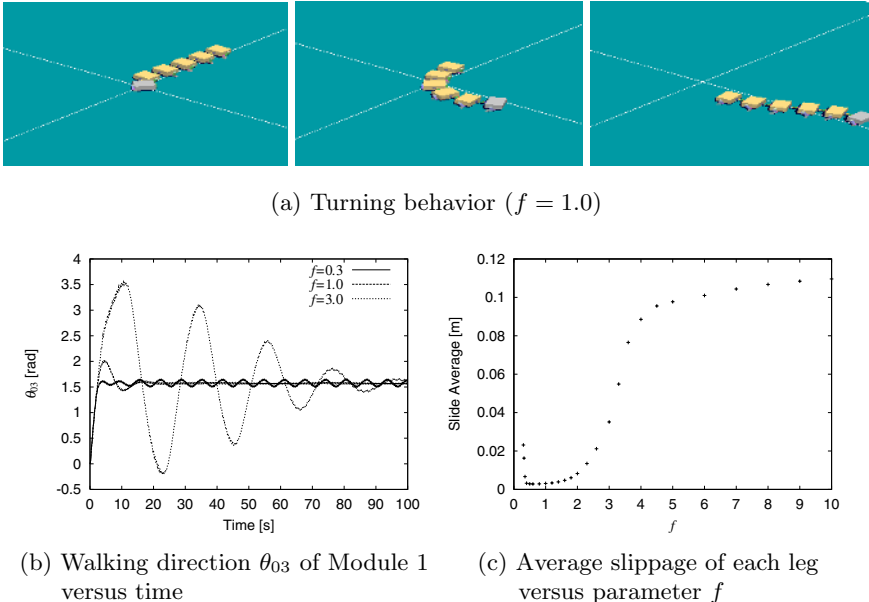


Fig. 9. Turning behavior

$t = 0$ [s] when the robot starts to turn. At that time, we changed the compliances of the yaw joints of the couplers, except for Coupler 1, by changing parameter f similar to (5), while Coupler 1 is fixed. Fig. 9a shows the turning behavior for changed parameter $f = 1$. Fig. 9b shows the profile of the walking direction θ_{03} of the first module for the three kinds of changed parameter f . Fig. 9c shows the average slippage of each leg to the ground compared to changed parameter f . These results suggest that in the region where compliances are very small, the modules cannot follow the first module efficiently because the amount of slippage has become too large, and so many modules are lagged. On the other hand, in the region where compliances are very large, the modules can follow effectively, but the legs slip and the robot can not walk efficiently due to the appearance of meandering. When the compliances are set just before the value at which walking becomes unstable, the robot can walk and turn most efficiently.

5 Conclusion

In this paper, we analyzed the dynamic properties of walking of a multi-legged robot. We found that walking degenerates into meandering through Hopf bifurcation by changing the compliances of the yaw joints of the couplers. This transfer of walking pattern is an example of the destabilization due to

the follower forces [1]. Then, based on the dynamic properties of the robot, we propose a turning strategy. Numerical simulations verified that the robot can turn effectively with fewer slips by decreasing the walking stability of the robot. Note that this means that the maneuverability of the robot is increased by compliance controls.

References

1. Bolotin, V. V. (1963) Nonconservative Problems of the Theory of Elastic Stability. Pergamon Press, New York.
2. Dean, J., Kindermann, T., Schmitz, J., Schumm, M., and Cruse, H. (1999) Control of walking in the stick insect: from behavior and physiology to modeling. *Autonomous Robots* 7(3):271–288.
3. Jindrich, D. and Full, R. J. (1999) Many-legged maneuverability: dynamics of turning in hexapods. *J. Exp. Biol.* 202:1603–1623.
4. Kubow, T. M. and Full, R. J. (1999) The role of the mechanical system in control: a hypothesis of self-stabilization in hexapedal runners. *Phil. Trans. R. Soc. Lond. B* 354:849–861.
5. Quinn, R. D., Nelson, G. M., Bachmann, R. J., Kingsley, D. A., Offi, J., and Ritzmann, R. E. (2001) Insect designs for improved robot mobility. *Proc. of 4th Int. Conf. on Climbing and Walking Robots (CLAWAR 2001)*, pp. 69–76.
6. Schmitt, J. and Holmes, P. (2000) Mechanical models for insect locomotion: dynamics and stability in the horizontal plane I. Theory. *Biol. Cybern.* 83:501–515.
7. Schmitt, J. and Holmes, P. (2000) Mechanical models for insect locomotion: dynamics and stability in the horizontal plane II. Application. *Biol. Cybern.* 83:517–527.
8. Schmitz, J., Dean, J., Kindermann, T., Schumm, M., and Cruse, H. (2001) A biologically inspired controller for hexapod walking: simple solutions by exploiting physical properties. *Biol. Bull.* 200:195–200.
9. Watson, J. T., Ritzmann, R. E., Zill, S. N., and Pollack, A. J. (2002) Control of obstacle climbing in the cockroach, *Blaberus discoidalis*. I. Kinematics. *J. Comp. Physiol. A* 188:39–53.
10. Watson, J. T., Ritzmann, R. E., and Pollack, A. J. (2002) Control of climbing behavior in the cockroach, *Blaberus discoidalis*. II. Motor activities associated with joint movement. *J. Comp. Physiol. A* 188:55–69.

A Behaviour Network Concept for Controlling Walking Machines

Jan Albiez¹, Tobias Luksch², Karsten Berns², and Rüdiger Dillmann¹

¹ Forschungszentrum Informatik Karlsruhe,
Interactive Diagnosis- and Service Systems,
Haid-und-Neu-Str. 10–14, 76131 Karlsruhe, Germany

² AG Robtersysteme, Fakultät für Informatik
Universität Kaiserslautern
D-67653 Kaiserslautern, Germany

Abstract. The high complexity of the mechanical system and the difficult task of walking itself makes the task of designing the control for legged robots a difficult one. Even if the implementation of parts of the desired functionality, like posture control or basic swing/stance movement, can be solved by the usage of classical engineering approaches, the control of the overall system tends to be very unflexible. This paper introduces a new method to combine aspects of classical robot control and behaviour based control. Inspired by the activation patterns in the brain and the spinal cord of animals we propose a behaviour network architecture using special signals like activity or target rating to influence and coordinate the behaviours. The general concept of a single behaviour as well as their interaction within the network is described. This architecture is tested on the four-legged walking machine BISAM and experimental results are presented.

1 Introduction

Walking robots have been a field of increasing activity in the last years. Especially the ability to adapt to unstructured terrain and the resulting demands on the control architecture have been in the focus of researchers. These efforts can be separated into two different approaches, one being the classical engineering approach using and refining the known methods of loop-back control structures and dynamic modelling to control the robot, e.g. [16]. The other way is to adopt as much from biological paragons for locomotion as possible regarding both mechanical design and control architecture, e.g. [7] and [22]. The methods proposed in this paper follow the second approach by applying a reflex or behaviour based control architecture to a four-legged walking machine, this way performing sensor-based adaptation to motion on irregular terrain.

Biological research of the last years has identified several key elements being used in nature for adapting locomotion. These range from the geometrical structure of legs [34] and dynamic properties of muscles [29] to neural networks used for walking by insects [11]. The results of this research suggest a transfer of these principles to legged robots. Due to the high complexity of

real walking machines and the impracticality of mimicking especially nature's activators and sensors, up to now only some of the ideas have been transferred to the control architectures of real robots. In [21,22] a neuro-oscillator based pattern generator is introduced. The adaptation to the terrain is solved by directly influencing the activation of the oscillator neurons. [6] also uses neuro-oscillators which are parametrized using the results from the analysis of lobsters. [17] proposes a reflex based gait generation system, triggered by the input of a camera system mounted on the robot. A distributed control system for a hexapod using reflexes to stabilize the body is presented in [14].

In the last years several methods were successfully applied to control the four-legged walking machine BISAM [8]. These include the usage of coupled neuro-oscillators for gait generation [18] and the application of radial basis function neural networks and reinforcement learning methods for posture control while trotting [1]. All these methods were successfull but lacked a certain extensibility when confronted with more demands than they were initially designed for (e.g. both dynamically stable trott and statically stable walking). Thus the necessity arrised to build an architecture being able to handle these demands.

2 Activation, activity, target rating and behaviours

There have been several approaches to use behaviour based control in mobile robots over the last years. The main area of application have been wheel driven, kinematically extremly simple robots, with the main focus on the robot's task eg. navigation and group behaviour [13,5,27]. Therefore these architectures concentrate on the coordination of a set of high level behaviours operating mostly on the same semantic level and producing abstract commands for the robot's hardware. Since the coordaintion of behaviours is crucial part in behaviour based robotics a lot of work has been done there. Examples include comfort zones [25] or case based reasoning [26]; a good overview on behaviour coordination can be found in [30].

There have only been a few attempts to use behaviour based architectures on the lower levels of the control architecture for kinematically more complex robots like walking machines. The best known and most successful is the subsumption architecture [9,15] used on several hexapods. A more biological inspired approach for a lobster robot is proposed in [7]. But there are several drawbacks to these architectures, among them a general tendency towards scalability problems, weaknesses when adding new behaviours or trying reusing existing ones and in most cases a highly problem specific approach (see [4]).

When considering the insights gained through PET and EEG scans and spinal cord activity plots of animals performing certain tasks [20,29], as well as the problems when dealing with real sensor information and highly complex robots, the following key aspects can be identified:

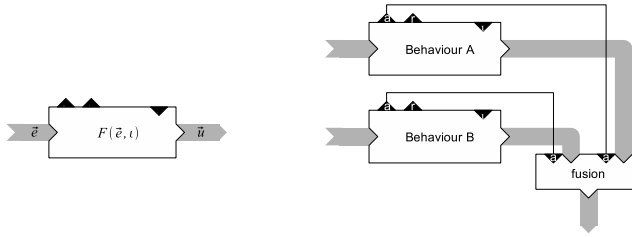


Fig. 1. (left) Basic behaviour block, (right) Behaviour fusion using activities as weight

- A certain action of an animal always creates activity in the same area of the animal's brain or its spinal cord.
- Such an active area can result in the stimulation of further regions as well as inhibit activity in others.
- Even though the classical approach to robot control has difficulties handling the complexity of the whole system, these established methods should be applied to solve simpler sub-problems.
- As hierarchical systems have been approved in robotics as well as in nature it is advisable to use some kind of leveled system with an increasing degree of abstraction regarding sensor data and motor signals.

Taking these observations into consideration, we designed a control architecture consisting of a hierarchical network of behaviours. Each behaviour or reflex¹ is developed using methods of classical control system design or artificial intelligence. Only the interaction of the behaviours and their placement in the network will result in the desired actions of the overall system.

Each such behaviour \mathcal{B} as used in this architecture can formally be defined as

$$\mathcal{B} = (\mathbf{e}, \mathbf{u}, \iota, F, r, a).$$

This functional unit uses the input vector \mathbf{e} and generates the output vector \mathbf{u} . It possesses another dedicated input value ι to activate the behaviour on a scale between 0 (disabled) and 1 (fully activated). This allows to ensure the robot's safety to a certain degree by activating only a defined set of behaviours and enables the usage of the behaviour as an abstract actor by other higher level behaviours. The transfer function F can then be defined as

$$F : \Re^n \times [0; 1] \rightarrow \Re^m; \quad F(\mathbf{e}, \iota) = \mathbf{u}.$$

¹ A reflex refers to a simple behaviour close to the hardware thus being more reactive than deliberative

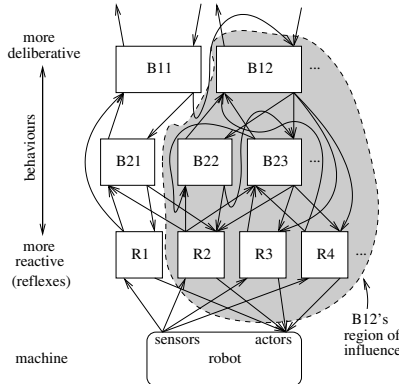


Fig. 2. Behaviour coordination network

Each behaviour generates two further output values, the target rating r and the activity a . These are set apart from the control output u as they are not used for control purposes but more treated as kind of sensor information about the behaviour's state. The target rating r evaluates the system state from the restricted view e of the behaviour.

$$r : \Re^n \rightarrow [0; 1]; r(e) = r$$

It is constantly calculated even if the behaviour is deactivated and generates no output. A value of 0 indicates that the robot's state matches the behaviour's goal, a value of 1 that it does not. The activity a reflects the magnitude of the behaviour's action:

$$a : \Re^m \rightarrow [0; 1] : a(u) \sim \|u\|$$

Apart from giving crucial visualisable information for the control system developer, ι , r and a are responsible for the interaction between the behaviours within the network. The network itself is a hierarchical distribution of the behaviours according to their functionality. The more reflex-like a behaviour is the lower it is placed inside the network (see figure 2). Higher behaviours are using the functionality of lower ones via their ι inputs like these could be using motor signals to generate robot movement. From this activation mechanism emerge the regions of influence \mathcal{R} as shown in figure 2 which are recursively defined as

$$\mathcal{R}(B) = \bigcup_{B_i \in \text{Act}(B)} \{B_i \cup \mathcal{R}(B_i)\},$$

$$\mathcal{R}(B) = \emptyset, \quad \text{if} \quad \text{Act}(B) = \emptyset,$$

where $\text{Act}(B)$ is the set of behaviours being influenced by B via ι . This affiliation of a behaviour to a region is not exclusive, it only expresses its

cooperation with other behaviours. The activity of the complete network will concentrate in the region of one high level behaviour.

The state variables a and r are used to pass information about a behaviour to others. The target rating r hints on the behaviour's estimation of the situation whereas the activity a describes how much it is working on changing this situation thus influencing other behaviours decisions and actions.

The activity also acts as a mean for the fusion of the outputs of competing behaviours (see figure 1). Either only the output of the behaviour with the highest activity (winner takes it all) is used or the average of all outputs weighted by the activities is calculated.

3 The walking machine BISAM

BISAM (Biologically InSpired wAlking Machine), developed at the FZI, consists of one main body and four equal legs (figure 3). The main body is

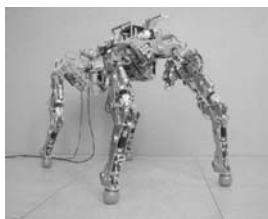


Fig. 3. The quadrupedal walking machine BISAM. Due to the five active degrees of freedom in the body and the ability to rotate the shoulder and hip, BISAM implements key elements of mammal-like locomotion.

composed of four segments being connected by five rotary joints. Each leg consists of four segments connected by three parallel rotary joints and attached to the body by a fourth. The joints are all driven by DC motors and ball screw gears. The height of the robot is 70 cm, its weight is about 23 kg. 21 joint angle encoders, four three dimensional foot sensors and two inclinometers mounted on the central body provide the necessary sensoric input. A more detailed description of the development and specification of BISAM can be found in [8,19]. Research on BISAM aims at the implementation of mammal-like movement and different gaits like statically stable walking and dynamic trotting with continuous gait transitions. Due to this target, BISAM is developed with joints in the shoulder and in the hip, a mammal-like leg-construction and small foot contact areas. These features have strong impact on the applicable methods for measuring stability and control. For example, caused by BISAM's small feet the ZMP-Criterion [32] is not fully adequate to describe the aspired movements.

The control design has to consider the high number of 21 active joints and especially the five joints in the body. One common way to reduce the model complexity is to combine joints and legs by the approach of the virtual leg, as used in many walking machines [31,23,35]. This approach poses problems when modelling BISAM's body joints and lead to a strong reduction in the flexibility of the walking behaviour [28]. A second way is to reduce the mechanical complexity of the robot so it is possible to create an exact mathematical model of the robot [10].

Taking the described problems into consideration BISAM was used as the first platform to implement the proposed behaviour based architecture ([3,2]). This first implementation has been expanded to a complete and consistent framework, which allows BISAM to automatically switch between standing, a free gait and a normal walking gait.

4 Implementing a behaviour network

Up to now we have implemented a behaviour network for BISAM which realises stable standing and a free gait. The sub-network controlling one leg is shown in figure 4. Note that the stance behaviour is inhibited by the swing behaviour via the activity to guarantee that stancing will stop as soon as the leg is cleared for swinging. The two "helper" behaviours, preparing a swing phase and keeping the ground contact, are the most reactive in this group and as such are placed at the bottom.

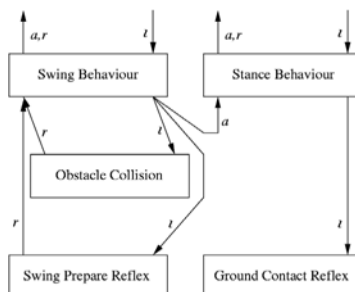


Fig. 4. Behaviour network for one leg

The overall network of BISAM is shown in figure 5. For clarity reasons the networks of the legs are only shown as blocks, since they operate independent from each other. Above them reside the posture behaviours as described in ([3]). The walking behaviours on the highest level only activate lower behaviours and don't generate direct control signals at all. The fusion knots between the walking and the posture behaviours guarantee that only the output of the active walking behaviour is used. The transition between standing and different gaits is done by the walking behaviours themselves.

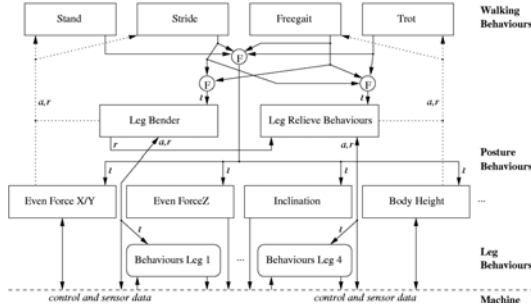


Fig. 5. Behaviour network of the complete robot

To demonstrate the activities and the coordination of the behaviours a simple step on even terrain as performed in free gait is described here. In figure 6 the swing phase of the leg is represented by its x-coordinate (uppermost plot) and several involved behaviours are visualized by their activation ι , activity a and target rating r (top-down). All behaviour plots scale from 0 to 1. Not all behaviours involved in actual walking are described here but are ignored for reasons of simplicity.

Between two swing cycles the free gait will try to stabilize the robot on four legs while adapting the posture to the terrain. The force distributing reflex (first behaviour in figure 6) represents the posture control being activated after the swing leg hits the ground (high ι). At once its activity increases, the posture of the robot is corrected, so the target rating decreases accordingly.

At the beginning of a new swing cycles the leg relieve behaviour is activated. It tries to remove most of the weight from the selected swing leg by shifting the robot's posture. The better the relieve situation of the swing leg is rated, the more the swing behaviour is activated. As soon as the swing behaviour decides to start swinging, its activity increases, the leg is lifted from the ground. Simultaneously the stance behaviour is inhibited which will no longer activate the ground contact reflex (bottom-most plot in figure 6). The target rating of the ground contact reflex will shoot up as soon as the leg leaves the ground, but the reflex cannot change the situation as it is not activated; its acitivity a remains Zero.

It is to be noted here that walking on unstructured terrain won't differ greatly from the situation above. The main differnece will be some more acitivity of the posture reflexes, the swing and stance mechanisms remain the same. Obstacles are hidden from them by the posture control and the collision reflex.

5 Conclusion and outlook

This paper introduced an hierarchical activation based behaviour architecture. Three dedicated signals, the activity a , the activation ι and the target

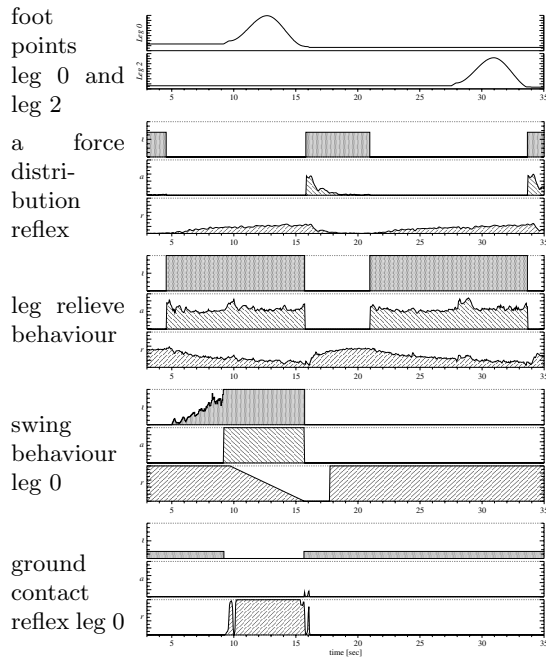


Fig. 6. Some of the behaviours involved while walking on even terrain in free gait

rating r are used to coordinate the interaction of behaviours within the network. Such a network for stable standing and a free gait was successfully implemented for a complex four-legged walking robot. Future work will mainly consist of the design and testing of different gait transition schemes and the integration of more sensors to allow anticipatory activation of the behaviours on BISAM. Furthermore there is ongoing work on using this architecture on other Robot's of FZI, namely the six-legged walking machines AirBug and Lauron III and the new four-legged Panter.

References

1. Albiez, J., Ilg, W., Luksch, T., Berns, K., and Dillmann, R. (2001). Learning reactive posture control on the four-legged walking machine bisam. In *International Conference on Intelligent Robots and Systems (IROS)*, Hawaii, USA.
2. Albiez, J., Luksch, T., Berns, K., and Dillmann, R. (2002a). An activation based behaviour control architecture for walking machines. In *Proceedings of the 7th International Conference on Simulation of Adaptive Behaviour SAB*, Edinburgh, UK.
3. Albiez, J., Luksch, T., Ilg, W., Berns, K., and Dillmann, R. (2002c). Reactive reflex based control for a four-legged walking machine. In *Proceedings of the 7th International Conference on Intelligent Autonomous Systems IAS*, Los Angeles, California, USA.

4. Arkin, R. (2000). *Behavior-Based Robotics*. MIT Press.
5. Arkin, R., Kahled, A., Weitzenfeld, A., and Cervantes-Prez, F. (2000). Behavioral models of the praying mantis as a basis for robotic behavior. *Journal of Autonomous Systems*.
6. Ayers, J., Witting, J., Olcott, C., McGruer, N., and Massa, D. (2000a). Lobster robots. In Wu, T. and Kato, N., (Eds.), *Proceedings of the International Symposium on Aqua Biomechanisms*.
7. Ayers, J., Witting, J., Wilbur, C., Zavracky, P., McGruer, N., and Massa, D. (2000b). Biomimetic robots for shallow water mine countermeasures. In *Proc. of the Autonomous Vehicles in Mine Countermeasures Symposium*.
8. Berns, K., Ilg, W., Deck, M., Albiez, J., and Dillmann, R. (1999). Mechanical construction and computer architecture of the four-legged walking machine BISAM. *IEEE Transactions on Mechatronics*, 4(1):1–7.
9. Brooks, R. (1986). A robust layered control system for a mobile robot. *IEEE Journal of Robotics and Automation*, RA-2(1):14–23.
10. Buehler, M., Cocosco, A., Yamazaki, K., and Battaglia, R. (1999). Stable open loop walking in quadruped robots with stick legs. In *Proceedings of the IEEE International Conference on Robotics and Automation*, pages 2348–2354, Detroit.
11. Cruse, H., Dürr, V., and Schmitz, J. (2001). Control of a hexapod walking - a decentralized solution based on biological data. In *Proc. of the 4th International Conference on Climbing and Walking Robots (CLAWAR)*, Karlsruhe, Germany.
12. Dürr, V. and Krause, A. (2001). The stick insect antenna as a biological paragon for an actively moved tactile probe for obstacle detection. In *Proc. of the 4th International Conference on Climbing and Walking Robots (CLAWAR)*.
13. Endo, Y. and Arkin, R. (2001). Implementing tolman's schematic sowbug: Behaviour-based robotics in the 1930's. In *Proceedings of the 2001 IEEE International Conference on Robotics and Autonomous Systems*.
14. Espenschied, K., Quinn, R., Chiel, H., and Beer, R. (1996). Biologically-based distributed control and local reflexes to improve rough terrain locomotion in a hexapod robot. *Robotics and Autonomous Systems*, 18:59–64.
15. Ferrell, C. (1995). Global behavior via cooperative local control. volume 2, pages 105 – 125.
16. Gienger, M., Löffler, K., and Pfeiffer, F. (2001). In *Proc. of the IEEE International Conference on Robotics and Automation (ICRA)*.
17. Hosoda, K., Miyashita, T., and Asada, M. (2000). Emergence of quadruped walk by a combination of reflexes. In *Proceedings of the International Symposium on adaptive Motion of Animals and Machines*, Montreal.
18. Ilg, W., Albiez, J., and Jedele, H. (1998a). A biologically inspired adaptive control architecture based on neural networks for a four-legged walking machine. In *Proceedings of the 8th International Conference on Artificial Neural Networks*, pages 455–460, Skoevde.
19. Ilg, W., Berns, K., Jedele, H., Albiez, J., Dillmann, R., Fischer, M., Witte, H., Biltzinger, J., Lehmann, R., and Schilling, N. (1998b). Bisam: From small mammals to a four legged walking machine. In *Proceedings of the Fifth International Conference on Simulation of Adaptive Behaviour*, pages 400–407, Zurich.
20. Kandel, E., Schwartz, J., and Jessell, T. M. (2000). *Principles of Neural Science*. McGraw-Hill, 4th ed. edition.

21. Kimura, H. and Fukuoka, Y. (2000). Biologically inspired dynamic walking on irregular terrain - adaptation at spinal cord and brain stem. In *International Symposium on Adaptive Motion of Animals and Machines*, Montreal.
22. Kimura, H., Fukuoka, Y., Hada, Y., and Takase, K. (2001). Three-dimensional adaptive dynamic walking of a quadruped robot by using neural system model. In *Proc. of the 4th International Conference on Climbing and Walking Robots (CLAWAR)*, Karlsruhe. FZI.
23. Kimura, H., Shimoyama, I., and Miura, H. (1990). Dynamics in the dynamic walk of a quadruped robot. *Advanced Robotics*, 4(3):283–301.
24. Löffler, K., Gienger, M., and Pfeiffer, F. (2001). Simulation and control of a biped jogging robot. In *Proceedings of the 4th International Conference on Climbing and Walking Robots (CLAWAR)*.
25. Likhachev, M. and Arkin, R. (2000). Robotic comfort zones. In *Proceedings of the SPIE: Sensor Fusion and Decentralized Control in Robotic Systems*, volume 4196, pages 27–41.
26. Likhachev, M. and Arkin, R. (2001). Spatio-temporal case-based reasoning for behavioral selection. In *Proceedings of the 2001 IEEE International Conference on Robotics and Automation (ICRA)*, pages 1627–1634.
27. Mataric, M. J. (1997). Behavior-based control: Examples from navigation, learning, and group behavior. *Journal of Experimental and Theoretical Artificial Intelligence*, Special issue on Software Architectures for Physical Agents, 9(2-3):323–336.
28. Matsumoto, O., Ilg, W., Berns, K., and Dillmann, R. (2000). Dynamical stable control of the four-legged walking machine bisam in trot motion using force sensors. In *Intelligent Autonomous Systems 6*.
29. Pearson, K. (1995). Proprioceptive regulation of locomotion. *Current Opinions in Neurobiology*, 5(6):768–791.
30. Pirajianian, P. (1999). Behaviour coordination mechanisms - state-of-the-art. Technical Report IRIS-99-375, Institute for Robotics and Intelligent Systems, School of Engineering, University of Southern California.
31. Raibert, M. H. (1986). *Legged Robots That Balance*. MIT Press, Cambridge, MA.
32. Vukobratovic, M., Borovac, B., Surla, D., and Stokic, D. (1990). *Biped Locomotion*. Springer-Verlag, Heidelberg, Berlin, New York.
33. Witte, H., Hackert, R., Fischer, M. S., Ilg, W., Albiez, J., Dillmann, R., and Seyfarth, A. (2001a). Design criteria for the leg of a walking machine derived by biological inspiration from quadruped mammals. In *Proc. of the 4th International Conference on Climbing and Walking Robots (CLAWAR)*, Karlsruhe, Germany.
34. Witte, H., Hackert, R., Lilje, K., Schilling, N., Voges, D., Klauer, G., Ilg, W., Albiez, J., Seyfarth, A., Germann, D., Hiller, M., Dillmann, R., and Fischer, M. (2001b). Transfer of biological principles into the construction of quadruped walking machines. In *Second International Workshop On Robot Motion And Control*, Bukowy Dworek, Poland.
35. Yoneda, K. and Hirose, S. (1992). Dynamic and Static Fusion Gait of a Quadruped Walking Vehicle on a Winding Path. In *Proceedings of the IEEE/RSJ International Conference on Intelligent Robots and Systems*, pages 143–148, Nizza.

Part 6

Adaptation at Higher Nervous Level

Control of Bipedal Walking in the Japanese Monkey, *M. fuscata*: Reactive and Anticipatory Control Mechanisms

Futoshi Mori¹, Katsumi Nakajima² and Shigemi Mori¹

¹ Department of Biological Control System, National Institute for Physiological Sciences, Okazaki, Aichi 444-8585, Japan

² Department of Physiology, Kinki University School of Medicine, Osaka-Sayama, Osaka 589-8511, Japan

Abstract. While the young Japanese monkey, *M. fuscata*, is growing, it can be trained operantly to maintain an upright posture and use bipedal (Bp) walking on a moving treadmill belt. For Bp locomotion, the animal generates sufficient propulsive force to smoothly and swiftly move the center of body mass (CoM) forward. The monkey can also adapt its gait to meet changing environmental demands. This appears to be accomplished by use of CNS strategies that include reactive and anticipatory control mechanisms. In this chapter, we provide evidence that the Bp walking monkey can select the most appropriate body-leg kinematic parameters to solve a variety of walking tasks. This recently developed non-human primate model has the potential to advance understanding of CNS operating principles that contribute to the elaboration and control of Bp walking in the human.

1 Introduction

Locomotion is a complex motor behavior that requires the integrated control of multiple, moving body segments including the head, neck, trunk, and limbs. Appropriate control of each body segment in space is necessary for the stable execution of both bipedal (Bp) and quadrupedal (Qp) locomotion, and for adapting posture and gait to a variety of external disturbances. For these needs, the CNS must integrate the control of (1) antigravity support, (2) stepping movements, (3) equilibrium, and (4) propulsive force generation [1, 2]. To advance understanding of such CNS control in the human, it was considered necessary to develop a Bp walking, non-human primate model. Its use should enable the multifaceted and interlocking study of behavioral, biomechanical, neuroanatomical, and neurophysiological mechanisms. To this end, we recently used operant conditioning to train the Japanese monkey, *M. fuscata*, to stand upright and use Bp walking on a moving treadmill belt [3-8]. In this chapter, we focus on how this model adapts its Bp walking pattern to accommodate changes in treadmill inclination (uphill, downhill), and other postural and gait perturbations. Relevant preceding human studies include those that have addressed changes in walking speed and/or slope [9-14], obstacles on a walking path [15-20], and stair ambulation [21, 22].

2 Reactive control of Bp locomotion on a slanted treadmill belt

Previous human studies have shown that gait adaptation on an inclined surface is achieved by changing the pattern of lower limb kinematics [10-12, 14]. Recently, it was also demonstrated that a trunk tilt is necessary in the healthy human subject to move the CoM ahead of the base of support, thereby assisting forward propulsion [13]. These postural adaptations were shown to be task-specific and made possible by recruiting reactive control mechanisms, which presumably involve use of neuronal circuitry in subcortical structures of the brain.

We have recently shown that in the face of changes in treadmill speed, our Bp walking *M. fuscata* model can automatically adapt its upright posture and lower limb kinematics, including body axis angle, stride length, and stepping frequency. This suggested that *M. fuscata* can select body-leg kinematic parameters most appropriate for the execution of a given walking task. These adaptations must involve use of reactive control mechanisms [23, 24]. To further study this capability, we examined the monkey's trunk and limb kinematics during Bp walking on a slanted treadmill surface. An additional focus was to compare the results to those obtained in previous work on the human.

2.1 Trunk adaptation to changes in treadmill inclination

In uphill walking, the limbs need to generate a larger acceleration force to transfer the CoM forward. Similarly, in downhill walking, the limbs generate a larger deceleration force to prevent excessive forward transfer of the CoM. Figure 1 shows representative Bp walking patterns of *M. fuscata* on an uphill (+15°, A), level (0°, B) and downhill (-15°, C) treadmill set at a fixed belt speed (1.3 m/s). Lines are drawn on the animal sketches in Figure 1 to depict relevant kinematic and joint angles: i.e., ear-hip angle and the angles at the hip, knee, and ankle joint. The line between ear and hip represents the body axis. The body axis angle is defined as the intercept of the body axis line and a reference line passing through the hip joint and vertical to the treadmill surface.

Figure 1A-C show the instantaneous postural shift when the monkey placed the foot of its left, forward limb on a moving treadmill belt: i.e., touchdown, the onset of the stance (ST) phase of the left limb. Subsequently, the monkey lifted the foot of the right, rearward limb up from the surface of the treadmill belt: i.e., take-off, the onset of the swing (SW) phase of the right limb. In uphill walking (Fig. 1A), the monkey inclined its body axis maximally during the ST phase of both limbs. The extent of forward body axis inclination was much larger than that observed during level walking. In downhill walking (Fig. 1C), the monkey also inclined its body axis maximally during the ST phase of both limbs. The extent of body axis inclination

was much smaller, however, than that observed during level walking. These results show that in order to appropriately propel the CoM forward, the monkey was able to reactively adapt its body axis angle to changes in treadmill inclination.

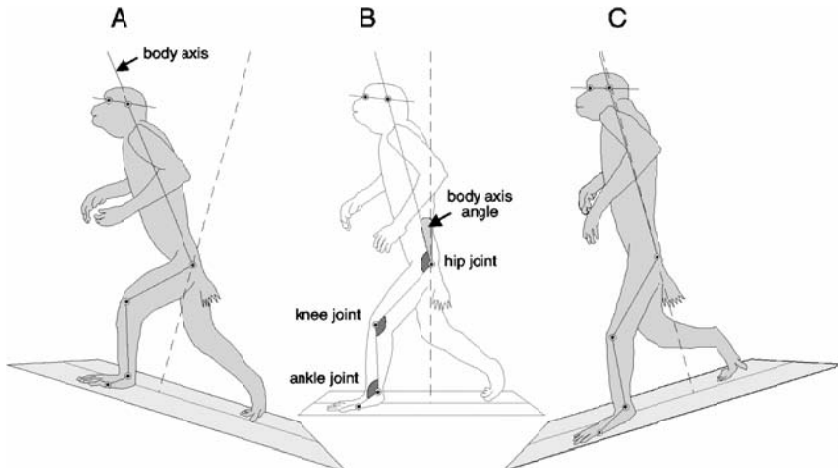


Fig. 1. Sketches of Bp walking monkey on the uphill (15° , A), level (0° , B) and downhill (-15° , C) treadmill belt at the same speed (1.3m/s). In Fig.1, Fig. 2 and 3, the treadmill belt moved from left to right, and the monkey walked from right to left. Dotted line in each sketch represents the reference vertical line to the treadmill belt (see the text). Body axis, body axis angle, lower limb joints (hip, knee and ankle) and each joint angles were defined as shown in sketches A and B. Note the body axis angle is much larger during uphill walking than during downhill walking. Modified from [7].

At a fixed treadmill speed (1.3m/s), we found that the body axis angle increased proportionately with an increase in treadmill grade (from -15° to 15°). An uphill increase from 0° to 7° to 15° resulted in an increase in the maximum body axis angle from 15° to 24° to 37° , respectively. Similarly, a downhill increase in treadmill grade from 0° to -7° to -15° resulted in a decrease in the maximum body axis angle from 15° to 8° to 2° , respectively. Such a relationship between changes in treadmill grade and body axis angle was nearly linear across all three of the tested treadmill speeds (0.7, 1.0 and 1.3m/s). On the treadmill belt at the same grade, the extent of body axis inclination became more pronounced as treadmill speed increased. All of the above changes have also been seen during human Bp walking [13].

2.2 Lower limb adaptation to changes in the treadmill inclination

Throughout a single uphill vs. level step cycle, the monkey exhibited a larger flexion of the hip joint, lesser extension of the knee joint, and larger ankle dorsi-flexion during the mid-SW and early-ST phase. Also, there was a larger knee joint extension in the late ST phase. Throughout a single downhill vs. level step cycle, the monkey exhibited a larger extension of the knee joint and a lesser flexion of the hip joint during the late SW and early ST phase. In addition, there was a lesser extension of the hip joint and larger flexion of the knee joint during the late ST and early SW phase.

During level treadmill walking at a fixed treadmill speed (0.7m/s), the duration of the ST and SW phase of the step was ~ 0.60 and ~ 0.25 s, respectively. Uphill and downhill walking at the same speed involved more prolonged and shortened ST-phase duration, respectively. This relationship was maintained across treadmill speeds of 1.0 and 1.3m/s. The duration of the SW phase of the step cycle, however, did not change significantly. We also found a linear relationship between treadmill grade and stride length: i.e., a progressively longer stride for an increase in treadmill grade from -15° to $+15^\circ$. There were clear associations between stride length, and treadmill grade and speed. During uphill walking, step-cycle frequency decreased as stride length and treadmill speed increased, with the reverse during downhill walking.

Presumably, the increase in body axis angle during uphill walking enables the limbs to generate greater momentum to propel the CoM forward and counteract the resistance due to gravity. It thus becomes necessary for the body axis to have a greater degree of forward inclination, especially at faster treadmill speeds. The need to generate this greater momentum is also accompanied by a progressive increase in stride length, as the treadmill slope becomes steeper. During downhill walking, the body is moved forward and downward by the mechanical effect of the slope. To counteract these external constraints, lower limb joints need to absorb more energy and decrease the forward momentum of the body [25]. This decrease is accompanied by a progressive decrease in stride length, as the treadmill inclination becomes steeper in downhill conditions. During downhill walking, a backward tilt of the body axis is needed to move the CoM relatively backward and upward, and thereby help decrease the forward and downward momentum caused by gravity.

Taken together, the above results suggest that the operant-trained Bp locomotion of *M. fuscata* is smooth and versatile during changes in treadmill inclination. By recruiting reactive control mechanisms and selecting appropriate kinematic parameters the animal is better able to couple movements of head, body, and lower limbs during walking on a slanted treadmill. Again, healthy human subjects make quite similar adjustments [10-13] to those described above for *M. fuscata*.

3 Reactive and anticipatory control of Bp locomotion on an obstacle-attached treadmill belt

In routine, daily locomotion, the feet often collide with unexpected obstacles, thereby requiring compensatory postural and gait adjustments to prevent stumbling and falling, and reestablish smooth and stable locomotion [5, 19]. Tripping and slipping perturbations commonly occur when the swing foot strikes a small object on the walking path. They are the major cause of falls during Bp walking in the elderly human [26]. Both occur primarily during the SW phase of the trailing limb, when the CoM is outside the base of supporting limb. The nature of postural and gait adjustments to unexpected perturbations have been studied experimentally in the human by having the subject walk on an obstacle-obstructed pathway [16-19], or a moving treadmill belt [15, 20]. Previous studies have already demonstrated that the Bp walking human recruits anticipatory control mechanisms to adjust posture and gait before encountering unexpected obstacles [24]. Anticipatory adjustments of posture and gait occur in a proactive way during all phases of the step cycle, with visuomotor coordination playing a crucial role [27-29]. We have therefore examined the extent to which *M. fuscata* can recruit anticipatory control mechanisms during its Bp walking on an obstacle-attached treadmill belt.

3.1 Reactive and compensatory adjustments during perturbed locomotion

Unexpected obstacles that impede the smooth trajectory of the swing foot during Bp walking activate a variety of sensory receptors, and perturb the stability of moving body segments. Visual, vestibular, proprioceptive and exteroceptive afferent inputs must be integrated to produce responses that ensure the removal of the limb from the obstacle, as well as the safe continuation of Bp walking. The relationship between the walking subject and the environment is mediated primarily through the visual system [29]. Other sensory modalities such as vestibular afferents also provide information about body orientation and equilibrium. Vestibular information is also used to maintain clear vision during movements of the head and keep the head stable in space [26]. Cutaneous and muscle afferents, which originate from both the trailing and leading limbs, contribute to the control of SW and ST phases of the limbs, and also to the transition from SW to ST and vice versa [30].

Figure 2 shows the monkey's adoption of a defensive posture, and some other compensatory processes, after slipping up an obstacle during the late SW phase. Stumbling occurred routinely when the trailing foot failed to clear the obstacle. This was presumably due to the absence of visual sampling of the up-coming obstacle. Such stumbling usually occurred when the toe of the trailing limb stepped on or slipped up the obstacle during its late SW phase. A late SW perturbation poses a greater threat for a fall, because the CoM is already well anterior to the supporting foot.

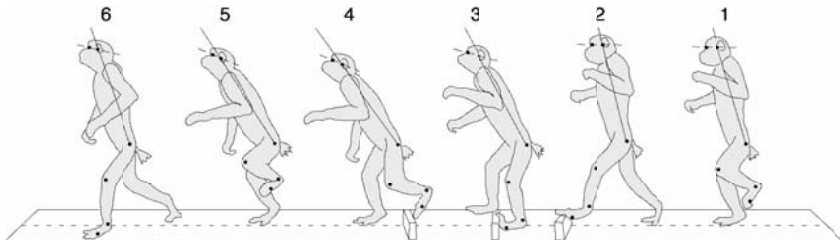


Fig. 2. Serial sketches of perturbed bipedally walking monkey. The monkey slipped on the obstacle at 2 and showed defensive posture during 3 and 5 with the correction of the perturbed posture.

Immediately after foot-obstacle contact (2 in Fig. 2), the monkey moved its body axis slightly backward. This was followed by a rapid and pronounced ($\sim 40^\circ$) forward movement of the body axis (4 in Fig. 2). Subsequently, the animal (1) shortened the SW period of the leading limb, (2) lowered the CoM to the treadmill belt, and (3) extended its left (and/or right) forelimb forward and/or downward, and (4) extended its lower limb joints to raise the lowered CoM upward. This serial postural compensation was usually accomplished within a few hundred milliseconds. The first three of these defensive compensatory reactions of multiple motor segments stabilized the perturbed posture. The last (fourth) one, an extension of the lower limb joints, especially the hip and knee joints, helped to restore the animal's head and body position to their pre-perturbed position in space. All four reactions made it possible for the animal to restore its posture and walk safely and smoothly without interruption. Presumably, such a serial recovering of normal posture and gait is based on the recruitment of reactive control mechanisms. Interestingly, correction of the head position always occurred first, followed by that of the body axis and finally the limbs. It seems likely that the restoration of head position in space is a critical determinant of the nature and extent of subsequent reactive responses.

3.2 Anticipatory avoidance strategy during obstacle-encountered locomotion

During Bp walking along an unperturbed straight path, finely controlled locomotor mechanisms, such as visuo-motor coordination, may not be necessary. Once the walking circumstances are dramatically changed, however, there is need in the CNS to make use of both external and internal sensory information. These include visual, vestibular, proprioceptive, and exteroceptive inputs (indeed, as many as are available), which help prepare the posture for the impending perturbations. It has been well demonstrated that visual and vestibular information interacts with that from other sensory systems to maintain postural stability over a wide range of environmental condition [26].

The most powerful means of ensuring such stability is to proactively avoid the perturbation by the recruitment of anticipatory control mechanisms.

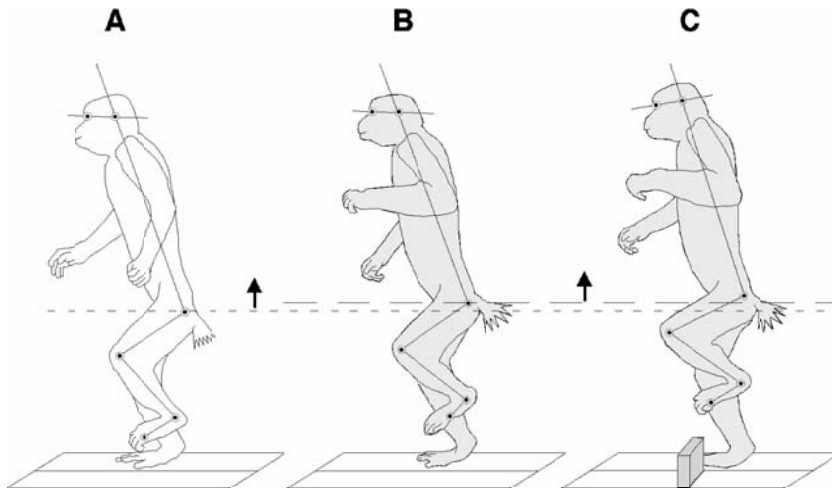


Fig. 3. Sketches of Bp walking monkey's instantaneous posture. A; control (no obstacle) level walking, B; obstacle is 3-4 steps ahead of walking monkey and out-of-site, C; successful clearance of the obstacle. Treadmill speed is 1.0 m/s. Modified from [7]. Arrows indicate the elevating hip position by “biasing strategy” (see the text).

Figure 3 shows the instantaneous upright posture of a Bp walking monkey during control (no obstacle) level walking (A) vs. when the obstacle is 2-3 steps ahead (B) vs. out-of-site (C). The task was to clear a 7-cm high rectangular obstacle, which was attached to the left walking path on the moving treadmill. In the control walking condition, the CoM was supported by the right limb alone. This involved moderate flexion of the left limb at the hip and knee joints (Fig. 3A). During walking on the obstacle-attached treadmill belt, the monkey flexed the hip and knee joints of the trailing limb to greater extent than in the control condition (Fig 3B). This was done even when the obstacle was out of sight. This finding shows that the monkey adopted a preparatory posture, thereby anticipating the up-coming obstacle (anticipatory control). For this, the monkey presumably using the learned memory of both how to clear the obstacle and the consequence of failing to do so.

We have also found that the number of stumbles in a single trial of the obstacle-clearance walking task, which consisted of ~100 successive step cycles, decreased after several trials. Apparently, the monkey perceived the up-coming obstacles by their visual sampling, and gradually learned how to clear them, using what in humans has been termed a “hip-knee flexion strategy”

[17]. This strategy involved the monkey simultaneously increasing the extent of flexion of the left trailing hip and knee joints. This enabled the animal to have enough clearance space over the obstacle, and it allowed use of the leading right limb alone for supporting the CoM and maintaining equilibrium (Fig. 3C). Our kinematic analyses of the hip and knee joints of the trailing limb revealed that they used larger flexions for obstacles of higher height. This result demonstrated that the monkey was able to use visual information about obstacle height to help select the most appropriate hip-knee flexion strategy to clear the obstacle.

Patla and Rietdyk have proposed that the human uses two different strategies to clear obstacles on a walking path [18]. The first involves an exaggerated “flexing” of the swing limb to increase ground clearance (flexion strategy). They termed the second one “biasing” for an exaggerated upward motion of the swing phase trajectory (elevating strategy). The upward bias in the swing limb trajectory is reflected in the vertical position of the hip. If it is higher there is a bias, whereas if only limb flexion is used to produce a higher limb elevation, the hip’s vertical position remains as during normal unperturbed locomotion. To lift the trailing foot higher, *M. fuscata* recruited not only the human’s hip-knee flexion strategy, but also the elevating strategy (Fig. 3C). The monkey also adapted its foot trajectory in relation to obstacle height: i.e., the hip was elevated higher as a function of obstacle height and a greater parabolic foot trajectory was used. Such findings also indicate the pronounced similarity between the locomotion strategies of the monkey vs. human.

3.3 Anticipatory control based visuo-motor coordination

Figure 3C shows an example of a successful obstacle clearance. During this clearance, hip-knee flexion was further enhanced by additional dorsi-flexion of the ankle joint (i.e., Fig. 3B vs. C). The monkey changed its foot trajectory from that used during control Bp walking. It was easier for the monkey to clear the obstacle when it was met during the early to mid-SW phase of the trailing limb. Probably, this was because it allowed sufficient time to calculate the new parabolic trajectory of the foot, which was required for clearance of the upcoming obstacle. Presumably, this was more challenging during the late SW phase of trailing left limb, when the swinging left foot began to approach the top surface of the obstacle. At this moment, the monkey needed an extra effort to lift the foot upward and over the obstacle. With repeated practice of this obstacle clearance task, however, the monkey became to modulate the foot trajectory even during the late SW phase.

When the monkey cleared the obstacle during the mid-swing phase of the trailing limb, the trajectory of the foot was nearly parabolic. When the obstacle was cleared during the late SW-phase, however, the foot trajectory took on a double parabolic shape, with a second trajectory initiated in the middle of the first one. Possibly, this new foot trajectory was achieved by the

recruitment of a visuo-motor coordination based on an anticipatory control mechanism. This proposition is supported by the fact that when the monkey could not sample sufficient visual information, it could not change its foot trajectory. Rather, it always stumbled over the obstacle even when using a preparatory locomotor posture. Sampled visual information apparently helped scaling of the toe clearance as a function of obstacle size, thereby providing a large safety margin as is also observed in the human [18].

4 Summary

Our analysis of the Bp walking of *M. fuscata* demonstrates quite clearly that this non-human primate model and the human make use of similar body-limb kinematics for the integration of posture and locomotion under a variety of circumstances.

When the monkey walked on a slanted treadmill belt, it utilized optimal kinematic parameters for coordination of multiple motor segments. When it encountered an obstacle, it changed its foot trajectory to advance (anticipatory control) and produce a larger-than-usual clearance space above the obstacle. Moreover, when the monkey stumbled over the obstacle, it quickly recovered from its perturbed posture, and continued smooth Bp locomotion. All of these findings suggest that the CNS of the Bp walking monkey received and transformed in an integrative manner salient visual, vestibular, proprioceptive, and exteroceptive sensory information. The result was an output of command motor signals, which were appropriate for the task at hand. This accommodation appeared to make use of reactive and anticipatory control mechanisms. These allowed the monkey to continuously adjust its ongoing locomotor patterns and accompanying postures.

At the present stage of our kinematic studies, a number of questions relevant to the underlying CNS mechanisms remain unanswered. We do not know how reactive and anticipatory control mechanisms interact to produce command signals to the motoneurons that innervate multiple motor segments. Nor do we know the subcortical and cortical neural networks that provide reactive and anticipatory control of posture and locomotion. Nonetheless, it is clear that our *M. fuscata* model has much potential for the further study of brain mechanisms that integrate posture and locomotion under normal, environmentally perturbed and pathological states.

References

1. Martin, J. P., 1967. The Basal Ganglia and Posture, Pitman Medical Publishing, London.
2. Mori, S., 1997. Neurophysiology of locomotion: Recent advances in the study of locomotion. In: Gait Disorders of Aging (J. C. Masdeu, L. Sundarsky, L. Wolfson, eds), Lippincott-Raven, Philadelphia, pp. 55-78.

3. Mori, F., Nakajima, K., Gantchev, N., Matsuyama, K., and Mori, S., 1999. A new model for the study of the neurobiology of bipedal locomotion: The Japanese monkey, *M. fuscata*. In: From basic motor control to functional recovery (N. Gantchev and G. N. Gantchev, eds), Academic Publishing House, Sofia, pp. 47-51.
4. Nakajima, K., Mori, F., Takasu, C., Tachibana, A., Okumura, T., Mori, M., and Mori, S., 2001. Integration of upright posture and bipedal locomotion in non-human primates. In: Sensorimotor Control (R. Dengler and A. R. Kossev, eds), IOS Press, Amsterdam, pp. 95-102.
5. Mori, F., Tachibana, A., Takasu, C., Nakajima, K., and Mori, S., 2001. Bipedal locomotion by the normally quadrupedal Japanese monkey, *M. fuscata*: Strategies for obstacle clearance and recovery from stumbling, *Acta Physiol. Pharmacol. Bulg.* 26: 147-150.
6. Nakajima, K., Mori, F., Takasu, C., Mori, M., Matsuyama, K., and Mori, S., 2003. Biomechanical constraints in hindlimb joints during the quadrupedal vs. bipedal locomotion of *M. fuscata*. In: Brain Mechanisms for the integration of Posture and Movement (S. Mori, M. Wiesendanger, and D. G. Stuart, eds), Elsevier, Amsterdam, pp. 183-190.
7. Mori, F., Nakajima, K., Tachibana, A., Takasu, C., Mori, M., Tsujimoto, T., Tsukada, H., and Mori, S., 2003. Reactive and anticipatory control of posture and bipedal locomotion in a non-human primate. In: Brain Mechanisms for the integration of Posture and Movement (S. Mori, M. Wiesendanger, and D. G. Stuart, eds), Elsevier, Amsterdam, pp. 191-198.
8. Tachibana, A., Mori, F., Boliek, C. A., Nakajima, K., Takasu, C., and Mori, S., 2003. Acquisition of operant-trained locomotion in juvenile Japanese monkeys (*Macaca fuscata*): a longitudinal study. *Motor Control* 7: 395-420.
9. Murray, M. P., Kory, R. C., Clarkson, B. H., and Sepic, S. B., 1966. Comparison of free and fast speed walking patterns of normal men. *Am. J. Phys. Med.* 45: 8-24.
10. Wall, J. Z. C., Nottrodt, J. W., Charteris, J., 1981. The effect of uphill and downhill walking on pelvic oscillations in the transverse plane. *Ergonomics* 24: 807-816.
11. Kawamura, K., Tokuhiro, A., Takachi, H., 1991. Gait analysis of slope walking: a study on step length, stride width, time factors and deviation in the center of pressure. *Acta Med. Okayama* 45: 179-184.
12. Vogt, L., and Banzer, W., 1999. Measurement of lumbar spine kinematics in incline treadmill walking. *Gait Posture* 9: 18-23.
13. Leroux, A., Fung, J., and Barbeau, H., 2002. Postural adaptation to walking on inclined surfaces: I. Normal strategies. *Gait Posture* 15: 64-74.
14. Cromwell, R. L., 2003. Movement strategies for head stabilization during incline walking. *Gait Posture* 17: 246-253.
15. Dietz, V., Quaterni, J. Q., and Sillem, M., 1987. Stumbling reactions in man: significance of proprioceptive and pre-programmed mechanisms. *J. Physiol.* 386: 149-163.
16. Patla, A., Beuter, A., and Prentice, S., 1991. A two stage correction of limb trajectory to avoid obstacles during stepping. *Neurosci. Res. Commun.* 8: 153-159.
17. McFadyen, B. J., and Winter, D. A., 1997. Anticipatory locomotor adjustments during obstructed human walking. *Neurosci. Res. Commun.* 9: 37-44.

18. Patla, A. E., and Rietdyk, S., 1993. Visual control of limb trajectory over obstacles during locomotion: effect of obstacle height and width. *Gait Posture* 1: 45-60.
19. Eng, J. J., Winter, D. A., and Patla, A. E., 1994. Strategies for recovery from a trip in early and late swing during human walking, *Exp. Brain Res.* 102: 339-349.
20. Schillings, A. M., Van Wezel, B. M. H., and Duysens, J., 1996. Mechanically induced stumbling during human treadmill walking, *J. Neurosci. Methods* 67: 11-17.
21. Heller, M. O., Bergmann, G., Deuretzbacher, G., Dürselen, L., Pohl, M., Claes, L., Haas, N. P., and Duda, G. N. 2001. Musculo-skeletal loading conditions at the hip during walking and stair climbing. *J. Biomechanics* 34: 883-893.
22. Riener, R., Rabuffetti, M., and Frigo, C., 2002. Stair ascent and descent at different inclinations. *Gait Posture* 15: 32-44.
23. Mori, S., 1987. Integration of posture and locomotion in acute decerebrate cats and in awake, freely moving cat. *Prog. Neurobiol.* 28: 161-195.
24. McFadyen, B. J., and Bélanger, M., 1997. Neuromechanical concepts for the assessment of the control of human gait. In: *Three-dimensional analysis of bipedal locomotion* (P. Allard, A. Cappozzo, A. Lundberg and C. L. Vaughan, eds), John Wiley & Sons, Chichester, pp. 49-66.
25. Redfern, M. S., and DiPasquale, J., 1997. Biomechanics of descending ramps. *Gait Posture* 6: 119-125.
26. Horak, F.B., Mirka, A., and Shupert, C.L. 1989. The role of peripheral vestibular disorders in postural dyscontrol in the elderly. In: *The Development of Posture and Gait Across the Lifespan* (M. Woolacott, and A. Shumway-Cook, eds), Univ. of South Carolina Press, Columbia, pp. 253-279.
27. Georgopoulos, A. P., and Grillner, S., 1986. Visuomotor coordination in reaching and locomotion. *Science* 245: 1209-1210.
28. Drew, T., 1991. Visuomotor coordination in locomotion. *Curr. Opin. Neurobiol.* 1: 652-657.
29. Patla, A.E. Visual control of human locomotion. 1991. In: *Adaptability of Human Gait* (A.E. Patla, ed) Elsevier Science Publishers B.V. North-Holland,
30. Zehr, E.P., and Stein, R.B. 1999. What functions do reflexes serve during human locomotion? *Prog. Neurobiol.* 58: 185-205.

Dynamic Movement Primitives –A Framework for Motor Control in Humans and Humanoid Robotics

Stefan Schaal^{1,2}

¹ Computer Science and Neuroscience, University of Southern California, Los Angeles, CA 90089-2520, USA

² ATR Human Information Science Laboratory, 2-2 Hikaridai, Seika-cho, Soraku-gun, 619-02 Kyoto, Japan

Abstract. Given the continuous stream of movements that biological systems exhibit in their daily activities, an account for such versatility and creativity has to assume that movement sequences consist of segments, executed either in sequence or with partial or complete overlap. Therefore, a fundamental question that has pervaded research in motor control both in artificial and biological systems revolves around identifying movement primitives (a.k.a. units of actions, basis behaviors, motor schemas, etc.). What are the fundamental building blocks that are strung together, adapted to, and created for ever new behaviors? This paper summarizes results that led to the hypothesis of Dynamic Movement Primitives (DMP). DMPs are units of action that are formalized as stable nonlinear attractor systems. They are useful for autonomous robotics as they are highly flexible in creating complex rhythmic (e.g., locomotion) and discrete (e.g., a tennis swing) behaviors that can quickly be adapted to the inevitable perturbations of a dynamically changing, stochastic environment. Moreover, DMPs provide a formal framework that also lends itself to investigations in computational neuroscience. A recent finding that allows creating DMPs with the help of well-understood statistical learning methods has elevated DMPs from a more heuristic to a principled modeling approach. Theoretical insights, evaluations on a humanoid robot, and behavioral and brain imaging data will serve to outline the framework of DMPs for a general approach to motor control in robotics and biology.

1 Introduction

When searching for a general framework of how to formalize the learning of coordinated movement, some of the ideas developed in the middle of the 20th century still remain useful. At this time, theories from optimization theory, in particular in the context of dynamic programming [1, 2], described the goal of learning control in learning a policy. A policy is formalized as a function that maps the continuous state vector \mathbf{x} of a control system and its environment, possibly in a time dependent way, to a continuous control vector \mathbf{u} :

$$\mathbf{u} = \pi(\mathbf{x}, \alpha, t) \quad (1)$$

The parameter vector α denotes the problem specific adjustable parameters in the policy π —not unlike the parameters in neural network learning. At the first glance, one might suspect that not much was gained by this overly general formulation. However, given some cost criterion that can evaluate the quality of an action \mathbf{u} in a particular state \mathbf{x} , dynamic programming, and especially its modern relative, reinforcement learning, provide a well founded set of algorithms of how to compute the policy π for complex nonlinear control problems. Unfortunately, as already noted in Bellman’s original work, learning of π becomes computationally intractable for even moderately high dimensional state-action spaces. Although recent developments in reinforcement learning increased the range of complexity that can be dealt with [e.g. 3, 4, 5], it still seems that there is a long way to go to apply general policy learning to complex control problems.

In most robotics applications, the full complexity of learning a control policy is strongly reduced by providing prior information about the policy. The most common priors are in terms of a desired trajectory, \mathbf{x}_d , usually hand-crafted by the insights of a human expert. For instance, by using a PD controller, a (explicitly time dependent) control policy can be written as:

$$\begin{aligned}\mathbf{u} &= \pi(\mathbf{x}, \alpha(t), t) = \pi(\mathbf{x}, [\mathbf{x}_d(t), \dot{\mathbf{x}}_d(t)], t) \\ &= \mathbf{K}_x(\mathbf{x}_d(t) - \mathbf{x}) + \mathbf{K}_{\dot{x}}(\dot{\mathbf{x}}_d(t) - \dot{\mathbf{x}})\end{aligned}\quad (2)$$

For problems in which the desired trajectory is easily generated and in which the environment is static or fully predictable, as in many industrial applications, such a shortcut through the problem of policy generation is highly successful. However, since policies like in are usually valid only in a local vicinity of the time course of the desired trajectory, they are not very flexible. When dealing with a dynamically changing environment in which substantial and reactive modifications of control commands are required, one needs to modify trajectories appropriately, or even generate entirely new trajectories by generalizing from previously learned knowledge. In certain cases, it is possible to apply scaling laws in time and space to desired trajectories [6, 7], but those can provide only limited flexibility, as similarly recognized in related theories in psychology [8]. Thus, for general-purpose reactive movement, the “desired trajectory” approach seems to be too restricted.

From the viewpoint of statistical learning, Equation constitutes a nonlinear function approximation problem. A typical approach to learning complex nonlinear functions is to compose them out of basis functions of reduced complexity. The same line of thinking generalizes to learning policies: a complicated policy could be learned from the combination of simpler (ideally globally valid) policies, i.e., policy primitives or movement primitives, as for instance:

Indeed, related ideas have been suggested in various fields of research, for instance in computational neuroscience as Schema Theory [9] and in mobile robotics as behavior-based or reactive robotics [10]. In particular, the latter

approach also emphasized to remove the explicit time dependency of ?, such that complicated “clocking” and “reset clock” mechanisms could be avoided, and the combination of policy primitives becomes simplified. Despite the successful application of policy primitives in the mobile robotics domain, so far, it remains a topic of ongoing research [11, 12] how to generate and combine primitives in a principled and autonomous way, and how such an approach generalizes to complex movement systems, like human arms and legs.

Thus, a key research topic, both in biological and artificial motor control, revolves around the question of movement primitives: what is a good set of primitives, how can they be formalized, how can they interact with perceptual input, how can they be adjusted autonomously, how can they be combined task specifically, and what is the origin of primitives? In order to address the first four of these questions, we suggest to resort to some of the most basic ideas of dynamic systems theory. The two most elementary behaviors of a nonlinear dynamic system are point attractive and limit cycle behaviors, paralleled by discrete and rhythmic movement in motor control. Would it be possible to generate complex movement just out of these two basic elements? The idea of using dynamic systems for movement generation is not new: motor pattern generators in neurobiology [13, 14], pattern generators for locomotion [15, 16], potential field approaches for planning [e.g., 17], and more recently basis field approaches for limb movement [18] have been published. Additionally, work in the dynamic systems approach in psychology [19-23] has emphasized the usefulness of autonomous nonlinear differential equations to describe movement behavior. However, rarely have these ideas addressed both rhythmic and discrete movement in one framework, task specific planning that can exploit both intrinsic (e.g., joint) coordinates and extrinsic (e.g., Cartesian) coordinate frames, and more general purpose behavior, in particular for multi-joint arm movements. It is in these domains, that the present study offers a novel framework of how movement primitives can be formalized and used, both in the context of biological research and humanoid robotics.

2 Dynamic movement primitives

Using nonlinear dynamic systems as policy primitives is the most closely related to the original idea of motor pattern generators (MPG) in neurobiology. MPG are largely thought to be hardwired with only moderately modifiable properties. In order to allow for the large flexibility of human limb control, the MPG concept needs to be augmented by a component that can be adjusted task specifically, thus leading to what we call a *Dynamic Movement Primitive* (DMP). We assume that the attractor landscape of a DMP represents the desired kinematic state of a limb, e.g., positions, velocities, and accelerations. This approach deviates from MPG which are usually assumed to code motor

commands, and is strongly related to the idea developed in the context of “mirror laws” by Bühler, Rizzi, and Koditschek [24, 25]. As shown in Figure 1, kinematic variables are converted to motor commands through an inverse dynamics model and stabilized by low gain feedback control. The motivation for this approach is largely inspired by data from neurobiology that demonstrated strong evidence for the representation of kinematic trajectory plans in parietal cortex [26] and inverse dynamics models in the cerebellum [27, 28]. Kinematic trajectory plans are equally backed up by the discovery of the principle of motor equivalence in psychology [e.g., 29], demonstrating that different limbs (e.g., fingers, arms, legs) can produce cinematically similar patterns despite having very different dynamical properties; these findings are hard to reconcile with planning directly in motor commands. Kinematic trajectory plans, of course, are also well known in robotics from computed torque and inverse dynamics control schemes [30]. From the view point of movement primitives, kinematic representations are more advantageous than direct motor command coding since this allows for workspace independent planning, and, importantly, for the possibility to superimpose DMP. However, it should be noted that a kinematic representation of movement primitives is not necessarily independent of dynamic properties of the limb. Proprioceptive feedback can be used to modify the attractor landscape of a DMP in the same way as perceptual information [25, 31, 32].

$$\mathbf{u} = \pi(\mathbf{x}, \alpha, t) = \sum_{k=1}^K \pi_k(\mathbf{x}, \alpha_k, t) \quad (3)$$

2.1 Formalization of DMPs

In order to accommodate discrete and rhythmic movements, two kinds of DMPs are needed, a point attractive system and a limit system. Although it is possible to construct nonlinear differential equations that could realize both these behaviors in one set of equations [e.g., 33], for reasons of robustness, simplicity, functionality, and biological realism (see below), we chose an approach that separates these two regimes. Every degree-of-freedom (DOF) of a limb is described by two variables, a rest position and a superimposed oscillatory position, , as shown in Figure 1. By moving the rest position, discrete motion is generated. The change of rest position can be anchored in joint space or, by means of inverse kinematics transformations, in external space. In contrast, the rhythmic movement is produced in joint space, relative to the rest position. This dual strategy permits to exploit two different coordinate systems: joint space, which is the most efficient for rhythmic movement, and external (e.g., Cartesian) space, which is needed to reference a task to the external world. For example, it is now possible to bounce a ball on a racket by producing an oscillatory up-and-down movement in joint space, but using the discrete system to make sure the oscillatory movement remains under the

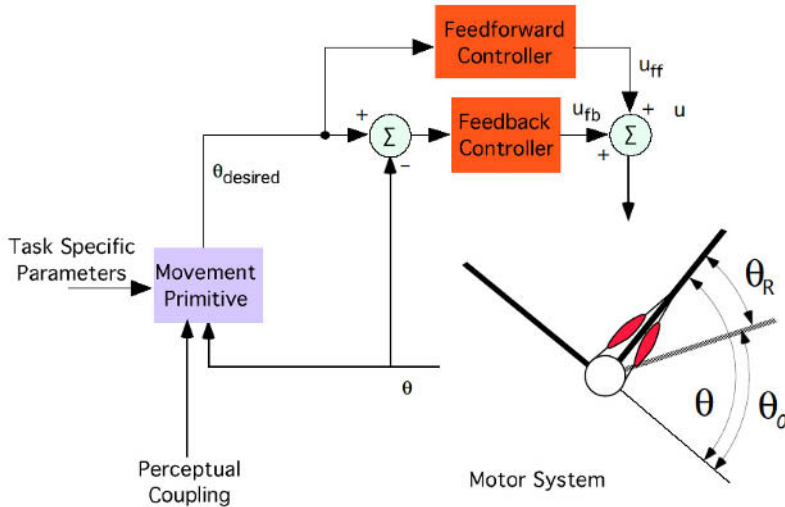


Fig. 1. Sketch of control diagram with dynamic movement primitives. Each degree-of-freedom of a limb has a rest state and an oscillatory state .

ball such that the task can be accomplished—this task actually motivated our current research [34].

The key question of DMPs is how to formalize nonlinear dynamic equations such that they can be flexibly adjusted to represent arbitrarily complex motor behaviors without the need for manual parameter tuning and the danger of instability of the equations. We will develop our approach in the example of a discrete dynamic system for reaching movements. Assume we have a basic point attractive system, for instance, instantiated by the second order dynamics

$$\mathbf{u} = \pi(\mathbf{x}, \alpha, t) = \sum_{k=1}^K \pi_k(\mathbf{x}, \alpha_k, t) \quad (4)$$

where g is a known goal state, α_z and β_z are time constants, τ is a temporal scaling factor (see below) and y ,

correspond to the desired position and velocity generated by the equations, interpreted as a movement plan. For appropriate parameter settings and $f=0$, these equations form a globally stable linear dynamical system with g as a unique point attractor. Could we find a nonlinear function f in Equation to change the rather trivial exponential convergence of y to allow more complex trajectories on the way to the goal? As such a change of Equation enters the domain of nonlinear dynamics, an arbitrary complexity of the resulting equations can be expected. To the best of our knowledge,

this has prevented research from employing generic learning in nonlinear dynamical systems so far. However, the introduction of an additional canonical dynamical system (x, v)

$$\mathbf{u} = \pi(\mathbf{x}, \alpha, t) = \sum_{k=1}^K \pi_k(\mathbf{x}, \alpha_k, t)$$

and the nonlinear function f

$$\mathbf{u} = \pi(\mathbf{x}, \alpha, t) = \sum_{k=1}^K \pi_k(\mathbf{x}, \alpha_k, t)$$

can alleviate this problem. Equation is a second order dynamical system similar to Equation , however, it is linear and not modulated by a nonlinear function, and, thus, its monotonic global convergence to g can be guaranteed with a proper choice of α_v and β_v , e.g., such that Equation is critically damped. Assuming that all initial conditions of the state variables x, v, y, z are initially zero, the quotient $x/g \in [0, 1]$ can serve as a phase variable to anchor the Gaussian basis functions ψ_i (characterized by a center c_i and bandwidth h_i), and v can act as a “gating term” in the nonlinear function such that the influence of this function vanishes at the end of the movement. Assuming boundedness of the weights w_i in Equation , it can be shown that the combined system in Equations , asymptotically converges to the unique point attractor g .

Given that f is a normalized basis function representation with linear parameterization, it is obvious that this choice of a nonlinearity allows applying a variety of learning algorithms to find the w_i . For instance, if a sample trajectory is given in terms as $y_{demo}(t)$, $\dot{y}_{demo}(t)$ and a duration T , e.g., as typical in imitation learning [35], a supervised learning problem can be formulated with the target trajectory $f_{target} = \tau \dot{y}_{demo} - z_{demo}$ for the right part of Equation , where z_{demo} is obtained by integrating the left part of Equation with y_{demo} instead of y . The corresponding goal is $g = y_{demo}(t = T) - y_{demo}(t = 0)$, i.e., the sample trajectory was translated to start at $y=0$. In order to make the nominal (i.e., assuming $f=0$) dynamics of Equations and span the duration T of the sample trajectory, the temporal scaling factor τ is adjusted such that the nominal dynamics achieves 95% convergence at $t = T$. For solving the function approximation problem, we chose a nonparametric regression technique from locally weighted learning (RFWR) [36] as it allows us to determine the necessary number of basis functions N , their centers c_i , and bandwidth h_i automatically—in essence, for every basis function ψ_i , RFWR performs a locally weighted regression of the training data to obtain an approximation of the tangent of the function to be approximated within the scope of the kernel, and a prediction for a query point is achieved by a ψ_i -weighted average of the predictions of all local models. Moreover, the parameters w_i learned by RFWR are also independent of the number of basis functions, such that they can be used robustly for categorization of different learned DMPs.

In summary, by anchoring a linear learning system with nonlinear basis functions in the *phase space* of a *canonical dynamical system with guaranteed attractor properties*, we are able to learn complex attractor landscapes of nonlinear differential equations without losing the asymptotic convergence to the goal state. Ijspeert et al [37] demonstrate how the same strategy as described for a point attractive system above can also be applied to limit cycle oscillators, thus creating oscillator systems with almost arbitrarily complex limit cycles. It is also straightforward to augment the suggested approach of DMPs to multiple DOFs: there is only one canonical system (cf. Equation), but for each DOF a separate function f is learned. Even highly complex phase relationships between different DOFs, as for instance needed for locomotion, are easily and stably realizable in this approach.

2.2 Application to humanoid robotics

We implemented our DMP system on a 30 DOF Sarcos Humanoid robot. Desired position, velocity, and acceleration information was derived from the states of the DMPs to realize a compute-torque controller. All necessary computations run in real-time at 420Hz on a multiple processor VME bus operated by VxWorks. We realized arbitrary rhythmic “3-D drawing” patterns, sequencing of point-to-point movements and rhythmic patterns like ball bouncing with a racket. Figure 2a shows our humanoid robot in a drumming task. The robot used both arms to generate a regular rhythm on a drum and a cymbal. The arms moved in 180-degree phase difference, primarily using the elbow and wrist joints, although even the entire body was driven with oscillators for reasons of natural appearance. The left arm hit the cymbal on beat 3, 5, and 7 based on an 8-beat pattern. The velocity zero crossings of the left drum stick at the moment of impact triggered the discrete movement to the cymbal. Figure 2b shows a trajectory piece of the left and the right elbow joint angles to illustrate the drumming pattern. Given the independence of a discrete and rhythmic movement primitives, it is very easy to create the demonstrated bimanual coordination without any problems to maintain a steady drumming rhythm.

Another example of applying the DMP is in the area of imitation learning, as outlined in the previous section. Figure 3 illustrates the teaching of a tennis forehand to our humanoid, using an exoskeleton to obtain joint angle data from the human demonstration. The learned multi-joint DMP can be re-used for different targets and at different speeds due to the flexible appearance of the goal parameter g and time scaling τ —in the example in Figure 3, the Cartesian ball position is first converted to a joint angle target by inverse kinematics algorithms, and subsequently each DOF of the robot receives a separate joint space goal state for its DMP component.

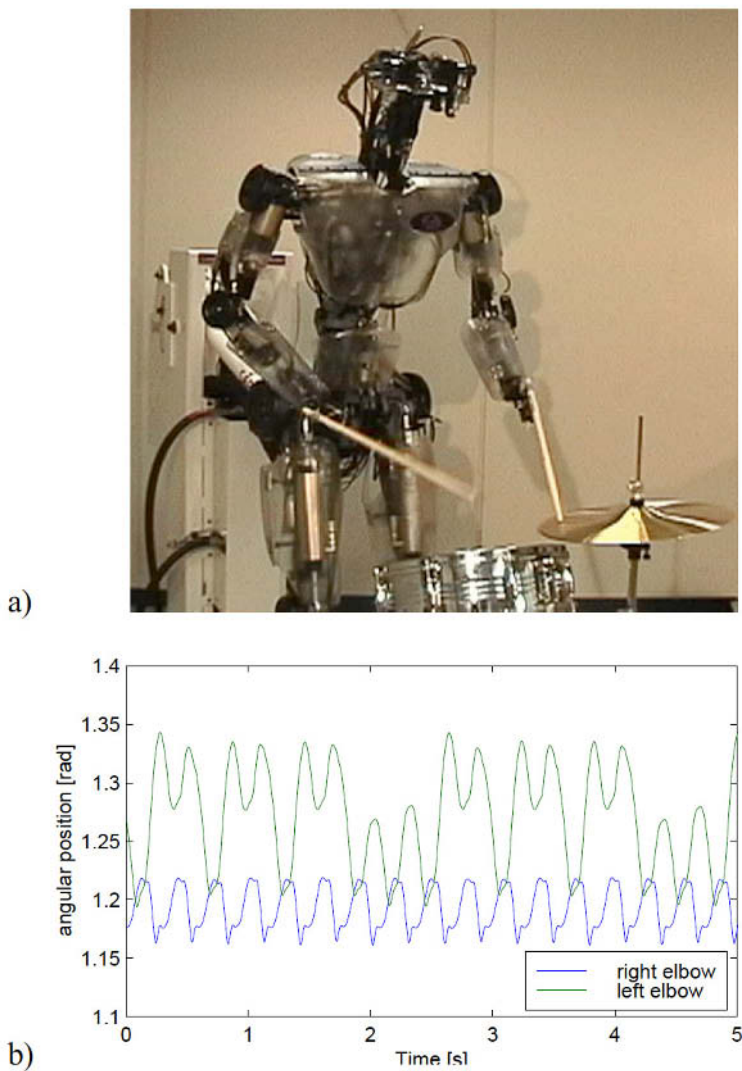


Fig. 2. a) Humanoid robot in drumming task, b) coordination of left and right elbow, demonstrating the superposition of discrete and rhythmic DMPs.

3 Parallels in biological research

Our ideas on dynamic movement primitives for motor control are based on biological inspiration and complex system theory, but do they carry over to biology? Over the last years, we explored various experimental setups that could actually demonstrate that dynamic movement primitives as outlined above are indeed an interesting modeling approach to account for various phenomena in behavioral and even brain imaging experiments. The remainder of this paper will outline some of the results that we obtained.

3.1 Dynamic manipulation tasks

From the viewpoint of motor psychophysics, the task of bouncing a ball on a racket constitutes an interesting testbed to study trajectory planning and visuomotor coordination in humans. The bouncing ball has a strong stochastic component in its behavior and requires a continuous change of motor planning in response to the partially unpredictable behavior of the ball.

In previous work [34], we examined which principles were employed by human subjects to accomplish stable ball bouncing. Three alternative movement strategies were postulated. First, the point of impact could be planned with the goal of intersecting the ball with a well-chosen movement velocity such as to restore the correct amount of energy to accomplish a steady bouncing height [38]; such a strategy is characterized by a constant velocity of the racket movement in the vicinity of the point of racket-ball impact. An alternative strategy was suggested by work in robotics: the racket movement was assumed to mirror the movement of the ball, thus impacting the ball with an increasing velocity profile, i.e., positive acceleration [25]. The dynamical movement primitives introduced above allow yet another way of accomplishing the ball bouncing task: an oscillatory racket movement creates a dynamically stable basin of attraction for ball bouncing, thus allowing even open-loop stable ball bouncing. This movement strategy is characterized by a negative acceleration of the racket during impacting the ball [39]—a quite non-intuitive solution: why would one break the movement before hitting the ball?

Examining the behavior of six subjects revealed the surprising result that dynamic movement primitives captured the human behavior the best: all subjects reliably hit the ball with a negative acceleration at impact, as illustrated in Figure 4. Manipulations of bouncing amplitude also showed that the way the subjects accomplished such changes could easily be captured by a simple re-parameterization of the oscillatory component of the movement, similarly as suggested for our DMPs above.

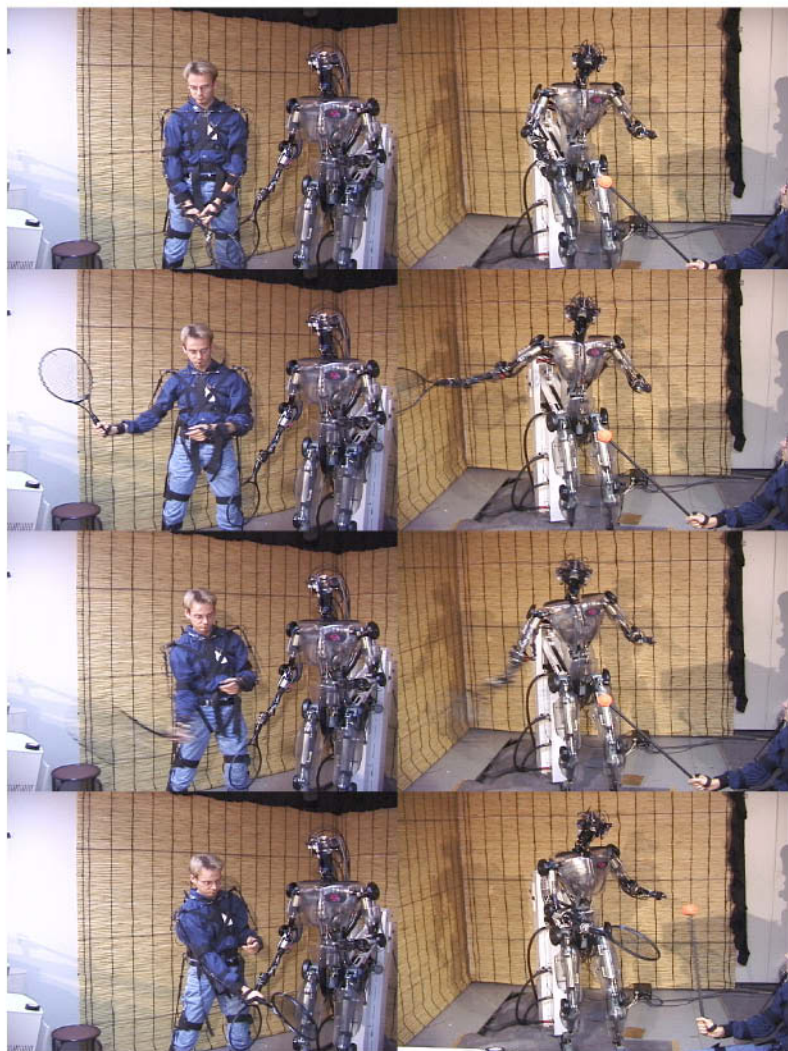


Fig. 3. Left Column: Teacher demonstration of a tennis swing, Right Column: Imitated movement by the humanoid robot.

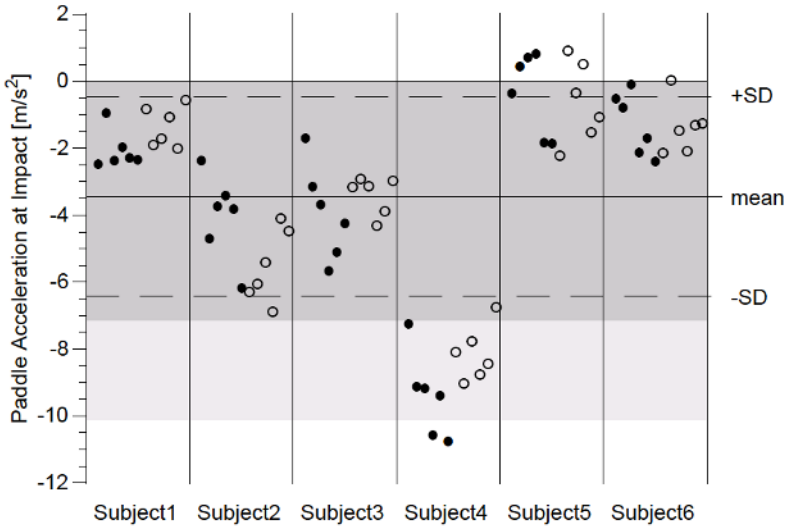


Fig. 4. Trial means of acceleration values at impact, $\ddot{x}_{P,n}$, for all six experimental conditions grouped by subject. The symbols differentiate the data for the two gravity conditions G . The dark shading covers the range of maximal local stability for $G_{reduced}$ the light shading the range of maximal stability for G_{normal} . The overall mean and its standard deviation refers to the mean across all subjects and all conditions.

3.2 Apparent movement segmentation

Invariants of human movement have been an important area of research for more than two decades. Here we will focus on two such invariants, the 2/3 power law and piecewise planar movement segmentation, and how a parsimonious explanation of those effects can be obtained. Studying handwriting and 2D drawing movements, Viviani and Terzuolo [40] first identified a systematic relationship between angular velocity and curvature of the endeffector traces of human movement, an observation that was subsequently formalized in the “2/3 power law” [41]:

$a(t)$ denotes the angular velocity of the endpoint trajectory, and $c(t)$ the corresponding curvature; this relation can be equivalently expressed by a 1/3 power-law relating tangential velocity $v(t)$ with radius of curvature $r(t)$:

Since there is no physical necessity for movement systems to satisfy this relation between kinematic and geometric properties, and since the relation has been reproduced in numerous experiments (for an overview see [42]), the 2/3-power law has been interpreted as an expression of a fundamental constraint of the CNS, although biomechanical properties may significantly contribute [43]. Additionally, Viviani and Cenzato [44] and Viviani [45] investigated the role of the proportionality constant k as a means to reveal

movement segmentation: as k is approximately constant during extended parts of the movement and only shifts abruptly at certain points of the trajectory, it was interpreted as an indicator for segmented control. Since the magnitude of k also appears to correlate with the average movement velocity in a movement segment, k was termed the “velocity gain factor.” Viviani and Cenzato [44] found that planar elliptical drawing patterns are characterized by a single k and, therefore, consist of one unit of action. However, in a fine-grained analysis of elliptic patterns of different eccentricities, Wann , Nimmo-Smith, and Wing [46] demonstrated consistent deviations from this result. Such departures were detected from an increasing variability in the log-v-log-r-regressions for estimating k and the exponent β of Equation (2), and ascribed to several movement segment each of which having a different velocity gain factor k .

The second movement segmentation hypothesis we want to address partially arose from research on the power law. Soechting and Terzuolo [47, 48] provided qualitative demonstrations that 3D rhythmic endpoint trajectories are piecewise planar. Using a curvature criterion as basis for segmentation, they confirmed and extended Morasso’s [49] results that rhythmic movements are segmented into piecewise planar strokes. After Pellizzetti, Massay, Lurito, and Georgopoulos [50] demonstrated piecewise planarity even in an isometric task, movement segmentation into piecewise planar strokes has largely been accepted as one of the features of human and primate arm control.

We repeated some of the experiments that led to the derivation of the power law, movement segmentation based on the power law, and movement segmentation based on piecewise planarity. We tested six human subjects when drawing elliptical patterns and figure-8 patterns in 3D space freely in front of their bodies. Additionally, we used an anthropomorphic robot arm, a Sarcos Dexterous Arm, to create similar patterns as those performed by the subjects. The robot generated the elliptical and figure-8 patterns solely out of joint-space oscillations, as described for the DMPs above. For both humans and the robot, we recorded the 3D position of the fingertip and the seven joint angles of the performing arm.

Figure 5 illustrates data traces of one human subject and the robot subject for elliptical drawing patterns of different sizes and different orientations. For every trajectory in this graph, we computed the tangential velocity of the fingertip of the arm and plotted it versus the radius of curvature raised to the power $1/3$. If the power law were obeyed, all data points should lie on a straight line through the origin. Figure 5a,b clearly demonstrates that for large size patterns, this is not the case, indicating that the power seems to be violated for large size patterns. However, the development of two branches for large elliptical patterns in Figure 5a,b could be interpreted that large elliptical movement patterns are actually composed of two segments, each of which obeys the power law. The rejection of the latter point comes from the robot data in Figure 5c,d. The robot produced strikingly similar features

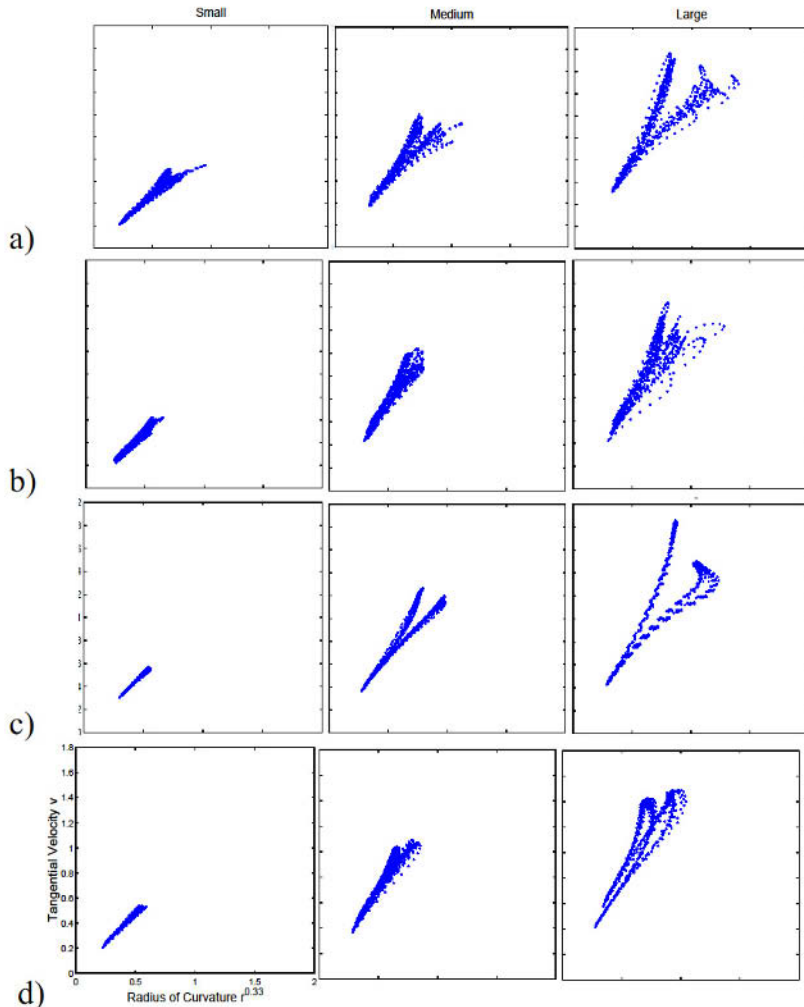


Fig. 5. Tangential velocity versus radius of curvature to the power $1/3$ for ellipses of small, medium, and large size for elliptical pattern orientations in the frontal and oblique workspace plane: a) human frontal; b) human oblique; c) robot frontal; d) robot oblique.

in the trajectory realizations as the human subjects. However, the robot simply used oscillatory joint space movement to create these patterns, i.e., there was no segmented movement generation strategy. Some mathematical analysis of the power law and the kinematic structure of human arms could finally establish that the power law can be interpreted as an epiphenomenon of oscillatory movement generation: as long as movement patterns are small enough, the power law holds, while for large size patterns the law breaks down [51, 52].

Using figure-8 patterns instead of elliptical patterns, we were also able to illuminate the reason for apparent piecewise-planar movement segmentation in rhythmic drawing patterns. Figure 6 shows figure-8 patterns performed by human and robot subjects. If realized with an appropriate width-to-height ratio, figure-8 patterns look indeed like piecewise planar trajectories and invite the hypothesis of movement segmentation at the node of the figure-8. However, as in the previous experiment, the robot subject produced the same features of movement segmentation despite it used solely joint space oscillations to create the patterns, i.e., no movement segmentation. Again, it was possible to explain the apparent piecewise planarity from a mathematical analysis of the kinematics of the human arm, rendering piecewise planarity to be an epiphenomenon of oscillatory joint space trajectories and the non-linear kinematics of the human arm. [51].

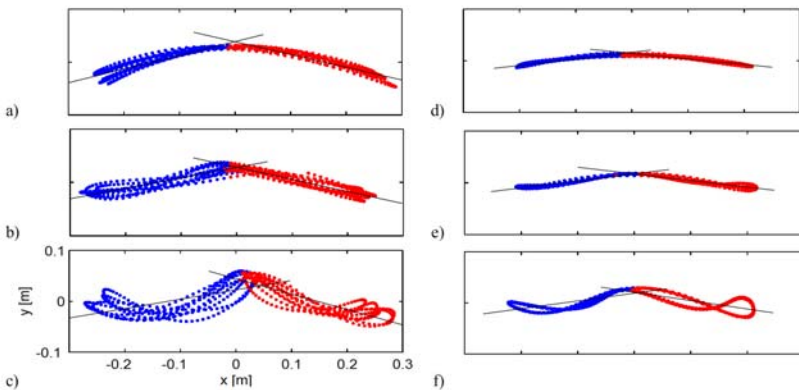


Fig. 6. Planar projection of one subject's figure-8 patterns of small, medium, and large width/height ratio: a-c) human data; d-f) corresponding robot data.

3.3 Superposition of discrete and rhythmic movement

In another experiment, we addressed the hypothesis of DMP that two separate movement primitives generate discrete and rhythmic movement. Subjects

performed oscillatory elbow movements around a given point in space and shifted the mean position of the elbow at an auditory signal to another point. In previous work [53], it was argued that such a discrete shift terminates the oscillatory elbow movement and restarts it after the shift. Using the model of dynamic movement primitives, we were able to demonstrate that a simple coupling structure between the discrete and rhythmic movement system can actually explain all the phenomena observed in this experiment, including phase resetting, a restricted set of onset phases for the discrete movement within the rhythmic movement, and kinematic features of the trajectory after the discrete shift [54, 55].

3.4 Brain activation in discrete and rhythmic movement

A last set of experiments addressed the question whether discrete and rhythmic movements make use of different brain centers. In a 4Tesla scanner, subjects performed either continuous oscillations with the wrist at two different frequencies, or discrete flexion and extension movements with pseudo-random movement start times. Both conditions were executed either with or without metronome pacing, and even with the foot instead of the wrist in three subjects. SPM99 based data analysis, including averaging across 11 subjects, provided highly statistically significant results (Figure 7). While rhythmic movement was confined to activation in primary contralateral motor cortices, supplementary motor cortex, and ipsilateral cerebellum, discrete movement elicited additional activation in contralateral premotor and parietal areas, and also in various ipsilateral cortical regions. These results indicate that discrete movements, even as simple as wrist flexion-extension movements, recruit significantly more cortical areas than rhythmic movement, and that discrete and rhythmic movement may have different movement generating principles in the brain. Thus, the model of rhythmic and discrete movement primitives may even have physiological significance.

4 Conclusion

The present study describes research towards generating flexible movement primitives out of nonlinear dynamic attractor systems. We focused on motivating appropriate dynamic systems such that discrete and rhythmic movements could be generated with high-dimensional movement systems. We also described some implementations of our system of Dynamic Movement Primitives on a complex anthropomorphic robot. In the last sections of the paper, we outlined various behavioral and imaging studies that resulted from our more theoretically motivated model. We believe that the combination of robotic, theoretical, and biological work that we pursued for the presented studies exemplifies a new path towards research in biomimetic robotics and computational neuroscience. Both disciplines can offer different and new ideas

Experiment 1

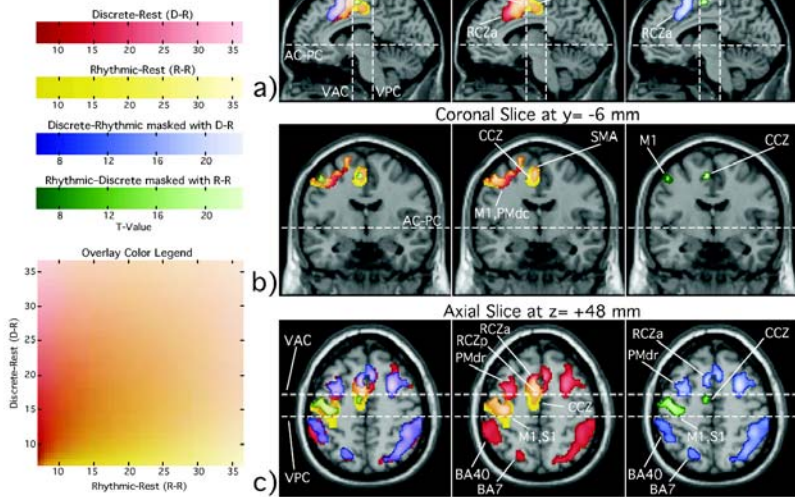


Fig. 7. Difference in brain activation between discrete and rhythmic movement obtained by contrasting discrete and rhythmic wrist movement. See legend on the left of the figure for explanations of which contrasts are displayed (note that this plot may not be clear in a black-and-white printout—download a PDF version at <http://www-clmc.usc.edu/publications>). RHYTHMIC-REST and DISCRETE-REST in the middle plot of all subfigures demonstrate the main effects of brain activity during RHYTHMIC and DISCRETE movement conditions—when there is overlap between the two contrasts, the Overlay Color Legend on the left of the subfigures is used to highlight the degree of overlap. RHYTHMIC-DISCRETE shows brain areas where rhythmic movement has stronger activity than discrete movement. Analogously, DISCRETE-RHYTHMIC displays areas that showed significantly more activation than rhythmic movement. The right plot of all three subfigures shows the RHYTHMIC-DISCRETE and DISCRETE-RHYTHMIC contrasts in isolation for the sake of clarity—no overlap is possible. The left plot in all subfigures superimposes the activities from the other plots in the subfigure to allow an easy comparison of activation locations. All results shown are statistically significant at a level of $p < 0.00001$, corrected for multiple comparisons within the entire brain volume. Abbreviations are [56]: AC: anterior commissure; PC: posterior commissure; VAC: vertical line perpendicular to the AC-PC, passing through the AC; PAC: vertical line perpendicular to the AC-PC, passing through the PC; CCZ: caudal cingulate zone; RCZ: rostral cingulate zone, divided in an anterior (RCZa) and posterior (RCZp) part; SMA: caudal portion of the supplementary motor area, corresponding to SMA proper; pre-SMA: rostral portion of the supplementary motor area; M1: primary motor cortex; S1: primary sensory cortex; PMdr: rostral part of the dorsal premotor cortex; PMdc: caudal part of the dorsal premotor cortex; BA7: Brodmann area 7 in parietal cortex; BA40: Brodmann area 40 in parietal cortex.

and techniques that will ultimately lead to reciprocal benefits in both disciplines.

Acknowledgments

This work was made possible by awards #9710312/#0010312 and #0082995 of the National Science Foundation, award AC#98-516 by NASA, an AFOSR grant on Intelligent Control, the ERATO Kawato Dynamic Brain Project funded by the Japanese Science and Technology Agency, and the ATR Human Information Processing Research Laboratories.

References

1. R. Bellman, *Dynamic programming*. Princeton, N.J.: Princeton University Press, 1957.
2. P. Dyer and S. R. McReynolds, *The computation and theory of optimal control*. New York: Academic Press, 1970.
3. G. Tesauro, "Temporal difference learning of backgammon strategy," in *Proceedings of the Ninth International Workshop Machine*, D. Sleeman and P. Edwards, Eds. San Mateo, CA: Morgan Kaufmann, 1992, pp. 9-18.
4. D. P. Bertsekas and J. N. Tsitsiklis, *Neuro-dynamic Programming*. Belmont, MA: Athena Scientific, 1996.
5. R. S. Sutton and A. G. Barto, *Reinforcement learning : An introduction*. Cambridge: MIT Press, 1998.
6. J. M. Hollerbach, "Dynamic scaling of manipulator trajectories," *Transactions of the ASME*, vol. 106, pp. 139-156, 1984.
7. S. Kawamura and N. Fukao, "Interpolation for input torque patterns obtained through learning control," presented at International Conference on Automation, Robotics and Computer Vision (ICARCV'94), Singapore, Nov., 1994, 1994.
8. R. A. Schmidt, *Motor control and learning*. Champaign, Illinois: Human Kinetics, 1988.
9. M. A. Arbib, "Perceptual structures and distributed motor control," in *Handbook of Physiology, Section 2: The Nervous System Vol. II, Motor Control, Part 1*, V. B. Brooks, Ed.: Bethesda, MD: American Physiological Society, 1981, pp. 1449-1480.
10. R. A. Brooks, "A robust layered control system for a mobile robot," *IEEE Journal of Robotics and Automation*, vol. 2, pp. 14-23, 1986.
11. R. R. Burridge, A. A. Rizzi, and D. E. Koditschek, "Sequential composition of dynamically dexterous robot behaviors," *International Journal of Robotics Research*, vol. 18, pp. 534-555, 1999.
12. W. Lohmiller and J. J. E. Slotine, "On contraction analysis for nonlinear systems," *Automatica*, vol. 6, 1998.
13. A. I. Selverston, "Are central pattern generators understandable?," *The Behavioral and Brain Sciences*, vol. 3, pp. 555-571, 1980.
14. E. Marder, "Motor pattern generation," *Curr Opin Neurobiol*, vol. 10, pp. 691-8., 2000.

15. M. Raibert, *Legged robots that balance*. Cambridge, MA: MIT Press, 1986.
16. G. Taga, Y. Yamaguchi, and H. Shimizu, "Self-organized control of bipedal locomotion by neural oscillators in unpredictable environment," *Biological Cybernetics*, vol. 65, pp. 147-159, 1991.
17. D. E. Koditschek, "Exact robot navigation by means of potential functions: Some topological considerations," presented at Proceedings of the IEEE International Conference on Robotics and Automation, Raleigh, North Carolina, 1987.
18. F. A. Mussa-Ivaldi and E. Bizzi, "Learning Newtonian mechanics," in *Self-organization, Computational Maps, and Motor Control*, P. Morasso and V. San-guineti, Eds. Amsterdam: Elsevier, 1997, pp. 491-501.
19. D. Sternad, M. T. Turvey, and R. C. Schmidt, "Average phase difference theory and 1:1 phase entrainment in interlimb coordination," *Biological Cybernetics*, vol. no.67, pp. 223-231, 1992.
20. J. A. S. Kelso, *Dynamic patterns: The self-organization of brain and behavior*. Cambridge, MA: MIT Press, 1995.
21. S. Grossberg, C. Pribe, and M. A. Cohen, "Neural control of interlimb oscillations. I. Human bimanual coordination," *Biol Cybern*, vol. 77, pp. 131-40, 1997.
22. C. Pribe, S. Grossberg, and M. A. Cohen, "Neural control of interlimb oscillations. II. Biped and quadruped gaits and bifurcations," *Biol Cybern*, vol. 77, pp. 141-52, 1997.
23. M. T. Turvey, "The challenge of a physical account of action: A personal view," 1987.
24. M. Bühler, "Robotic tasks with intermittent dynamics," Yale University New Haven, 1990.
25. A. A. Rizzi and D. E. Koditschek, "Further progress in robot juggling: Solvable mirror laws," presented at IEEE International Conference on Robotics and Automation, San Diego, CA, 1994.
26. J. F. Kalaska, "What parameters of reaching are encoded by discharges of cortical cells?," in *Motor Control: Concepts and Issues*, D. R. Humphrey and H. J. Freund, Eds.: John Wiley & sons, 1991, pp. 307-330.
27. N. Schweighofer, M. A. Arbib, and M. Kawato, "Role of the cerebellum in reaching movements in humans. I. Distributed inverse dynamics control," *Eur J Neurosci*, vol. 10, pp. 86-94, 1998.
28. N. Schweighofer, J. Spoelstra, M. A. Arbib, and M. Kawato, "Role of the cerebellum in reaching movements in humans. II. A neural model of the intermediate cerebellum," *Eur J Neurosci*, vol. 10, pp. 95-105, 1998.
29. N. A. Bernstein, *The control and regulation of movements*. London: Pergamon Press, 1967.
30. J. J. Craig, *Introduction to robotics*. Reading, MA: Addison-Wesley, 1986.
31. S. Schaal and D. Sternad, "Programmable pattern generators," presented at 3rd International Conference on Computational Intelligence in Neuroscience, Research Triangle Park, NC, 1998.
32. M. Williamson, "Neural control of rhythmic arm movements," *Neural Networks*, vol. 11, pp. 1379-1394, 1998.
33. G. Schöner, "A dynamic theory of coordination of discrete movement," *Biological Cybernetics*, vol. 63, pp. 257-270, 1990.
34. S. Schaal, D. Sternad, and C. G. Atkeson, "One-handed juggling: A dynamical approach to a rhythmic movement task," *Journal of Motor Behavior*, vol. 28, pp. 165-183, 1996.

35. S. Schaal, "Is imitation learning the route to humanoid robots?", *Trends in Cognitive Sciences*, vol. 3, pp. 233-242, 1999.
36. S. Schaal and C. G. Atkeson, "Constructive incremental learning from only local information," *Neural Computation*, vol. 10, pp. 2047-2084, 1998.
37. A. Ijspeert, J. Nakanishi, and S. Schaal, "Learning attractor landscapes for learning motor primitives," in *Advances in Neural Information Processing Systems 15*, S. Becker, S. Thrun, and K. Obermayer, Eds.: Cambridge, MA: MIT Press, 2003.
38. E. W. Aboaf, S. M. Drucker, and C. G. Atkeson, "Task-level robot learning: Juggling a tennis ball more accurately," presented at Proceedings of IEEE International Conference on Robotics and Automation, May 14-19, Scottsdale, Arizona, 1989.
39. S. Schaal and C. G. Atkeson, "Open loop stable control strategies for robot juggling," presented at IEEE International Conference on Robotics and Automation, Georgia, Atlanta, 1993.
40. P. Viviani and C. Terzuolo, "Space-time invariance in learned motor skills," in *Tutorials in Motor Behavior*, G. E. Stelmach and J. Requin, Eds. Amsterdam: North-Holland, 1980, pp. 525-533.
41. F. Lacquaniti, C. Terzuolo, and P. Viviani, "The law relating the kinematic and figural aspects of drawing movements," *Acta Psychologica*, vol. 54, pp. 115-130, 1983.
42. P. Viviani and T. Flash, "Minimum-jerk, two-thirds power law, and isochrony: Converging approaches to movement planning," *Journal of Experimental Psychology: Human Perception and Performance*, vol. 21, pp. 32-53, 1995.
43. P. L. Gribble and D. J. Ostry, "Origins of the power law relation between movement velocity and curvature: Modeling the effects of muscle mechanics and limb dynamics," *Journal of Neurophysiology*, vol. 76, pp. 2853-2860, 1996.
44. P. Viviani and M. Cenzato, "Segmentation and coupling in complex movements," *Journal of Experimental Psychology: Human Perception and Performance*, vol. 11, pp. 828-845, 1985.
45. P. Viviani, "Do units of motor action really exist?," in *Experimental Brain Research Series 15*. Berlin: Springer, 1986, pp. 828-845.
46. J. Wann, I. Nimmo-Smith, and A. M. Wing, "Relation between velocity and curvature in movement: Equivalence and divergence between a power law and a minimum jerk model," *Journal of Experimental Psychology: Human Perception and Performance*, vol. 14, pp. 622-637, 1988.
47. J. F. Soechting and C. A. Terzuolo, "Organization of arm movements. Motion is segmented," *Neuroscience*, vol. 23, pp. 39-51, 1987.
48. J. F. Soechting and C. A. Terzuolo, "Organization of arm movements in three dimensional space. Wrist motion is piecewise planar," *Neuroscience*, vol. 23, pp. 53-61, 1987.
49. P. Morasso, "Three dimensional arm trajectories," *Biological Cybernetics*, vol. 48, pp. 187-194, 1983.
50. G. Pellizzari, J. T. Massey, J. T. Lurito, and A. P. Georgopoulos, "Three-dimensional drawings in isometric conditions: planar segmentation of force trajectory," *Experimental Brain Research*, vol. 92, pp. 326-227, 1992.
51. D. Sternad and D. Schaal, "Segmentation of endpoint trajectories does not imply segmented control," *Experimental Brain Research*, vol. 124, pp. 118-136, 1999.

52. S. Schaal and D. Sternad, "Origins and violations of the 2/3 power law in rhythmic 3D movements," *Experimental Brain Research*, vol. 136, pp. 60-72, 2001.
53. S. V. Adamovich, M. F. Levin, and A. G. Feldman, "Merging different motor patterns: coordination between rhythmical and discrete single-joint," *Experimental Brain Research*, vol. 99, pp. 325-337, 1994.
54. D. Sternad, E. L. Saltzman, and M. T. Turvey, "Interlimb coordination in a simple serial behavior: A task dynamic approach," *Human Movement Science*, vol. 17, pp. 392-433, 1998.
55. D. Sternad, A. De Rugy, T. Pataky, and W. J. Dean, "Interaction of discrete and rhythmic movements over a wide range of periods," *Exp Brain Res*, vol. 147, pp. 162-74, 2002.
56. N. Picard and P. L. Strick, "Imaging the premotor areas," *Curr Opin Neurobiol*, vol. 11, pp. 663-72., 2001.

Coupling Environmental Information from Visual System to Changes in Locomotion Patterns: Implications for the Design of Adaptable Biped Robots

Aftab E. Patla, Michael Cinelli and Michael Greig

Gait and Posture Lab, Department of Kinesiology, University of Waterloo,
Waterloo, Ontario N2L3G1

Abstract. Information at a distance provided by vision is critical for adaptive human locomotion. In this paper we focus on which visually observable environmental features from the visual images on the retina are extracted and how they are coupled to changes in appropriate locomotion patterns. Studies related to environmental features that pose a danger to the mobile agent are described: these include obstacles; sliding doors and undesirable foot landing area in the travel path. Both static and dynamic environmental features result in changing optic flow patterns: environmental features that change independently pose an added challenge. Key results from these studies are discussed in terms of issues that are important for the implementation of visually guided adaptable biped robot.

1 Introduction

“Locomotion is controlled by information; control lies in the animal-environment system” (Gibson, 1979). The fact that sensory information plays a critical role in the control of locomotion is not an issue: rather the challenge has been to identify the roles played by various sensory inputs and delineate the transformation of the sensory input into appropriate motor output (Dickinson et al., 2000). A sensory modality that is able to provide information at a distance is essential for adaptive locomotion in unstructured and changing environments. Research has shown that vision is the only modality that can provide accurate and precise advance information about inanimate features of the environment (Patla, Davies & Niechweij, 2003). It is not surprising that most animals rely on vision to guide locomotion and Gibson in 1938 stated that “locomotion is guided chiefly by vision”.

The importance of vision for the control of adaptive locomotion was recognized early on. Liddell & Phillips (1944) showed that following pyramidotomy (which involves the cutting of the primary motor pathway from the cortex to the spine) cats were unable to walk in challenging environments where visually guided limb movements were essential. This proves that vision will mediate through higher cortical centers when visual information is necessary to safely move in a complex environment. Researchers have quantified cortical motor signals which represent one of the outputs from the visual system

(Drew et al., 1986). The challenge has been on the sensory side, specifically controlling the visual input, determining the spatial and temporal link and the transformation between the sensory input and motor output and identifying the many roles visual input plays in controlling locomotion. Psychophysical studies examining perceptual responses to visual inputs (abstraction of naturally occurring stimuli pattern during locomotion) focus on the sensory side without examining how the relevant information is used to guide action. Recording of neural activity in animals in response to similar stimuli or functional neuro-imaging studies in humans while fruitful also do not provide insights into the actual information and strategies used during adaptive locomotion. In our lab we have manipulated the environment, and/or visual input and examined the spatial and temporal characteristics of the changes that occur in the gait patterns.

2 The twelve postulates for visual control of human locomotion

Based on a series of experiments done in our lab, we have been able to come up with a set of postulates that provide unique insights into visual control of human locomotion (Patla, 1997; Patla, 1998; Patla, 2003). These are grouped under a series of questions that have guided our research.

Q1: What information does vision provide, that is unique and cannot be easily substituted by other sensory modalities?

P1. Vision provides unique, accurate and precise information at the right time and location about the environment at a distance (Exteroceptive), information about posture and movements of the body/body segment and information about self-motion (Ex-proprioceptive). For example, environmental information provided by haptic sense, used so effectively by visually impaired individuals, is not accurate or precise enough and takes much longer to obtain the information (see Patla, Davies & Niechweij, 2003).

Q2. Where and when are different types of visual information used?

P2. Environmental information, both visually observable and visually inferred, is used in a sampled feed-forward control mode to adapt basic walking patterns by influencing whole body motor patterns.

P3. Postural and movement information about the lower limbs is used in a sampled on-line control mode to fine-tune the adaptive swing limb trajectory (Patla et al., 2002).

P4. Self-motion information is used in a sampled on-line control mode to maintain postural orientation and balance during locomotion.

Q3. How is this visual information acquired?

P5. Combination of whole body, head and eye movements are used to acquire visual information. The most common gaze pattern during adaptive locomotion does not involve active gaze transfer to objects of interest: rather

gaze is anchored in front of the feet and is carried by the moving observer giving rise to optic flow (Patla, 2003). This has clear implications for the control of moving image capture in legged robots: as long as the video cameras are stabilized and oriented appropriately relative to the terrain, relevant information can be extracted from the optic flow.

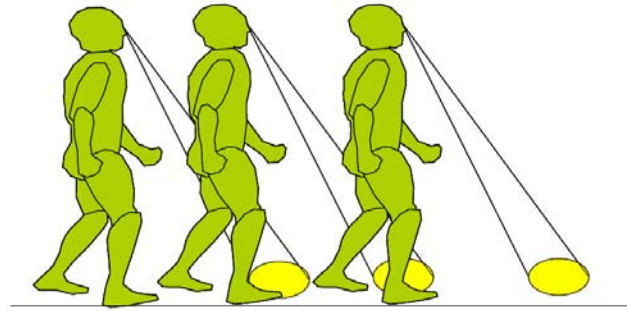


Fig. 1. Dominant gaze behavior is similar to carrying a torch shining at a fixed distance on the ground ahead of the person.

Q4. What are the characteristics of the visual-to-motor transformation?

P6. Visual-motor transformation for adaptive locomotion is not just dependent on visual input: prediction of future limb trajectory along with a priori rules influences the selection of an adaptive strategy.

P7. Proactive adaptive gait strategies involve global modifications to movement patterns and exploit inter-segmental dynamics to provide simple and efficient control.

P8. The duration and the pattern of available visual information influence accuracy and precision of local and global control of posture and balance during locomotion.

P9. The dynamic temporal stability margin during adaptive locomotion is constrained within narrow limits, necessitating a fast backup reactive system (reflexes) to ensure stability in case of error in visual-motor transformation.

P10. Visual-motor transformation for control of locomotion is primarily carried out in the occipito-parietal stream.

P11. Cognitive factors play an important role in both the selection of adaptive strategies and modulation of locomotion patterns.

Q5. What happens when there is conflicting information from other modalities?

P12. Visual information dominates over inappropriate kinesthetic information and voluntarily generated vestibular information for the control of swing limb trajectory.

3 Challenges for applying this knowledge to building of adaptable biped robots

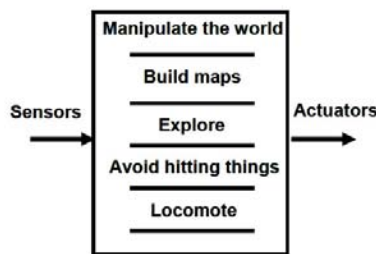
Creating an internal, environmentally detailed map from the visual images has clearly been recognized as not the way to use visual information to control a biped robot. Besides being prohibitively time consuming and hence too slow to implement any changes quickly, it is also not the way the biological system has evolved and functions. We know that the same visual information is processed differently and in different areas to guide action versus aiding perception (Milner & Goodale, 1991). Gibson (1958) proposed similar functional visuo-motor loops to serve different locomotor functions. He argued that our movements through the world result in changes of the images on the retina: this optic flow provides rich sources of information to guide movements. Information present in the visual stimulus under ecological conditions is sufficient and can be used to guide movements accurately and precisely (Gibson, 1979). The brain is tuned to pick up the appropriate visual information in the stimulus, similar to the tuner picking up a radio signal. The relevant information present in the stimulus is a complex, higher order spatial-temporal structure, which Gibson called an invariant. One such invariant is the variable “Tau” that provides information about time to contact with an object and has been argued to guide interceptive action (see review by Lee, 1998). Other invariants would control other actions. Gibson’s ideas are mirrored in the revised architecture for robots proposed by Brooks (1989). Figure 2 below summarizes the convergence of engineering, behavioral and biological thinking on how vision is used to control locomotor functions.

3.1 Geometric versus non-geometric features of the environment: role of past experience in interpreting visual information

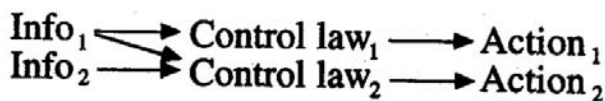
Most geometric features of the environment are available in the changing image on the retina as the person moves through that environment. In contrast, non-geometric features such as surface properties (for example compliance and frictional characteristics) require some inference based on past experience. For example, the potential for slipping on a banana peel in the travel path is inferred from past experience and is not directly available in the changing visual image.

Our work has shown that accommodating surfaces with different physical properties involve major modifications once contact has been made: while there are some changes to the pattern prior to landing, these are based on knowledge and/or prior experience with the surfaces (Marigold & Patla, 2002; Marigold et al., 2003). Modulations following ground contact probably rely more on information from other modalities (somatosensory for example) than vision. It is best therefore to focus on the extraction of visually observable environmental features from the visual images and linking them to changes in appropriate biped locomotor patterns.

(a)



(b)



(c)

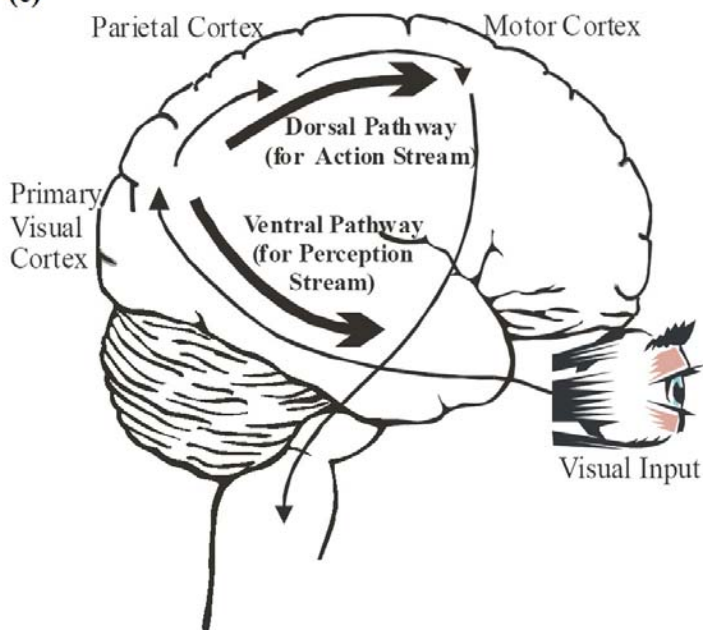


Fig. 2. a) Engineering architecture for control adaptable robots; b) Gibson's ideas about visual control of locomotion; c) Concept of cortical visual processing in animals adapted from Milner & Goodale (1991).

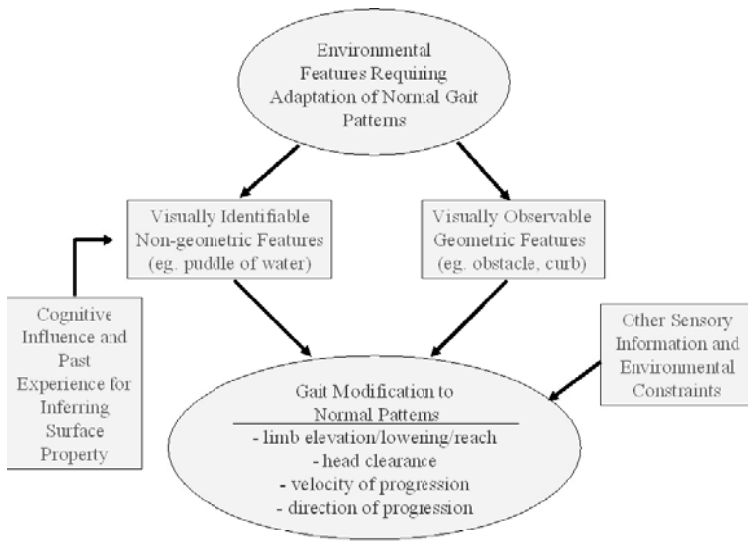


Fig. 3. Schematic flow chart showing the inputs besides vision to adapt normal gait patterns for different environments.

The focus of this paper will be on studies related to environmental features that pose a danger to the locomotor agent: obstacles, moving/oscillating doors and undesirable foot landing area in the travel path are examples of such hazards. Both static and dynamic environmental features result in changing optic flow patterns. Environmental features that change independent of the mobile agent pose an added challenge. Key results from these studies are discussed in terms of issues that are important for implementation of visuo-motor algorithms for adaptable biped robot.

4 Avoiding collisions with obstacles in the travel path

Avoiding a collision with obstacles in the travel path is a defining feature of legged locomotion. The ability to step over or under an obstacle besides going around it, allows legged animals to travel over terrains that are not accessible on wheels. This ability also minimizes damage to the terrain; wheeled vehicles that roll over the uneven terrain transfer their weight on the surface and can potentially harm the environment. The decision not to alter the travel path direction and instead step over or under an obstacle has been argued to be based on perceiving affordances in the environment (Gibson, 1979). Affordances are based on visual information about the environment scaled to an individual's own body size or capability. For example, if an obstacle exceeds a certain height in relation to the person's own stature, the individual chooses to go around rather than over (Patla, 1997). To capture the complexity and flexibility of adaptive human gait behavior during collision avoidance

in legged robots is a daunting task. We have to take baby steps so to speak before we run with the task of implementing the full repertoire of behavior.

4.1 Approaching and stepping over a single static obstacle in the travel path

We begin with the simplest task of getting a legged robot to approach and step over an obstacle that is static in its travel path. At first glance this would seem a trivial task and relatively easy to achieve, but this is not the case. This task has been studied in healthy individuals quite extensively with a wealth of knowledge available (see review by Patla, 1997). While the primary focus has been on mapping the changes in motor patterns as a function of obstacle characteristics (see Patla and Rietdyk, 1993), researchers have also examined the nature of the contribution of visual and proprioceptive sensory systems to adaptive locomotion (Patla, 1998; Sorensen, Hollands and Patla, 2002; Mohagheghi et al., 2003). It has been shown that dominance of visual input, which has the capability to provide information at a distance, can be used to plan and modify step patterns (Patla, 1998).

Lewis & Simo (1999) implemented a unique learning algorithm to teach a biped robot to step over an obstacle of a fixed height. Depending on what part of the swing limb trajectory made contact with the obstacle, preceding foot placements were adjusted. Limb elevation was set for the obstacle height (presumably early on) and the foot placement was modified in the approach phase to ensure success. Depending on which part of the robot leg touched the obstacle, the step length was either shortened (if the leg touches during the lowering phase) or lengthened. The reduction in variability in foot placement as the robot approached the obstacle was implemented by imposing a cost penalty for making large changes in step length. Visual information about the location of the obstacle was therefore being updated on-line to modulate step length during the approach phase while obstacle height information was programmed in for a fixed height obstacle. An intriguing question such an implementation poses is whether it is possible to dissociate the two critical pieces of information necessary for task performance. If possible, the visuo-motor algorithm could then be simplified by extracting obstacle height information separately and early in the approach phase. On-line obstacle location information could then be used to modulate primarily the foot placement during the approach phase.

What we were interested in is seeing if humans use similar techniques during obstacle avoidance. The easiest way to test the algorithm proposed by Lewis & Simo (1999) is to examine the performance of the obstacle avoidance task in an open-loop mode with the visual information about the obstacle height and location available prior to gait initiation. The basic question being: Can obstacle location and height information acquired prior to gait initiation be used to successfully step over the obstacle? The experiment and key results are described next.

Information about an obstacle in the travel path was acquired at a distance: the person was either standing (static viewing) or visually sampling during three steps before (dynamic sampling). The experimental set-up is shown below.

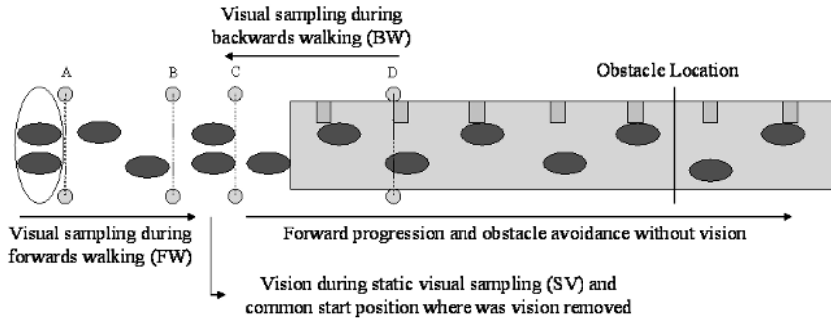


Fig. 4. Experimental set-up for obstacle avoidance following obstacle viewing under different conditions.

Compared to the full vision condition, visual information acquired at a distance followed by open-loop control has a failure rate of $\sim 50\%$. The challenge is to determine what information is required on-line to ensure success in this task: is it obstacle height or obstacle location? Two pieces of evidence suggest that obstacle height information is relatively robust, while the lack of on-line obstacle location information to modulate foot placement is the reason why individuals fail in this seemingly simple task carried out in open loop mode.

First evidence comes from examination of the types of errors that led to failure. The graph below (Figure 5a) showing the different error types shows that a large proportion of failure occurs during the limb lowering phase. The second piece of evidence comes from the comparison of the limb elevation for the successful versus failure trials. Both the accuracy and precision of limb elevation is similar for the successful and failure trials (Figure 5b). Therefore limb elevation is appropriate, but where it occurs relative to the obstacle is not correct. Thus poor foot placement in the approach phase is responsible for the high failure rates.

As would be predicted, variability in foot placement when the task is performed open-loop and results in failure is higher (Figure 5c). It is interesting to see that even in open loop control the variability of foot placement is regulated as the individual approaches the obstacle. Thus previously acquired visual information about obstacle location coupled with on-line kinesthetic information about limb movement can be used to tighten the foot placement as one nears the obstacle. Clearly the reduction in variability of foot placement in the absence of on-line visual information while possible is not sufficient:

the magnitude of reduction in foot placement variability is not sufficient to compensate if the initial foot placement variability is very high. Thus on-line visual information about obstacle location is necessary.

Previous research suggests how to extract obstacle height information relatively easily (Sinai et al., 1998; Ooi et al., 2001). Sinai et al. (1998) have shown that we use the ground surface as a reference frame for simplifying the coding of an obstacle location, and use angle of declination below the horizon to estimate absolute distance magnitude with the eye level as a reference (Ooi et al., 2001). Obstacle height can be inferred from the difference in angle of declination between the top and bottom edge of the obstacle, using the eye level as a reference and assuming the obstacle is located on a continuous terrain. Obstacles that are not anchored to the ground pose a challenge however and probably need additional processing.

4.2 Avoiding collision with a moving/changing obstacle in the travel path

During locomotion we often encounter potential obstacles that are moving (vehicular or pedestrian traffic in the travel path) or changing in size and shape. Common examples of obstacles that change shape and size include a pet that decides to stand up as one is stepping over or sliding entrance doors in department stores. Here the obstacle in the travel path is changing size and shape independently. The individual has to extract appropriate information about the dynamically changing environment and make appropriate changes to their own movement to ensure safe travel. While we know a lot about how locomotion is adapted to static environmental features, how and when behavior changes are coupled to the changes in environment is not well understood.

We focus on two experiments: in the first experiment individuals were required to avoid head-on collision with an object that was moving towards them in the same travel path while in the second experiment individuals were required to steer through gaps in the sliding doors, which oscillated at different frequencies.

Individuals are able to correctly estimate time-to-contact and implement an appropriate response. This has been shown in interception tasks with the upper limb (Savelsbergh et al., 1992; Watson and Jakobson, 1997; Port et al., 1997). When self-motion information was manipulated either on a computer screen (Delucia and Warren, 1994) or during a locomotor task (Bardy et al., 1992), individuals timed their response accordingly. We wanted to study a realistic simulation of head-on collision avoidance during a locomotor task. Individuals were given no specific instructions: they were asked to avoid hitting the object if it is in their travel path. The object, a life size manikin, approached the person at different velocities (2.2 m/s to 0.8 m/s) from the opposite end of the travel path. The expected response was to change the direction of locomotion and veer off the collision path. What we found was that

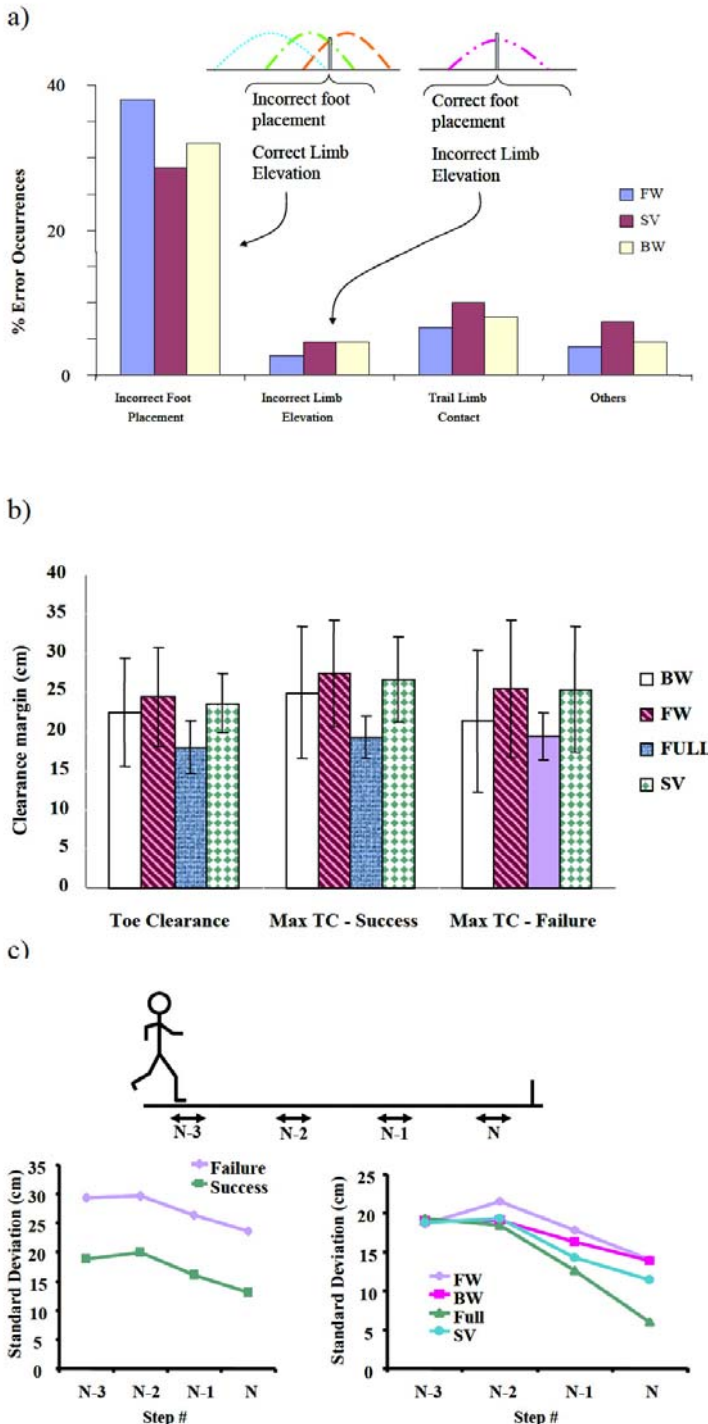


Fig. 5. (a) Collision error types; b) obstacle toe clearance and maximal toe elevation for successful and failed trials; (c) foot placement consistency during successful (for all conditions) and unsuccessful trials.

the time of initiation in change of travel path was independent of the velocity of the object, but the velocity of lateral displacement of the body center of mass was modulated as a function of object velocity. Thus the subjects were using vision to acquire action-relevant information and adapt their gait patterns to avoid collision. Since there were no precise temporal constraints on the individual's response, the coupling between the changing environment and changes in walking patterns were primarily guided by safety and initiation of change was not modulated as a function of environmental changes (Tresilian, 1999).

In the next study we increased the accuracy and precision demands of the locomotor task by having individuals approach and go through sliding doors that are continuously opening and closing. Montagne et al. (2002) used a virtual reality set-up to investigate the changes in locomotor speed to pass safely through the opening. The experimental set-up involved subjects walking on a treadmill while viewing the virtually manipulated environment. They showed that individuals modified their velocity of locomotion based on visual information about the door oscillation frequency and amplitude, but because of treadmill constraints subjects chose not to stop or slow down. Clearly the use of a virtual reality environment influenced the outcome.

We used a physical set-up shown below (Figure 6a) and monitored the person's movement pattern to identify the responses when there were no constraints on the subject's response. We identified on-going changes to the locomotor patterns as individual's approached the oscillating doors (Figure 6b). The challenge to the individual was increased by varying the oscillating speed of the doors.

Everyday behavior is controlled by a simple coupling between an action and specific information picked up in optical flow that is generated by that action. Safe passage through a set of sliding doors requires individuals to use information about the environment and their own body movement (ex-propriospecific). In order to achieve this goal, individuals must try to keep the rate of gap closure between them and the doors and that of the doors at a constant rate. This action is known as tau coupling (Lee, 1998). Tau coupling forces individuals to adjust their approach to the moving doors (controllable) so that they can pass through the doors at an optimal point. This optimal point is determined by the fit between properties of the environment and properties of the organism's action system termed affordance (Warren and Whang, 1987).

Approach to the moving doors is the same as an approach to an object in that it requires spatiotemporal information between the doors and the moving observer. Time to Contact (TTC) is the concept that explains the spatiotemporal relationship between an object and the point of observation. In the case of moving doors, TTC will only tell the individuals when they will reach the doors but will not tell the individuals what position the doors will be in when they get there. Tau coupling data from this study were determined by

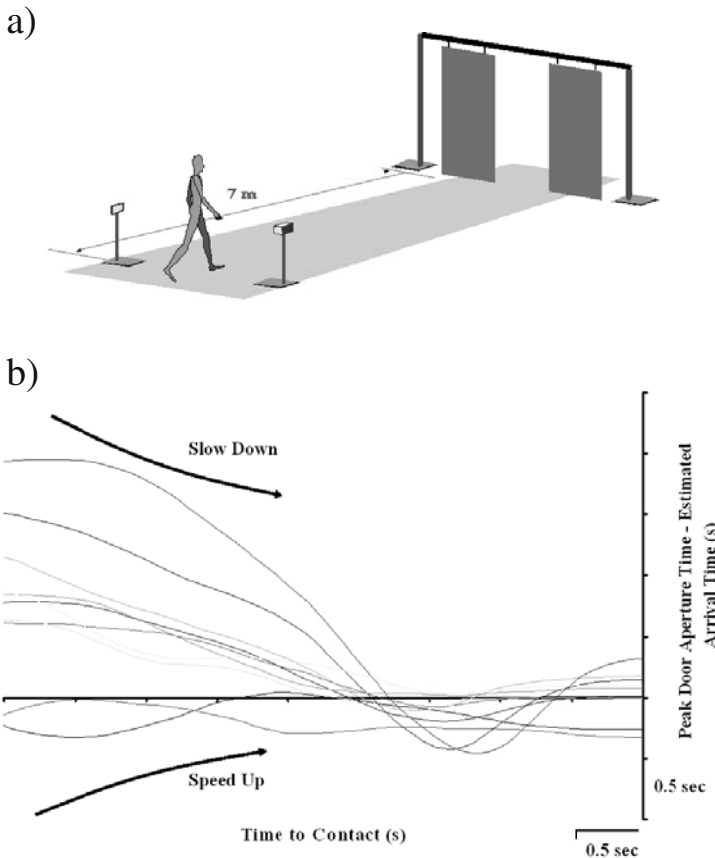


Fig. 6. a) Sliding door experimental setup; (b) coupling of speed of locomotion with door opening.

subtracting the time when the peak door aperture occurred in the appropriate cycle from the estimated time of arrival at the door. If this temporal difference was zero, then the individuals have timed their arrival when the doors are opened widest. This is the ideal coupling between the individual's action and changing environment, and provides the safest margin. Non-zero temporal difference indicates arrival when either the doors are opening wide (positive temporal difference representing earlier arrival with respect to maximum door opening time) or closing in (negative temporal difference representing later arrival with respect to maximum door opening time).

Reduction in magnitude of the temporal difference can be achieved by modulating the velocity of progression: for positive temporal difference slowing down is needed, whereas for the negative temporal difference, an increase in speed of locomotion is required (Figure 6b). Clearly the margin for error is

dependent on the maximum door opening and opening and closing cycle time. Smaller maximum door aperture and cycle time imposes tighter constraint on the action: if it is not timed precisely within small temporal limits, safety could be compromised. Thus this paradigm offers a unique opportunity to observe dynamic perception-action coupling during locomotion.

Typical profiles of speed from several trials for one individual from one of the experiments are shown in Figure 6b. These profiles show both an increase and decrease in speed of locomotion, depending on the trial, to time the arrival at the door close to when the door is at its maximum. The adjustments in speed of locomotion are gradual and occur during the approach phase and are completed about 2s before arrival at the door. This funnel like control seen in the profile is similar to studies in upper limb control literature (cf. Bootsma & Oudejans, 1993).

The overriding theme that emerges from the studies discussed so far is that on-line visual information about the environment and self-motion is needed to continuously modify and adapt walking patterns. So far control of action is dependent on sensory information which specifies the change needed. In the next section we look at another common locomotor adaptation that is not completely specified by the sensory input.

5 Avoiding stepping on a specific landing area in the travel path

Path planning is an integral component of locomotion, and most often refers to route plans to goals that are not visible from the start. The choice of a particular travel path is dependent on a number of factors such as energy cost (choosing the shorter of possible paths) and traversability (choosing a path that has been selected and traversed by others). We consider this global path planning. The focus here is on adjustments to gait that one routinely makes to avoid stepping on or hitting undesirable surfaces, compromising dynamic stability, possibly incurring injuries. These on-line adaptations to gait termed local path planning include selection of alternate foot placement, control of limb elevation, maintaining adequate head clearance and steering control (Patla et al., 1989; 1991). We have been exploring the factors that influence local path planning in several experiments and show that visual input alone does not specify a unique action: other factors play a role in decision making. The focus of the experiments was determining what guides the selection of alternate foot placement during locomotion in a cluttered environment.

Visual input alone in most cases is able to identify which area of the travel surface to avoid, although in many cases prior experience and knowledge plays an important role. For example, avoiding stepping on a banana peel is clearly based on prior experience or knowledge that it can be a slippery surface. For now we concentrate on the class and type of surfaces that are visually

determined to be undesirable to step on and an alternate foot placement is required. While sensory input can tell you where not to step, it does not specify where you should step. Our work (Patla et al., 1999) has shown that the choices we make are not random, but systematic.

The first critical observation from our work is that choice for the same target area to be avoided is dependent on where in relation to the target area one normally lands (see conditions 'a' and 'b' in Figure 7). This suggests that visual input about the target area, shape and size is not enough: this has to be coupled with prediction of where the foot in relation to the target (to be avoided) would land. The latter has to be based on prediction from the ongoing interaction between visual and proprioceptive input. We believe that this is done to predict the magnitude of the foot displacement that would be needed for the different choices such as stepping long, short, medial or lateral. This is based on the second critical information from these studies: the dominant alternate foot placement choices are the ones that require smallest foot displacement from the normal landing spot among the possible choices. This we have argued minimizes the effort required to modify the normal step pattern and possibly reduces metabolic cost.

If there is a unique single choice among the possible alternate foot placement, the decision is simple, and is primarily based on available and predicted sensory input. This would be relatively easy to implement in an algorithm. The problem arises when more than one choice meets this criterion.

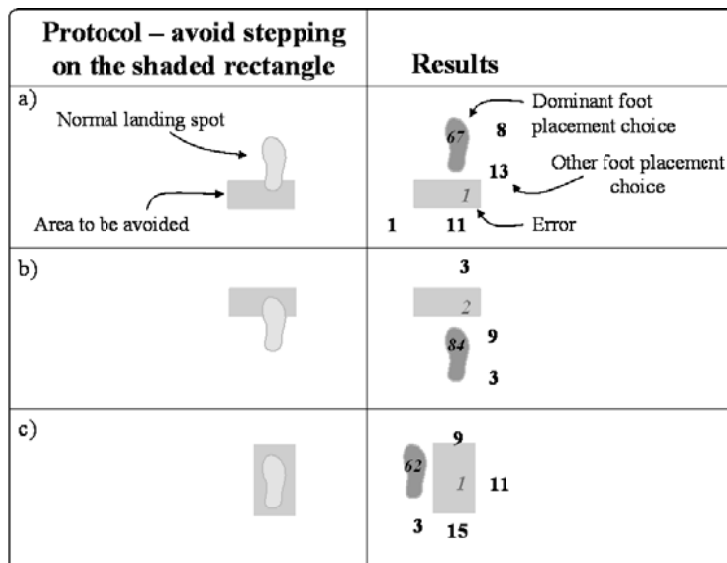


Fig. 7. Protocol and results from three conditions used by Patla et al., 1999.

When more than one possible foot placement choice satisfies this criterion, sensory input alone is clearly not sufficient. See for example, the condition ‘c’ in Figure 7: stepping medial or lateral involves similar magnitude of foot displacement from its normal landing spot. Despite that there is a dominant choice of stepping medially. Here we have argued that the control system has a set of hierarchical rules that guide the choice. These rules are based on functional determinants of locomotion such as dynamic stability and maintenance of travel in the intended direction.

For example, given a choice between stepping medial or lateral, stepping medial would minimize disturbance to balance but is dependent on step length and situational constraints. When stepping medial or long result in the same magnitude of foot displacement from the normal landing spot, stepping long is preferred since that ensures both dynamic stability and forward progression. Our work has shown that individuals prefer choices that are in the path of progression (stepping long or short versus stepping medial or lateral). When there is choice between stepping long or short, they prefer stepping long. Stepping medially (narrow) is preferred over stepping laterally (wide). The relative weight given to the determinants is probably influenced by any temporal constraints on the response (Moraes, Lewis & Patla, 2003). A schematic decision tree guiding foot placement is shown in Figure 8. Clearly such an algorithm would have to be built-in for a legged robot to safely traverse a cluttered environment.

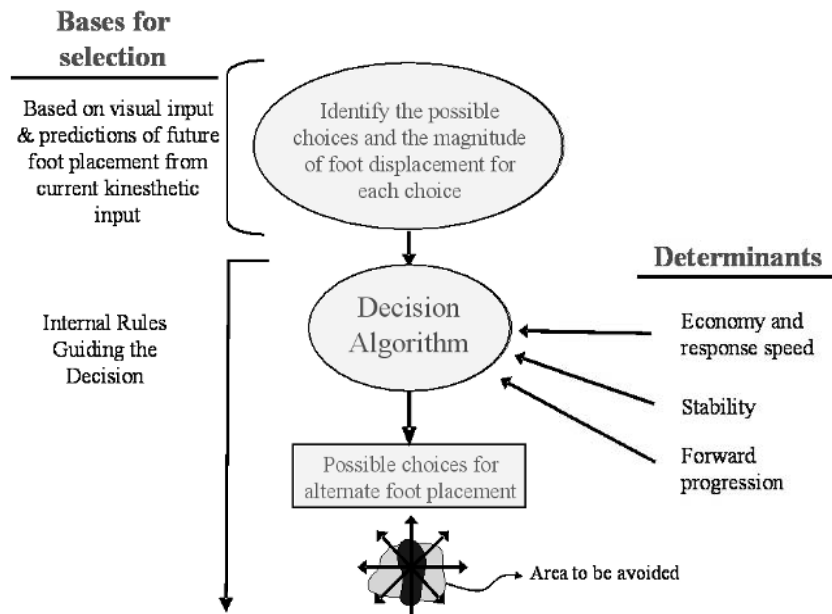


Fig. 8. Schematic of decision process for choosing a foot placement

6 Conclusions

In several studies we have attempted to focus on how and which visually observable environmental features are extracted to control adaptive human locomotion. These studies provide insights into possible algorithms for visual control of biped robots.

Acknowledgements

This work was supported by a grant from Office of Naval Research, USA.

References

1. Bardy, B.G., Baumberger, B., Fluckiger, M. and Laurent, M. (1992). On the role of global and local visual information in goal-directed walking. *Acta Psychologica* (Amsterdam), 81(3):199-210.
2. Bootsma, R.J., Oudejans, R.R.D. (1993). Visual information about time-to-collision between two objects. *Journal of Experimental Psychology: Human Perception and Performance*, 19(5):1041-1052.
3. Brooks, R.A. (1989). A robot that walks: Emergent behavior from a carefully evolved network. *Neural Computation* 1(2):253-262.
4. Delucia, P.R. and Warren, R. (1994). Pictorial and motion-based information during active control of self-motion: Size arrival effects on collision avoidance. *Journal of Experimental Psychology: Human Perception and Performance*, 20:783-798.
5. Dickinson, M.H., Farley, C.T., Full, R.J., Koehl, M.A.R., Kram, R., Lehman, S. (2000). How animals move: An integrative view. *Science*, 288:100-106.
6. Drew, T., Dubuc, R., Rossignol, S. (1986). Discharge patterns of reticulospinal and other reticular neurons in chronic, unrestrained cats walking on a treadmill. *Journal of Neurophysiology*, 55(2):375-401.
7. Gibson, J.J. and Crooks, L.E. (1938). A theoretical field-analysis of automobile-driving. *American Journal of Psychology*, 51:453-471.
8. Gibson, J.J. (1958). Visually controlled locomotion and visual orientation in animals. *British Journal of Psychology*, 49:182-189.
9. Gibson J.J. (1979). *The ecological approach to visual perception*. Boston, MA: Houghton Mifflin.
10. Lee, D.N. (1998). Guiding Movement by Coupling Taus: Ecological Psychology. 10(3-4): 221-250.
11. Lewis, M.A. & Sim, L.S. (1999). Elegant stepping: A model of visually triggered gait adaptation. *Connection Science*, 11(3&4):331-344.
12. Liddell, E.G.T., & Phillips, C.G. (1944) Pyramidal section in the cat. *Brain*, 67:1-9
13. Marigold, D.S. and Patla, A.E. (2002). Strategies for dynamic stability during locomotion on a slippery surface: effects of prior experience and knowledge. *Journal of Neurophysiology*, 88:339-353.

14. Marigold, D.S., Bethune, A.J. and Patla, A.E. (2003). Role of the unperturbed limb and arms in the reactive recovery response to an unexpected slip during locomotion. *Journal of Neurophysiology*, 89:1727-1737.
15. Milner A.D. & Goodale, M.A. (1993). Visual pathways to perception and action. *Progress in Brain Research*, 95:317-337.
16. Mohagheghi, A.A., Moraes, R. and Patla, A.E. (2003). The effects of distant and on-line visual information on the control approach phase and step over an obstacle during locomotion. *Experimental Brain Research* (in press).
17. Montagne, G., Buekers, M., De Rugy, A., Camachon, C. and Laurent, M. (2002). The control of human locomotion under various task constraints. *Experimental Brain Research*, 143:133-136.
18. Moraes, R., Lewis, M.A. and Patla, A.E. (2003). Strategies and determinants for selection of alternate foot placement during human locomotion: influence of spatial but not temporal constraints. *Experimental Brain Research* (accepted pending revisions).
19. Ooi, T.J., Wu, B. and He, Z.J. (2001). Distance determined by the angular declination below the horizon. *Nature*, 414:197-200.
20. Patla, A.E., Robinson, C., Samways, M., & Armstrong, C.J. (1989). Visual control of step length during overground locomotion: Task-specific modulation of the locomotion synergy. *Journal of Experimental Psychology: Human Perception and Performance*, 15(3): 603-617.
21. Patla, A.E., Prentice, S., Robinson, C., & Neufeld, J. (1991). Visual control of locomotion: Strategies for changing direction and for going over obstacles. *Journal of Experimental Psychology: Human Perception and Performance*, 17(3): 603-634.
22. Patla, A.E. and Rietdyk, S. (1993). Visual control of limb trajectory over obstacles during locomotion: effect of obstacle height and width. *Gait and Posture*, 1:45-60.

P
23. Patla A.E. (1997). Understanding the roles of vision in the control of human locomotion. *Gait and Posture*. 5:54-69.
24. Patla A.E. (1998). How is human gait controlled by vision? *Ecological Psychology* (Invited peer-reviewed paper), 10 (3-4): 287-302.
25. Patla A.E., Prentice S.D., Rietdyk S., Allard F. and Martin C. (1999). What guides the selection of foot placement during locomotion in humans.. *Experimental Brain Research*, 128:441-450.
26. Patla, A.E., Niechwiej, E., Racco, V., Goodale, M.A., (2002). Understanding the contribution of binocular vision to the control of adaptive locomotion. *Experimental Brain Research*, 142:551-561.
27. Patla, A.E., (2003). Gaze behaviours during adaptive human locomotion: Insights into the nature of visual information used to regulate locomotion. In: *Optic flow and beyond*. Edited by: L. Vania, S. Rushton, in press.
28. Patla, A.E., Davies, C., Niechwiej, E. (2003). Obstacle avoidance during locomotion using haptic information in normally sighted humans. *Experimental Brain Research* (in press).
29. Port, N.L., Lee, D., Dassonville, P. and Gergopoulos, A.P. (1997). Manual interception of moving targets: I. Performance and movement initiation. *Experimental Brain Research*, 116(3):406-420.

30. Savelsbergh, G.J.P., Whiting, H.T.A., Burden, A.M. and Bartlett, R.M. (1992). The role of predictive visual temporal information in the coordination of muscle activity in catching. *Experimental Brain Research*, 89:223-228.
31. Sinai, M.J., Ooi, T.J. & He, Z.J. (1998). Terrain influences the accurate judgement of distance. *Nature*, 395:497-500.
32. Sorensen, K.L. Hollands, M.A. and Patla A.E. (2002). The effects of human ankle muscle vibration on posture and balance during adaptive locomotion. *Experimental Brain Research*, 143(1):24-34.
33. Tresilian, J.R. (1999). Visually timed action: time-out for “tau”? *Trends in Cognitive Sciences*, 3:301-310.
34. Warren, W.H. Jr. and Whang, S. (1987). Visual guidance of walking through apertures: body-scaled affordances. *Journal of experimental psychology. Human perception and performance*, 13(3):371-383
35. Watson, MK and Jakobson, L.S. (1997). Time to contact and the control of manual prehension. *Experimental Brain Research*, 117(2):273-280.